Problems associated with the cds. photovoltaic cell.

Buckley, Robert William

Problems associated with the CdS Photovoltaic Cell

by

R.W. Buckley B.Sc.

A thesis presented in candidature of the degree of Doctor of Philosophy

University of Durham

September 1973

The people that walked in darkness have seen a great light; they that dwell in the land of the shadow of death, upon them hath the light shined.

Isaiah 9.2

Acknowledgements

I would like to extend my thanks to all those who have helped me in any way over the past three years and especially to those mentioned below.

To the Science Research Council for their award of a C.A.P.S. Research Studentship.

To Dr. J. Woods, my supervisor, for his never-failing help and encouragement.

To Professor D.A. Wright for the use of the research facilities of the Department and to the technical staff headed by Mr. F. Spence whose help and advice have been invaluable.

To Mr. J.R. Cutter for providing the single crystal material.

To the Research Group led by Dr. L. Clark at I.R.D. Newcastle for providing much valuable information.

To the Durham University Methodist Society for helping me to lead a balanced life throughout the period of the work.

To my parents for all their encouragement over the years.

And finally to my wife Helen for her understanding and support.

RuBuckley

Abstract

The cadmium sulphide solar cell is based on the CdS-Cu_2S heterojunction and is the only serious contender to the established silicon cell for the conversion of solar energy into electrical power. The cells can be fabricated in thin film or single crystal form.

The first part of this thesis describes an investigation into the electrical properties of vacuum deposited CdS films as a function of various parameters such as evaporation rate, source temperature, substrate temperature and film thickness. The Hall mobilities and resistivities of the samples have been measured. The main object was to produce low resistivity films for use in CdS solar cells. By evaporating CdS in a totally enclosed system, films with resistivities less than 10 Ωcm were produced. Much of the CdS film behaviour can be explained in terms of evaporation and condensation kinetics, in particular the decrease in resistivity with increasing thickness observed in all films evaporated from a single source can be attributed to the deviation from stoichiometry of the source as the evaporation proceeds.

Some of the films were photoluminescent. Measurements of the spectral distribution of the luminescence enabled a correlation to be made between optical and electrical properties of the films.

The second part of the thesis deals with an investigation of the photovoltaic properties of the CdS-Cu_2S heterojunction. Cells with efficiencies up to 3.3% were fabricated on thin films and single crystals.

The formation of a Cu_2S layer on CdS is explained in terms of a simple diffusion model. The existence of a photoconductive i-CdS region in the heat treated cells is demonstrated by the presence of long time constants and quenching effects. The importance of the preliminary surface treatment given to the CdS layer and the stoichiometry of the Cu_2S is also demonstrated. An attempt has been made to adjust the stoichiometry of the Cu_2S layer by utilizing its electrochemical properties.

CONTENTS

			Page
CHAPTER	1	INTRODUCTION	1
		References	3
CHAPTER	2	PHOTO-EFFECTS AND II-VI COMPOUNDS	4
		2.1 The photovoltaic effect	4
		2.2 Solar cells	6
		2.3 II-VI compounds	10
		2.4 Properties of cadmium sulphide	14
		2.5 Properties of copper sulphide	15
		2.6 Conclusions	18
		References	19
CHAPTER	3	THE CdS SOLAR CELL	22
		3.1 History	22
		3.2 Other II-VI photovoltaic devices	24
		3.3 Suggested mechanisms at the CdS-Cu_2S junction	25
		3.4 Clevite model for solar cell	28
		3.5 CdS layer	30
		3.6 The copper sulphide layer	32
		References	34
CHAPTER	4	CdS THIN FILMS	36
		4.1 The Preparation of CdS Thin Films	36
		4.2 The Properties of CdS Films	41
		4.3 Conclusions	44
		References	46
CHAPTER	5	THE PREPARATION OF CdS THIN FILMS	49
		5.1 Vacuum Systems	49
		5.2 Vacuum Chamber Fixtures	49
		5.3 Source Material	52
		5.4 Masks	53
		5.5 Substrates	53
		References	58

		Page
CHAPTER 6	THE ELECTRICAL PROPERTIES OF CdS THIN FILMS	59
	6.1 Introduction	59
	6.2 Electrical Contacts	60
	6.3 Apparatus	60
	6.4 Current Characteristics	61
	6.5 Effect of Film Thickness of Electrical Resistivity	63
	6.6 Effect of Evaporation Parameters on Electrical Resistivity	68
	6.7 Film Structure	70
	6.8 Conclusions	71
	References	73
CHAPTER 7	DISCUSSION OF THE EFFECT OF THE EVAPORATION PARAMETERS ON THE PROPERTIES OF THE THIN FILMS	74
	7.1 Introduction	74
	7.2 Evaporation Kinetics	74
	7.3 Transport Properties	83
	References	90
CHAPTER 8	LUMINESCENCE IN CdS THIN FILMS	91
	8.1 Introduction	91
	8.2 Experimental Details	94
	8.3 Experimental Results	96
	8.4 Interpretation	97
	8.5 Summary	99
	References	101

		Page
CHAPTER 9	PHOTOVOLTAIC MEASUREMENTS	102
	9.1 Introduction	102
	9.2 Cell Fabrication	102
	9.3 Cell Evaluation	104
	9.4 Barrier Layer Formation	106
	9.5 Cell Properties	109
	9.6 Cell degradation and Cu_2S Stoichiometry	115
	9.7 Summary	122
	References	124
CHAPTER 10	DISCUSSION OF PHOTOVOLTAIC MEASUREMENTS	125
	10.1 Introduction	125
	10.2 Rate of formation of Cu_2S	125
	10.3 Cell Performance	129
	10.4 Thin Film Cells	133
	10.5 Cu_2S Stoichiometry	134
	10.6 Conclusions	137
	References	138
CHAPTER 11	SUMMARY	139
	11.1 CdS Thin Films	139
	11.2 CdS:Cu_2S Photovoltaic Cells	140
	11.3 Suggestions for future work	142
	11.4 Epilogue	142

CHAPTER 1

INTRODUCTION

During the past decade there has been great interest in the cadmium sulphide-copper sulphide heterojunction because of its possible application as a lightweight, flexible, photovoltaic cell suitable for satellite power sources. Its potential for terrestrial applications is also promising. Applications to date, particularly for space use, have been hindered by instabilities in the cell, which lead to a degradation of the output on exposure to illumination or on thermal cycling. A study of these problems forms the basis for the work described in this thesis. The ultimate aim is to develop space qualified, stable, high efficiency, CdS solar cells.

The work has been carried out under the Science Research Council's C.A.P.S. scheme in co-operation with the International Research and Development Company of Newcastle-upon-Tyne.

A schematic representation of the structure of a typical CdS thin film cell is shown in Figure 1.1. The cell consists of a substrate, the CdS film, a "barrier layer" of cuprous sulphide, a grid to reduce the sheet resistance of the top contact and a protective plastic layer. A single crystal version of the cell can also be made by forming the barrier layer of cuprous sulphide on a single crystal slice of CdS, the opposite side of which is in ohmic contact with a metal base, usually copper.

Both these structures are of the heterojunction type since cuprous sulphide is a degenerate p-type semi-conductor while cadmium sulphide is n-type. The operation

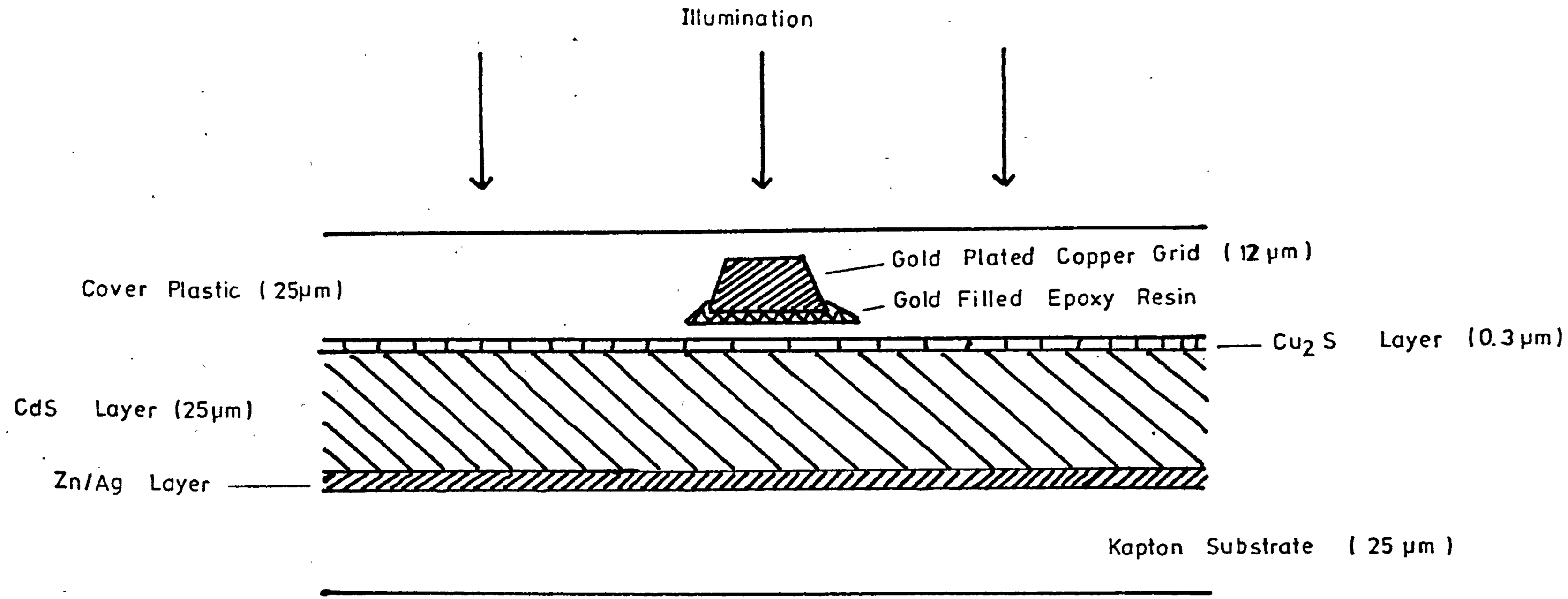

Figure 1.1

Schematic Cross-Section Of a CdS Thin Film Solar Cell

of the photovoltaic cell is however not straightforward and will be discussed later.

The CdS film has to be of low resistivity, to minimize the series resistance of the device, (Clark et al 1970) and the Cu_2S layer, which is chemically plated on top of this film, has to be stoichiometric in order to increase the efficiency and stability of the final cell (Nakayama et al 1971). The device once fabricated is then baked at a temperature of about 200°C. for a few minutes in order to form an intrinsic layer of CdS between the n-type CdS and p-type Cu_2S. This layer is essential for the photovoltaic operation of the cell (Shiozawa et al 1969). These requirements will be discussed more fully in Chapter 3.

The work described in this thesis can be divided into two parts.

(a) A study has been carried out into the electrical properties of evaporated films of CdS in an attempt to grow films with resistivities less than 100Ωcm and to determine which parameters are important in controlling the resistivity of the resultant films.

(b) Solar cells in both single crystal and thin film form have been fabricated. Performances were noted as a function of heat treatment in different ambients to investigate the formation of the i-CdS layer. The rate of formation of the Cu_2S layer was also studied in an attempt to elucidate the diffusion mechanism which brings about this chemical change. Finally attempts were made to form stoichiometric Cu_2S on CdS by applying potentials to the Cu_2S surface during formation.

References

Clark et al (1971), Proc. Brighton Power Conference p.643

Nakayama et al (1971), Japan J.A.P. 10 1415

Shiozawa et al (1969), Aerospace Research Labs. Report ARL 69-0155

CHAPTER 2

PHOTO-EFFECTS AND II-VI COMPOUNDS

2.1 The Photovoltaic Effect

The photovoltaic effect (P.V.E.) is one of the three major photoelectric effects which were discovered during the nineteenth century. In 1839 Bequerel discovered that if one of two identical electrodes immersed in an electrolyte was illuminated, a potential difference was produced between them. This effect occurs because incident photons liberate electrons (or holes) near the junction of two dissimilar materials and these electrons are then accelerated through an external circuit by the electric field established at the boundary of the two materials. The wet cell arrangement is inconvenient and no practical applications were found for the P.V.E. until a similar effect was discovered in selenium (Adams and Day 1877). Later the effect was observed in other semi-conducting materials, e.g. Cu/Cu_2O (1927), AgS, ZnS, PbS. Present day photovoltaic studies are based on the newer materials, Si, CdS, CdTe, InP, GaAs which are more suited to the generation of electrical power than Cu/Cu_2O and Se which are used mainly in light meters.

The Bequerel P.V.E. is difficult to explain fully. Early models proposed by Frenkel (1933, 1935), Landau and Lifshitz (1936), Davydov (1938) and Mott (1939) concluded that the photo- E.M.F. arose as a result of a non-equilibrium of minority carriers. The most recent explanation of the mechanism of the Bequerel type cell came from Williams (1960) who described such a cell with CdS electrodes. Chopin et al (1954) discovered P.V. action in p-n junctions of silicon and used much of the then new p-n junction theory to explain

the operation of his device. An attempt by Reynolds et al later that year to apply this theory to the Cu or Cu_2S:CdS cell was unsuccessful, as this cell is composed of a complicated p-i-n junction. No model for this device has yet been universally accepted.

The second photoelectric process to be reported was the photoconductive effect (P.C.E.) which was discovered in selenium by Smith (1873). The resistivity of the sample was reduced when the selenium was irradiated with light of an appropriate wavelength; no photo-E.M.F. was generated if identical electrodes were used. The photoconductivity of most of the group II-group VI compounds has been studied. In practical devices a compromise has to be reached between the required speed of response and sensitivity (Rose 1963, Bube 1955, 1960).

For completeness mention should be made of the third photoelectric process, namely the photoemissive effect (P.E.E.) first reported by Hertz in 1887. This effect however is not relevant to the present work.

A photovoltaic effect can be produced in a number of different situations:-

(a) Bulk effects occur when the sample is illuminated non-uniformly or when it has a non-uniform impurity distribution.

Wallmark (1957) reported a transverse P.V. potential which was developed in certain samples when they were illuminated non-uniformly. Illumination perpendicular to the junction gave rise to a potential difference parallel to it.

(b) Barrier effects are obtained whenever an electrostatic barrier exists within the sample, which can cause charge separation of optically created electron-hole pairs. Illumination of the sample produces an E.M.F. perpendicular to the barrier. This barrier may be a diffusion potential between p and n regions of a semiconductor homo or heterojunction, or between a metal and a semiconductor. The CdS solar cell, which is essentially a n-CdS/p-Cu_2S heterojunction, is a p-n junction with further complications arising from an interposed compensated layer of CdS.

(c) Thin films of most II-VI compounds and certain single crystal semi-conductors can develop a photovoltage larger than the forbidden gap. This can be several hundred volts per cm. of sample length, (Goldstein and Pensak 1959, Brandhorst et al 1968) and depends on the sample perfection or method of production of the thin film. It has been suggested that this anomalous effect is associated with the cubic/hexagonal stacking faults which are present in ZnS for example, and that the stacking faults are the sources of the potential barriers (Neumark 1962). The two phases have slightly different energy gaps and it is suggested that the potential discontinuities are additive and can therefore give a total barrier of several hundred electron volts, (Ogawa et al 1965, Gagliano et al 1967). The high impedance of the materials involved precludes any useful application being made.

2.2. Solar Cells

Initially semiconducting photovoltaic devices were used only to detect or measure radiation, but over the past

decade improved technology has allowed the liberated electrons to be collected more efficiently so that useful conversion of solar energy into electrical power has been achieved.

On a cloudless summer day at latitude $55^{o}N$ at sea level about 800 watts m^{-2} of solar energy fall on the earth. To generate power it would seem more efficient to convert this energy directly into electricity instead of burning fossil fuels etc. This is the hope for P.V. devices now that materials with theoretically low conversion losses have been reported. A 20% 'limit conversion efficiency' was calculated for p-n junctions in silicon with higher values for GaAs, InP and AlSb (Cummerow 1954, Pfann and Roosbroeck 1954, Pittner 1954, Prince 1955, Rappaport 1959 and Wolf 1960). The greatest advance towards achieving these high efficiencies have been made as a result of the U.S. space project. As the available solar energy beyond the earth's atmosphere under conditions known as air mass zero is 1400 watts m^{-2}, an acceptable sized array of solar cells even with a low conversion efficiency will provide adequate power for a communications satellite.

In choosing materials and arrays for solar cells the following requirements have to be met:

(a) The cost must be low.

(b) The fabrication process should lend itself to mass production.

(c) The absorption spectrum of the cell should match, as well as possible, the sun's spectral output.

A cell should have:

(i) A high resistance to radiation (for space use).

(ii) A large area and be flexible.

(iii) A high power to weight ratio.

(iv) Low reflection losses at its surfaces.

(v) A high efficiency for the production of e-h pairs from the absorbed energy.

(vi) A high carrier collection efficiency.

(vii) A high voltage factor(V.F.) which is the ratio of the open circuit voltage to the energy gap.

(viii) A low density of surface and interface states, especially on large area cells.

(ix) A high curve factor(C.F.) which is the ratio of the maximum power to the product of open circuit voltage and short circuit current, (also known as the fill-factor).

(x) A low internal series resistance, (partly overcome by using gridded electrodes).

The first cells to be fabricated were single crystal cells of which the most efficient to date has been the p-n junction silicon cell (Tudenberg 1960). More recently gallium arsenide cells have been produced but both Si and GaAs cells necessitate the growth of large single crystals and the costly machining of these into thin wafers. Moreover the size of each cell is limited to a few square centimetres by the size of the original crystal and by the fragility of the cut wafer. The present day conversion efficiencies of silicon cells are at best 15% but more usually 12% - 13%. These values degrade in satellite use to around 6% in a matter of a few months when the cells are subjected to particle radiation in the Van Allen belt. Brucker et al, 1966, and workers at R.C.A. have suggested however that this damage can be minimized by using silicone coatings or by doping the silicon with lithium.

The power to weight ratios of single crystal cells are in the region of 40 watts/lb.

The power level of the single crystal silicon solar cells used on all the un-manned space missions flown to date has been limited to powers of less than 1 KW. Future missions may well require powers in the multi KW. range, and since the current solar cell systems may not be practical for such high powers considerable research has been devoted to the development of a solar cell with a thin film structure. Thin film cells (Moss 1961) offer the advantages of cheapness, light weight, mechanical flexibility, and a larger total output power from a practical array. The design criteria and goals relevant to the thin film solar cell programme are shown in Table 2.1, and are due to Perkins (1967). Considerable effort has been directed to the production of such cells with cadmium telluride (CdTe) and GaAs and with cadmium sulphide in particular for which the spectral response with a peak at 0.5 μm is well matched to solar radiation.

Whilst some properties of the cells can be improved with better technology others have a theoretical limit controlled by the basic properties of the material concerned. Consideration of these factors gives rise to a curve of efficiency as a function of band gap. Loferski (1956) and Wolf (1960) favour this as a means of determining a figure of merit. The curve has a maximum around an energy gap of 1.6 eV for AMO sunlight illumination. Silicon (1.1 eV) is therefore seen to be worse than gallium arsenide (1.34 eV) or aluminium antimonide (1.52 eV). CdS cells were assumed to be equally bad (2.4 eV) but, as will be discussed later, they have an effective energy gap of about 1.3 eV.

TABLE 2.1

Design criteria and goals for the thin film solar cell programme
(after Perkins 1967)

Design Criteria	Goals	Si cells current status
Efficient cell structure	10%	14% (max.)
Environmental Earth Resistance Space	Stable 5-10 years	Stable at least 5-10 years
Suitable configuration a. lightweight b. low cost c. large flexible area	 >100 w/lb (array) <£4/w (array) 1 ft^2	 10-20 w/lb (array) ~£160/w (array) 2-4 cm^2 rigid, fragile

This suggests that the CdS/Cu_2S cell may present a strong challenge to the supremacy of Si cells. Theoretically CdTe (Vodakov et al 1960, Cusano 1963), AlSb (Pittner 1954) and InP should be better and devices using these materials have been constructed, but low carrier mobilities, difficulties of growth and high cost, make them economically unattractive.

2.3 II-VI Compounds

2.3.1 Preparation

By II-VI compounds we mean compounds formed between elements of Group IIb and Group VIb of the periodic table.

Crystals of all the II-VI's have been grown both from the melt and the vapour phase. The first report of the growth of a II-VI crystal from the vapour phase was that of Lorenz (1891). His technique was modified much later by Frerichs (1946). Separate sources for the elements are required with this dynamic method which employs a carrier gas so that the system is in a continuous state of externally induced flow. The basic requirement for growth is a flow of the group II and group VI elements in the vapour phase. These elements can either be separate or formed from the dissociation of a permanent compound. The gaseous species diffuse or flow to a region where they become supersaturated and growth takes place.

Reynolds and Czyzak (1950) and Greene et al (1958) developed a static method of crystal growth in which transport occurs by diffusion through the gas phase. This method requires the starting components in powder form. Further modifications to it were carried out by Piper and

Polich (1961) and since then the method has been used with good results on several II-VI compounds.

Growth from the melt has many advantages in the preparation of large volume single crystals. However the required conditions of high temperatures and not insignificant pressures make the technique a difficult one. Only those compounds with relatively low melting points, e.g. CdTe, CdSe, ZnTe can be fused without the need for a high pressure autoclave or protective equipment (Lorenz 1962). Cadmium sulphide has been successfully grown from the melt by Medcalf and Fahrig (1958) and Fischer (1963), but it is usually grown from the vapour phase by methods similar to those of Piperand Polich. At the present time large single crystals of CdS can be grown readily this way. The optimum conditions are now well established and if there is need for improvement it is in the area of source purity.

2.3.2 Structure

The II-VI compounds crystallise in two main modifications, namely the cubic zinc blende (sphalerite) and the hexagonal wurtzite. In addition closely related polytypes may exist which have tetrahedrally co-ordinated arrangements that are substantially derivative structures of zinc blende and wurtzite. Some compounds are transformed by pressure into a rock salt structure in which the atoms have octahedral co-ordination, and although these phases are unstable under normal conditions they may sometimes be retained at low temperatures. The compounds with a rock salt structure appear to be typically ionic but in general the bonding in II-VI's spans the complete range from ionic to covalent.

The crystals encountered in practice are usually non-ideal and contain defects and imperfections which often control the semiconducting properties. Crystals typically contain point defects such as vacancies or impurity atoms, line or plane defects, i.e. dislocations and stacking faults and more complex defects resulting from the coalescence of elementary ones. Because of the extensive polytypism of some of these compounds such as ZnS, gross defect structures associated with intergrowths of several crystal forms are commonly encountered.

2.3.3 Bonding

The bonds found in II-VI compounds are not adequately described by any one extreme type, but have characteristics intermediate with those usually associated with ionic and covalent bonding. The energy band gaps of the compounds are intermediate between those of metals and the elemental semiconductors (Si and Ge). As stated previously, the bonding is a mixture but no matter what the nature of the bonding, ionic or covalent, the spins of the bonding electrons are paired so that the net spin of the electrons is zero. A perfect compound free of defects is therefore diamagnetic. It is in fact the presence of defects, or more often the fabrication of material with control over the number and nature of the defects that gives rise to the interesting electrical, magnetic and optical properties of the II-VI compounds.

2.3.4 Electrical Properties

Nearly all the II-VI compounds can be made photoconducting. The predominant energy transfer process in these

materials is brought about by the charge carriers. The exciting radiation creates free carriers of both polarities in such quantities that all other transport mechanisms may be obscured by ambipolar diffusion. It appears possible to achieve very high photosensitivity in all the II-VI compounds and the range of bandgaps allows for a range in response maxima from the near ultra-violet to the near infra-red.

The photoconductivity of II-VI compounds is characterised in the following ways:

(a) Electrons are the majority contributors to the photocurrent. Free electrons and holes are created by the absorption of radiation, the holes however are rapidly captured at sites where recombination with free electrons occurs at a later time.

(b) The centres that give rise to the high photosensitivity are compensated acceptors. They have a capture cross section for holes 10^4-10^6 times larger than their subsequent capture cross section for free electrons. These centres are associated with intrinsic crystal defects or defect impurity complexes.

(c) Many of the characteristic properties of a particular II-VI photoconductor (e.g. the dependence of photocurrent on intensity, photosensitivity on temperature, optical quenching, speed of response etc.) depend directly on the location of the energy level of the sensitizing centres. These sensitizing levels are about 1.1 eV above the valence band in sulphides, 0.6 eV above in selenides and 0.3 eV (predicted) in tellurides.

2.4 Properties of Cadmium Sulphide

CdS is a IIb-VIb semi-insulating compound which has a direct band gap of 2.4 eV and normally crystallizes in the hexagonal wurtzite structure. Under certain growth conditions a meta-stable cubic sphalerite structure may predominate. Thin films with a cubic structure can be grown on cubic crystalline substrates with similar dimensions of the unit cell (Wilcox and Holt 1969).

As the energy gap is direct the optical absorption coefficient changes as the square of the incident photon energy and has very high values for energies greater than the band gap.

CdS starts to sublime at 700°C and melts under several atmospheres pressure at 1500°C. Consequently crystals can be grown either from the vapour phase or from the high pressure liquid phase.

Unlike group IV or III-V semiconductors the II-VI compounds are not amphoteric and do not show intrinsic behaviour at room temperature. CdS can only be made n-type and any attempt to diffuse in acceptor impurities results in self compensation by vacancies to maintain charge neutrality. Anderson and Mitchell (1968) and Chernow et al (1968) thought they had obtained p-type CdS by ion implantation techniques but Tell and Gibson (1969) showed that this p-type conductivity was almost certainly due to radiation damage rather than introduced chemical impurity. Consequently in the CdS solar cell, Cu_2S is used as the p-type material of a heterojunction since it can be grown epitaxially on n-type CdS by a method which will be described later.

Pure CdS crystals have a high resistivity of about 10^{12} Ωcm which is lowered under illumination. The Hall mobility may also be dependent on the light intensity. At room temperature in the dark the Hall mobility of electrons is around 300 $cm^2\ v^{-1}\ sec^{-1}$ in good single crystals whereas the hole mobility is of the order of 10. In single crystals it is possible that all the following processes limit the carrier mobilities:- ionized impurity scattering, acoustic mode scattering, polar optical mode scattering, piezo-electric scattering. In films geometrical effects and intergranular boundaries will also be important.

CdS has been studied extensively over the past twenty years (Aven and Prener 1967) mainly because of the interest in its photoconductive and luminescent properties. Since hexagonal CdS has no centre of inversion symmetry, the material is piezoelectric and much interest has also centred on acoustoelectric effects and CdS transducers. Laser emission has been obtained under high energy density excitations with an electron beam. A rather unusual property of conductivity has also been discovered by Wright et al, (1968)

2.5 Properties of Copper Sulphide

Cuprous sulphide (Cu_2S) exists in several different crystalline structures and chemical formulae. A general review of the electrical and optical properties of 'copper sulphide' has been given by Abdullaev et al (1968) and Vlasenko and Kononets (1971). By 'Cu_2S' we mean all sulphides of monovalent copper represented by the general formula Cu_xS where $1.8 \leqslant x \leqslant 2$.

A layer of chalcocite (x=2) can be formed epitaxially on CdS by dipping the latter into a hot solution of Cu^+ ions. The following substitution reaction takes place

$$CdS + 2Cu^+ \longrightarrow Cu_2S + Cd^{++}$$

On heating gently in air some chalcocite forms djurleite (x=1.96) and further heat treatment produces some digenite (x=1.8). Further information on these phase changes is given by Roseboom (1966).

Singer and Faeth (1967) and Cook (1970) reported the complete transformation of a single crystal of CdS to a cracked but single crystal of Cu_2S by a chemical plating process. The cracks are formed by the strain present in the Cu_2S as a result of the volume mismatch between the two sulphides.

Cu_2S has an indirect band gap of 1.2 eV and a second threshold for direct transitions at 1.8 eV (Marshall and Mitra 1965). Its optical absorption coefficient changes slowly with photon energy up to 1.8 eV and then increases more rapidly. Consequently high energy photons ($h\nu > 1.8$ eV) are absorbed near the surface of the Cu_2S when the cell is illuminated from that side. This however leads to a poor conversion efficiency for short wavelength illumination as the electrons and holes are created close to surface recombination centres. Some light of energy between 1.2 eV and 2.4 eV will however pass through the Cu_2S and be absorbed in the i-CdS layer.

Copper sulphide is a p-type semiconductor which has a hole mobility of about 10 $cm^2\ v^{-1}\ sec^{-1}$ (Martinuzzi et al 1970). It shows appreciable ionic conduction at room

temperature with a mobility of 3×10^{-6} cm^2/v sec, due to the high diffusion rate of Cu^+ in Cu_2S which increases with temperature (Hirahara 1951). When subjected to high temperatures Cu_2S loses copper by chemical and structural changes (Cook et al 1970). In vacuo copper whiskers are formed on the surface. This process is reversible but on heating in air the copper which migrates to the surface is oxidised. This process is irreversible and leads to the formation of Cu_2O on the surface whereas in the bulk heating leads to a composition change as follows

$$Cu_2S \longrightarrow Cu_{1.96}S \longrightarrow Cu_{1.8}S$$

This reaction is responsible for the degradation of unencapsulated cells and will be discussed later. CdS solar cells also have a high resistance to radiation damage, this is possibly due to the high mobility of Cu^+ ionsin Cu_2S which permits rapid annealing of 'knock-on' damage.

The interface region between the n-type CdS and the p-type Cu_2S is important. This is a 1 μm thick layer of Cu compensated CdS known as the i-CdS region. It is formed by heating a plated sample at 200°C for a few minutes. Such heat treatment is an essential step in the preparation of an efficient cell. By using tracer techniques it has been shown (Clark 1959, Woodbury 1965, Szeta and Somorjai, 1966) that the diffusion rate of Cu in CdS is anisotropic. Diffusion proceeds more rapidly perpendicular to the c axis than parallel to it. Purohit (1969) showed that these diffusion rates were much slower when the copper ions originated from Cu_2S rather than elemental copper. This therefore suggests that only prolonged heat treatment would

cause the copper to penetrate right through the CdS to the substrate and effect the shunt resistance. This is found to be the case in practice.

2.6 Conclusions

The heterojunction between CdS and Cu_2S is sufficiently promising to compete with other photovoltaic cells and has the following advantages.

(a) It is easy and potentially cheap to fabricate in thin film form (Clark et al 1971).

(b) It has a high power to weight ratio in thin film form (> 100 watts/lb).

(c) The cell has a high resistance to radiation damage (Brucker et al 1966).

(d) It is flexible and easy to handle in store and has a long operating lifetime.

(e) The spectral response is well matched to the solar spectrum.

(f) The cell's I(v) characteristics display a large VF and CF.

The major problem with the cells is the degradation they suffer when subjected to thermal cycling and long term simulated solar illumination tests. Degradation under long term illumination has been identified as due to two phenomena, darkening of the cover plastic under UV irradiation and a loss in power output due to a more fundamental cell degradation mechanism known as load effect degradation. The latter is manifested when cells are exposed to sunlight under open circuit or near open circuit conditions and will be discussed in more detail in a later chapter.

References

Abdullev et al (1968), Phys. Stat. Solid 26 65

Adams and Day (1877), Proc. Roy. Soc. A25 113

Anderson and Mitchell (1968), App. Phys. Lett. 12 334

Aven and Prener (1967), Physics and Chemistry of II-VI compounds (editors) (North Holland)

Bequerel (1839), Compt. Rend. 9 145

Brandhorst et al (1968), J.A.P. 39 6071

Brucker et al (1966), Proc. I.E.E.E. 54 895

Bube (1955), Proc. I.R.E. Dec. 1836

Bube (1960), Photoconductivity of solids (Wiley)

Chernow et al (1968), Appl. Phys. Lett. 12 339

Chopin et al (1954), J.A.P. 25 676

Clark (1959), J.A.P. 30 957

Clark and Woods (1966), B.J.A.P. 17 319

Clark and Woods (1968), J. Cryst. Growth 3 126

Clark et al (1971), Proc. Brighton Power Conference 1971

Cook et al (1970), J.A.P. 41 3058

Cummerow (1954), Phys. Rev. 95 16

Cusano (1963), Solid State Electron. 6 217

Davydov (1938), Zn. Tekh. Fiz. 5 79

Fisher (1963), U.S.A.F. Contract Report No. AF19 (604) 80 18

Frenkel (1933), Nature 132 312

Frenkel (1935), Physik Z. Sovietunion 8 185

Frerichs (1946), Naturwiss 33 387

Gagliano et al (1967), J. Phys. Chem. Sol. 28 737

Goldstein and Pensak (1959), J.A.P. 30 155

Greene et al (1958), J. Chem. Phys. 29 1375

Hertz (1887), Ann. Physik 31 421

Hertz (1887), Ann. Physik 31 983

Hirahara (1951), J. Phys. Soc. Jap. 6 422

Landau and Lifshitz (1936), Physik Z. Sovientunion 8 185

Loferski (1956), J.A.P. 27 777

Lorenz (1891), Chem. Ber. 29 1509

Lorenz (1962), J. Phys. Chem. Sol. 23 1449

Marshall and Mitra (1965), J.A.P. 36 3882

Martinuzzi et al (1970), Phys. Stat. Sol. (a) 2 K9

Medcalf and Fahrig (1958), J. Electrochem. Soc. 105 719

Moss (1961), R.C.A. Review 22 29

Mott (1939), Proc. Roy. Soc. A171 281

Neumark (1962), Phys. Rev. 96 533

Ogava et al (1965), Japan J.A.P. 4 948

Perkins (1967), Adv. Energy Conv. 7 265

Pfann and Roosbroeck (1954), J.A.P. 25 1422

Piper and Polich (1961), J.A.P. 32 1278

Pittner (1954), Phys. Rev. 96 1708

Prince (1955), J.A.P. 26 534

Purohit (1969), J.A.P. 40 4677

Rappaport (1959), R.C.A. Review 20 373

R.C.A. (1966), Direct Energy digest Aug 2

Reynolds et al (1954), Phys. Rev. 96 533

Reynolds and Czyzak (1950), Phys. Rev. 79 543

Rose (1963), 'Theory of Photoconductivity'

Roseboom (1966), Economic Geology 61 641

Rudenberg (1960), Proc. 14th Annual Power Conf. Atlantic City 1960

Singer and Faeth (1967), App. Phys. Lett. 11 130

Smith (1873), Am. J. Sci. 5 307

Stanley (1956), J. Chem. Phys. 24 1279

Szeta and Somorjai (1966), J. Chem. Phys. 44 3490

Tell and Gibson (1969), J.A.P. 40 5320

Vlasenko and Kononets (1971), Ukr. Fiz. Zh. (USSR) 16 237

Vodakov et al (1960), Sov. Phys. Sol. St. 2 1

Wallmark (1957), Proc. I.R.E. 45 474

Wilcox and Holt (1969), J. Mat. Sci. 4 672

Williams (1960), J. Chem. Phys. 32 1505

Wolf (1960), Proc. I.R.E. 48 1246

Woodbury (1958), J.A.P. 36 2287

Wright et al (1968) B.J.A.P. 1 1593

CHAPTER 3

THE CdS SOLAR CELL

3.1 History

The discovery of the CdS photovoltaic cell is attributed to Reynolds (1954) who while studying the properties of various rectifying contacts on CdS observed a strong photovoltaic effect. In direct sunlight with copper contacts, open circuit voltages (OCV) of 0.45 volts and short circuit currents (SCC) of 15 m Amps/cm^2 were observed. An anomalous response of the cell to light with wavelengths greater than the band gap of CdS was also noted. By the end of 1954 single crystal cells 1% efficient and 0.5 cm^2 in area were being produced. Over the five years that followed a greater effort was put into the understanding of the basic properties of the CdS, e.g. electrical and optical properties of doped and undoped crystals, methods of cutting, polishing etc. The first report of the preparation of a thin film solar cell was that of Nadjakov et al (1954). They evaporated a thin film of CdS on to comb like grids of aluminium or gold on glass substrates. Low photocurrents were observed. Had they tried copper electrodes they might have formed the Cu_2S layer which, as is now evident, gave Reynolds his high photocurrents. Copper electrodes were later examined by Fabricus (1962) and found to be successful.

In 1962 Shirland et al formed thin film cells on conducting metal substrates. At the same time plastic substrates were investigated to determine the viability of flexible cells. By the mid 1960's the objective of growing thin films of CdS on metallised plastic substrates and

plating the Cu_2S layer chemically was well established. The early thin film cells had been limited by a sheet resistance, particularly that formed at the contact with the Cu_2S. If this contact was small, a large sheet resistance resulted; however if it was large there was a masking of the Cu_2S which lowered the output of cell. This problem was overcome by using gold plated copper grids to make the top contact to the Cu_2S layer. During this early period many different arrays and constructions of solar cells were investigated, i.e. backwall (illumination through CdS), frontwall (illumination through Cu_2S), and various hybrids. These have been described in detail by many authors, see for example Shirland (1966), McMahan (1967).

The increase in efficiency of CdS cells over the last ten years as reported in the literature and at conferences is shown in Fig. 3.1. In 1967 attempts were made to improve (1) the protection against atmospheric humidity, and (2) the stability of cells against thermal cycling, by packaging them in epoxy cements with transparent plastic covers, (Hietaneh and Shirland; Spakovski, Bowman et al). Degradation of the cells then emerged as an important disadvantage especially the process known as load-effect degradation. This was traced (1968) to the electrolytic deposition of copper in microscopic Cu_2S fingers penetrating as far as the rear surface of the cell. This plating out of copper eventually short-circuited the cell. However the effect only occurred above a threshold of 390 mv at $25^{o}C$, which is approximately equal to or slightly above the normal operating point of the cell. Furthermore, this degradation was found to be reversible (Palz et al, 1968)

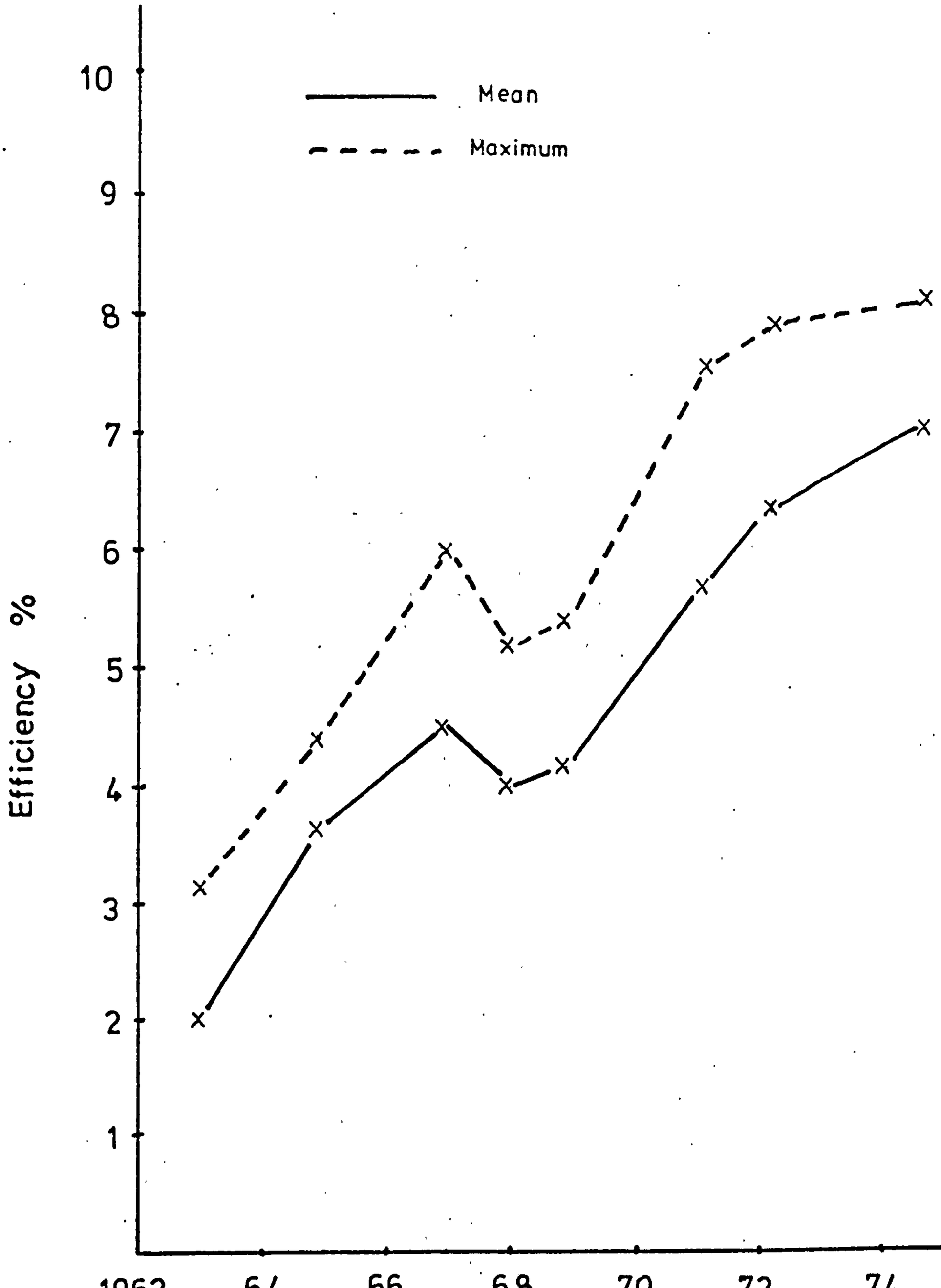

Figure 3.1

Progress In CdS Cell Efficiencies Reported At Conferences And In The Literature

and the output was recovered when the cell potential was lowered below the threshold. However there still remains the problem that when operated in temperatures greater than 60°C as required in sun orientated arrays, the cells degrade significantly when illuminated.

Recently the stability and efficiency of the cells has been improved. Bogus and Mattes, Palz et al, and Mytton et al (1972) working independently identified the problem as being associated with the oxidation of cuprous sulphide. This is a reaction which appears to be accelerated under illumination and which proceeds at an increasing rate with increasing temperature. The preferred way of minimizing the rate of the reaction which occurs when cells are tested in air or poor vacuum is to ensure exact stoichiometry in the Cu_2S layer. Palz reported no degradation at 60°C for such cells tested in vacuum conditions as experienced in space. A bonus which has resulted from ensuring exact stoichiometry of the Cu_2S layer has been a small rise in cell efficiencies. At the present time therefore work on the cell is devoted to methods of measuring and controlling the Cu_2S stoichiometry.

3.2 Other II-VI Photovoltaic devices

Whilst progress was being made with the thin film, CdS-Cu_2S solar cell, other modifications and materials were being investigated. Brockemuehl (1961) and later Bugatti and Muller (1963) developed Reynolds' ideas of a photovoltaic effect at a rectifying junction using aluminium, copper and gold on CdS. They produced devices giving

photovoltages which increased linearly with light intensity. By evaporating CdS on selenium Kunioka and Sakai (1965) formed a photovoltaic cell with a spectral sensitivity close to that of the eye. Photovoltages of up to 0.2 V were obtained by Goryuonva et al (1969) with a thin film of Cu_2S formed on top of $CdSnP_2$ single crystals. Philips (1971) produced a junction between sintered CdS and copper which had an efficiency of 8%. Photovoltaic measurements have also been made on heterojunctions of CdS-SnS (Stoyanov 1971), Cu_2Te-CdTe (Cusano 1963), Cu_2S-CdSe (Otake 1971), and CdS-PbS (Watanabe and Mitra 1972). Recently Bonnet and Rabenhorst (1972) have reported efficiencies of 6% from CdTe-CdS abrupt junctions and are now seeking to make a graded heterojunction from the same materials to improve the cell performance. The CdS-Cu_2S heterojunction however is still thought to offer the best possibilities for commercial applications.

3.3 Suggested mechanisms at the CdS-Cu_2S junction

Many models have been put forward to explain the experimental observations made on CdS solar energy converters. Initially a variety of processes were suggested according to the construction involved. Some of the models suggested are listed below:

(a) Electrons are emitted photoelectrically from the plated copper into n-CdS (Williams and Bube 1960).

(b) Two junctions exist in series, i.e. metal/n^+-CdS CdS/n-CdS (Bockemuehl et al 1961) for cells formed by diffusing copper into high resistivity CdS.

(c) A nCdS/pCdS homojunction is formed with a copper impurity band which gives p-type conduction. (Reynolds and Czyzak 1954, Woods and Champion 1959, Grimmeis and Memming 1962, Fabricus 1962).

(d) A pCu_2Te/n-CdTe heterojunction is produced in which the p layer plays only a minor role in the light absorption and energy conversion (Cusano 1963), (the theory extended to Cu_2S/CdS cells).

(e) A heterojunction in Cu_2Te/CdTe and Cu_2S/CdS cells can be deduced from theoretical calculations (Keating 1965).

(f) A severly localised P.V.E. at interface states between pCu_2S and nCdS, which results in electrons being emitted from these states into the CdS. The long wavelength response of such a cell is due to absorption by impurities in the CdS (Balkanski and Chone 1966).

(g) An impurity P.V.E. at copper centres in CdS (Duc Cuong and Blair 1966) is attributed to the creation of additional minority carriers by electron transitions from the valence band to the impurity levels.

(h) An impurity P.V.E. arises at copper centres in CdS. A surface barrier is also created by a copper contact (Shitaya and Sato 1968).

(i) An impurity P.V.E. occurs in addition to a p^+-Cu_2S/n-CdS heterojunction process. Light absorption occurs in the Cu_2S layer for a Mott-barrier type of cell. This structure also includes an i layer formed after heat treatment (Nakayama 1969).

(j) Impurity P.V.E. (1.8 eV response) and photoemission from the Cu_2S (1.2 eV response) are the dominant processes. (Gill et al 1968).

(k) A p-n heterojunction (Chamberlain and Skarman 1966, Pavelets and Fedorous 1966).

(l) Keating (1963) reported electroluminescence in Cu_2S/CdS which was attributed to hole injection from Cu_2S into CdS.

Further models have been suggested by Potter and Schalla, 1967, (Lewis model), Hill and Keramidas, 1966, (Harshaw model), Shiozawa et al 1966 (Clevite model) and Van Aerschot et al 1968 (E.S.R.O. model). All contain some common features but differ about the details of the variation of the potential energy with distance from the Cu_2S/CdS contact. The Clevite model is commonly agreed to be the most satisfactory, particularly as it has been amended to conform with most of the experimental data.

Any satisfactory model must explain the following observations:

(a) The barrier height is reduced under illumination, as evidenced by a cross over of the dark and illuminated I(v) curves,(Fig. 3.2.)

(b) The enhancement and quenching effects which occur under illumination with light of particular wavelengths, when superimposed on steady 'white' illumination.

(c) The wide spectral response with low energy threshold at 1.2 eV.

(d) The slow response times to certain wavelengths of heat treated cells.

(e) The slow drift of cell characteristics under forward-bias conditions.

(f) The sharp dip in the spectral response of the

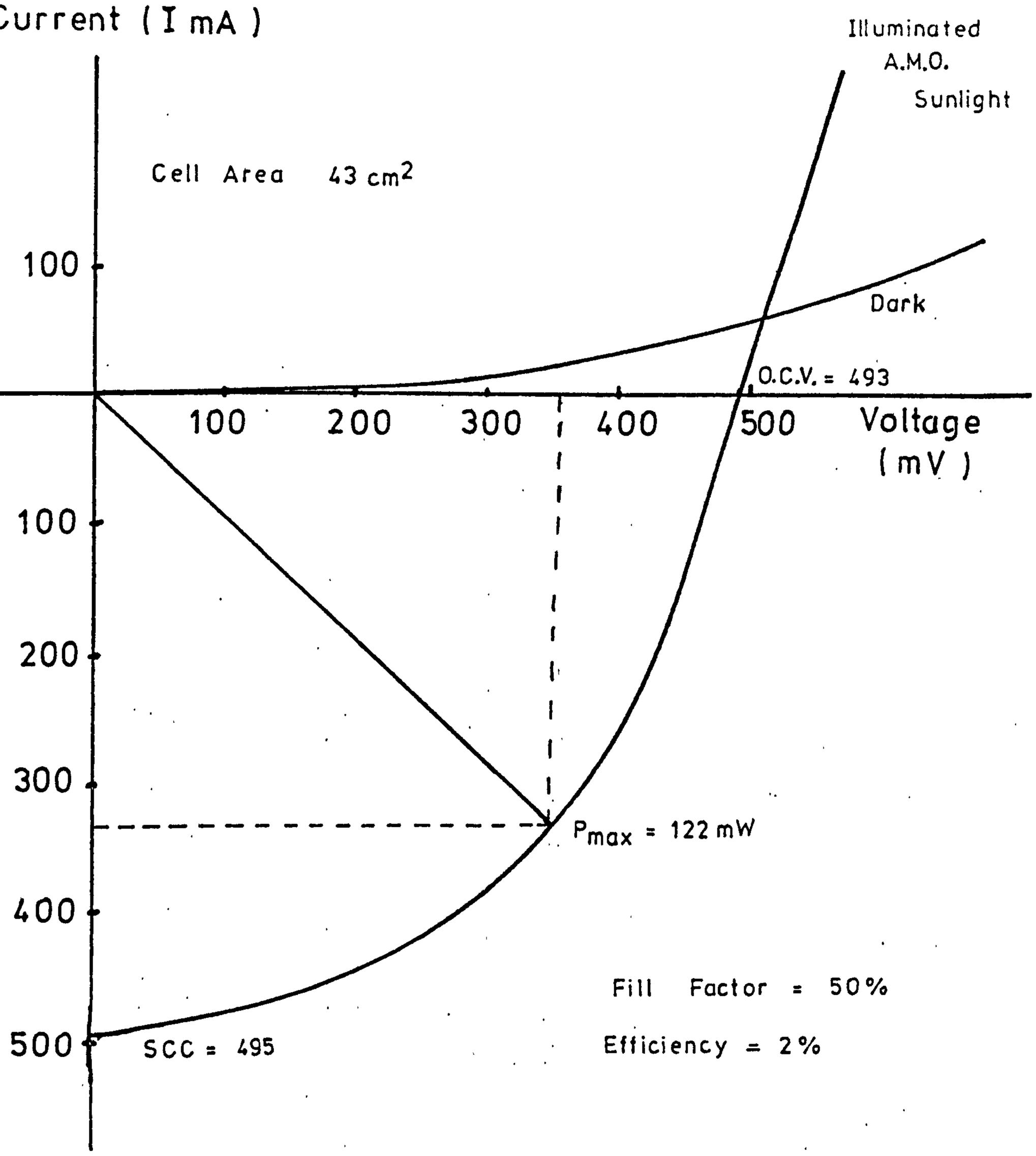

Figure 3.2

I (V) For A Large Area CdS Solar Cell

photocurrent at the band gap of CdS when the Cu_2S layer is thin.

(g) The reduction in junction capacitance on heating.

(h) The improved 'squareness' of the I(v) curves after heating.

(i) The highest observed OCV is 800 mv at 4 K with the equivalent of five suns illumination.

(j) The effects of doping the CdS with donors, e.g. the enhancement spectrum moves to longer wavelengths when indium is introduced.

(k) Radiation resistance, module growth, and effects associated with high Cu^+ mobility.

(l) Degradation after heating for several minutes, which is connected with a composition change in the Cu_2S layer.

3.4 Clevite Model for Solar Cell

The Clevite model suggested by Shiozawa et al can explain most of the features listed above. Figure 3.3 shows the energy band diagram according to their model under illumination and short-circuit conditions. The cell is considered to be a p-i-n heterojunction between p-type Cu_2S, intrinsic CdS and n-type CdS. In the intrinsic region the CdS donors are compensated by copper acceptors diffused in from the Cu_2S during the heat treatments given to the cell in the course of processing. The n-type CdS has a carrier concentration in the range 10^{16} to 10^{18} cm^{-3} which is obtained by controlling the non-stoichiometry during the deposition of the film. Ohmic contact to the nCdS is provided by the ZnAg alloy which forms on the surface of

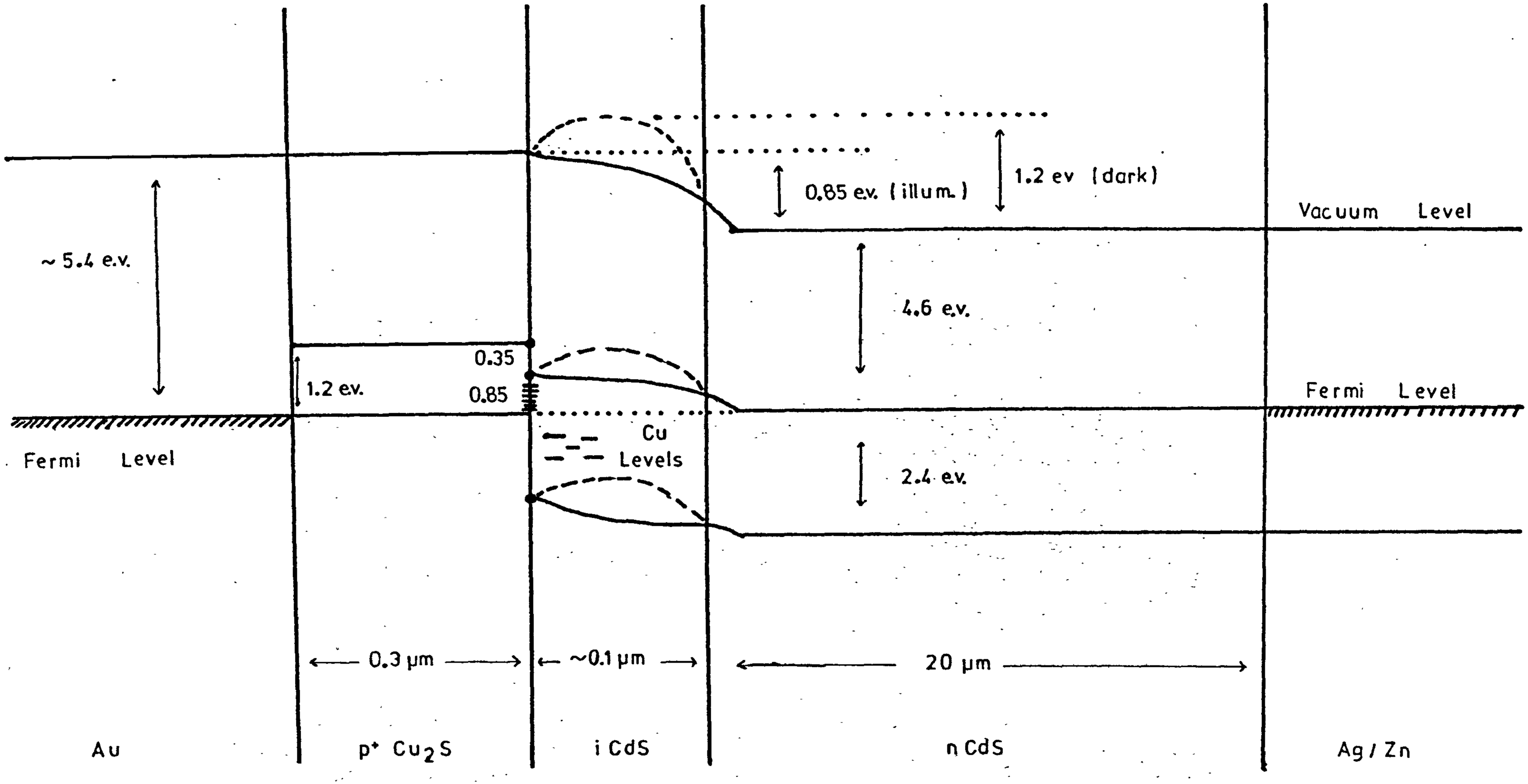

Figure 3.3

'Clevite' CdS Solar Cell Model (Illuminated Short Circuit Conditions)

the metallized substrate. Almost all of the light is absorbed in the p-Cu_2S which has a rough surface and therefore assists absorption by means of multiple reflections. A small proportion of the incident light passes through the Cu_2S to the i-CdS and increases its conductivity by a photoconductive process. Hence the quasi-Fermi level for electrons in the i-CdS moves upward under illumination toward the conduction band giving the band configuration shown in Fig. 3.3. The situation in the dark is shown by the dashed lines. This variation in the height of the barrier with intensity of illumination and the higher series resistance presented by the i-CdS region in the dark, account for the unusual cross over which occurs in the first quadrant of the I(v) characteristics measured under dark and illuminated conditions, (Fig. 3.2). When the cell is illuminated the principal photojunction is at the p-Cu_2S/i-CdS interface with a barrier height of 0.85 eV, and when the cell is in darkness the barrier is at the i-CdS/n-CdS interface with a height of 1.2 eV. There is also a small reverse-biased junction between the p-Cu_2S and i-CdS with a barrier height of 0.35 eV. Hence the CdS acts mainly as an n-type host on which an efficient photovoltaic p-n junction can be formed, and the majority of the absorption and photogeneration of the carriers takes place in the Cu_2S where the band gap of 1.2 eV is close to the optimum band gap of 1.4 eV for efficient solar energy conversion (Loferski 1956).

A slightly different energy band diagram has been suggested by Gill et al (1968). They place the conduction band of CdS 0.1 eV above the bottom of the conduction band

of Cu_2S instead of 0.35 eV below. This would form a narrow energy spike which would permit electrons to tunnel through it. Using this model an electrostatic barrier of 1.2 eV is obtained - far greater than the maximum observed OCV. Whether or not the model is feasible depends on the width of the spike. Gill assumed a value of 10^{17} cm^{-3} for the net donor concentration in the CdS. This is too high for heat-treated cells, but seems reasonable for unheated cells where tunnelling is a likely cause of the unstable and poorly shaped I(v) characteristics.

3.5 CdS layer

The normal operation of the photovoltaic junction is in reverse bias. Consequently the minority carriers (electrons) constitute the photocurrent and the photo-junction aids their motion from the Cu_2S to the CdS. The diffusion potential presents a barrier only for majority carrier motion across it. The current delivered by the cell in reverse bias therefore is

$$I = I_o\,(\exp(eV/AkT)-1) - I_L$$

where I_L = light generated current,

V = potential across junction,

I_o = reverse leakage current,

A = diode factor,

T = operating temperature.

If the shunt and series resistances are taken into account the equivalent circuit is as shown in Fig. 3.4. The series resistance of the cell is governed by the resistance of the various layers of the cell in the direction of

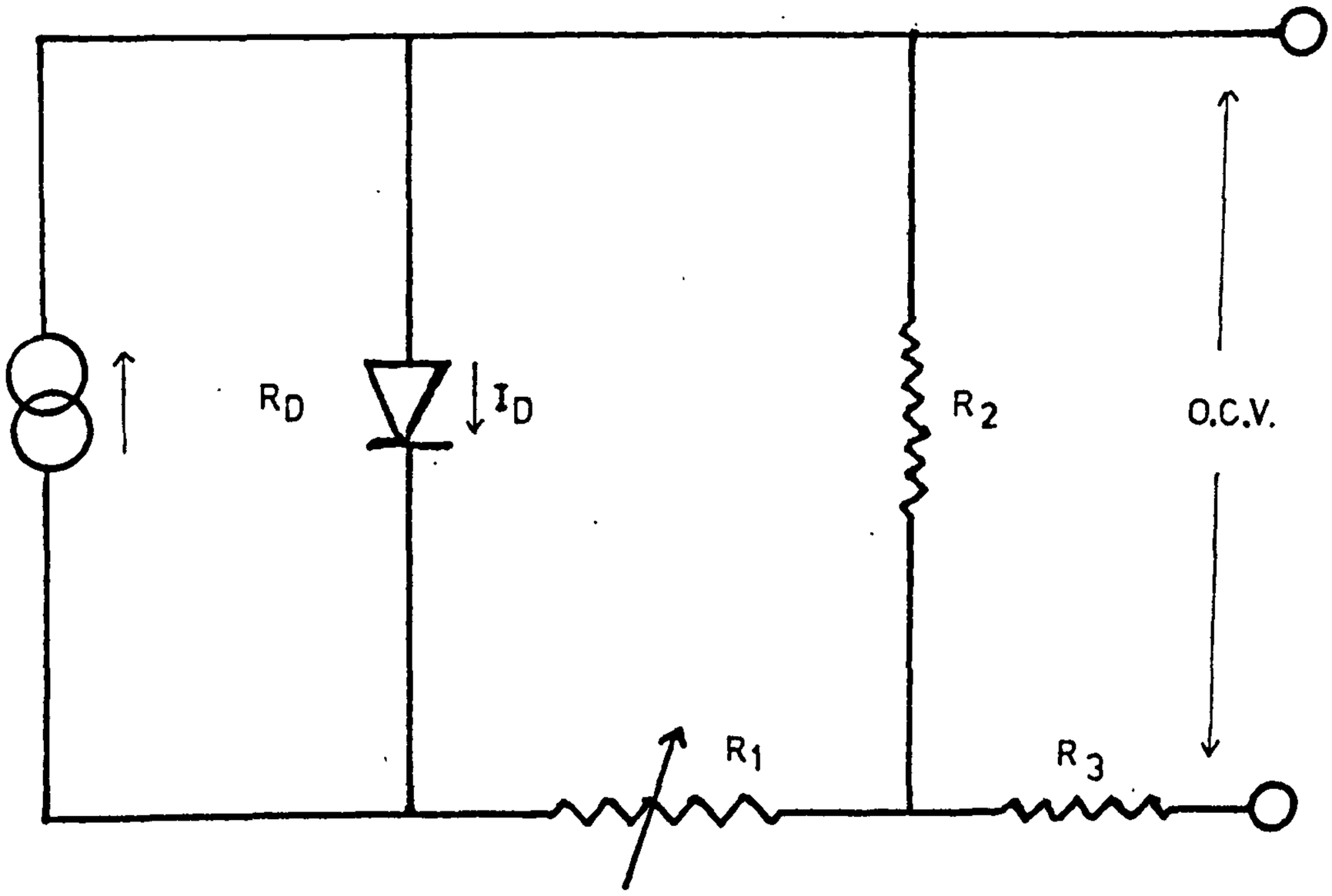

I_D = Recombination Current

R_D = Diode Effective Resistance (Voltage Dependent)

R_1 = i - CdS Resistance

R_2 = Shunt Resistance

R_3 = Lumped Series Resistance

Figure 3.4

CdS Solar Cell Equivalent Circuit

current flow. The series resistance of the i-CdS and n-CdS layers can be kept to negligible proportions by reducing the resistivity of the basic n-type CdS layer to values less than 100 Ωcm. The series resistance of the Cu_2S contact is kept to around 50 $m\Omega/cm^2$ by using a grid which allows 90-95% optical transmission. The ohmic contact to the CdS is made as thick as weight considerations allow. The shunt resistance of the cell is determined by the thickness of the CdS layer because Cu_2S is plated down grain boundaries during the plating process and will therefore reach the substrate more readily in thinner films. At present a thickness of 20 μm is required to ensure that the shunt resistance remains greater than 100Ω for a 50 cm^2 cell. Shunt resistances of less than 100Ω lead to a reduction in fill factor and efficiency. However since the density of CdS is high (4.8 grm/cc), the layer should not be too thick otherwise the weight of the cell will be unnecessarily increased.

The structure of the film is also important. Films with crystallites ranging from 1-3 μm in diameter are required. The crystals should be elongated to the full thickness of the film and highly orientated with the c-axis perpendicular to the substrate. When such films are etched in HCl some of the surface is removed and its uneveness is exaggerated by preferential etching down the grain boundaries. When the films are then dipped in the cuprous ion solution to form a thin layer of Cu_2S on the surface, the Cu_2S partially penetrates the grain boundaries thus providing a larger surface area at which the incident radiation may be absorbed. This feature is essential if

high conversion efficiencies are to be obtained.

3.6 The copper sulphide layer

A copper sulphide layer approximately 0.3μ thick is formed by immersing the CdS film in a hot bath (90°C) of cuprous ions buffered at a pH of 2.5. Although the solution is stabilized by the addition of a reducing agent, it is still possible that cupric ions may exist in the solution resulting in the possibility of forming Cu_xS where $1<x<2$. Generally x is very close to 2, but the Cu_xS phase diagram is so complex that very small changes in x can result in large changes in the properties of the resultant layers. Electrochemical studies by Rickert and Matthieu (1969) have shown that by controlling the potential of the Cu_xS as it is being formed, it is possible to prevent anything but stoichiometric Cu_2S being formed in the plating bath.

The importance of achieving strict stoichiometry in the Cu_2S layer is evidenced by the dependence of both the SCC and OCV on the composition of the Cu_xS (Palz et al, 1972). Similar results have also been obtained by Te Velde (1970), with Cu_xS layers grown topotaxially on CdS single crystals. The higher the SCC and OCV the higher the maximum power, Pm, provided the fill factor ($^{Pm}/_{SCC.OCV}$) is not adversely affected by an improvement in Cu_2S stoichiometry. (There is a possibility this might happen because the sheet resistance of stoichiometric Cu_2S is higher and hence the series resistance of the cell is increased). A major advantage however is that the stability of the cell increases as $x \rightarrow 2$, for two reasons:

(1) The critical potential at which copper will plate out of Cu_xS increases as $x \longrightarrow 2$. In fact the rate of deposition of copper is proportional to δ in the formula $Cu_{2-\delta}S$ (Mytton, 1972). Thus more stoichiometric Cu_2S leads to a higher critical potential and a slower rate of degradation when the cell is operated above that potential.

(2) It has already been mentioned that degradation under illumination is also accelerated at 60°C and above by the oxidation of Cu_2S. Bogus and Mathes (1972) and Palz (1972) showed that this effect was smaller in more stoichiometric Cu_2S layers.

A stoichiometric Cu_2S layer is therefore essential if a reasonable efficient cell (η>6%) with an acceptable lifetime (five years or more) is to be produced.

References

Balkanski and Chone (1966), Rev. de Phys. App. 1 179

Bogus and Mattes (1972), Proc. 9th P.V. Spec. Conf. Maryland, U.S.A.

Bonnet and Rabenhorst (1972), Proc. 9th P.V. Spec. Conf. Maryland, U.S.A.

Bowman et al (1967), A.I.A.A.J. 6 378

Brockemuehl et al (1961), J.A.P. 32 1324

Bujatti and Muller (1965), J. Electrochem. Soc. 112 702

Chamberlain and Skarman (1966), J. Electrochem. Soc. 113 86

Chamberlain and Skarman (1966), Solid State Elec. 9 819

Cusano (1963), Solid State Elec. 6 217

Duc Cuong and Blair (1966), J.A.P. 37 1660

Fabricus (1962), J.A.P. 33 1597

Gill et al (1968), Proc. 7th P.V. Spec. Conf. California, U.S.A.

Goryuonva et al (1969), Phys. Stat. Sol. (a) 2 K117

Grimmeis and Memming (1962), (a) J.A.P. 33 2217

Grimmeis and Memming (1962) (b) J.A.P. 33 2596

Hietanen and Shirland (1967), Proc. 6th P.V. Spec. Conf. Florida, U.S.A.

Keating (1965), J.A.P. 36 564

Kunioko and Sakai (1965), Solid State Elec. 8 961

Loferski (1956), J.A.P. 27 777

McMahan (1967), Proc. 6th P.V. Spec. Conf. Florida, U.S.A.

Mytton (1972), Private Communication

Mytton et al (1972), Proc. 9th P.V. Spec. Conf. Maryland, U.S.A.

Nadjakov et al (1954), Izu. Bulg. Akad. Nank. 4 4

Nakayama et al (1969), Japan J.A.P. 8 450

Otake et al (1971), OYO Buturi 40 1224

Palz et al (1968), Proc. 8th P.V. Spec. Conf. Seattle, U.S.A.

Palz et al (1972), Proc. 9th P.V. Spec. Conf. Maryland, U.S.A.

Pavelets and Fedorous (1966), Ukraryinsk, Fiz. Zhuranal 11 686

Philips et al (1969), Electron Comp. January 1971

Potter and Schalla (1967), N.A.S.A. T.N.D. - 3849

Reynolds (1954), Phys. Rev. 96 533

Reynolds and Czyzak (1954), Phys. Rev. 96 1705

Rickert and Matthieu (1969), E.S.R.O. CR-14

Shiozawa et al (1966), Contract A.F. 33(615)-5224 2nd QPR

Shiozawa et al (1969), Aerospace Res. Labs. AR2 69-0155

Shirland et al (1962), A.S.D. Tech. Doc. Rep. 62

Shirland (1966), Adv. En. Conv. 6 201

Shitaya and Sato (1968), Japan J.A.P. 7 1348

Spakowski (1967), Proc. 6th P.V. Spec. Conf. Florida, U.S.A.

Stoyanov et al (1971), Acad. Sc. Bulg. 94 1469

Te Velde (1968), Proc. 8th P.V. Spec. Conf. Seattle, U.S.A.

Van Aerschot et al (1968), Proc. 7th P.V. Spec. Conf. California, U.S.A.

Watanabe and Mitra (1972), Solid St. Elec. 15 5

Williams and Bube (1960), J.A.P. 31 968

Woods and Champion (1959), J. Elec. Control. 7 243

CHAPTER 4

CdS THIN FILMS

Thin films of II-VI compounds have provoked much interest recently particularly because of the demand for smaller and lighter devices. Although films of compounds such as ZnS have been studied for many years in the past, the requirements of high crystallinity have not been too important in most applications. Modern developments however have led to an increasing interest in the crystalline character of thin films and the requirement that their physical properties should approximate as closely as possible to those of the bulk material.

In addition to photovoltaic heterojunctions CdS thin films have been used as (1) ultrasonic transducers (Curtis 1969), (2) photoresistors, (3) phosphors, (4) electro-luminescent layers (Andrews and Haden 1969), (5) evaporated triodes and diodes (Dresner and Shallcross 1962), (6) heterojunction diodes (Aven and Cook 1961) and (7) insulated gate T.F.T's (Haering 1964).

In this section some of the methods used to fabricate thin films of II-VI compounds are reviewed with special reference to CdS.

4.1 The Preparation of CdS Thin Films

The method employed to grow a thin film can have a very strong influence on its final properties and consequently films suitable for different devices are often grown by completely different methods. A crude technique may be adequate if polycrystalline films are required, but

it is necessary to resort to more elaborate technology for the production of single crystal films. Reviews of the various methods in common use are given in the books by Anderson (1966) and Chopra (1969). Some of the methods reported for the successful production of CdS thin films are described below.

(a) Sintered layers of CdS powder were prepared by Micheletti and Mark (1968). They doped the layers with chlorine and sometimes copper in an attempt to increase the photosensitivity of their films. By painting a slurry of CdS and $CdCl_2$ on to a ceramic substrate Chockalingham et al (1970) produced photoconductive cells with a spectral response extending from 0.63 to 1.12 μm. Nakayama (1968) fabricated solar cells based on ceramic plates. Such cells were between 6% and 9% efficient. This method provides cheap but heavy devices.

(b) Micheletti and Mark (1967) formed CdS layers 3000-5000Å thick using a chemical spray technique. Cadmium chloride and thiourea in aqueous solution was sprayed on to a heated ceramic substrate. Further heating brought about the chemical decomposition of $CdCl_2$ and a polycrystalline film of CdS was formed, the other components escaped as vapour. Imaoka (1972) concluded that the orientation and Hall mobility of such layers depended on the actual chemicals used. Carrier mobilities for these films of a few thousandths $cm^2V^{-1}sec^{-1}$ were calculated by Wu et al (1972) from thermo-electric power measurements.

A chemical spray technique was also used by Chamberlin and Skarman (1966) to form a CdS/Cu_2S photovoltaic junction which produced an OCV of 1.04 volts and an SCC of

$2mA/cm^2$ when illuminated with 100 mW/cm^2 of visible radiation. Laurance (1959) also used a spray technique for fabricating photoconductive cells, decomposing the $CdCl_2$ in the presence of H_2S. Marchenko et al (1970) formed solar cells on films prepared in this way. Unfortunately all these methods present large problems of film contamination.

(c) Vapour phase reaction is a technique used for single-crystal growth which has been successfully adapted to the growth of thin films. The vapours of the constituent elements of the compound are allowed to react and form a film on a heated substrate. Films of CdS 1-2μm thick have been formed by Ratcheva et al (1972) using this method. Heyraud and Coquella (1968) produced films 15-25μm thick in the same way on substrates such as NaCl, KBr, KCl, CaF_2 and muscovite. They reported that the optical and photoelectric properties of such films were comparable to those of the bulk material. The method produces high quality films but is not practical for depositions on large amorphous substrates.

(d) Thick film technology based on 'silk-screened' layers is mainly concerned with the deposition of conductors and insulators. Witt et al (1966) have used silk-screened CdS layers in insulated gate thin film transistors (TFT's). The main problem with this technology is that the composition of the existing conductor inks is an industrial secret and the problems of the conduction mechanism in glassy solids have not been solved.

(e) Vacuum evaporation is an established technique

for the production of both thick and thin films. The major consideration in such methods is the choice of an optimum method of supplying energy to the source such that the vapour beam produced condenses on the substrate to form the film.

Sputtering methods utilize several different electrode and source arrangements. In sputtering the target surface i.e. the cathode, is bombarded by energetic particles which leads to the ejection of surface atoms. The ejected atoms can then be condensed in a similar way to evaporated ones. Litchensteiger (1969) reported p type conduction of CdS films sputtered in the presence of phosphine. Reactive sputtering of Cd in H_2S (Durand 1971) has been used to produce photoconducting layers and Honda et al (1971) have formed stoichiometric layers with excellent photoconductive properties by R.F. sputtering. However the process is difficult to control and the high electric fields present can affect the structure of the film.

Thermal evaporation of either CdS or a mixture of CdS and an excess of one component has been the most popular technique of thin film production. , (Nelson 1955, Wendland 1962 and Bleha 1969). Bujatti (1968) used a modified vacuum furnace to grow CdS thin films and, by controlling the temperature gradient at the substrate, obtained well orientated films of high resistivity. A close spaced sublimation technique where a single crystal or polycrystalline slice of starting material was sublimed from a position parallel and close to the substrate (sapphire) was described by Tyagi (1971). According to Tyagi the close juxtaposition of the source and substrate mean that

only a small temperature difference exists between them and therefore the evaporation proceeds under equilibrium conditions giving stoichiometric films with a large grain size. This method has the advantages that (1) it is economical (the material is only deposited where it is needed), (2) at a given temperature it produces a higher deposition rate than any other method and (3) it is possible to do a series of depositions on different substrates during one 'pump-down.' Such a method lends itself to the production of integrated circuits but cannot be used to form films on large amorphous substrates.

Co-evaporation of CdS and S was used by Pizzarello (1964) and Suzanne and Malé (1970) to ensure that stoichiometric proportions of the constituent elements arrived at the substrate. This seems a complex way of controlling the film properties. It is simpler to control the stoichiometry of the films by varying the evaporation rate of the CdS and the substrate temperature. (Dresner and Shallcross 1962, Sakai and Okimura 1964).

In order to reduce the number of controllable parameters in a CdS evaporation, it is necessary to evaporate the compound by supplying energy in some way for example in the form of a laser beam, an R.F.field, an electron beam or by thermal radiation or conduction from a resistively heated filament. Most workers in common with ourselves have used resistively heated or electron beam heated sources in vacua of about 10^{-6} torr. To ensure a low impurity content a U.H.V. environment of less then 10^{-8} torr is essential. This is impractical commercially owing to

expense and the long duty cycle of U.H.V. rigs. It would be of greater commercial use if reproducible devices could be fabricated in a high vacuum of about 10^{-6} torr.

4.2 The Properties of CdS Films

In the early work which was reported in the late 1950's the importance of controlling the magnitude of the various parameters when preparing a CdS thin film was not fully appreciated. The source material was often of dubious quality and post-deposition treatments were necessary to produce reasonable photoconductive properties. This resulted in the publication of many conflicting reports (Nelson 1955).

Veith (1950), Aitchson (1951) and Bramley (1955) who worked on photoconductive layers demonstrated the importance of controlling the pressure in the evaporation system, the substrate temperature and the purity of the charge. More recently it has been shown that the evaporation rate, the temperature of the source, the thickness of the deposited film, the nature of the substrate and the composition of the residual gas in the vacuum are all important parameters in determining the properties of a film. (Shalimova et al 1964, Thomas et al 1970, South 1971, Kamoshita 1972). Post-evaporation treatments of the film may override the importance of some of these by changing the structure of a film.

When films of CdS are deposited normally on to a heated substrate they have a hexagonal wurtzite structure with a fibre axis orientation. The films are polycrystalline with the individual c-axes aligned approximately

perpendicular to the substrate surface. (Shallcross 1967, Beringer and Corrsin 1963). With films deposited with the beam incident obliquely on the substrate the c-axes of the crystallites tend to align themselves parallel to the vapour beam (Forster 1967). This effect can be enhanced by increasing the deposition rate (Fukurushi and Niizeki 1969) and is of vital importance when CdS films are used as ultrasonic transducers. Both the substrate temperature and the thickness of the film influence the crystallite size, but for a film 20μ thick the crystallites may be several microns across (Berger et al 1968).

The substrate temperature also has a great influence on the structure of the film. At temperatures lower than 150°C a cubic sphalerite modification predominates. Films evaporated on to a substrate at room temperature contain so much excess cadmium that they are black in colour. As the substrate temperature increases above 150°C the films become orange, changing to yellow above 200°C where the structure is then hexagonal wurtzite. (Bujatti 1967, 1968, Galkin et al 1968). At temperatures above 400°C the substrate is hot enough for considerable re-evaporation to occur and it becomes increasingly difficult to form a deposit (Wendland 1962).

Using a freshly cleaved single crystal substrate and the correct evaporation conditions it is possible to grow epitaxial layers of either cubic or hexagonal CdS (Escofferey1964, Holloway and Wilkes 1968, Wilcox and Holt 1969). Chopra and Kahn (1962) were able to produce

differently orientated cubic and hexagonal films on different polished and cleaved faces of NaCl by controlling the evaporation rate and substrate temperature. The cleaner the system the less stringent are the epitaxial limits and the lower the defect content of the films. (Holt and Wilcox 1971).

The dark resistivity of the films changes with evaporating conditions. Although there are many conflicting reports it is generally agreed that the resistivity increases with increasing substrate temperature but decreases as the evaporation rate is increased. Variations in the dark resistivity with film thickness have also been reported by Bleha (1968), Wilson and Woods (1973) and Buckley and Woods (1973). The photosensitivity changes as expected increasing with the dark resistivity.

The electron Hall mobility (μ_H) is also affected by the evaporation conditions and crystallite size; being lower in polycrystalline films than in single crystal ones. A typical value of 10 $cm^2\ V^{-1}\ sec^{-1}$ (Mankarious 1964) can be explained in terms of the Petritz model (1956) for polycrystalline films of PbS, PbSe, PbTe. The model assumes that the carriers are scattered and trapped by intercrystalline boundaries and this therefore leads to an exponential dependence of μ_H on temperature and barrier height.

$$\mu_H = \mu_o \exp -(E/kT) \qquad \text{(Berger 1961)}$$

Unfortunately ionized impurity scattering leads to a dependence on μ as $T^{3/2}$ and the two mechanisms are difficult to distinguish experimentally (Shallcross 1967). Most workers however favour the Petritz model e.g. Neugebauer (1968)

and the existence of intercrystalline boundaries is supported by the measurements of Waxman et al (1965) on drift mobilities in CdS films.

Photoluminescence has been observed in CdS thin films by Bleha and Peacock (1970).

The photosensitivity and carrier mobility in CdS films have been increased by a post-evaporation bake in one of a variety of ambients viz. air, vacuum, H_2S, Ar (Berger et al 1964, Sakai and Okimura 1964, Esbitt 1965). Both increases and decreases in the dark resistivity of films treated in this way have been reported depending on the substrate temperature during the initial preparation (Wendland 1962). The effects can be explained as a result of (i) substantial recrystallization or (ii) a reaction between the CdS and O_2, as it is known oxygen is an active element which promotes changes in the photosensitivity of CdS (Kuwabara 1954).

Many workers have investigated the recrystallization of CdS films, which can be brought about by heating a film in contact with a thin metal layer. By evaporating a layer of silver on CdS and then annealing in an inert atmosphere at 500^{o}-600^{o}C, Addis (1963) increased the Hall mobility in his films from 1 to between 20 and 70 $cm^2\ V^{-1}\ sec^{-1}$. (c/f bulk value of 250). More recently similar experiments have been carried out by Kahle and Berger (1970).

A general review of the activation and recrystallization of II-VI compound layers is given by Vecht (1966).

4.3 Conclusion

In the preparation of thin films of CdS cleanliness

of the system and source material is very important. By controlling the evaporation parameters it is possible to produce films with a wide range of structures and properties. The following chapter gives a description of the apparatus used to prepare the thin films used in the present work.

References

Addis (1963) Trans. 10th Nat. Vac. Sump. P.354

Aitchson (1951) Nature 167 812

Anderson (1966) Use of Thin Films in Physical Investigations (Academic Press)

Andrews and Haden (1969) Proc. I.E.E.E. 57 99

Aven and Cook (1961) J.A.P. 32 360

Behringer and Corrsin (1963) J. Electrochem. Soc. 110 1083

Berger (1961) Phys. Stat. Sol. 1 739

Berger et al (1964) Phys. Stat. Sol. 7 679

Berger et al (1968) Phys. Stat. Sol. 28 K97

Bleha et al (1969) J. Vac. Sci. Tech. 7 135

Bleha and Peacock (1970) J.A.P. 41 4992

Bramley (1955) Phys. Rev. 98 246

Buckley and Woods (1973) J. Phys. D. 6 1084

Bujatti (1967) Phys. Lett. 24A 36

Bujatti (1968) J. Phys. D. 1 983

Chamberlin and Skarman (1966) J. Electrochem. Soc. 113 86

Chamberlin and Skarman (1966) Sol. St. Elec. 9 819

Chockalingham et al (1970) Indian J. Pure and Appl. Phys. Sept. 744

Chopra (1969) Thin film phenomena (McGraw-Hill)

Chopra and Kahn (1967) Surface Science 6 33

Curtis (1969) J.A.P. 40 433

Dresner and Shallcross (1962) Sol. St. Elec. 5 205

Dresner and Shallcross (1963) J.A.P. 34 2390

Durand et al (1971) Thin Solid Films 11 237

Esbitt (1965) Phys. Stat. Sol. 12 K35

Escofferey (1964) J.A.P. 35 2273

Forster (1967) J.A.P. 38 149

Fukurùshi and Niizeki (1969) Japan JAP 10 1274

Galkin et al (1968) Sov. Phys. Crystallog. 12 766

Haering (1964) Sol. St. Elec. 7 31

Heyraud and Coquella (1968) J. Cry. Growth 2 405

Holloway and Wilkes (1968) J.A.P. 39 5807

Holt and Wilcox (1971) J. Cry. Growth 9 193

Honda et al (1971) Fujitsu Sci. and Tech. J. March 161

Imaoka et al (1972) Oyo Buturi 40 729

Kahle and Berger (1970) Phys. Stat. Sol. (a) 2 717

Kamoshita (1972) J. Vac. Soc. Japan 15 205

Kuwabara (1954) J. Phys. Soc. Japan 9 97

Laurance (1959) Brit. J.A.P. 10 298

Lichtensteiger et al (1969) Appl. Phys. Lett. 15 418

Mankarious (1964) Sol. St. Elec. 7 702

Marchenko et al (1970) Ukr. Fiz. Zh. 15 295

Micheletti and Mark (1967) App. Phys. Lett. 10 136

Micheletti and Mark (1968) J.A.P. 39 5774

Nakayama (1968) Japan J.A.P. 8 450

Nelson (1955) J. Opt. Soc. America 45 774

Neugebauer (1968) J.A.P. 39 3177

Petritz (1956) Phys. Rev. 104 1508

Pizzarello (1964) J.A.P. 35 2730

Ratcheva et al (1972) Phys. Stat. Sol. (a) 10 209

Sakai and Okimura (1964) Japan J.A.P. 3 144

Shalimova et al (1964) Sov. Phys. Crystallog. 8 618

Shallcross (1967) R.C.A. Revue 28 569

South (1971) Ph.D. Thesis. Univ. of Wales (Bangor)

Suzanne and Malé (1970) Thin Solid films 5 379

Thomas et al (1970) Rev. Phys. App. 5 683

Tyagi (1971) Proc. Symp. on Electronics, Madras, India 1971

Vecht (1966) Physics of Thin Films 3 196

Veith (1950) Comptes Rend. Acad. Sci. 230 947

Waxman (1965) J.A.P. 36 168

Wendland (1962) J. Opt. Soc. America 52 581

Wilcox and Holt (1969) J. Mat. Sci. 4 672

Wilson and Woods (1973) J. Phys. Chem. Sol. 34 171

Witt et al (1966) Proc. I.E.E.E. 54 897

Wu et al (1972) J.A.P. 43 756

CHAPTER 5

THE PREPARATION OF CdS THIN FILMS

5.1 Vacuum Systems

Figure 5.1 is a schematic diagram showing the valves and pumps on the vacuum system used with an electron gun to produce some of the films to be discussed. Two gauges were used to measure pressure, an Edwards Series 70 Pirani II gauge for pressures between 3 and 10^{-3} torr and an Edwards IG5 ionization gauge for pressures below 10^{-3} torr. The lowest pressure obtainable using Silicone 705 pump fluid in the diffusion pump and liquid N_2 in the cold trap was 10^{-6} torr. Most of the evaporations were carried out at pressures below 10^{-5} torr.

A smaller system using A.E.I. components and built round a 3" diffusion pump was used to evaporate films from a resistively heated source.

A third system made by C.V.C. with an 18" bell jar was used at I.R.D. This system incorporated an oil diffusion pump and a cold trap and an automatic switching facility for the valves. Pressures of 10^{-7} torr were obtained within 30 minutes of the system starting. A Sloan deposit control meter (OMNI II) was installed to monitor the film thickness and deposition rate. A complete evaporation cycle could be controlled with the oscillating quartz crystal detector and relays.

5.2 Vacuum Chamber Fixtures

5.2.1 The System with a Resistively Heated Source

Figure 5.2 shows the arrangement of fittings in the

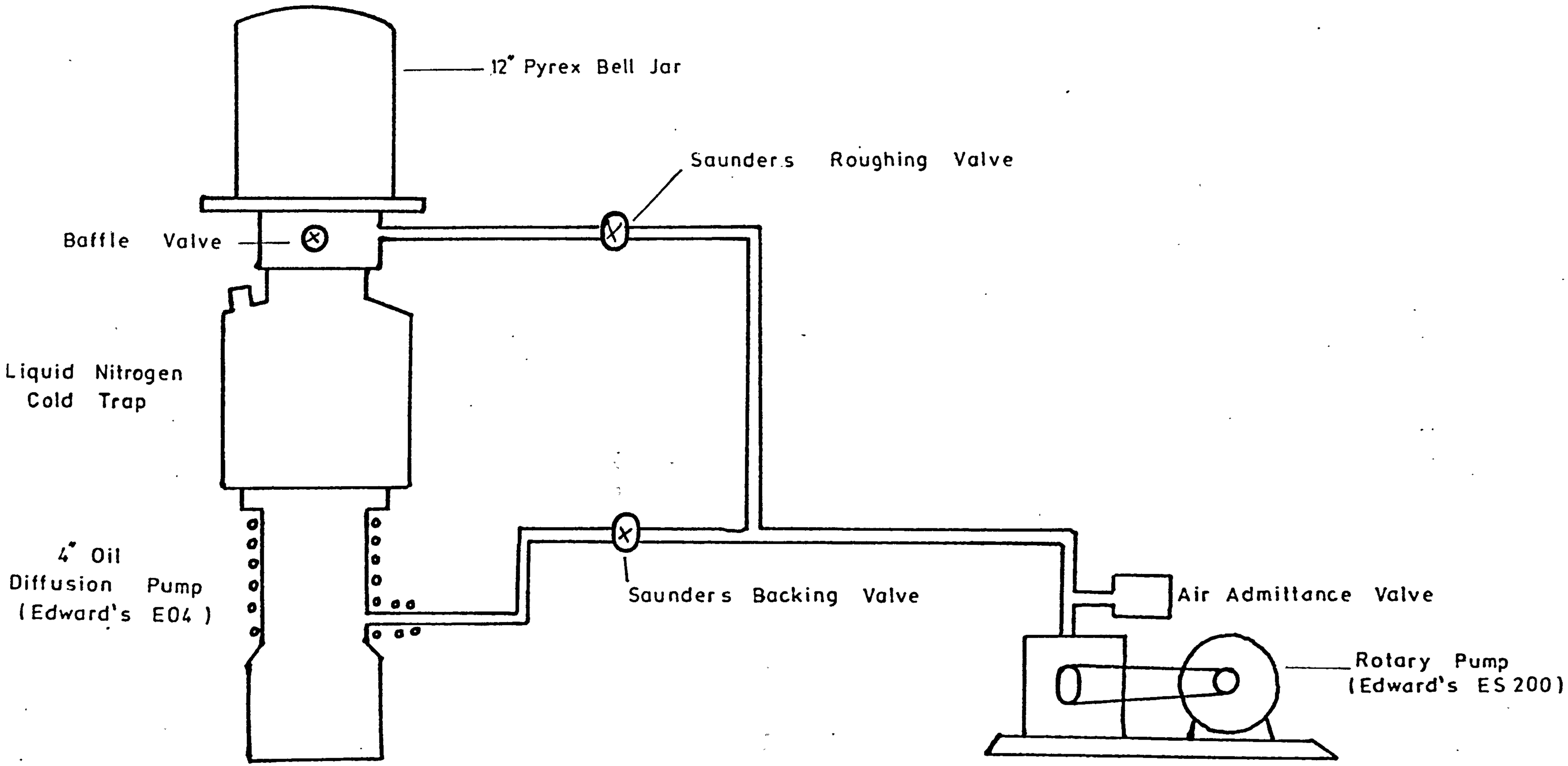

Figure 5.1

Schematic Diagram Of Pumps And Valves Of 12" Evaporator

Scale Approx. 1:3

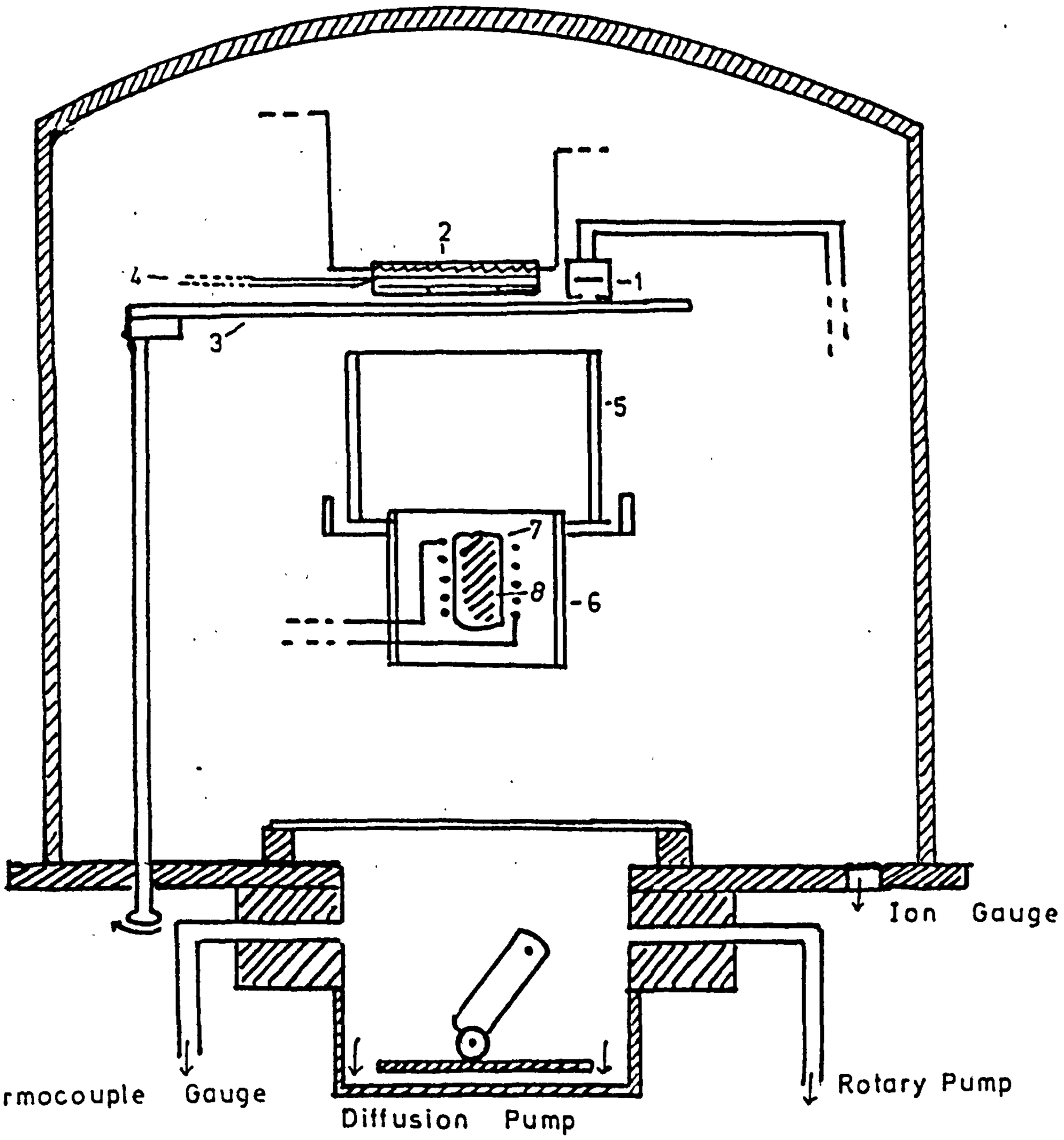

1. Deposit Thickness Monitor
2. Substrate Heater, Substate, and Copper Mask
3. Shutter
4. Thermocouple
5. Silica Cylinder
6. Mo Radiation Shield
7. Silica Crucible and Molydenum Heater
8. Charge and Quartz Wool Baffle

Figure 5.2

Bell Jar Fixtures - Resistively Heated System

bell jar for the resistively heated source pumped by the 3" oil diffusion pump. A silica crucible wound with molybdenum wire was used. This heating element was matched to a L.T. transformer enabling 30A at 30V to be drawn if required. A quartz wool baffle was mounted in the mouth of the crucible to prevent the spattering of CdS at high evaporation rates. A deposition rate of several thousand angstroms per minute was easily obtained.

The substrate and mask were clamped to a stainless steel block containing an insulated tungsten heating element. The temperature of the substrate was controlled by an Ether "mini controller" with a NiCr/NiAl thermocouple in contact with the substrate surface. Two substrates could be mounted on the block at one time enabling films to be evaporated consecutively. The volume between the source and the substrate was surrounded by a 9 cm diameter silica cylinder which was heated by radiation from the source. This was done in an attempt to retain both components of the vapour within the vicinity of the substrate and to increase the stoichiometry of the resultant films by preventing the preferential condensation of one of the elements on the cold walls of the bell jar. This "hot-wall" was found to be essential for reproducible results.

The quartz crystal of a Genevac (D.T.M.1) deposit thickness monitor was placed close to the substrate. The instrument was calibrated against the optical measurement of film thickness made after evaporation. This monitor enabled the growth rate of the film to be measured 'in-situ' so that the evaporation could be stopped when the required thickness had been deposited. A stainless steel shutter

operated through a rotary seal was situated immediately below the substrate and D.T.M. crystal. Either the crystal alone or the crystal and either one of the substrates could be exposed to the CdS vapour. Thus the substrates could be masked until outgassing had been completed and a steady evaporation rate attained. The substrates could then be exposed to the CdS vapour either simultaneously or consecutively.

5.2.2 The Electron Gun System

Figure 5.3 shows the lay-out of the components in the bell jar of the 4" pump system. The masks and substrates were mounted in a recess in a stainless steel disc 25 cm in diameter and 8 mm thick which was placed 10 cm above the electron gun. The substrate was heated by a 750 watt tungsten-halogen lamp. The temperature of the substrate was controlled by a Eurotherm "Phase Angle" controller and a NiCr/NiAl thermocouple in contact with the substrate. The Eurotherm was fitted with a current limit facility to prevent current surges during the initial switching due to the low "cold" resistance of the lamp. A stainless steel shutter which could be operated magnetically was placed immediately below the substrate.

A diagram of the Genevac E.B.U.1 electron beam evaporator is shown in Fig. 5.4. The molybdenum filament was optically screened from both source and substrate by a negatively biased focussing cage and washer. The electrons were focussed on to the surface of the evaporant which was contained in one of the four crucibles in the water cooled hearth. Each crucible could be positioned below the emitter

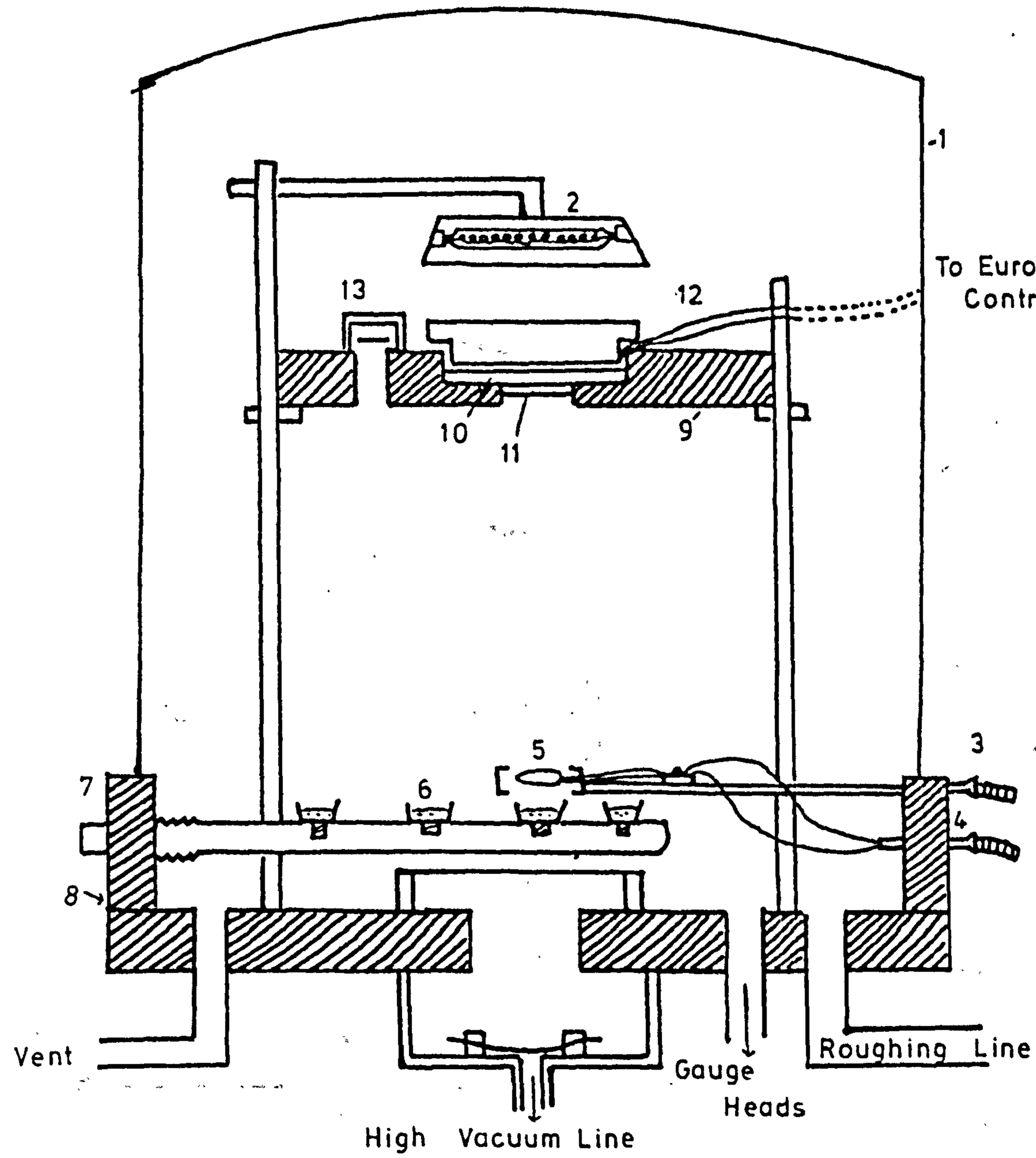

1. 12" Pyrex Bell Jar
2. W-I Lamp (substrate heater)
3. E.H.T. Leadthrough
4. Filament Leadthrough
5. Filament
6. Molybdenum Crucibles
7. Stainless Steel Collar
8. Viton 'O' Ring
9. Stainless Steel Substrate Holder
10. Substrate
11. Aluminium Mask
12. Thermocouple
13. Quartz Crystal Thickness Monitor

Figure 5.3

Bell Jar Fixtures — Electron Gun System

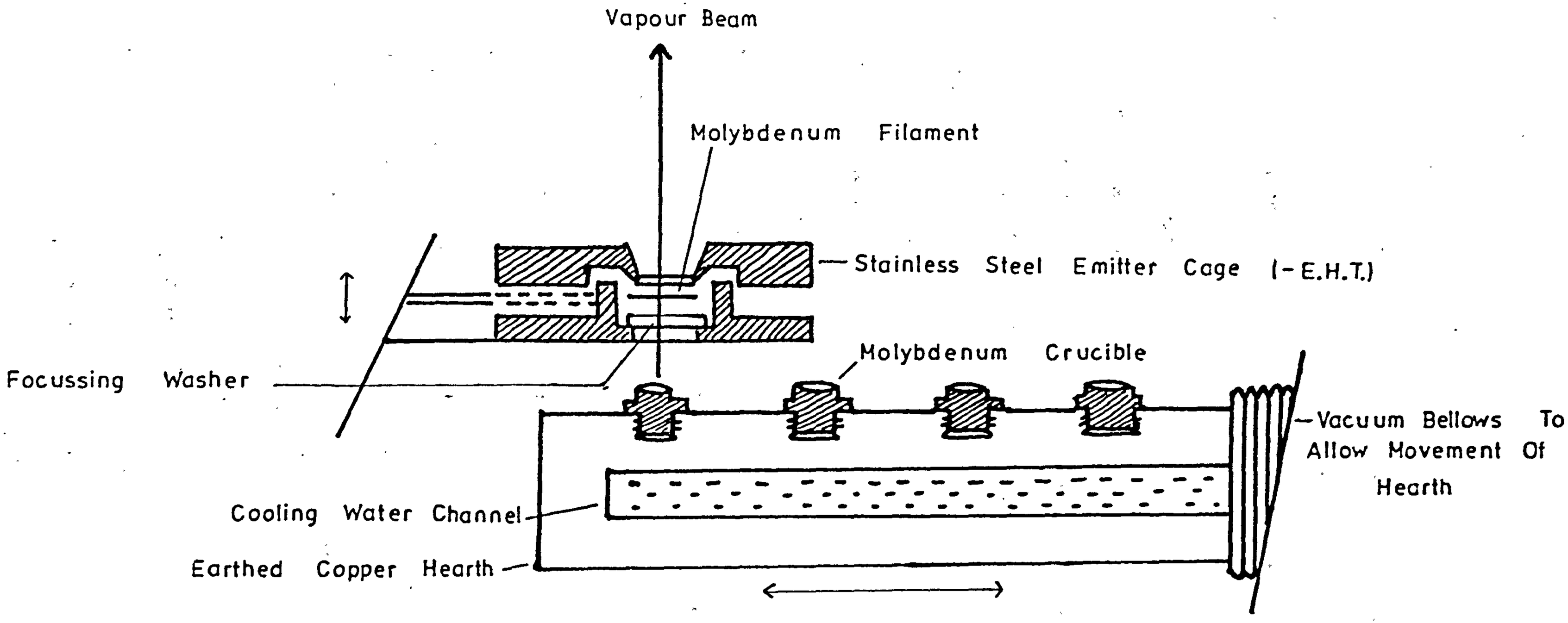

Figure 5.4

Genevac E B U 1 Electron Beam Evaporator

by moving the bellows seal through a stainless steel collar between the bell jar and baseplate.

A 10 kV, 20A at 7V variable power supply was constructed in the department to provide both the filament power and accelerating potential (Martin 1970). The supply incorporated safety interlocks to protect both the equipment and the operator. A stabilized maximum beam power of 150mA 10kV was available. Both the current and EHT were independently variable between these limits.

The combination of the electron gun and the "totally enclosed" substrate heater meant there were fewer sources of contamination in this system than in the resistively heated one.

5.2.3 I.R.D. System

The I.R.D. Co. system used a source as shown in Fig. 5.5 in an 18" bell-jar. This was a directly heated tantalum crucible containing 40 grms of powdered CdS when full. Evaporation rates greater than 1μm a minute were attained and it was possible for layers of CdS 20μm thick to be grown on substrates 8 cm square. A 'hotwall' was used with the source and substrate 36 cm apart. A shutter and substrate heater similar to those in our own resistively-heated system were incorporated in the chamber.

5.3 Source Material

Commercially produced CdS powder (B.D.H. Optran grade) was purified by resublimation in a flow of argon (Stanley 1956) to give rods and platelets of light yellow CdS.

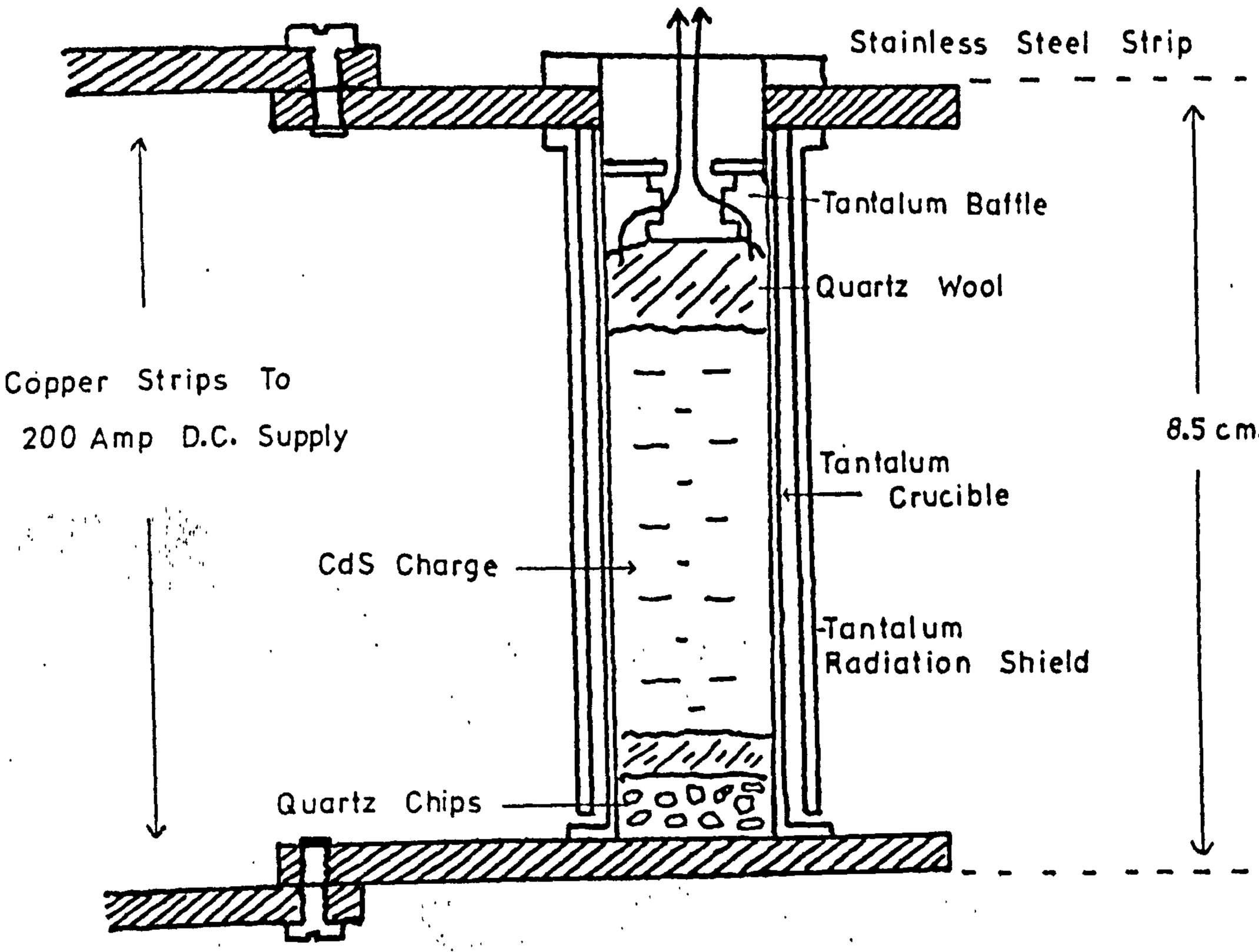

Figure 5.5

I.R.D. Tantalum Crucible

Mass spectrographic analysis of these crystals showed most impurities were present in quantities less than 0.1 ppm. The crystals were crushed and used as the source material for the vacuum evaporation. The I.R.D. sources were filled with "Leuchstoffurer" CdS powder.

5.4 Masks

Evaporation masks for the delineation of electrical contacts and samples on which the Hall coefficient could be measured were manufactured from 0.005" thick copper sheet by photochemical etching. Less complex patterns were machined from copper and duralumin sheet. The copper masks were cleaned in chromic acid before being placed in the vacuum chamber.

5.5 Substrates

There are many suitable substrate materials with contrasting properties. Those used included glass, NaCl, and metallised kapton (a polyimide plastic). The different substrates required different cleaning and handling techniques before film deposition was possible.

Much work has been done on the cleaning of glass substrates for vacuum evaporation. The most common methods used are; a series of chemical rinses, glow discharge cleaning (Holland 1955) and alcohol vapour degreasing (Putner 1959). Holland (1966) came to the conclusion that a thorough chemical wash was at least as good as ion bombardment. The best way to remove gross contamination is by ultrasonic agitation in a detergent type solvent followed by a degrease in propan-2-ol vapour.

Single crystal substrates required cleaving before the deposition of the film. The crystals were cleaved in air, immediately before being loaded into the system, by a cleaver of the type described by Harris (1969).

The metallised kapton substrates were cleaned by a gentle swabbing with acetone followed by propan-2-ol.

5.6 The Evaporation Cycle

The series of steps in the evaporation of a CdS film on to glass using the systems described is outlined below.

(a) The substrate was cleaned by ultrasonic agitation in "quadralene" US17 instrument cleaner, rinsed in distilled water, washing in propan-2-ol and then suspended in propan-2-ol vapour for several minutes to ensure that no stains persisted on the dry surface.

(b) The substrate and mask were placed on the substrate heater and the source crucible filled with crushed CdS flow crystals.

(c) The system was evacuated to a pressure less than 10^{-5} torr and the substrate heated to $50^{o}C$ above its required temperature for one hour.

(d) The CdS was outgassed gradually by increasing the source power.

(e) The evaporation rate and substrate temperature were set to the required value and the shutter opened when the steady state condition had been attained.

(f) The evaporation rate was monitored by the D.T.M.1 until the film had grown to the desired thickness when the shutter was closed. The source and substrate

heaters were then switched off.

(g) The substrate was allowed to cool to room temperature before the system was let up to air.

(h) Electrical contacts when desired were evaporated on to the CdS from a molybdenum boat in a separate glass vacuum system pumped by a small mercury diffusion pump and a cold trap.

5.7 A Totally Enclosed System

Following the success of the 'hot-wall' method a totally enclosed system was designed for the evaporation of CdS thin films. With this technique, which is described below, the evaporation chamber was not pumped during the formation of the film, thus allowing the evaporation to proceed under equilibrium conditions and ensuring that none of the constituents of the vapour were lost preferentially to exhaust.

The charge of crushed flow-run crystals was placed at the bottom of a vertical silica glass tube, with 12 mm bore and 25 cm long. The 1 cm square glass substrate was supported on small silica projections from the wall as near to the top of the silica tube as possible. The tube was rounded at the top end and joined to a 5 mm bore silica tube with which it was connected to a high vacuum system pumped by a mercury in glass diffusion pump and a cold trap. The whole tube was then heated to a temperature of 200^{o}C until outgassing was complete when the pressure lay in the range 9×10^{-7} to 4×10^{-6} torr. After cooling, the tube was sealed from the vacuum system leaving a volume of about 1 cm^{3} above the glass substrate (see Figure 5.6).

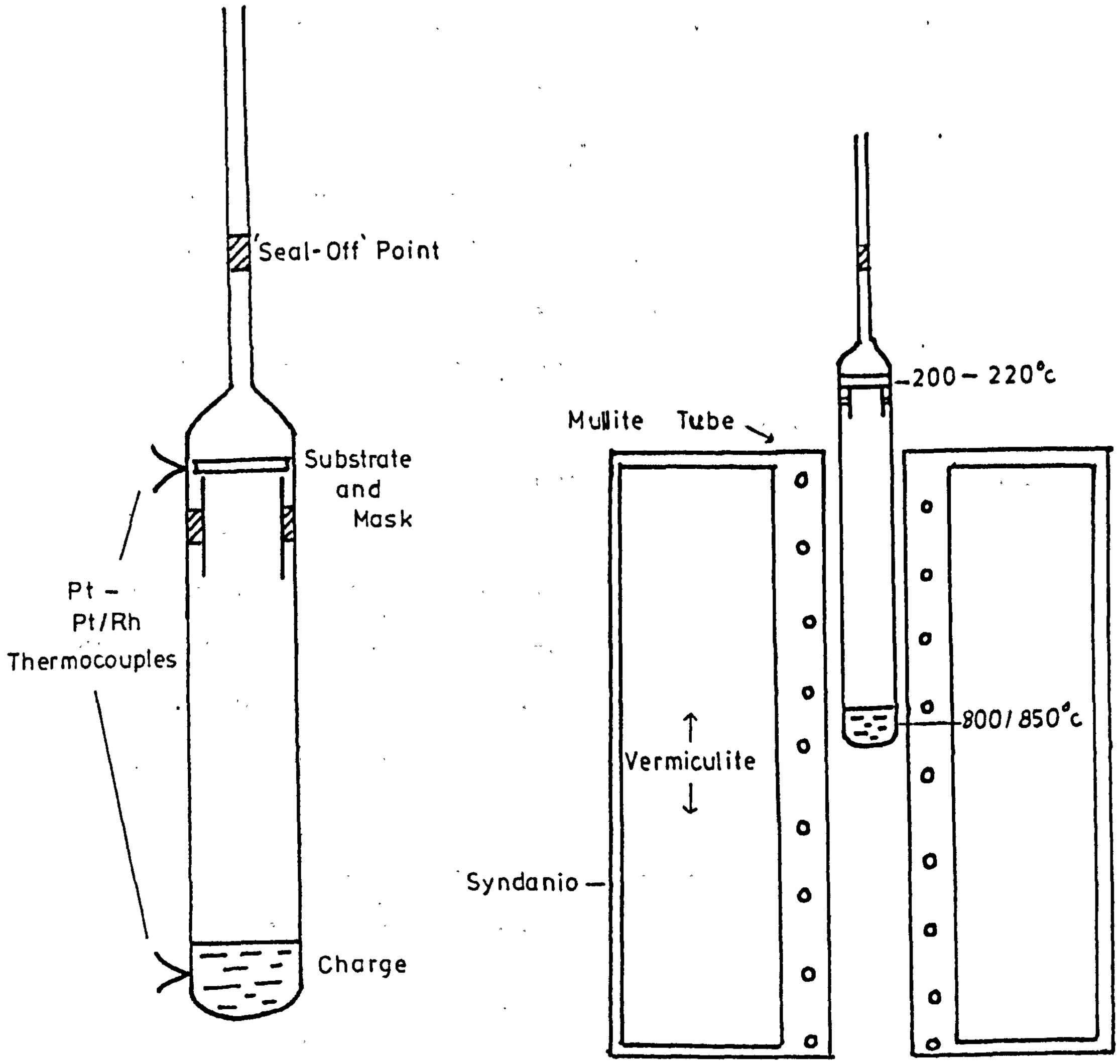

GROWTH TUBE

VERTICAL FURNACE

Figure 5,6

Method Of Growing Films In An Enclosed System

The evaporation was carried out by placing the tube in a vertical furnace similar to that used to grow single crystals (Clark and Woods 1968). By adjusting the position of the tube in the furnace some degree of control over the source and substrate temperatures was obtained. Using this system it was possible to grow films from 0.2 μm to 2 μm thick at a mean deposition rate of 40-50Å min^{-1}.

The source and substrate temperatures were measured with Pt, Pt/Rh thermocouples in contact with the outside of the tube. No direct monitoring of the deposition rate was possible and the mean rate was calculated by dividing the ultimate thickness of the film (measured using interference microscopy) by the total length of time the deposition had been in progress.

5.8 The Measurement of Film Thickness

The various methods used to measure film thickness are reviewed by Chopra (1969).

The thickness of the films was measured optically with a Watson interference objective. A reflecting metallised layer over the film edge is desirable with this method and the indium electrical contacts proved ideal for this purpose provided they were evaporated at a high rate in pressures below 10^{-5} torr.

With the interference head and a monochromatic source double beam Fizeau fringes were obtained by reflection from the metallised film and substrate. The metallic layer increases the fringe contrast and eliminates errors associated with phase changes which occur on reflection from dielectrics. The film thickness was calculated from the fringe displacement across the step,

see Fig. 5.7, which arose from the path differences of the reflected beams. This thickness is simply

$$t = \frac{n\lambda}{2}$$

where t = film thickness

n = number of fringes displacement

λ = wavelength of illumination.

The thicker films ($\approx$ 20μm) prepared at I.R.D. were measured directly using a calibrated microscope stage by focussing successively on the film and the adjacent substrate.

5.9 Conclusions

Samples were prepared in the systems described to determine the effects of the type of system and evaporation parameters on the resistivity of the CdS films. We were particularly interested in the conditions required to grow low resistivity films for use in photovoltaic junctions. The results are presented in the next chapter.

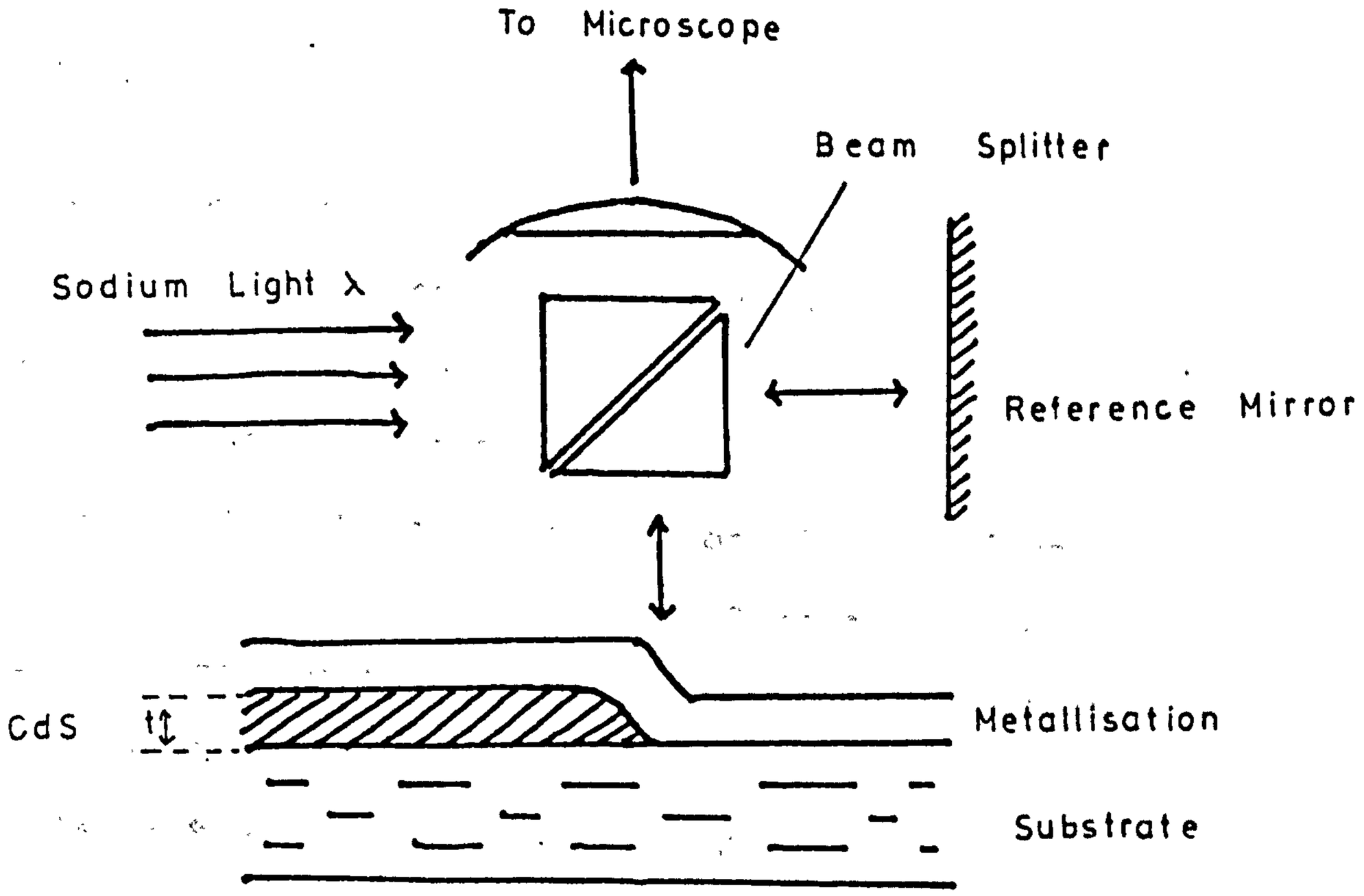

(1) FORMATION OF THE FRINGES

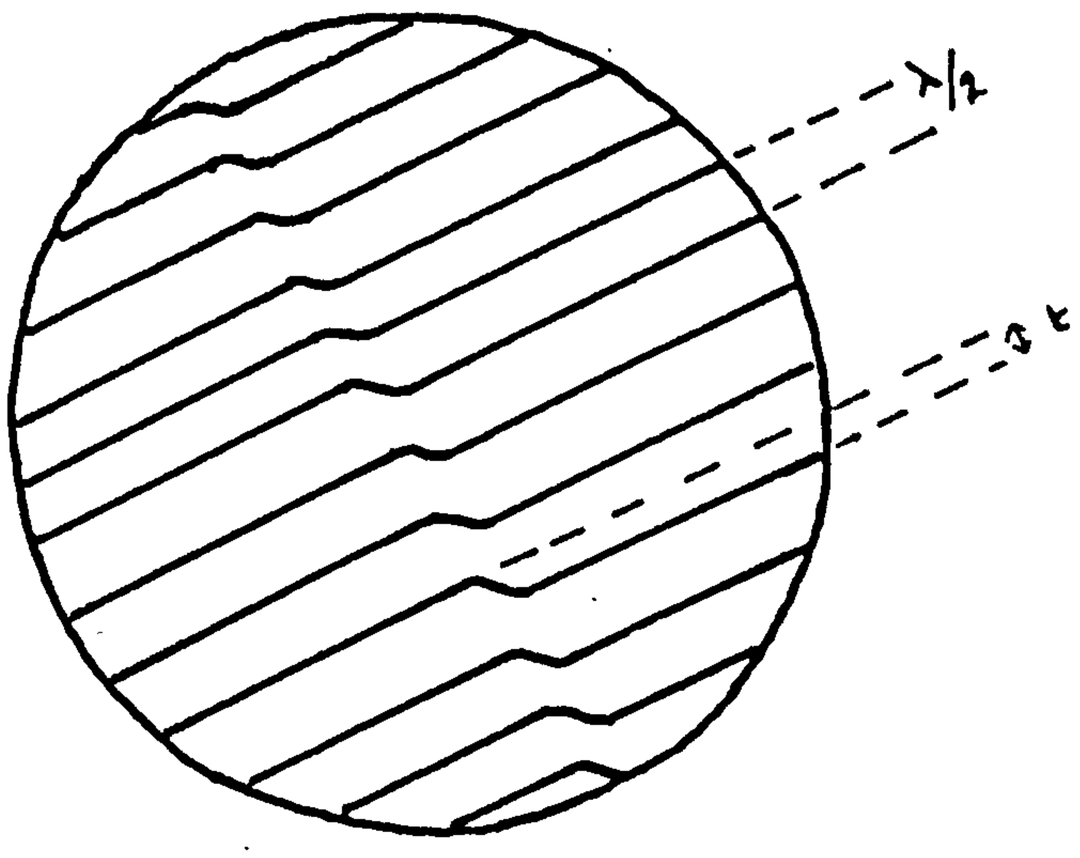

(2) APPEARRANCE OF THE FRINGE

Figure 5.7

Measurement Of Film Thickness

REFERENCES

Chopra (1969) "Thin Film Phenomena" (McGraw-Hill)

Clark and Woods (1968) J. Crystal Growth 3 126

Harris (1969) J. Phys. E. 2 432

Holland (1955) B.J.A.P. 9 410

Holland (1966) "The Properties of Glass Surfaces" (Chapman and Hall)

Martin (1970) M.Sc. Thesis, University of Durham

Putner (1959) B.J.A.P. 10 332

Stanley (1956) J. Chem. Phys. 24 1279

CHAPTER 6

THE ELECTRICAL PROPERTIES OF CdS THIN FILMS

6.1 Introduction

It was mentioned in Chapter 3 that the electrical resistivity of the underlying CdS thin film is an important parameter in controlling the properties of a P.V. heterojunction. An examination of the conditions required to produce CdS films of the correct resistivity is therefore of great importance. Low resistivity films are essential to ensure that the cell has a low series resistance thus enabling maximum power to be extracted. The low resistivity must be achieved without departing from the optimum composition at which the heterojunction can be formed. The effects on the dark resistivity of varying the film thickness, deposition rate and substrate temperature of CdS films deposited on glass by the different methods described in Chapter 5, have been investigated and are described below.

A large number of samples would have been necessary to cover the complete range of interest of all the parameters (substrate temperature from 20 to 350^{o}C, deposition rates from 10 - 10,000Å/min, and thicknesses from .1 – 10 μm). For example Davey (1963) working on germanium films found it necessary to produce twelve hundred samples. Operations on such a scale were beyond our scope so that the work was restricted to substrate temperatures between 200 and 220^{o}C where previous experiments have shown (Wilson and Woods 1973) that films of acceptable composition and resistivity were most likely to be produced.

6.2 Electrical Contacts

Mention should be made at this stage of the materials which form ohmic contacts with CdS which has an electron affinity of 4.22 eV. The most commonly used contact is indium which has a work function of 3.8 eV (Smith 1955, Schulman 1955) but silver (4.21 eV), zinc, aluminium (4.20 eV) and chromium (4.21 eV) also have suitable work functions (Learn et al 1966, Bujati 1968). Gold (ϕ = 4.46 eV) might be expected to form a blocking contact because its work function is so high. However when a CdS film is evaporated on to gold an ohmic contact is produced. This is attributed to the formation of a Au/Cd intermetallic compound in the surface regions of the CdS.

Gold contacts are more durable than those of the other materials. They have a high resistance to oxidation and gold does not diffuse into CdS as readily as indium. However the sticking coefficient of CdS on gold is higher than that of CdS on glass. Films on gold are therefore more non-uniform and consequently it was decided to use evaporated indium contacts in this work.

6.3 Apparatus

The electrical circuit used for the measurements is shown diagrammatically in Figure 6.1 while a scale drawing of the thin film sample and contacts is illustrated in Figure 6.2.

The current flowing along the sample was derived from a dry battery and monitored by a sensitive mirror

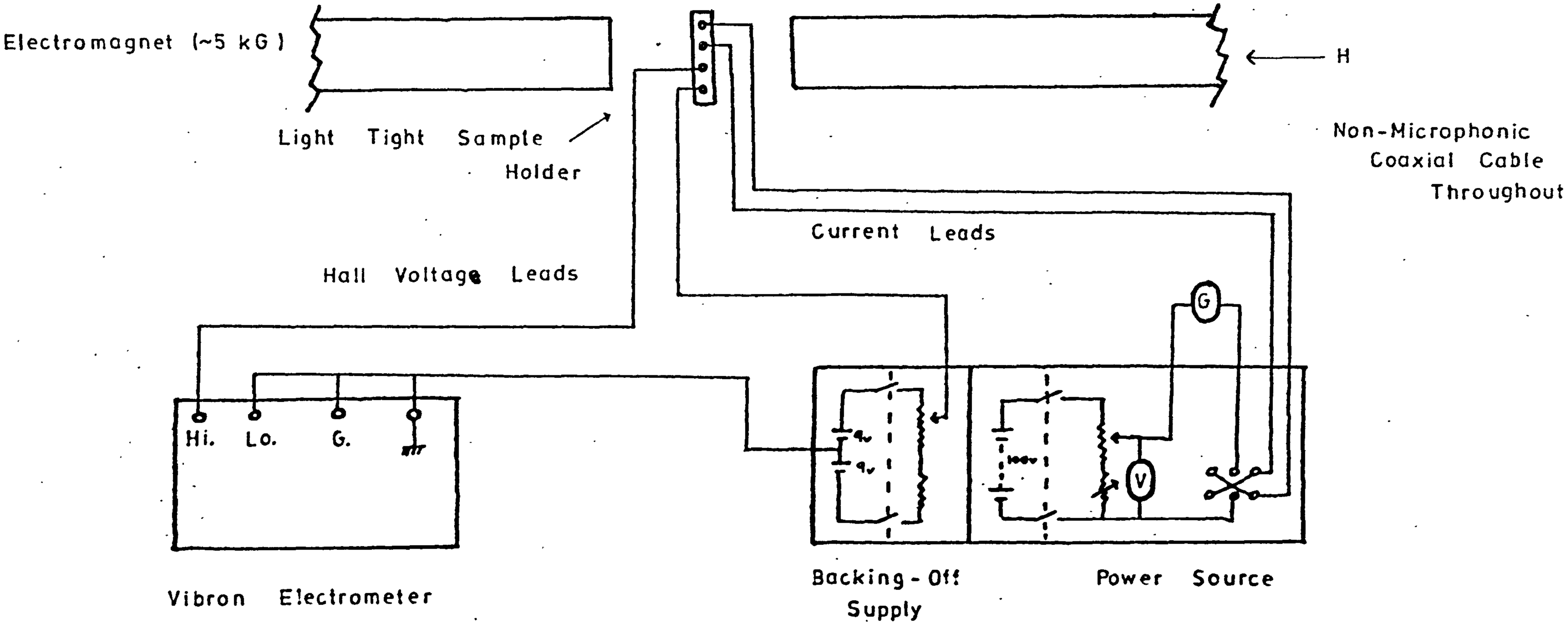

Figure 6.1

Circuit For Electrical Measurements On Thin Films

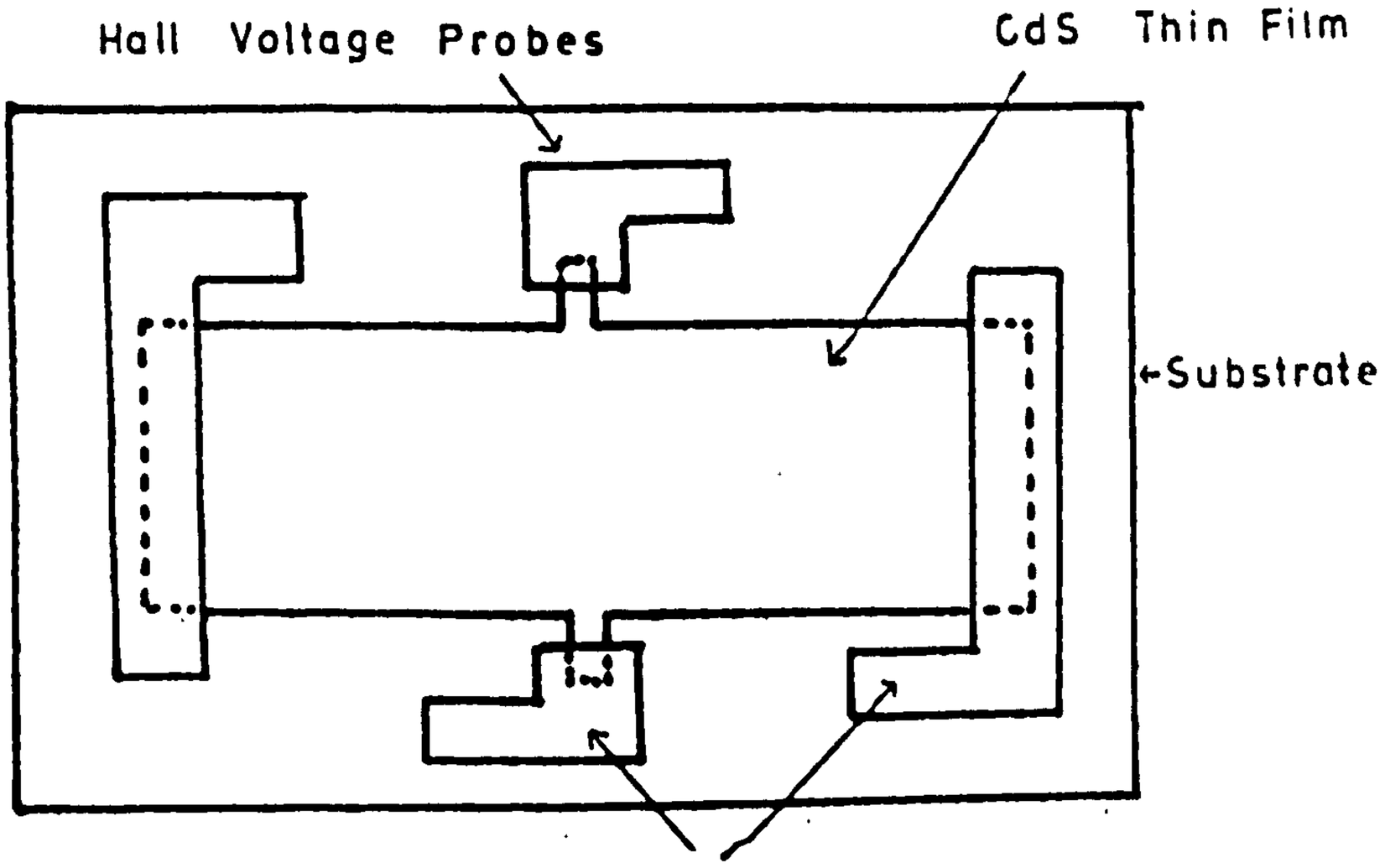

Figure 6.2

Thin Film Sample And Electrical Contacts

galvanometer (2,400 mms/ A). A field of 5 kG was obtained from an electromagnet. The field was uniform over the sample area across a gap of 2 cm in which the light tight sample holder was supported. Non-microphonic, co-axial, screened cable was used between the sample, meters and power supply since the high resistivity of a number of the samples made the use of an E.I.L. Vibron 33B Electrometer essential for the measurement of some Hall voltages. In order to off-set the out-of-balance voltage across the Hall probes, which was present in zero magnetic field because of slight contact misalignment, a variable backing-off battery supply was inserted into the Hall voltage measuring circuit. Since the length to width ratio of the thin films was greater than three no end effect corrections to the Hall voltage were necessary to compensate for possible short circuiting effects of large current contacts (Isenberg et al 1948).

When the photoconductivity was to be measured illumination was provided by the radiation from a tungsten-halogen lamp filtered by a 1 cm path of water. The intensity of the radiation was maintained at 150mW/cm^2 as determined by a calibrated Si photovoltaic cell. This apparatus will be described in more detail in Chapter 9.

6.4 Current Characteratistics

6.4.1 In order to check that the evaporated indium contacts were ohmic, a series of I(v) curves for 'forward' and 'reverse' voltages up to 100 volts were obtained for CdS

films evaporated under a wide range of conditions. Some of the resultant curves are shown in Figure 6.3. By varying the method of evaporation, substrate temperature, deposition rate and thickness it was possible to produce films with resistivities varying from 2.0 to 2.0×10^7 ohm cm.

Samples numbered with the prefix G were evaporated using the electron gun, with the prefix R by a resistively heated source and with the prefix E in a totally enclosed system. This convention has been used throughout this work.

Figure 6.3 shows that the higher resistivity samples were slightly non-ohmic. This is because the work function of In matches that of CdS less well as the Fermi level moves downwards from the conduction band. No difference was noted in the current flowing in any sample when the polarity was reversed. All the films in the lower resistivity range (the ones of most interest in the present investigation) were ohmic. The values of resistivity quoted in Figure 6.3 were measured at 50V. This was a suitable voltage to produce a measureable current without introducing high field effects, and has been used as a standard bias.

6.4.2 The effect of illuminating a sample and changing the intensity of the white light with neutral density filters was to produce a non-linear variation of photocurrent with intensity as shown in Figure 6.4. In this diagram L = 100% corresponds to illumination with sunlight at a.m.o. (air mass zero). The samples were mounted on a copper block which acted as a heatsink and thus ensured isothermal conditions.

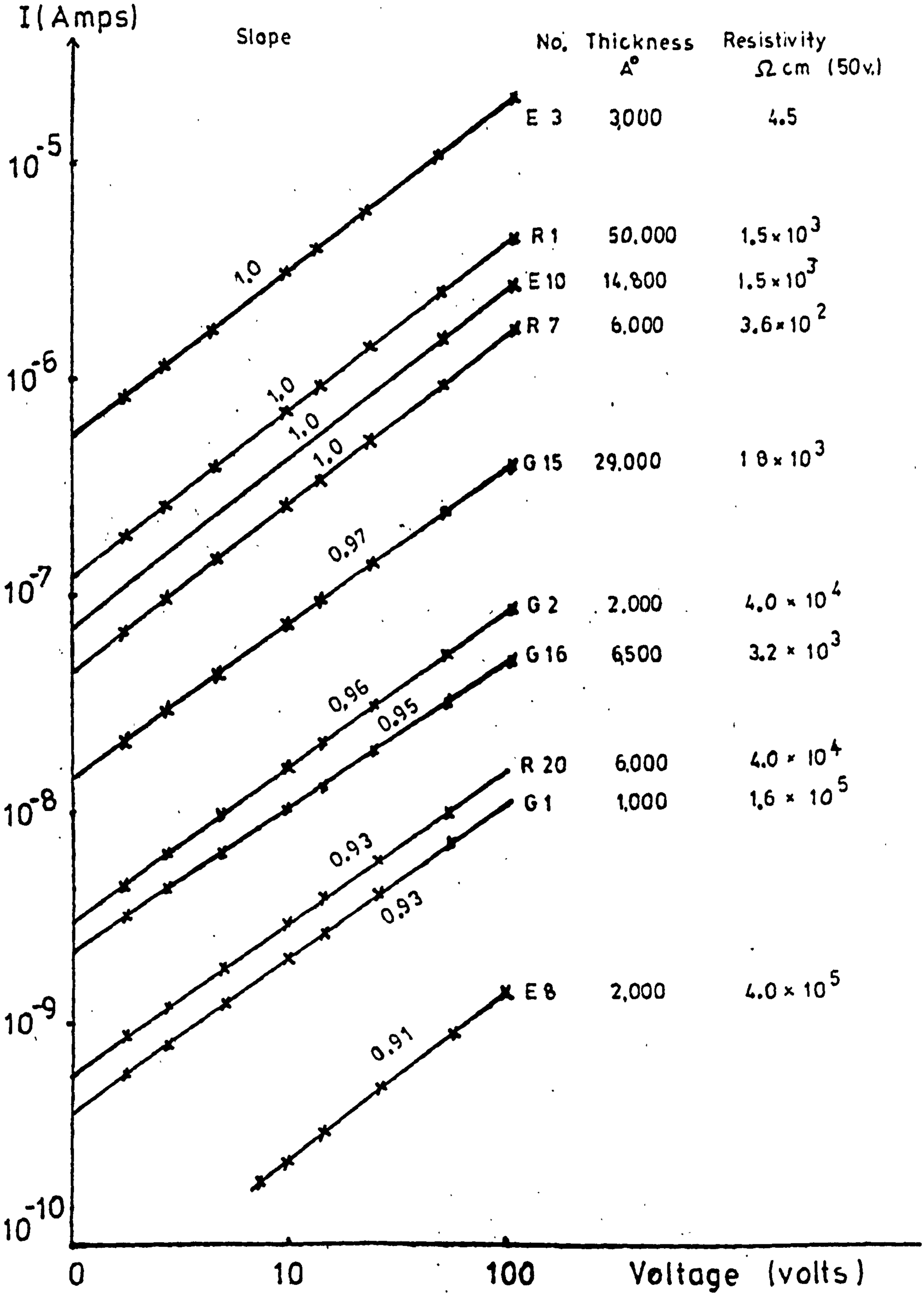

Figure 6.3

Dark I(V) Characteristics Of CdS Films On Glass

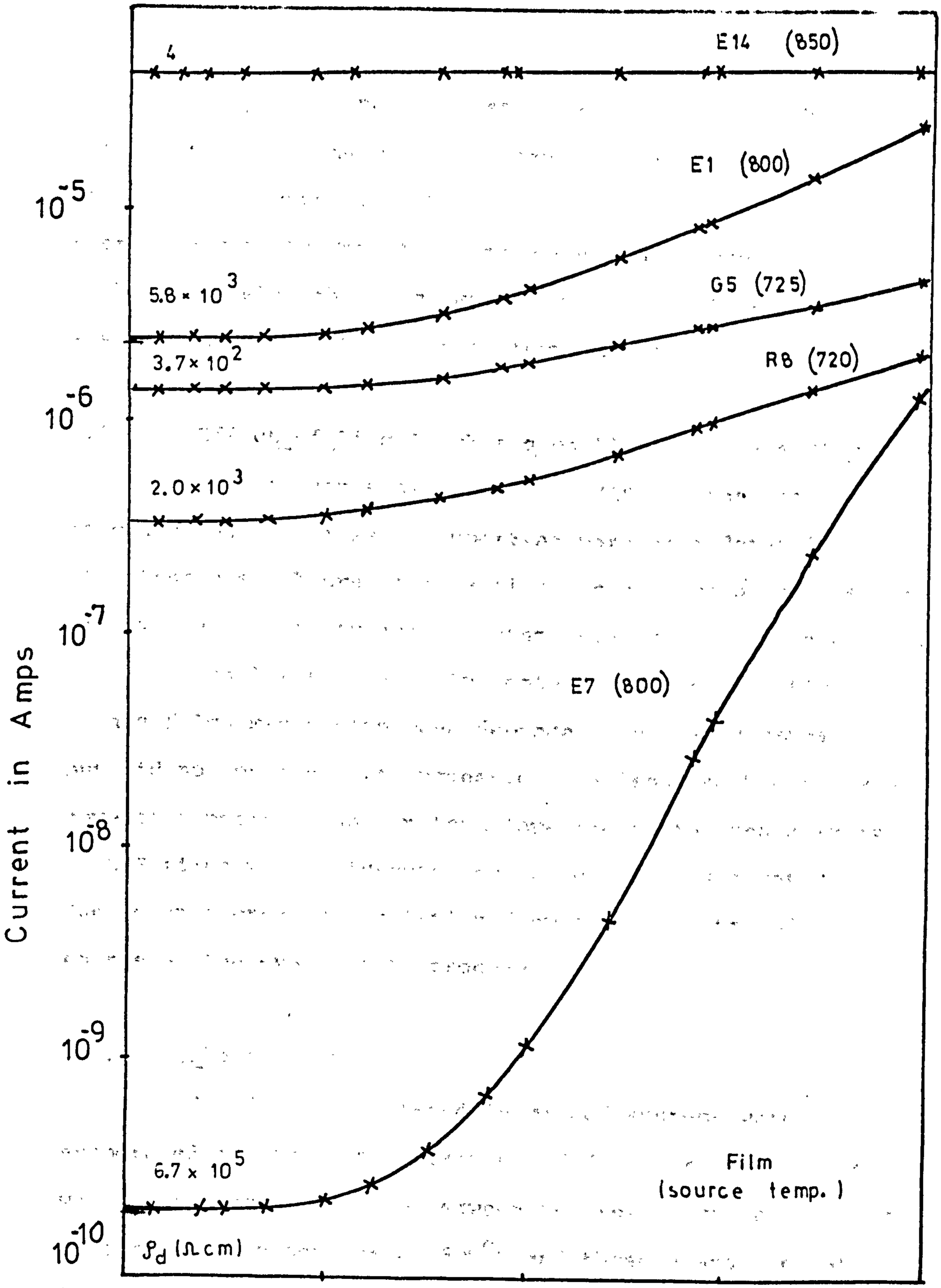

Figure 6.4

Photocurrent Versus Light Intensity For CdS Films

A typical spectral response of the photoconductivity of one of the more photosensitive enclosed films is shown in Figure 6.5. There was a large peak in the photoconductivity when the sample was illuminated with light of wavelength 0.5μm, which is at the optical absorption edge of CdS at room temperature.

6.5 Effect of Film Thickness on Electrical Resistivity

It has been shown by Addiss (1963) that the thickness of a film is an important parameter determining its structure. There is a parallel dependence of the resistivity, Hall mobility and photosensitivity on film thickness.

Shallcross (1966) indicated that the resistivity of his films might have been dependent on the thickness, but did not pursue this suggestion. Wilson and Woods (1973) however reported a non-uniform lowering of the resistivity of CdS films with thickness and suggested this might be due to an increasing deviation from stoichiometry of the source as the evaporation proceeds.

6.5.1 Closed System

The films evaporated in closed systems were evaporated at source temperatures of 800°C or 850°C. There was a striking difference between the resistivities of films evaporated from sources at 800°C and those evaporated at 850°C. The curves in Figure 6.6 show the resistivities of the two sets of films, deposited at 50Å min^{-1} as a function of film thickness. Each point plotted represents the mean of at least six films of the same thickness. Curve 'a'

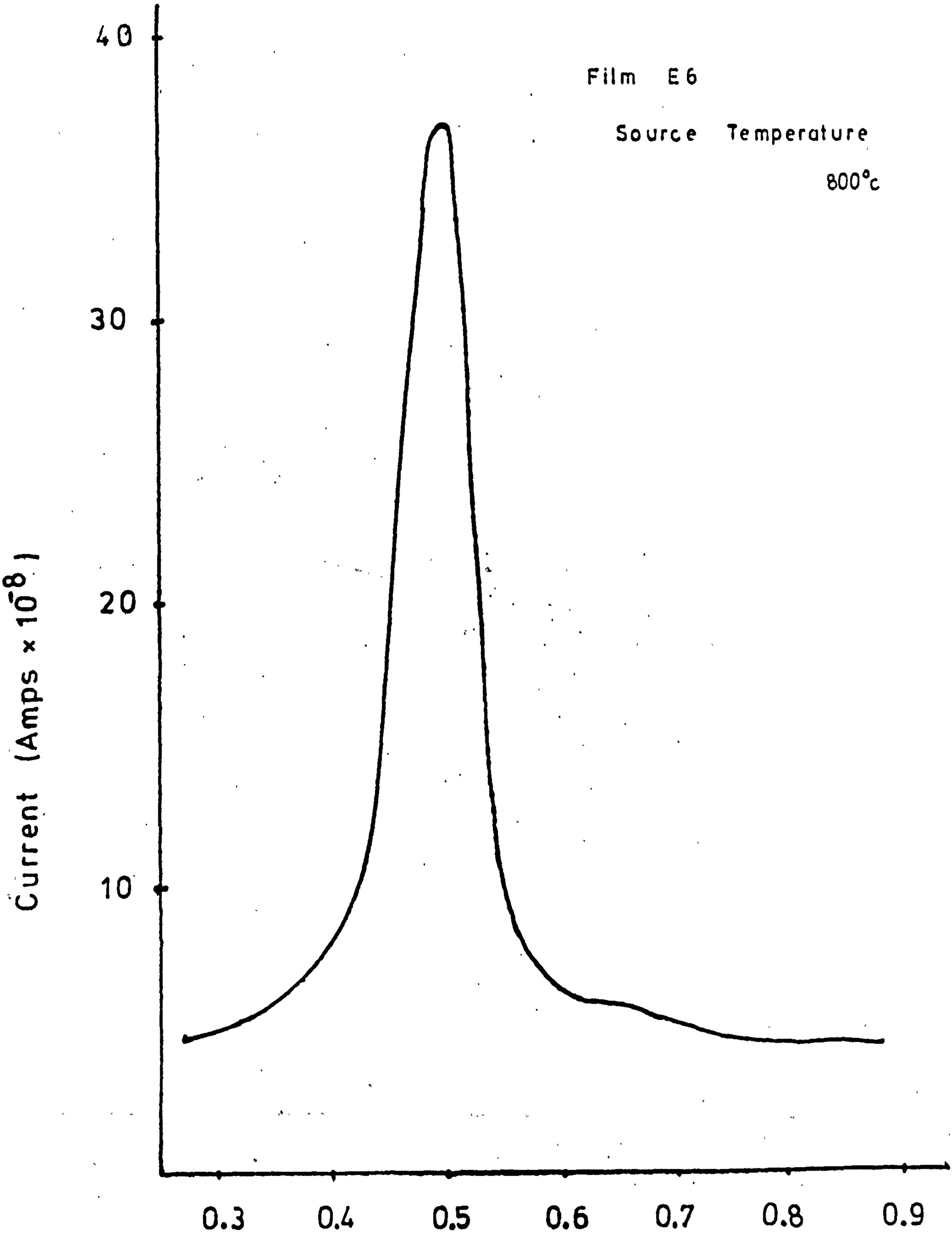

Figure 6.5

Spectral Response Of Photocurrent

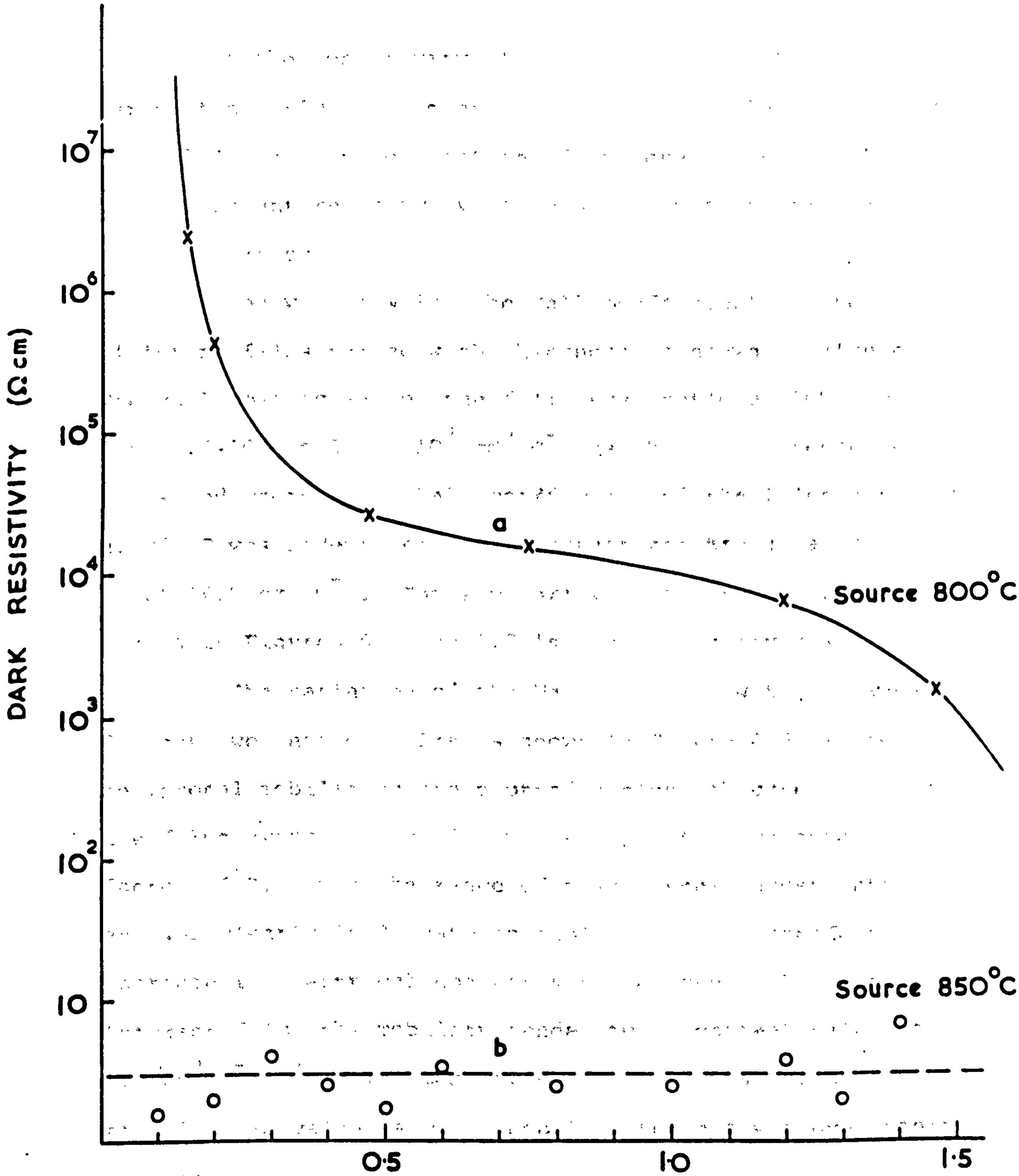

Figure 6.6

Enclosed Films: Resistivity Versus Thickness

shows that the resistivity of the films evaporated at 800°C varied from 2×10^6 ohm cm at a thickness of 0.15 μm to 10^3 ohm cm at 1.47 μm. In contrast the films evaporated at 850°C had a constant resistivity of about 3 ohm cm regardless of their thickness.

The way in which the Hall coefficient of the different films varied with thickness is shown in Figure 6.7. The Hall coefficient of the films evaporated at 800°C changed from 3.6×10^6 to 5.5×10^3 $cm^3\ C^{-1}$ as their thicknesses were increased whereas the Hall coefficient of the films evaporated at 850°C was independent of thickness and had a value of about 14.0 $cm^3\ C^{-1}$. The similarity in the shape of the curves in Figures 6.6 and 6.7 is strikingly obvious.

The variation of the Hall mobility with thickness for the two sets of films is shown in Figure 6.8, where reciprocal mobilities are plotted against thickness. With the films evaporated at 800°C the mobility increased by a factor of 2.5 over the range of thicknesses investigated and was clearly inadequate to explain the thousandfold increase in electrical conductivity observed. With the thickest films the mobility tended to a constant value of 3.7 $cm^2\ v^{-1}\ s^{-1}$. The mobilities of the films evaporated at 850°C had values almost identical to this whatever their thickness.

The Hall measurements allow a distinction to be made between the contributions of the carrier concentration and the mobility to changes in the resistivities of the films. The obvious similarities between the changes in the Hall coefficient and the resistivity of the films evaporated

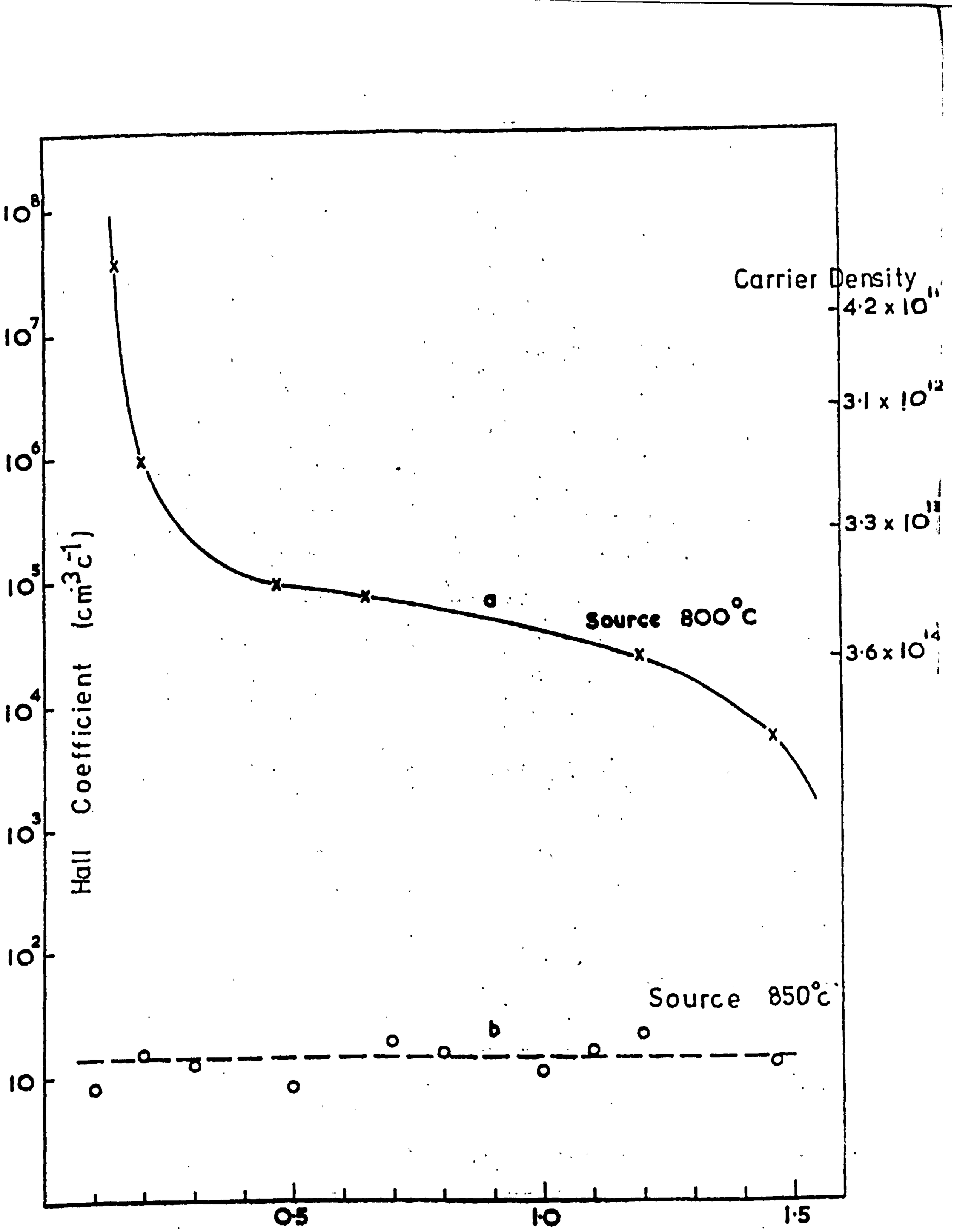

Figure 6.7

Enclosed Films Hall Coefficient Versus Thickness

in the closed system from a source at 800°C demonstrates that the change in resistivity is almost entirely due to an increase in carrier concentration with thickness. In fact the carrier concentration increased from $8x10^{11}$ to $8x10^{14}$ cm^{-3} as the thickness increased to 1.5 μm. The carrier concentration of the films evaporated at 850°C was about $5.0x10^{17}$ cm^{-3}.

The variation in the Hall mobility, μ, with thickness illustrated by curve 'a' in Figure 6.8 can be explained in terms of the model put forward by Fleitner (1961) which attributes the variation to diffuse scattering of the electrons at the surfaces of the films. According to Fleitner's model

$$\mu = \mu_K (1 - 2\lambda/t)$$

where μ_K is the bulk mobility of CdS modified by the effects of grain boundary and impurity scattering, t is the thickness of the film and λ is the effective mean free path between surface collisions. A good fit was obtained between this equation and the experimental results when values of $\mu_K = 4$ cm^2 V^{-1} s^{-1} and $\lambda = 500\text{Å}$ were used. The continuous line in Figure 6.8a has been plotted using these values.

6.5.2 Open Systems

Wilson and Woods (1973) have previously reported similar variations in the resistivity of CdS films with thickness. Their samples were prepared in a conventional 'open' vacuum system using a resistively heated source. To check that the results they obtained could be reproduced

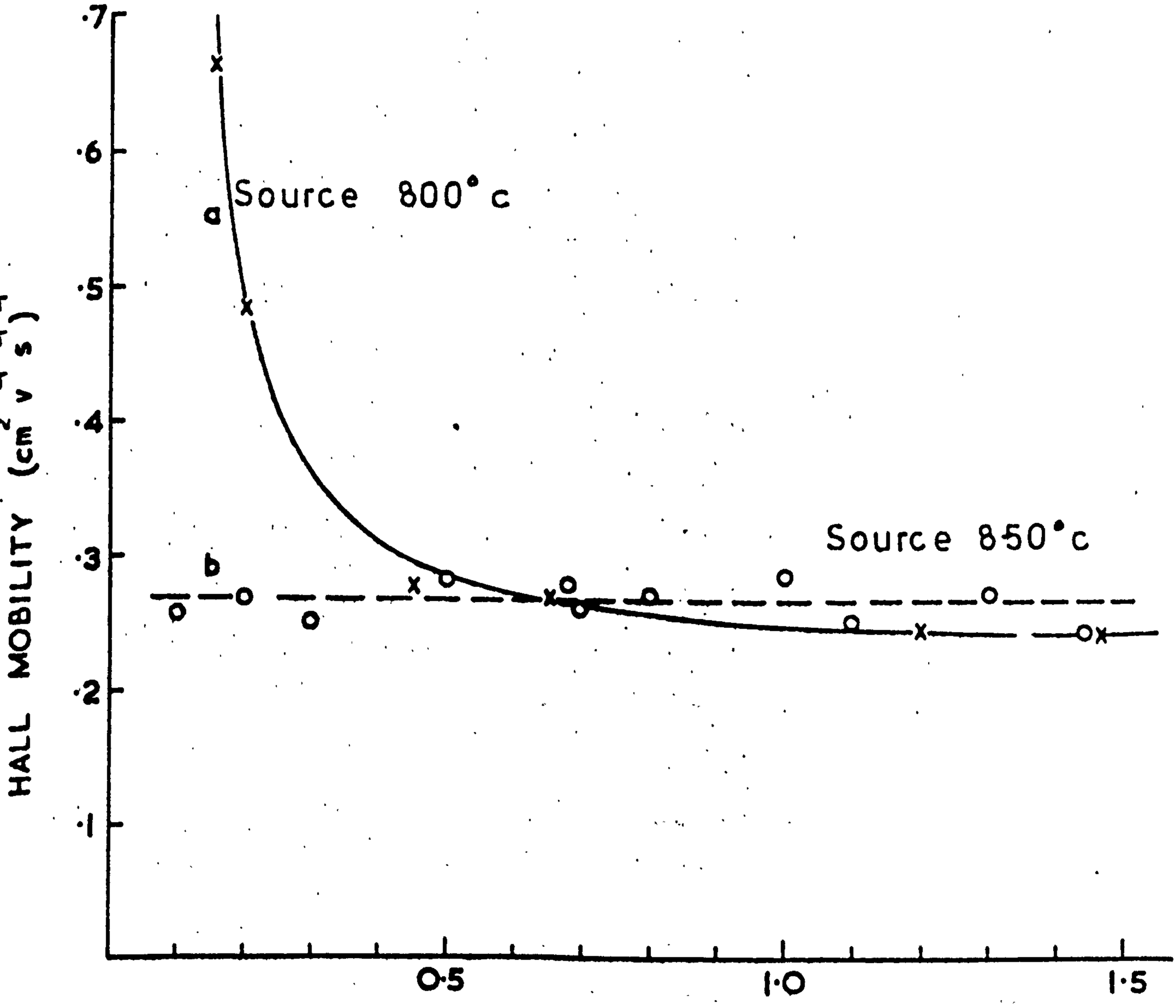

Figure 6.8

Enclosed Films: Hall Mobility Versus Thickness

using the starting material employed in the experiments described above, some films were grown using the identical open system, and identical source and substrate temperatures they had worked with. Excellent agreement was obtained.

To extend their work and to test the idea that the composition of the source varied with time, the following experiment was performed. Two glass substrates were placed side by side on the substrate heater in the vacuum system. A shutter was used to allow a film of CdS to be deposited on one substrate for ten minutes, whereupon the shutter was adjusted to stop the deposition on the first substrate and allow a film to be formed on the second substrate. This second deposition also lasted for ten minutes. A substrate temperature of 200°C and a source temperature of 720° were used. Throughout the evaporation the deposition rate was monitored and was approximately constant at 900Å/min. The experiment was then repeated with two new substrates and a new charge. Once again a film was formed on substrate 1 for the first ten minutes. For the second ten minutes both substrates were obscured from the source and finally for the third ten minutes a film was deposited on substrate 2. The source was heated for the whole 30 minutes duration of the experiment. The experiment was then repeated increasing the interval between the first and second depositions to 20 and then 30 minutes. The results are shown in Figure 6.9.

The tops of the tall rectangles show the resistivities of the films evaporated for the first ten minutes in each of the four experiments. The heights of the dashed rectangles show the resistivities of the films deposited on

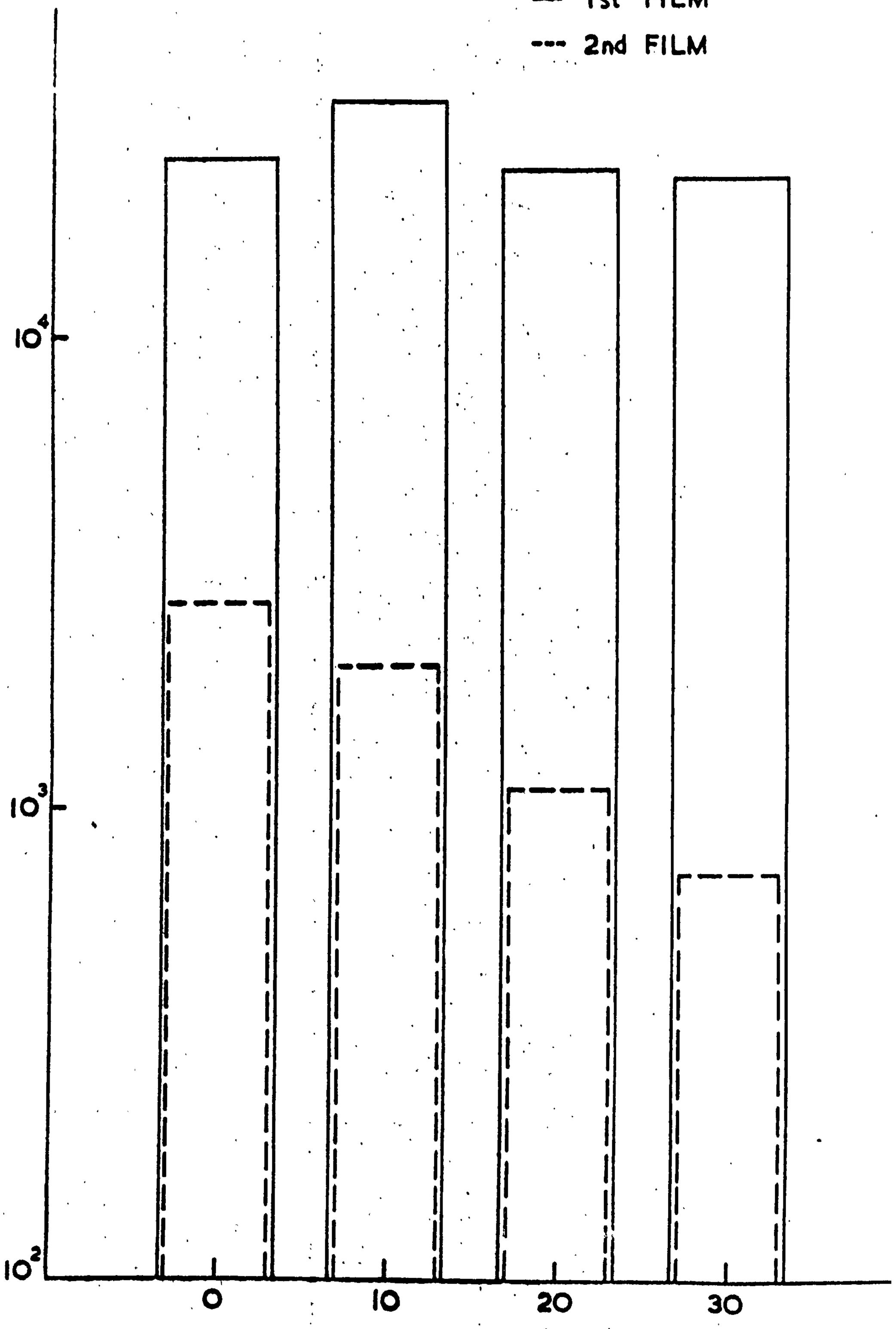

Figure 6.9

Resistivity Differences in CdS Thin Films

the second substrates. The numbers on the abscissa indicate the time in minutes between the first and second depositions. The results demonstrate quite clearly that with films of the same thickness the resistivity decreases with the length of time for which the source has been heated to the evaporation temperature prior to the deposition occurring.

A similar experiment was then performed in which the source was allowed to run for an increasing length of time before two films were evaporated consecutively at 900 Å/sec for 10 minutes. The results are shown in Figure 6.10. In this figure the ratio of two consecutively evaporated films (the resistivity of the film of substrate 1 : the resistivity of the film on substrate 2) is plotted against the time the source had been running prior to the evaporation of the initial film.

The small size of the source meant it was impossible to run it at the evaporation temperature for periods in excess of 50 minutes. As a result the point where both films would have the same resistivity could not be reached experimentally. However by extrapolating the curve we can estimate that this would occur when the source was heated to evaporation temperature for 50 minutes prior to the deposition of the first film.

6.5.3 Electron beam evaporation

Further films were evaporated in an 'open' vacuum system using an electron beam to heat the source. The variation in resistivity with thickness of these films

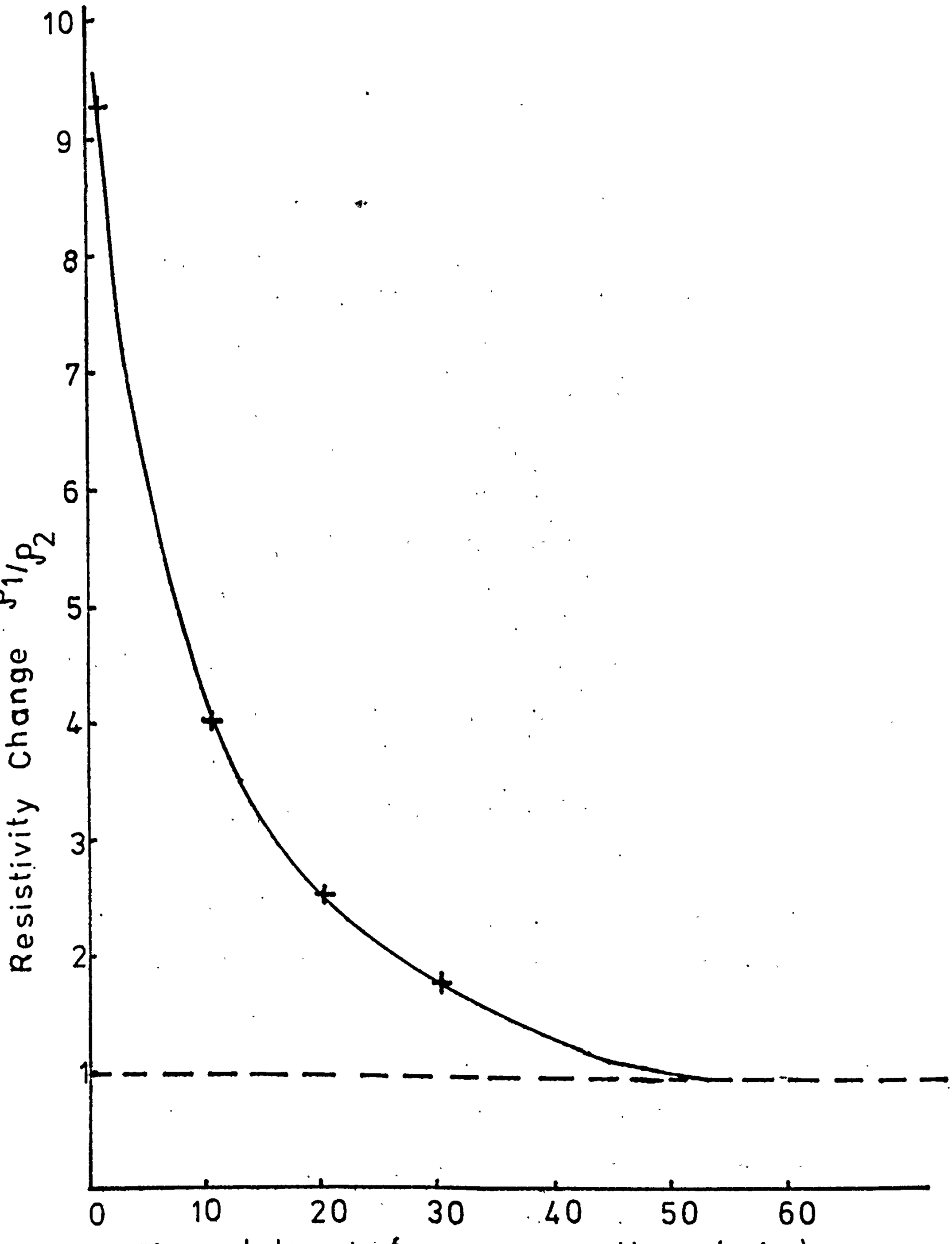

Figure 6.10

'Double Films'

Resistivity Change Versus Time Delay Before Films Evaporated

is shown in Figure 6.11. The resistivity of such films falls from 1.6×10^5 Ωcm at a thickness of 0.05μm to 3.4×10^3 Ωcm at 0.6μm, and thereafter appears to be approximately constant up to a thickness of 4μm. The Hall coefficient (Figure 6.12) follows an identical pattern suggesting the decrease in resistivity is predominantly due to an increase in carrier concentration as opposed to carrier mobility. This is confirmed by the variation of inverse Hall mobility with thickness shown in Figure 6.13.

6.6 Effect of Evaporation Parameters on Electrical Resistivity

6.6.1 So far the conditions required to produce a film of given resistivity have not been discussed. It has merely been stated that a variety of films with widely ranging properties can be produced by varying the substrate temperature and deposition rate. In this investigation studies have been made on more than 100 films which were deposited on glass from undoped resublimed Optran (B.D.H.) CdS.

The black films which result from deposition on a cold substrate were of no use for photovoltaic purposes as they were very rich in cadmium and consequently highly conductive ($\rho \approx 80\Omega$cm) and non-photosensitive. The requirement to avoid such films set a lower limit on the substrate temperature of around 150°C. At the other extreme great difficulty was experienced in depositing CdS on to a substrate held at a temperature in excess of 350°C. Near this temperature a thin pale yellow film was fabricated. The minimum deposition rate was limited by

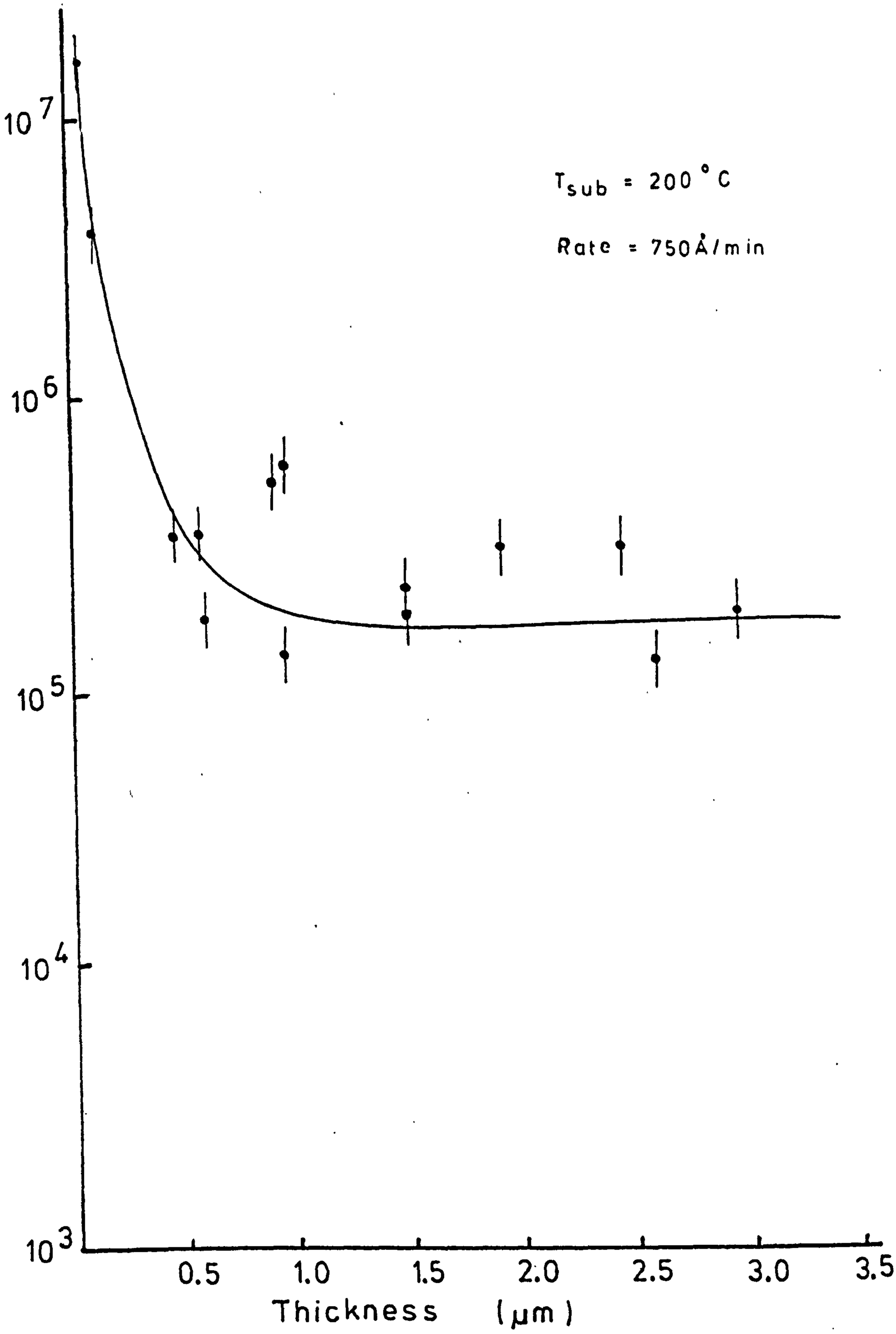

Figure 6.11

Electron Gun Films
Resistivity Versus Thickness

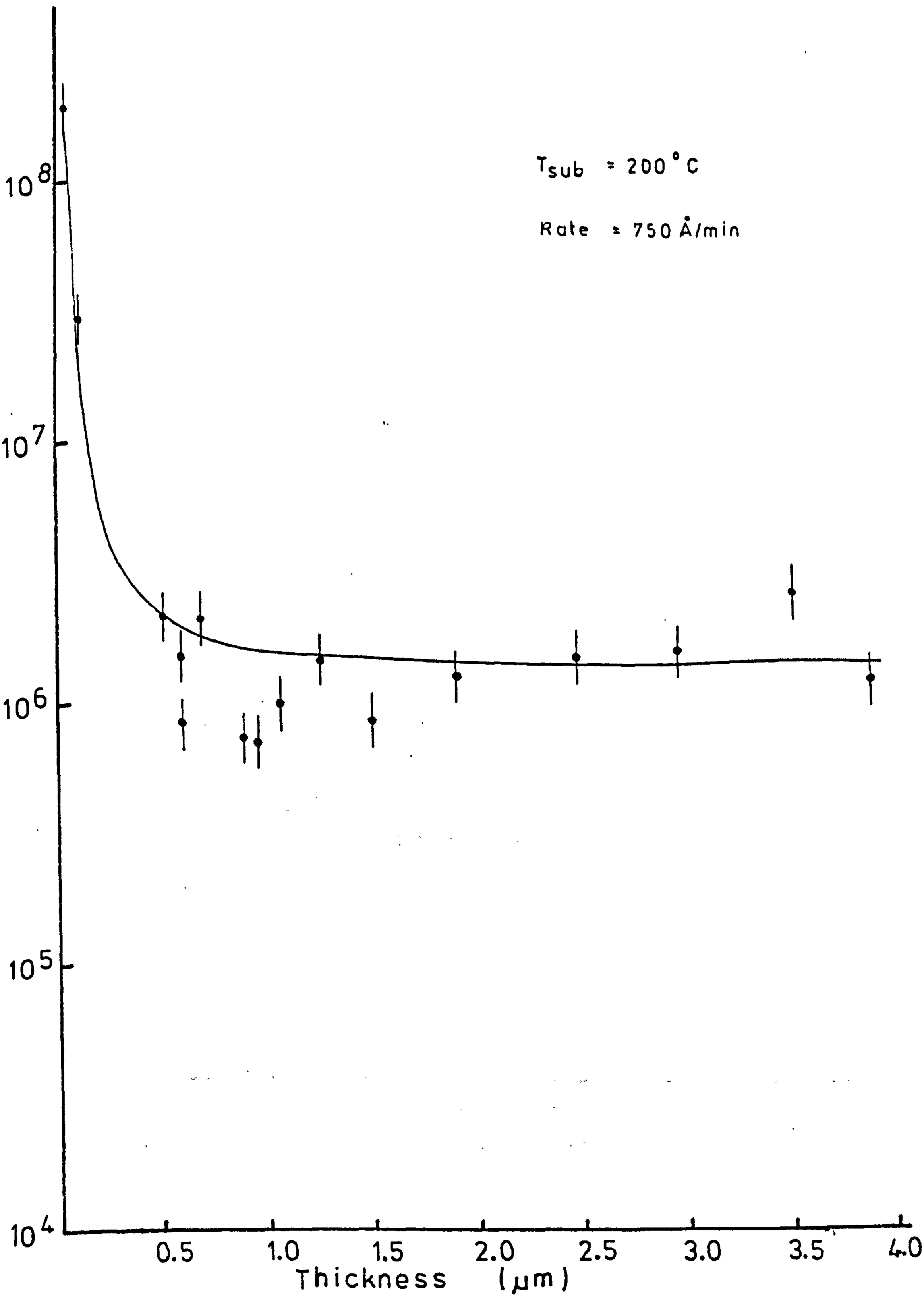

Figure 6.12

Electron Gun Films
Hall Coefficient Versus Thickness

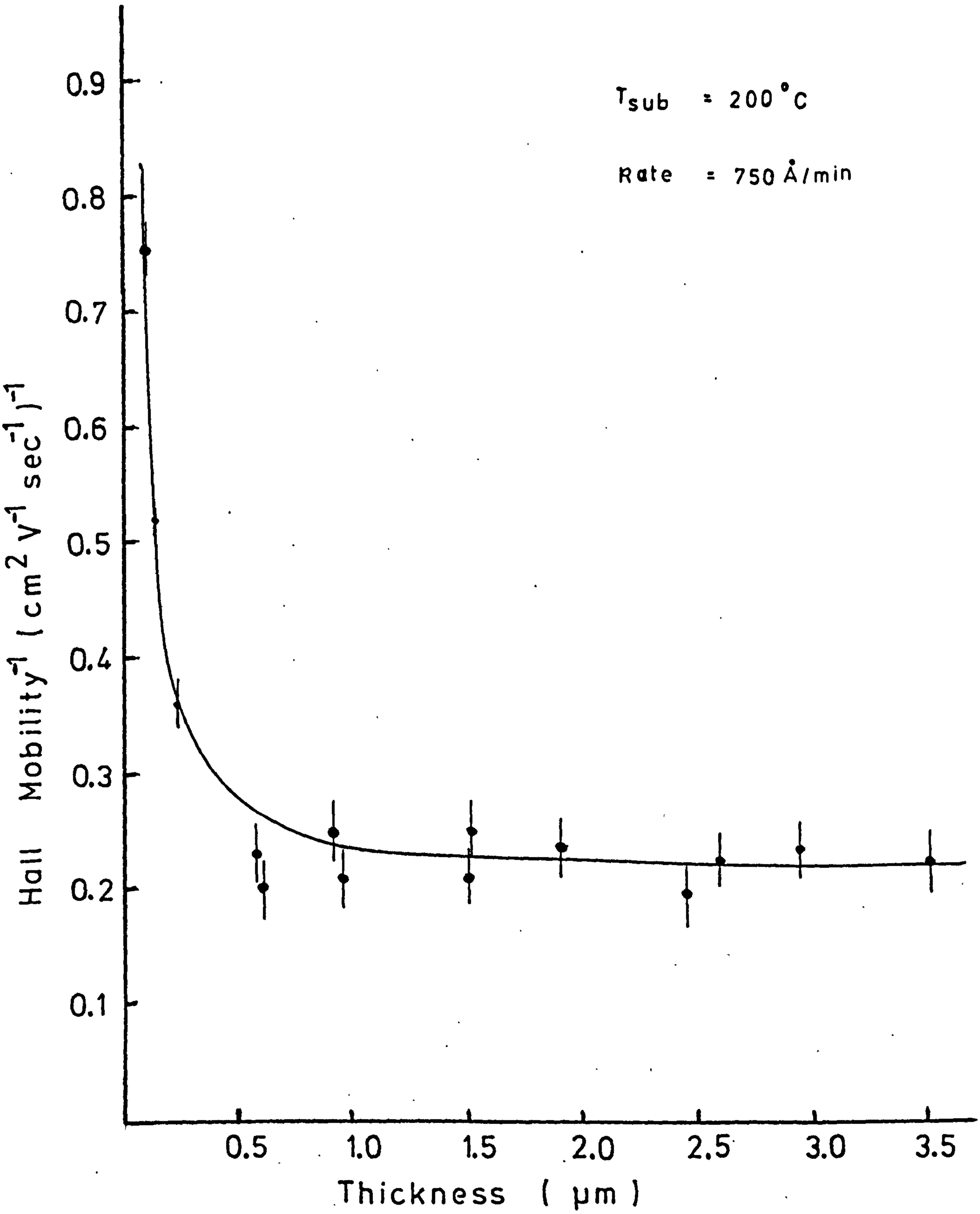

Figure 6.13

Electron Gun Films

Hall Mobility Versus Thickness

the time available for the evaporation and the maximum rate governed by the total power that could be supplied to the source.

6.6.2 Enclosed System

The measurement of substrate temperature in the enclosed system was not considered accurate enough (±20°C) for any meaningful plot of film resistivity against substrate temperature to be made. The thermocouple used in the system did however ensure that all the depositions were made on substrates with reproducible temperatures which varied by no more than 5°C, even though the actual temperature could only be estimated to within the error mentioned above.

By varying the position of the evaporation tube in the furnace it was possible to obtain a limited range of deposition rates. Figure 6.14 shows that the variation of resistivity with deposition rate was approximately linear. The predominant parameter in controlling film resistivity was however the source temperature. Figure 6.15 shows the distribution of film resistivities deposited at various rates from sources at 800°C and 850°C. This shows clearly that the variation in resistivity associated with changes in the source temperature is much greater than any change brought about by a variation in deposition rate.

6.6.3 Open System

The resistivity of films evaporated by an electron beam in a conventional vacuum system increased with

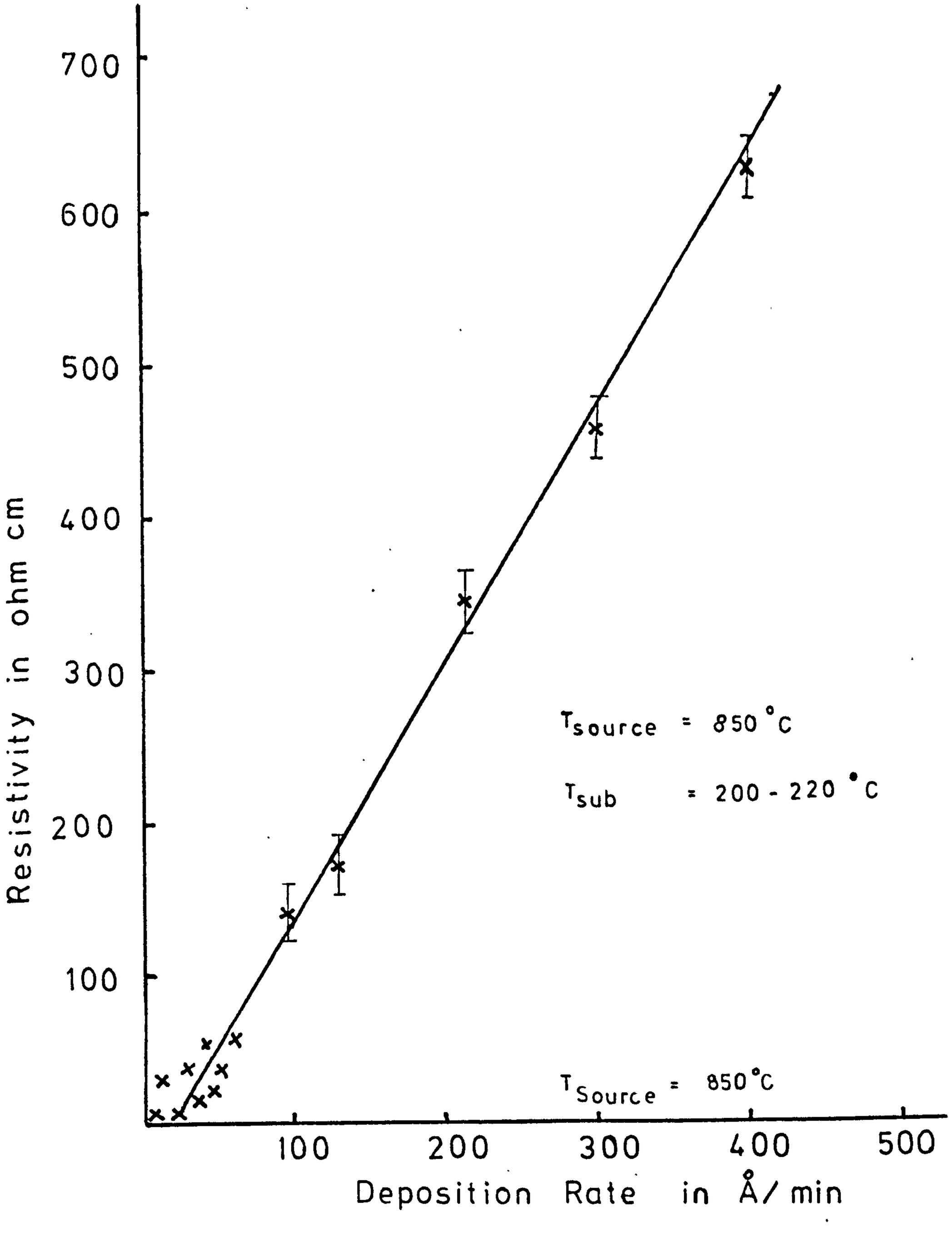

Figure 6.14

'Enclosed' Films

Resistivity Versus Deposition Rate

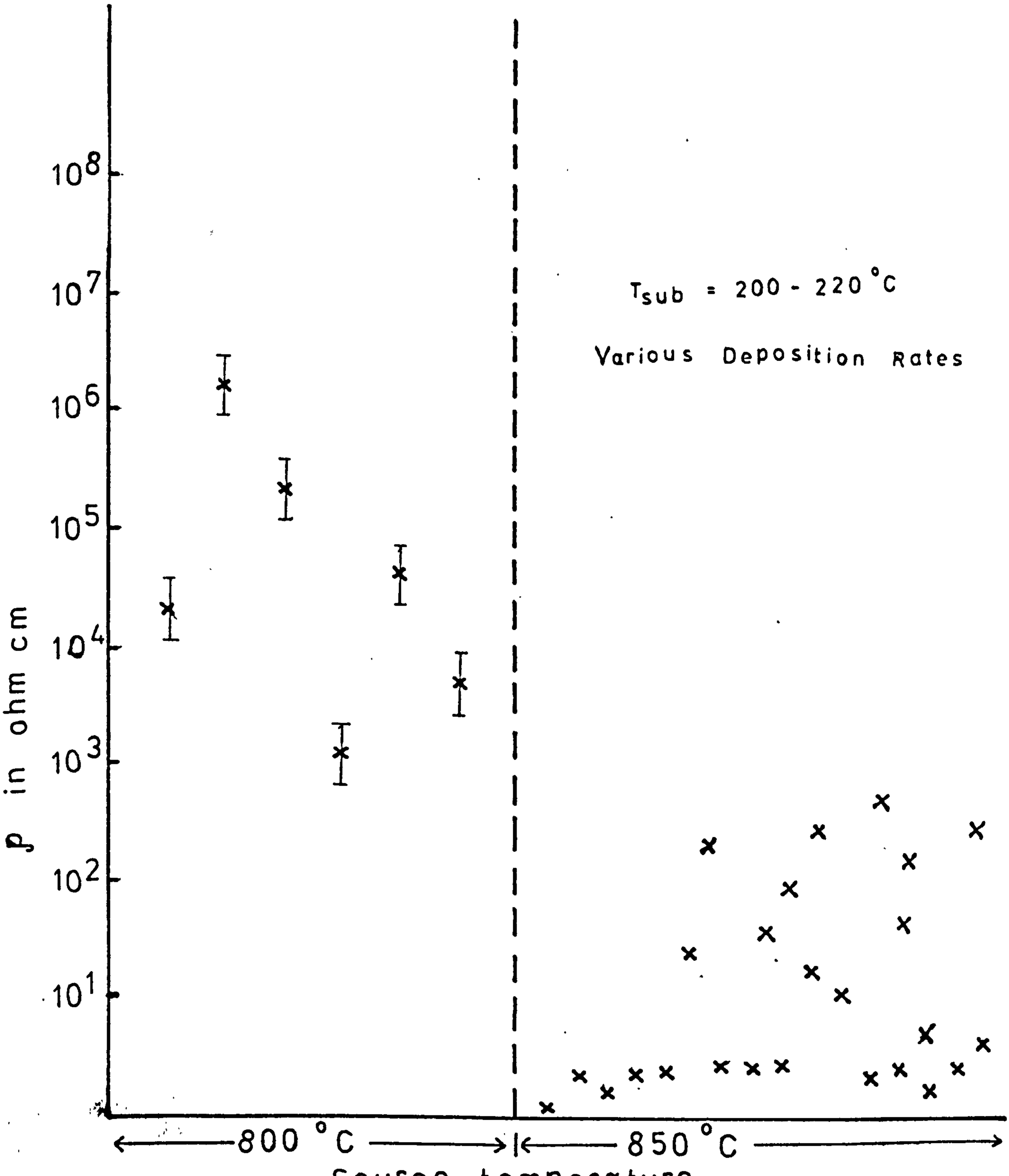

Figure 6.15

Enclosed Films
Resistivity Versus Source Temperature

substrate temperature as shown in Figure 6.16. This corresponded with a colour change from black for films evaporated at $T_{sub} \leqslant 150^{o}C$ to yellow for films evaporated at $T_{sub} \leqslant 300^{o}C$. A standard substrate temperature of $200^{o}C$ was therefore used for most of the films as this proved to be a good compromise between the required low resistivity and reasonable stoichiometry. The resistivity of films prepared by this method varied with deposition rate in a similar way to the resistivity of films grown in enclosed tubes. Figure 6.17 shows that there was a change in resistivity of two orders of magnitude as the deposition rate was increased from 500 to 3000Å/min.

6.7 Film Structure

All the films so far described in this investigation were polycrystalline with a preferred orientation of the c-axis perpendicular to the substrate (Wilson 1971).

It was possible however using the conventional vacuum system to grow epitaxial films of CdS on freshly cleaved (100) faces of rock-salt. Using a resistivity heated source epitaxial films were produced on substrates at $250^{o}C$ using deposition rates up to 15Å/sec. Epitaxial films could be produced using the electron beam system in slightly less stringent conditions, i.e. substrate temperature $250^{o}C$, deposition rate 10-200Å/sec. The degree of control over the enclosed system however was not great enough to allow such films to be grown.

The films were studied by transmission electron microscopy using a JEOL JEM 120 microscope. A typical diffraction pattern from an epitaxial film deposited in

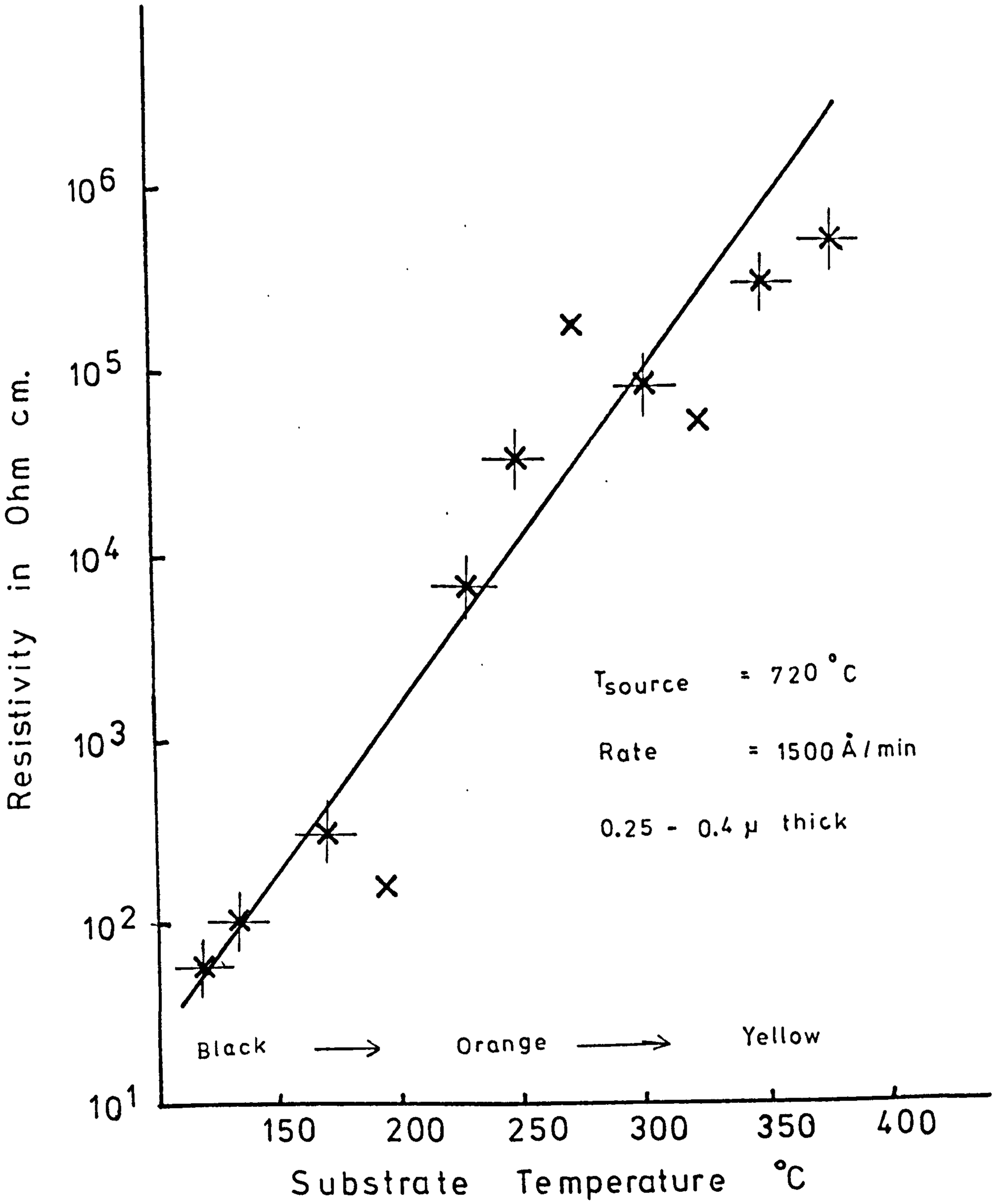

Figure 6.16

Electron Gun Films

Resistivity Versus Substrate Temperature

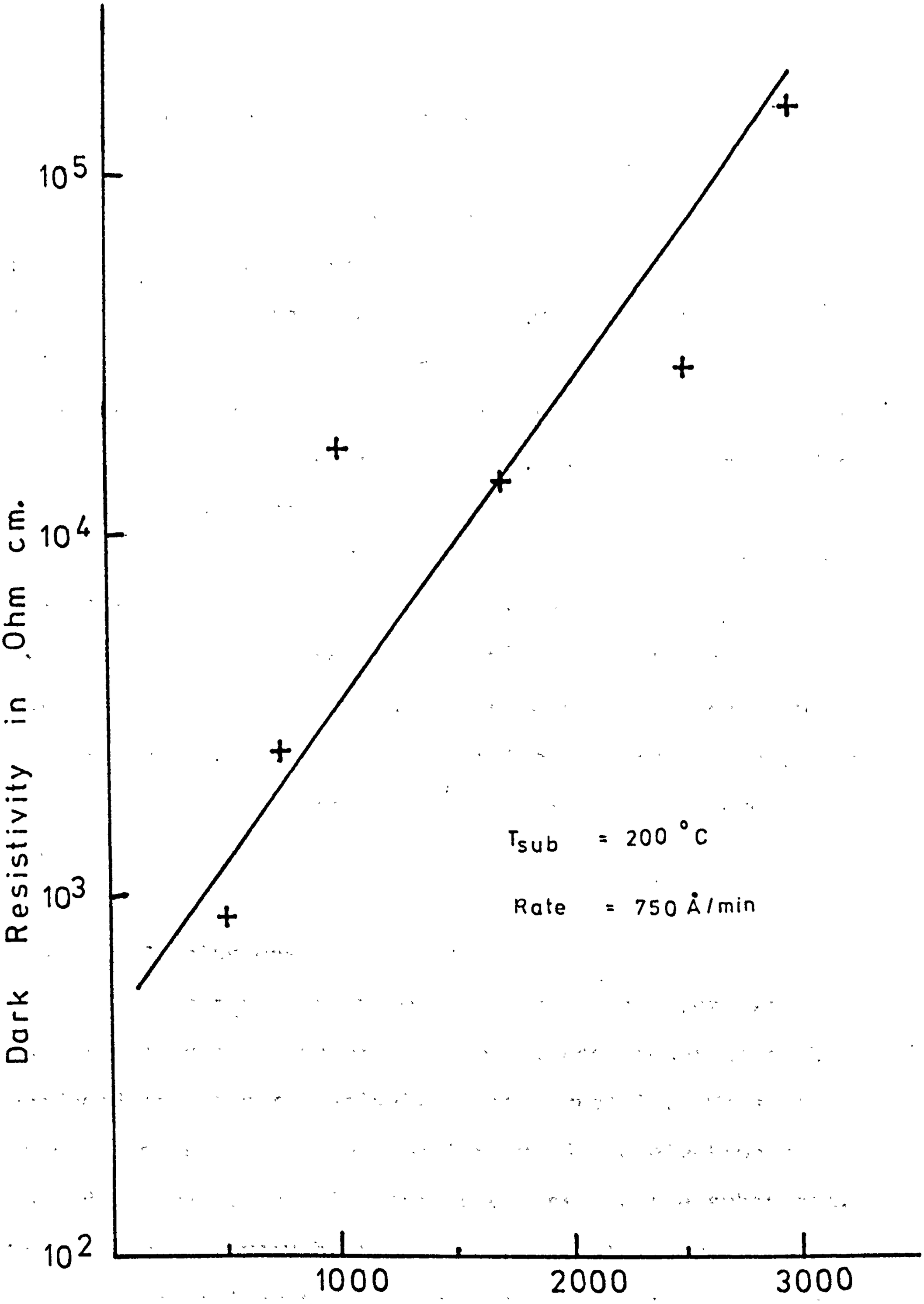

Figure 6.17

Electron Gun Films
Resistivity Versus Deposition Rate

the electron beam system is shown in Fig. 6.18. The pattern shows the film to have a cubic (sphalerite) structure but the splitting of many of the spots indicates the presence of twinning, included grains of hexagonal (wurtzite) structure material or planar defects. Holt and Wilcox (1971) strongly support the idea that this splitting is due to the presence of wurtzite grains in the film whereas Rawlins (1970) attributes the same effect in ZnS on silicon to twinning and double diffraction.

The epitaxial films evaporated from the resistively heated source at 12.8Å/min had dark resistivities around 7×10^5 Ωcm and mobilities of 30 $cmV^{-1}sec^{-1}$. These mobilities were higher than those observed in polycrystalline films of the same resistivity. However as the polycrystalline films were basically hexagonal (Wilson 1971) no valid direct comparison can be made.

6.8 Conclusions

Electron beam evaporation produced layers with dark resistivities one order of magnitude higher than those produced from the resistively heated crucible. This is thought to be due to the superiority of the electron beam method, where no hot filament is exposed to the substrate. With the resistively heated source some atoms from the filament would inevitably be carried on to the substrate and incorporated in the film. In addition, because of the geometry of the electron gun the source vapour passes through the electron beam and becomes charged, which may have a beneficial effect on the alignment of the first

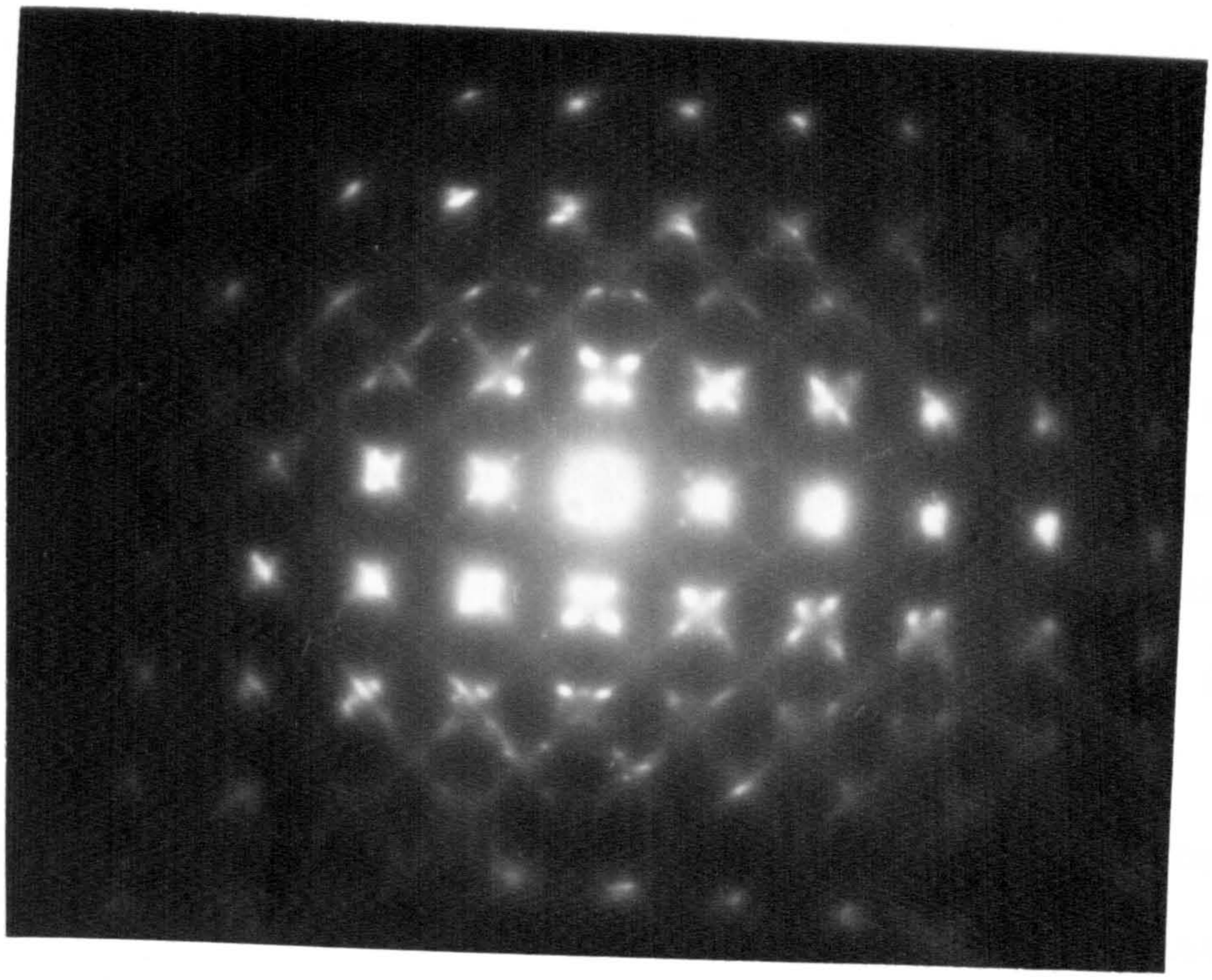

Figure 6.18

Transmission Electron Diffraction pattern ([001] zone axis) from a CdS Thin Film.

few monolayers deposited (Wilson 1971). The electron beam source however has a limited capacity and can only produce very thin layers (≤5 μm). Not only are these too thin for use as solar cells, but the results shown here indicate that their resistivities would be too high.

The method of growing films in the sealed enclosure had the advantage of having no source of contamination in the system other than impurities in the starting material and the silica glass. The method led to reproducible films of low resistivity which look promising for solar cell applications (see Chapter 9). Such a method is however difficult to modify for large area substrates and the inability to measure accurately the absolute values of substrate temperature and deposition rate is an additional drawback.

The following general conclusions can be made regarding the effects of the evaporation parameters on film resistivity:

(i) When evaporating from a single source at a temperature of 800^{o}C or less the resistivity increases as the thickness decreases.

(ii) The resistivity increases with substrate temperature in the range 125^{o}C ≤ Tsub ≤ 375^{o}C.

(iii) Resistivity is dependent on the source temperature and the method of evaporation employed.

(iv) As the deposition rate increases the resistivity of the film also increases.

REFERENCES

Addiss (1963) Trans. 10th Nat. Vac. Symp. p.354

Bujatti (1968) B.J.A.P. 1 581

Davey (1963) Solid State Electron. 6 205

Fleitner (1961) Phys. Stat. Sol. 1 483

Holt and Wilcox (1971) J. Crystal Growth 9 193

Isenberg et al (1948) Rev. Sci. Instrum. 19 685

Learn et al (1966) App. Phys. Lett. 8 144

Rawlins (1970) J. Mat. Sci. 5 881

Schulman (1955) Phys. Rev. 98 384

Shallcross (1966) Trans. Met. Soc. AIME 236 309

Smith (1955) Phys. Rev. 97 1525

Wilson (1971) Ph.D. Thesis, Univ. of Durham

Wilson and Woods (1973) J. Phys. D. 34 171

CHAPTER 7

DISCUSSION OF THE EFFECT OF THE EVAPORATION PARAMETERS ON THE PROPERTIES OF THE THIN FILMS

7.1 Introduction

The object of this chapter is to offer explanations for the experimental observations reported in the previous chapter and to provide some theoretical basis for these suggestions where possible.

The first section of this chapter is concerned with a theoretical study of the evaporation and condensation kinetics following a scheme suggested in an I.R.D. Co. Ltd. report (Syms et al 1966). This scheme was later used by Wilson (1971) to explain his results on CdS thin films evaporated from a resistively heated source and will be discussed now in relation to our films produced by electron beam deposition.

7.2 Evaporation Kinetics

7.2.1 CdS Vapourisation

We shall now study the process by which a source of CdS is vapourised and subsequently condensed on a heated surface.

Somorjai and Jepsen (1964) have studied the evaporation mechanism of CdS single crystals and have suggested this takes place in the following four stages:

$$CdS\ (solid) \rightleftharpoons Cd\ (surface) + S\ (surface)$$

$$Cd\ (surface) \rightleftharpoons Cd\ (gas)$$

$$2S\ (surface) \rightleftharpoons S_2\ (surface)$$

$$S_2\ (surface) \rightleftharpoons S_2\ (gas)$$

It is the first of these which is the rate controlling process and gives rise to a lower evaporation rate than that calculated from vapour pressure measurements using Langmuir's equation;

$$R = 5.83 \times 10^{-2} P (MT)^{-\frac{1}{2}}$$

where R is the evaporation rate in moles cm^{-2} s^{-1}

P is the saturated vapour pressure in torr

M is the molecular weight of the evaporant

and T is the temperature.

The ratio of the experimental values of the evaporation rate and this equilibrium value, R, is given by a factor 'a', the so-called evaporation coefficient. 'a' has a value of around 0.1 for the 0001 face of CdS but is temperature dependent. The values for other faces of CdS crystals are usually different but Somorjai and Stemple (1964) suggested that crevices form on some faces to expose small c facets, so it will be assumed therefore that for a source formed from crushed flow crystals 'a' has the value characteristic of a uniform c-face. The following additional assumptions will also be made; (i) that the evaporation of CdS is congruent and (ii) that no CdS molecules exist in the vapour with the source temperature employed.

For convenience of comparison with the results of Wilson (1971) the power supplied to the electron gun was regulated to give a source temperature of 725°C which was measured using a NiCr/NiAl thermocouple in thermal contact with the molybdenum crucible on the electron gun. At this source temperature the deposition rate was 1500Å/min.

Using the data obtained by Somorjai and Stemple (1964) for the evaporation rate of CdS from a base plane, which is shown in Figure 7.1, the evaporation rate from the crucible employed (surface area 0.8cm^2) is calculated to be

$$1.00 \times 10^{-6} \text{ moles of CdS } s^{-1} \text{ at } 725^{\circ}C.$$

From this value we can find the impingement rates of CdS on a small substrate held directly above the source at a distance of 10cm. Assuming the vapour from the crucible follows a cosine distribution law the quantity of vapour striking the substrate from a source at 725°C is found to be

$$3.18 \times 10^{-9} \text{ moles cm}^{-2} \text{ s}^{-1}$$

This impingement rate for CdS can be used to obtain the fluxes of cadmium and sulphur vapour at the substrate, remembering that the evaporation is congruent. At 725°C these are as follows:

$$3.18 \times 10^{-9} \text{ moles of Cd cm}^{-2} \text{ s}^{-1}$$

$$3.18 \times 10^{-9} \text{ moles of S cm}^{-2} \text{ s}^{-1} \quad \text{or}$$

$$1.59 \times 10^{-9} \text{ moles of } S_2 \text{ cm}^{-2} \text{ s}^{-1}$$

7.2.2 Effect of Substrate Temperature

What happens to the Cd and S_2 on reaching the substrate depends on the substrate temperature. The first process which occurs is that of nucleation. For any particular substrate and impingement rate, there will be a critical temperature above which nucleation will not occur. The critical temperatures for Cd and S_2 are rather low and it is unlikely therefore that the nucleation of the film

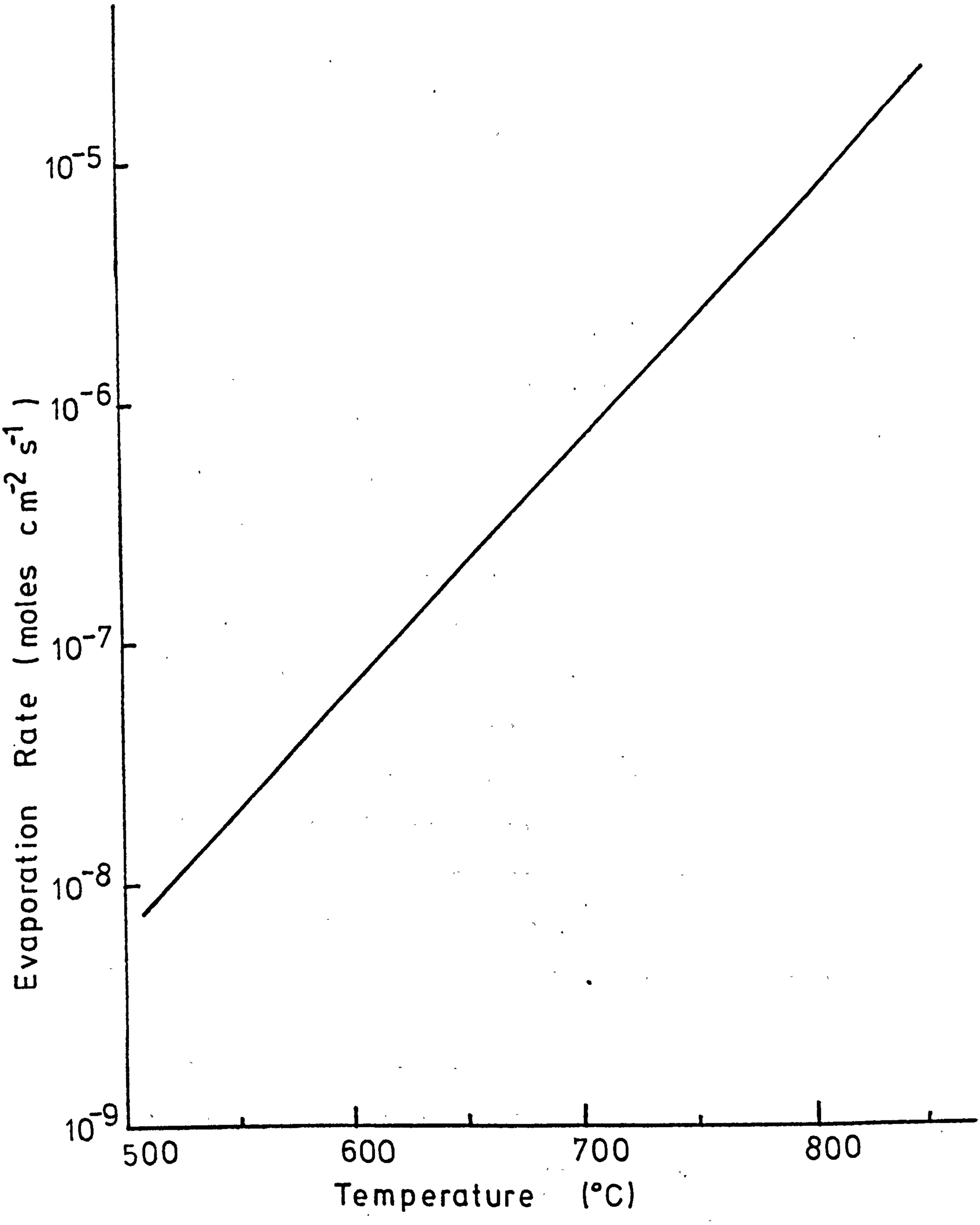

Figure 7.1

Evaporation Rate of CdS c-Face

(Somorjai and Stemple 1964)

is initiated by either Cd or S_2. It is more likely that nucleation will occur through Cd and S_2 combining on the surface of the substrate by the reverse reactions to those which occur on vapourisation. CdS will then nucleate on the substrate surface at a higher critical temperature than that for either Cd or S_2 at any given impingement rate. Once the nucleated layer has been formed condensation can take place at preferential sites in the film such as steps.

At temperatures below 600°C the stable configuration of sulphur molecules is S_8. It is therefore probable that a competing reaction to the formation of CdS (solid) will be the formation of S_8 (surface) from 8S (surface). The S_8 surface species will then condense fully or vapourise according to the substrate temperature. If the re-evaporation rate is high excess cadmium will be left on the substrate. Eventually as the substrate temperature is further increased the excess cadmium will also have a high rate of re-evaporation and only CdS will be deposited until a temperature is reached above which no deposit will be formed at all.

This description provides a qualitative explanation of the varying properties of CdS films prepared under different conditions. As the substrate temperature is increased over a series of films with the evaporation rate fixed the compositions of the various films will change from having excess free cadmium and sulphur, to excess cadmium, to stoichiometric CdS until it eventually becomes increasingly difficult to form any deposit at all.

7.2.3 Condensation and Re-evaporation

We now require to calculate the condensation rates of cadmium, sulphur and cadmium sulphide as a function of substrate temperature to gain an idea of the magnitudes of the critical temperature. If it is assumed that the condensation coefficients of Cd and S_2 are unity at all practical substrate temperatures i.e. all the Cd and S_2 impinging on the substrate sticks, at least momentarily regardless of substrate temperature, then the condensation rates of Cd and S_2 will be identical to the impingement rates. Some of the surface cadmium and sulphur will then combine to form cadmium sulphide whilst the remainder re-evaporates.

We now require to calculate the rate of formation of CdS on the substrate. As we have assumed that the CdS dissociates completely when it evaporates from the source, no CdS molecules arrive at the substrate, and so the rate of formation of CdS cannot be calculated directly. We shall suppose that the mechanism of condensation on the substrate is the exact opposite of evaporation and use the product of the impingement rate of "CdS" and the evaporation coefficient of CdS as a good approximation to the rate of formation (condensation) of CdS. The use of a condensation coefficient (in this case equal to the evaporation coefficient) allows for the fact that not all the Cd and S_2 will go to form cadmium sulphide but some will form other phases or re-evaporate. Therefore the rate of condensation of CdS will be obtained from the CdS impingement rate and the temperature dependent

evaporation coefficient of CdS which has been measured by Somorjai (1964a) and which is reproduced in Figure 7.2.

The next step is to calculate the rate of re-evaporation of Cd, S_8 and CdS from the substrate. This can be done for Cd and S_8 by using the reported saturated vapour pressure (S.V.P.) curves and Langmuir's formula with an evaporation coefficient. From the "Handbook of Physics and Chemistry" (45th edition) we have S.V.P. of Cd as shown in Figure 7.3, which follows the following formula:

$$\log_{10} P_{Cd} \text{ (torr)} = 8.564 - \frac{5693.07}{T^{o}K}$$

The evaporation and condensation coefficients are taken as unity.

The measured S.V.P. of S_8 (Figure 7.3) is due to Bradley (1951) who determined the following formula and obtained a temperature independent value of 0.73 for the evaporation coefficient.

$$\log_{10} P_{S_8} \text{ (torr)} = 9.763 - \frac{5240}{T^{o}K}$$

The calculated evaporation rates of Cd and S_8 from a heated substrate are given in Figure 7.4. These were first calculated by Wilson (1971). The evaporation rate of CdS from the substrate is taken from the extrapolated data of Somorjai and Stemple (1964) as shown in Figure 7.5.

The last stage in the calculation is to find the actual composition of a film deposited on a heated substrate from a source at 725°C. To do this we require to use a sticking factor defined as the ratio of the evaporation rate from the substrate to the condensation

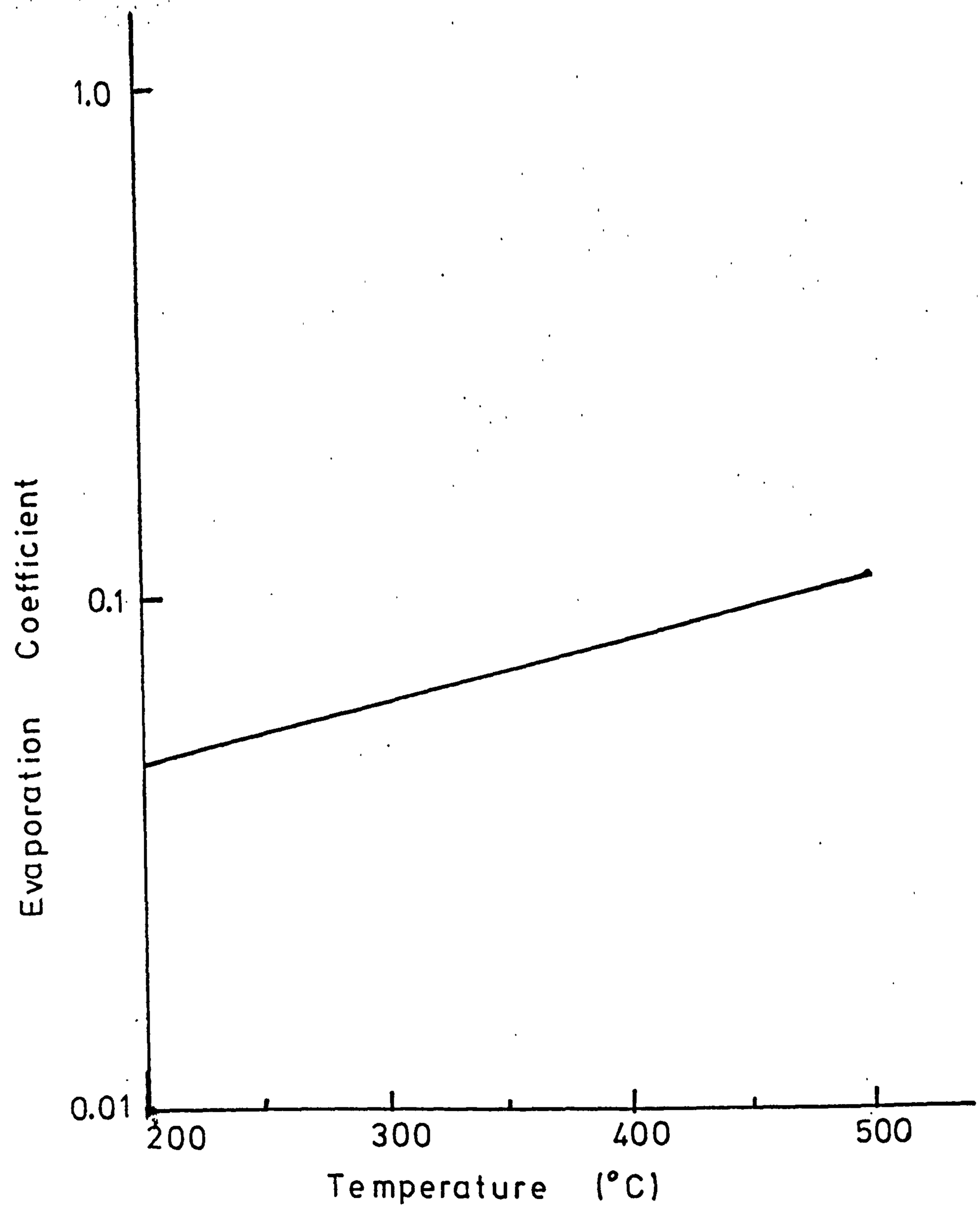

Figure 7.2

Evaporation Coefficient of CdS
(Somorjai 1964)

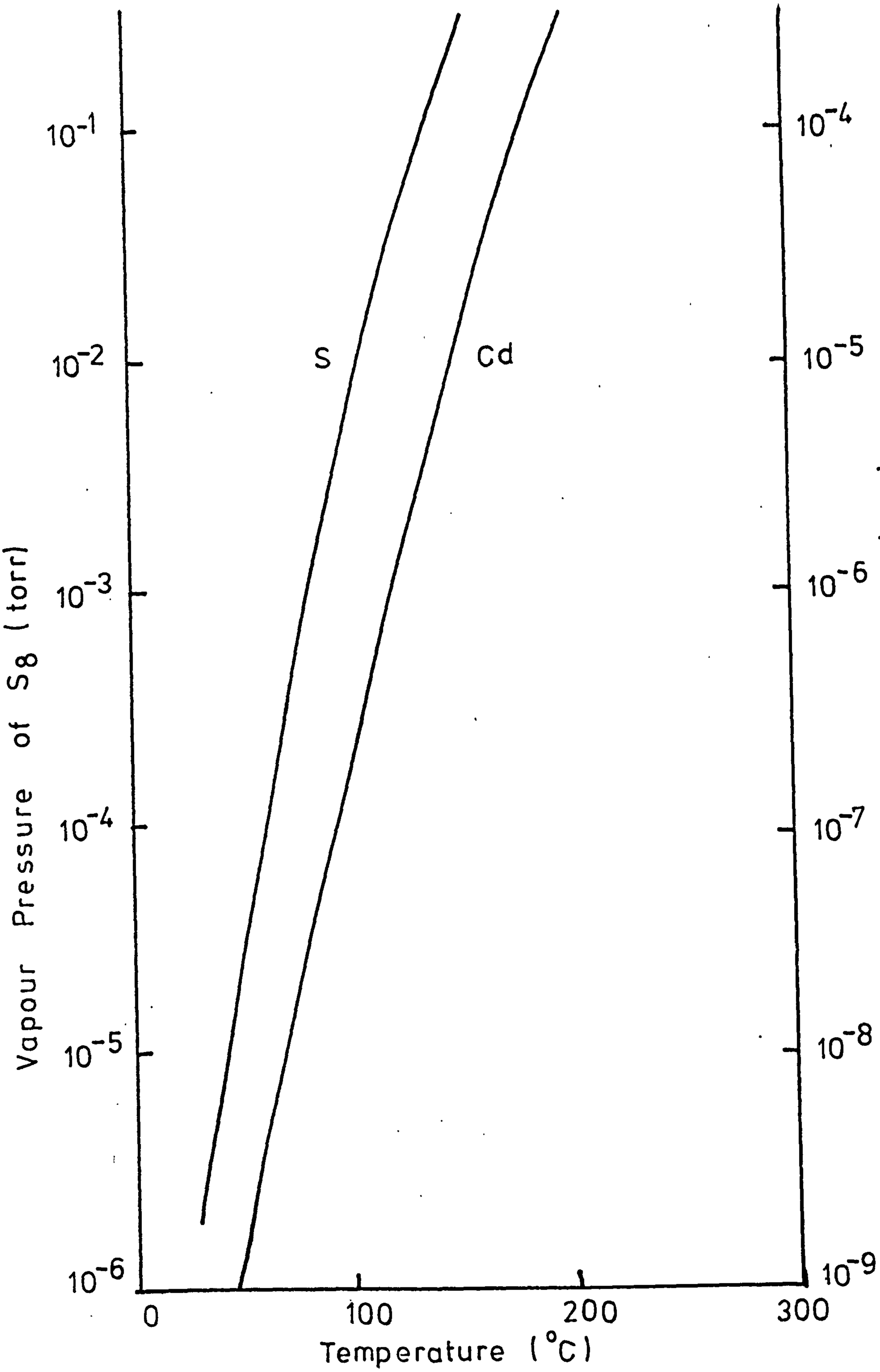

Figure 7.3
S.V.P. of Cd and S_8

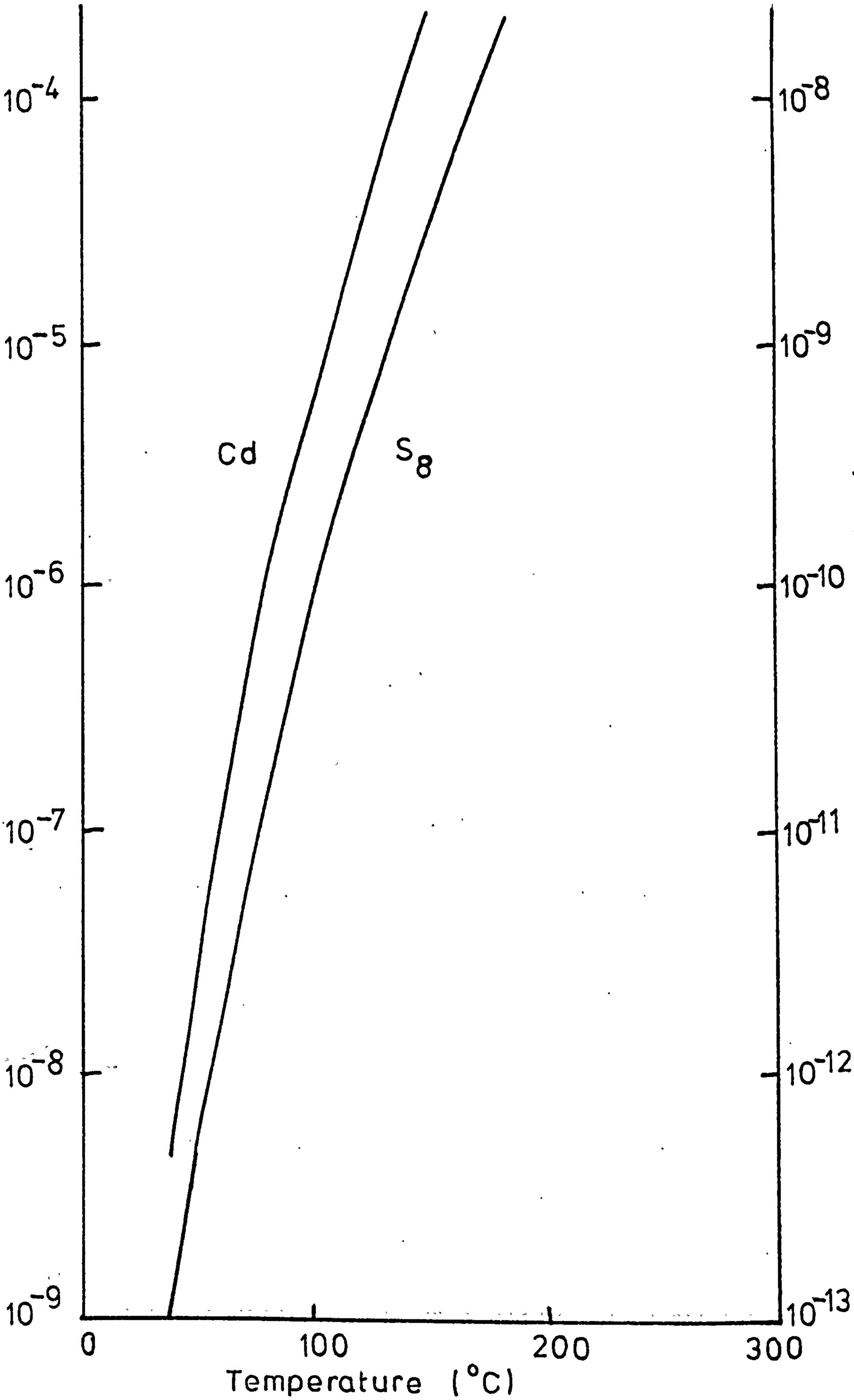

Figure 7.4

Evaporation Rates Of Cd And S_8
(Wilson 1971)

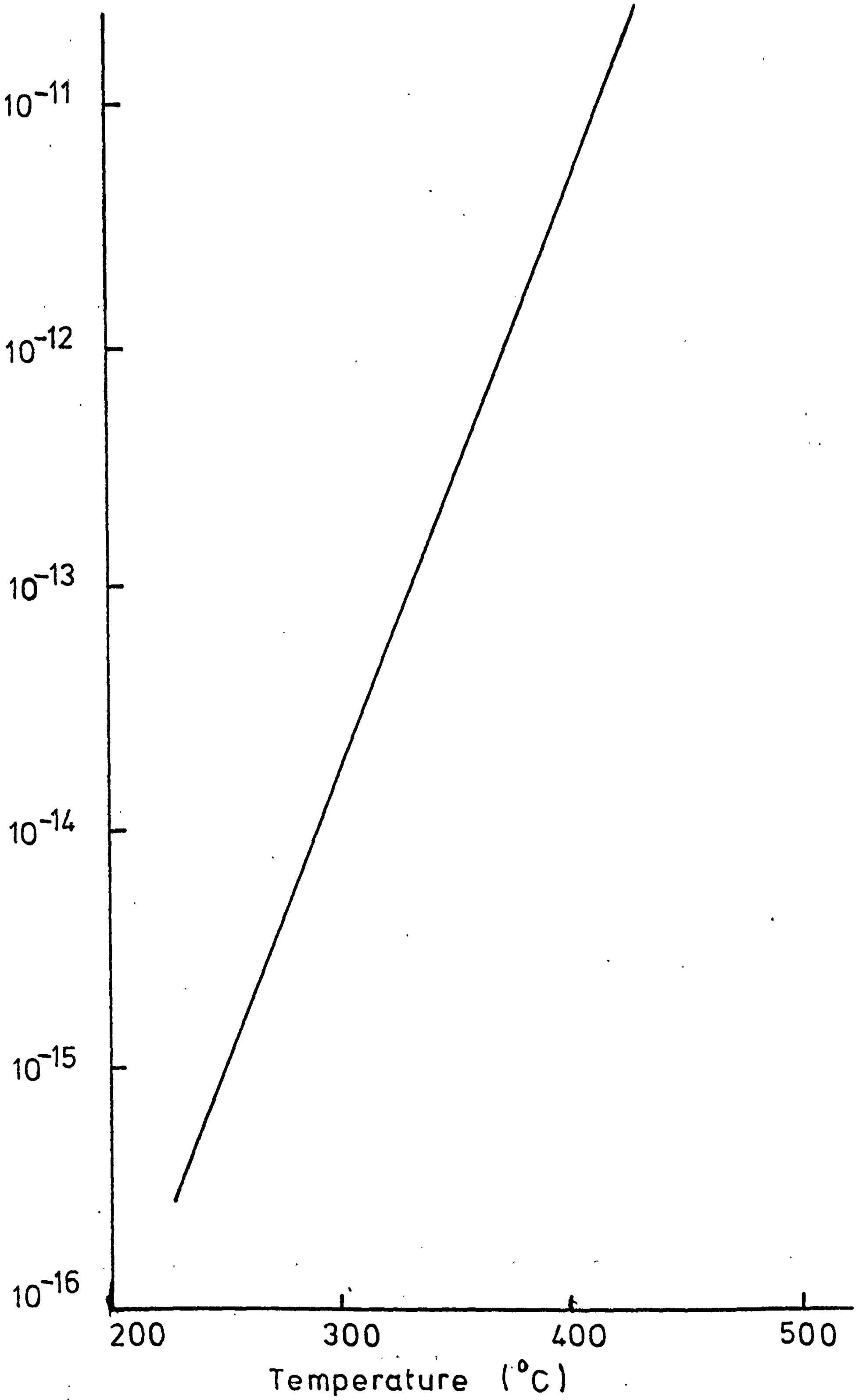

Figure 7.5

Evaporation Rate Of CdS C-Face
(extrapolated)

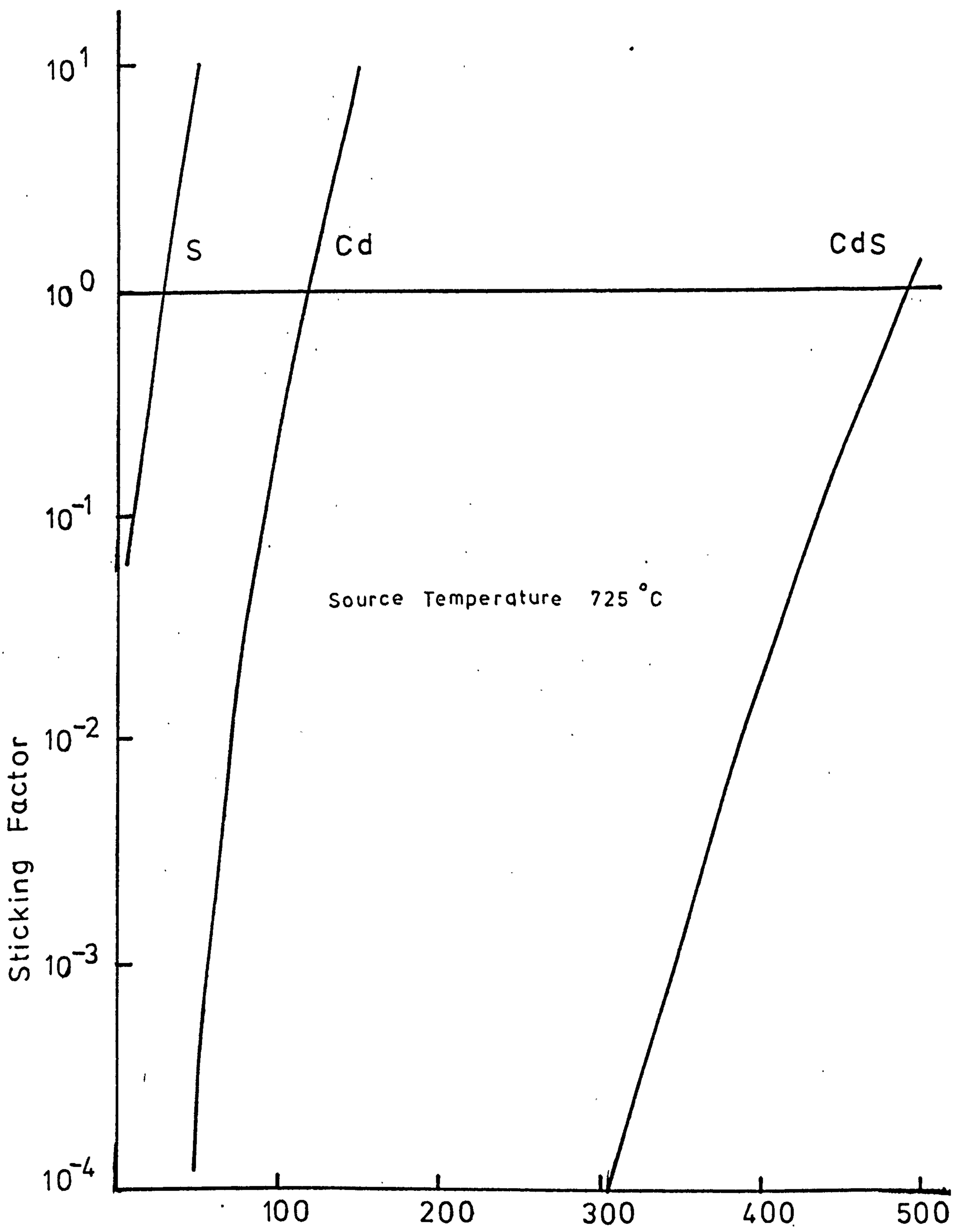

Figure 7.6

Sticking Factors For Cd, S, CdS

rate on the substrate. Values of this coefficient for Cd, S and CdS are shown in Figure 7.6. For values less than unity a deposit will form, for all values greater than unity no deposit will form. From this we find that for a source temperature of 725°C

(i) no free sulphur will form if the substrate temperature is above 28°C,

(ii) no free cadmium will form if the substrate temperature is above 117°C, and

(iii) there will be no deposit at substrate temperatures above 490°C.

7.2.4 Changes in Film Composition

These results show that there will be a gradual change in the composition of a series of films as the substrate temperature is increased. This explains the observed change in colour mentioned in Chapter 6.

At low substrate temperatures the excess cadmium present in the films makes them appear black and results in a low resistivity. In the range of substrate temperatures employed in the experimental work, namely 200-220°C, no free S or Cd normally exists and therefore the films have high resistivities. At much higher deposition rates however (i.e. higher source temperatures) excess cadmium is again deposited and films of lower resistivity are produced.

By calculating the critical substrate temperature for a variety of source temperatures (Table 7.1) it can be shown that it is the substrate temperature which has the major influence on the film composition. The effect of

TABLE 7.1

Critical substrate temperatures and source temperatures

Source temperature (assumed proportional to deposition rate)	Substrate temperature above which no free sulphur will form	Substrate temperature which which no free cadmium will form	Substrate temperature above which no deposit will form
680°C	20°C	106°C	460°C
700°C	24°C	112°C	480°C
725°C	28°C	117°C	490°C

the deposition rate is only secondary.

The results show that with a source at 725°C there would be no deposition on a substrate above 490°C and that it would be increasingly difficult to form a film above 400°C. This is somewhat higher than the value determined experimentally where it was found to be impossible to deposit films on substrates above 375°C. The validity of the assumptions used in the calculation must therefore be questioned.

7.2.5 Validity of the Assumptions

Wilson (1971) explaining why the observed critical temperature values were lower than those calculated suggested the discrepancy might be associated with errors in the assumptions made (1) concerning the physics of the mechanisms of evaporation/condensation process or (2) concerning the geometry and surface temperature of the source. The results described here led to the same discrepancy when an entirely difference source was used and consequently we conclude that it is the assumptions made concerning the physics of the evaporation/condensation process which are incorrect. We list below several reasons why these assumptions might be invalid:

(a) Evaporation and condensation are not the exact inverse of each other. In evaporation all the atoms are initially bound to the surface whereas in condensation some atoms may re-evaporate before bonding to the surface. This would lead to an inequality between the evaporation and condensation coefficients and lead to a lower critical

temperature than that previous calculated.

(b) Somorjai (1964b) suggested that the evaporation rate of CdS at a given temperature is reduced when the material is illuminated. This effect would also lower the maximum substrate temperature.

(c) It has been assumed that the evaporation coefficient 'a' is the same for crushed flow crystals as for the c-face of single crystals. An increase in 'a' above the c-face value would increase the impingement rate at a given temperature and give better agreement between the observed and calculated critical temperatures.

(d) The evaporation and condensation coefficients for cadmium are assumed to be unity. This is a reasonable assumption for a metal and for the sulphur S_2 molecule which has a low vapour pressure. However sulphur evaporates from the substrate as S_8 and this has a higher vapour pressure than the S_2 molecule.

(e) The degree of dissociation of CdS has been assumed to be 100%. Any deviation from this value would change the calculated impingement rates.

(f) The growth of the film may not take place via the recombination of Cd and S but from CdS molecules (Caveney 1970). However the qualitative agreement between the experimental results and the calculations strongly supports the idea that the CdS vapour in the vacuum system is completely dissociated.

Finally mention should be made of the use of the "hot-wall" in the resistively heated system. This has the effect of trapping the S_8 molecules close to the substrate,

thus ensuring that sulphur was not lost rapidly from the substrate by condensation on the cold surfaces of the apparatus. Its use resulted in the formation of stoichiometric CdS over a wider range of substrate temperatures than would otherwise have been possible.

7.2.6 Conclusions

Despite the uncertainties in the processes involved, the calculations provide reasonable explanations for the results described in Chapter 6. The theory predicts the dominance of substrate temperature over deposition rate in determining the properties of the film. Some dependence of resistivity on source temperature (deposition rate) is predicted by the theory but it does not explain the tremendous changes in resistivity observed in films grown in the enclosed system from sources at 800°C and 825°C. The reasons for this could be two-fold:

(1) The assumptions made may be even more questionable in the 'equilibrium situation.' There is certainly no direct dependence of source temperature on deposition rate in this method.

(2) The change in composition (and therefore resistivity) may be brought about by a mechanism completely different from that described above. This will be discussed in more detail later in this chapter.

7.3 Transport Properties

7.3.1 Film thickness effects

We have already seen that the variation of the

mobility with thickness (Figure 6.8) in films grown in an enclosed tube is insufficient to explain the decrease in resisitivity which occurs with increasing thickness (Figure 6.6). The decrease is in fact due to a change in carrier density with thickness (Figure 6.7).

Decreases in the resistivity of II-VI compound films with thickness have been reported previously and attributed to a variety of effects. For example Berger et al (1969) explained the effect in CdSe films as due to an increase in the size of the micro-crystallites in the film which manifests itself in terms of an increasing mobility. Vergunas (1967) suggested that the resistivity of CdS films decreased because of an increasing fibre axis orientation. This again would affect the mobility not the carrier density and the results reported here show that the decrease in resistivity is associated with an increase in carrier concentration. Furthermore Wilson and Woods (1973) have shown that in similar films the preferential orientation does not appear to change over a wide enough range of thickness to account fully for the observed changes in resistivity.

The other possible explanation of the decrease in resistivity is that the film changes its composition during growth. There are three possible ways in which this might happen:-

(1) The impurity content of the source might increase with time, particularly with resistively heated sources.

(2) A gettering process might occur, particularly in an open vacuum system.

(3) The excess cadmium content of the film might increase with time.

Wilson and Woods discounted the first two possibilities and our results with the closed system demonstrate that this was justifiable. Now CdS is believed to evaporate congruently under equilibrium conditions, i.e. the vapour has the same composition as the source. It is therefore possible to obtain a vapour which changes composition with time if the source itself changes composition with time. Somorjai and Jepsen (1964) have shown that a source rich in Cd or S has a different evaporation rate from a stoichiometric source but that the evaporation remains congruent. To explain the observed effects it is therefore necessary that the source becomes more Cd rich with time.

The solid equilibrium area of the CdS composition versus temperature diagram is of the shape shown in Figure 7.7 (Shiozawa et al 1968). The P_{min} locus shows the composition which has the lowest vapour pressure at any given temperature, i.e. the equilibrium condition. The partial pressures of cadmium and sulphur are related by the equilibrium constant of the reaction:

$$2CdS\ (solid) = 2Cd\ (gas) + S_2\ (gas)$$

as follows: $$K = p_{Cd}^2 \times P_{S_2}$$

If $P = P_{Cd} + P_{S_2}$, the lowest total pressure P_{min} is obtained when

$$\partial P/\partial P_{Cd} = \partial P/\partial P_{S_2} = 0 \quad \text{(Lorentz 1967)}$$

Consequently a source heated to 800°C will tend towards a

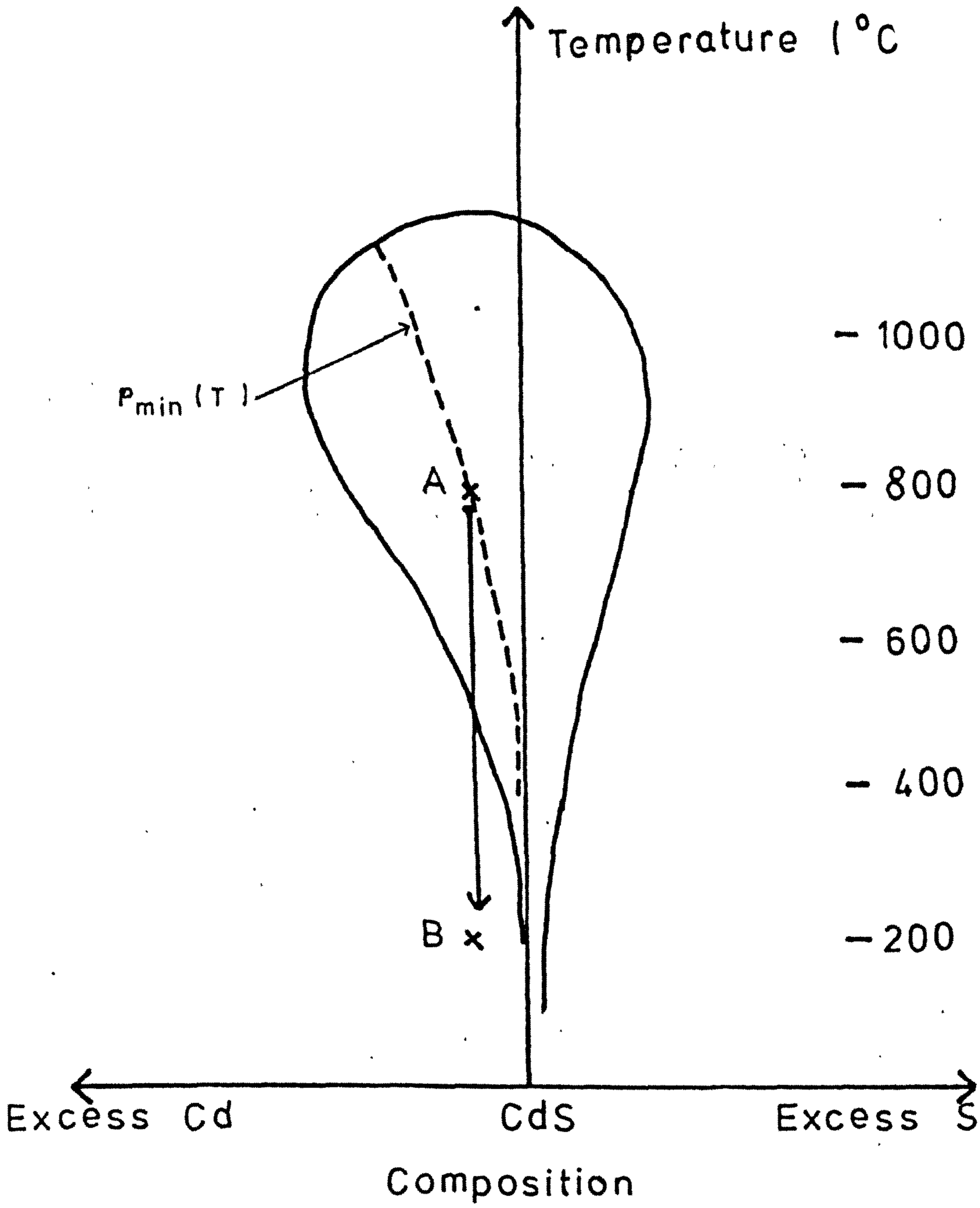

Figure 7.7

CdS Phase Diagram

point 'A' in composition and will become cadmium rich. The crux of the problem is the time taken to achieve this condition. If it takes many minutes the source will only reach a stable composition towards the end of the evaporation. If the change is rapid then the swing towards cadmium rich CdS will be completed during outgassing. The results obtained from consecutively evaporated films (Figure 6.10) indicate that, when the source is heated resistively to evaporation temperature (720^{o}C) in a conventional high vacuum system, this process takes approximately 50 minutes. This would explain the observed variation in resistivity with thickness.

A second look at the phase diagram shows that when the vapour in state A strikes a substrate and is cooled to a temperature represented by B, there will be more cadmium present than can exist in CdS. This cadmium must form a second phase or re-evaporate.

The results shown in Figures 6.9 and 6.10 which were obtained with an open system, demonstrate clearly that the decrease in resistivity is not a function of the actual thickness of the film, but of the length of time during which the source has been heated to the evaporation temperature prior to the deposition taking place. The results obtained from the samples deposited in the electron beam system (Figures 6.11-6.13) confirm this. The gun has a multiple source, so that the time each crucible is held at the evaporating temperature is much smaller than in the case of a resistively heated source. The variation in resistivity of these films with thickness

(Figure 6.11) is mostly due to an increase in carrier concentration but is also due to a change in mobility (Figure 6.13). This change in mobility can be explained in terms of the Fleitner surface scattering model in the same way as the change observed in the enclosed films evaporated from a source at 800°C.

We conclude therefore that a film deposited in the closed system from a source at 800°C becomes increasingly rich in cadmium as the evaporation proceeds. We also conclude that if the evaporation were continued for a much longer time the resistivity of the film would approach that of the films evaporated from a source at 850°C. The latter films presumably went through a similar cycle but on a much faster time scale so that they reached an equilibrium situation in the time required to form the thinnest film examined.

A final point to clarify is that if the source and the deposited film in a closed container both become cadmium rich, sulphur must segregate out somewhere within the system. In our system some deposition occurred on the walls of the silica tube near its seal-off point behind the substrate. This deposit was pale yellow in colour and probably contained CdS and excess sulphur. (In an open system the sulphur goes preferentially to exhaust).

7.3.2 Photosensitivity

All the films produced in the conventional high vacuum system were photosensitive to some extent (Figure 6.2)

but showed no photoluminescence under ultra-violet excitation at 77 K. Wilson (1971) showed that the photosensitivity of such films was due solely to the photocreation of carriers and not to any change in carrier mobility. These results were in agreement with Espevik et al (1971) who reached a similar conclusion for polycrystalline layers of PbS.

It is interesting to note that the films evaporated in a closed system at 850°C displayed no appreciable photoconductive effects and were non luminescent. The films evaporated at 800°C were luminescent (see Chapter 8) and displayed substantial photoconductive effects. These properties suggest that the films evaporated at 800°C approximate more closely to the bulk material than films evaporated at a higher source temperature or in a conventional system.

7.3.3 Hall Effect

The variation of mobility with thickness for films grown in the enclosed system from a source at 800°C (Figure 6.8a) was explained in terms of a surface scattering model in which the bands were assumed to be flat (Fleitner 1961). The mobility variation of the films deposited in the electron beam system (Figure 6.13) can be explained in the same way and Wilson and Woods (1973) used the same theory to explain the mobility variation with thickness in their CdS films evaporated from a resistively heated source. However the almost constant value of the mobility of films deposited in an enclosed system from a source at

850^{o}C (Figure 6.8b) is contrary to this theory. No explanation can be found for this anomaly other than to suggest that in such highly conducting crystallites (i) the flat band approximation is invalid or (ii) diffuse scattering at the surface of the film is not the chief factor determining the electron mobility.

REFERENCES

Berger et al (1969) Phys. Stat. Sol. 33 417

Bradley (1951) Proc. Roy. Soc. (London) 205A 553

Caveney (1970) J. Cryst. Growth 1 102

Espevik et al (1971) J.A.P. 42 3513

Fleitner (1961) Phys. Stat. Sol. 1 438

Lorentz (1967) II-VI Semiconducting compounds (ed. Thomas. pub. W.A. Benjamin Inc.)

Shiozawa et al (1968) Aerospace Research Labs. Report ARL 69-0155

Somorjai (1964a) Proc. Int. Symp. on Evap. and Condens. of Solids. Ohio 1962 (Gordon and Breach)

Somorjai (1964b) Surface Science 2 298

Somorjai and Jepsen (1964) J. Chem. Phys. 41 1389 and 1394

Somorjai and Stemple (1964) J.A.P. 35 3398

Syms et al (1966) I.R.D. Co. Ltd. Report 66-63

Vergunas et al (1967) Sov. Phys. Crystallog. 11 420

Wilson (1971) Ph.D. Thesis. Univ. of Durham

Wilson and Woods (1973) J. Phys. D. 34 171

CHAPTER 8

LUMINESCENCE IN CdS THIN FILMS

8.1 Introduction

The word luminescence describes the emission of radiation in excess of thermal radiation which results when a material adjusts itself from an excited to a ground state. The material must previously have been stimulated into the excited state. The form of stimulation is denoted by a prefix to the word luminescence and the phenomena of particular relevance to II-VI compounds are described below.

(1) Photoluminescence, in which the excitation is accomplished by the absorption of photons. The wavelengths of which may be in the infra-red, visible, ultra-violet or x-ray region of the spectrum.

(2) Cathodoluminescence which results when a material is bombarded by high energy electrons or cathode rays.

(3) Electroluminescence, where the excitation is produced by means of an A.C. or D.C. field applied across the crystal.

(4) Thermoluminescence which is actually a misnomer as the electrons are not initially excited thermally. Instead, the electrons are excited by other means at very low temperatures and become trapped in states lying in the forbidden-energy region. The low temperature retards the emptying of these states, so that luminescence does not occur until the temperature of the material is subsequently increased.

(5) Triboluminescence where the excitation is mechanical and is produced by briskly rubbing or abrading

the surface of a specimen.

The present investigation was concerned only with the photoluminescence of CdS films excited with ultraviolet radiation.

A particular feature affecting the luminescence of II-VI compounds is the presence of exciton states. Radiative recombination of excitons leads to the appearance of sharp lines on the long wavelength side of the absorption edge which for CdS lies at about 4800Å at 4.2 K. Excitons are bound electron-hole pairs which can be described in terms of "hydrogenic" levels close to the conduction band. These levels provide a series of discrete parabolic bands below the bottom of the conduction band.

The band-edge luminescence from CdS crystals at low temperatures (<25 K) is known to consist of both (1) sharp lines resulting from the recombination of free or bound excitons and (2) broad bands resulting from the recombination of holes bound at acceptors with either free electrons or electrons bound to shallow donors. The identification of the free and bound exciton states was made by Thomas and Hopfield (1959, 1962) and Hopfield and Thomas (1961) and subsequently by many other workers. The broad bands observed at 4.2 K were shown by Thomas et al (1964) and Colbow (1966) to result from the radiative recombination of a hole bound to an acceptor and an electron bound to a donor.

The model proposed by Pedrotti and Reynolds (1960) to explain the broad band emission in the green is illustrated in Figure 8.1. It assumes the presence of a shallow donor level and a somewhat deeper acceptor level

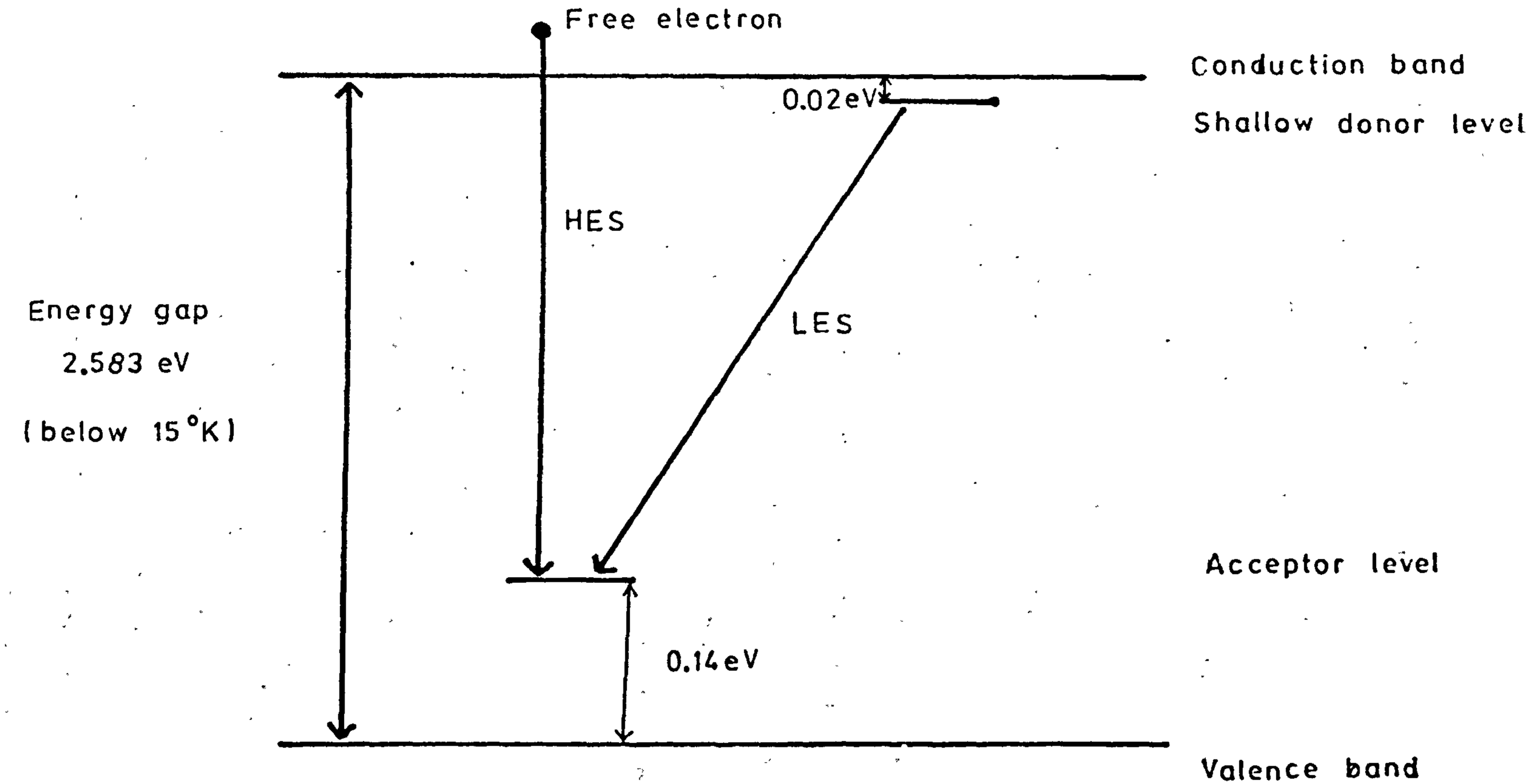

Figure 8.1

Band Diagram Of CdS

(Pedrotti and Reynolds)

in the forbidden gap. At 4.2 K radiative recombination between a bound electron in a shallow donor level and a bound hole in an acceptor produces an emission band. On the low energy side of this band further bands are observed which are due to the simultaneous emission of one or more longitudinal optical phonons. These additional bands are known as phonon replicas. They occur at known phonon intervals and have no corresponding absorption lines (Thomas and Hopfield 1962). This group of bands is called the Low Energy Series (L.E.S.) emission.

At 77 K the electrons in the shallow donor levels are thermally excited into the conduction band, so that the observed luminescence is due to the recombination of free electrons from the conduction band with bound holes. This band also has phonon replicas and the group is known as the High Energy Series (H.E.S.) emission. A knowledge of the wavelengths of these series and the band gap of CdS enables the donor and acceptor depths to be calculated. Pedrotti and Reynolds concluded that the shallow donor state lay 0.022 eV below the conduction band and the acceptor level 0.14 eV above the valence band.

The characterization of near band-edge luminescence from vacuum deposited CdS films has not received much attention. Shalimova et al (1964) observed green photoluminescence in polycrystalline films formed by sublimation. With films deposited at substrate temperatures below 350^{o}C, a very weak structureless peak centred around 5250$\mathring{A}$ was observed at 77 K. Vlasenko et al (1966) deposited CdS on glass substrates at room temperature in a vacuum of 10^{-5} torr.

The films were nonluminescent following deposition, but thermal processing in the presence of Group III donor elements or sulphur vapour led to the production of green emission at 77 K. Conradi (1969) studied the cathodoluminescence (at 4.2 and 77 K) from CdS films deposited on substrates at 100°C. No further heat treatment was given. The main spectral features observed were a single peak in the blue at 4890Å together with a structured green emission in the region from 5100-5500Å. Similar results were obtained by Bleha and Peacock (1970).

Of the films studied in the present work only those deposited in an enclosed tube from a source at 800°C showed any photoluminescence. The emission from two such films deposited at 50Å/min on substrates at 220°C was studied in detail; viz. Film E36 1.5 μm thick with a resistivity of $1x10^3$ cm and Film E41 0.3 μm thick with a resistivity of $1x10^5$ Ωcm. The difference in the resistivities was entirely due to the thickness effect described in Section 6.5.

8.2 Experimental Details

8.2.1 Cryostat

The film samples were mounted in an all metal helium cryostat shown diagrammatically in Figure 8.2 which was manufactured by the Oxford Instrument Co. Ltd. A conventional vacuum system incorporating an Edward's ES 150 rotary pump and EO1 oil diffusion pump was used to evacuate the cryostat.

Indium was used to attach the film to the cold copper finger. The cold finger was detached from the cryostat and heated until the indium covering the sample area

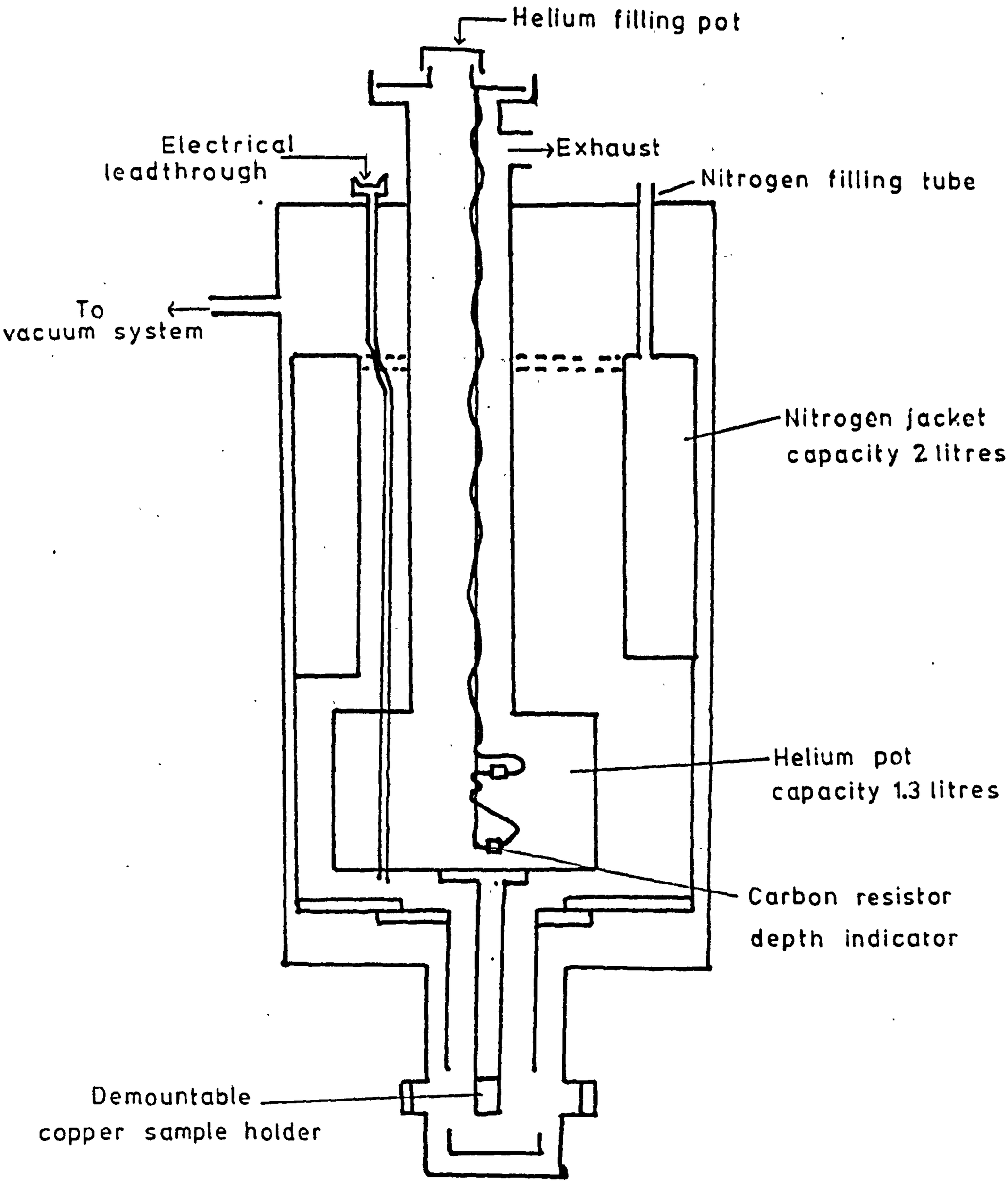

Figure 8.2

Metal Helium Cryostat

was molten. The heating was then stopped and the film and substrate placed on the indium before it resolidified. The indium proved a good thermal contact between the substrate and the cryostat.

A 0.03 at% Fe/Au versus chromel thermocouple was used to measure the temperature of the film under luminescent conditions. With liquid helium in the helium container a temperature of 10 K was obtained, with liquid nitrogen in the helium container temperatures in the range 77 K to 85 K were recorded.

8.2.2 Photo-excitation

Photo-excitation was provided by a 250 watt mercury lamp filtered by two Chance glass OX1A filters to pass 3650Å radiation. The transmission of these filters is shown in Figure 8.3a. Orr (1970) has shown that with such a combination of lamp and filters the radiant energy available to be focussed on to the sample is about 9 watts. The arrangement used to excite and collimate the luminescence into the optical spectrophotometer is shown in Figure 8.4. When required a set of neutral density filters (manufactured by Barr and Stroud Limited) was used to vary the intensity of the excitation.

8.2.3 Spectrophotometer

The spectrophotometer used in this investigation was an Optica CF4N1. This is a double beam recording instrument employing a grating. It was designed for use primarily to measure absorption. It has a spectral range from

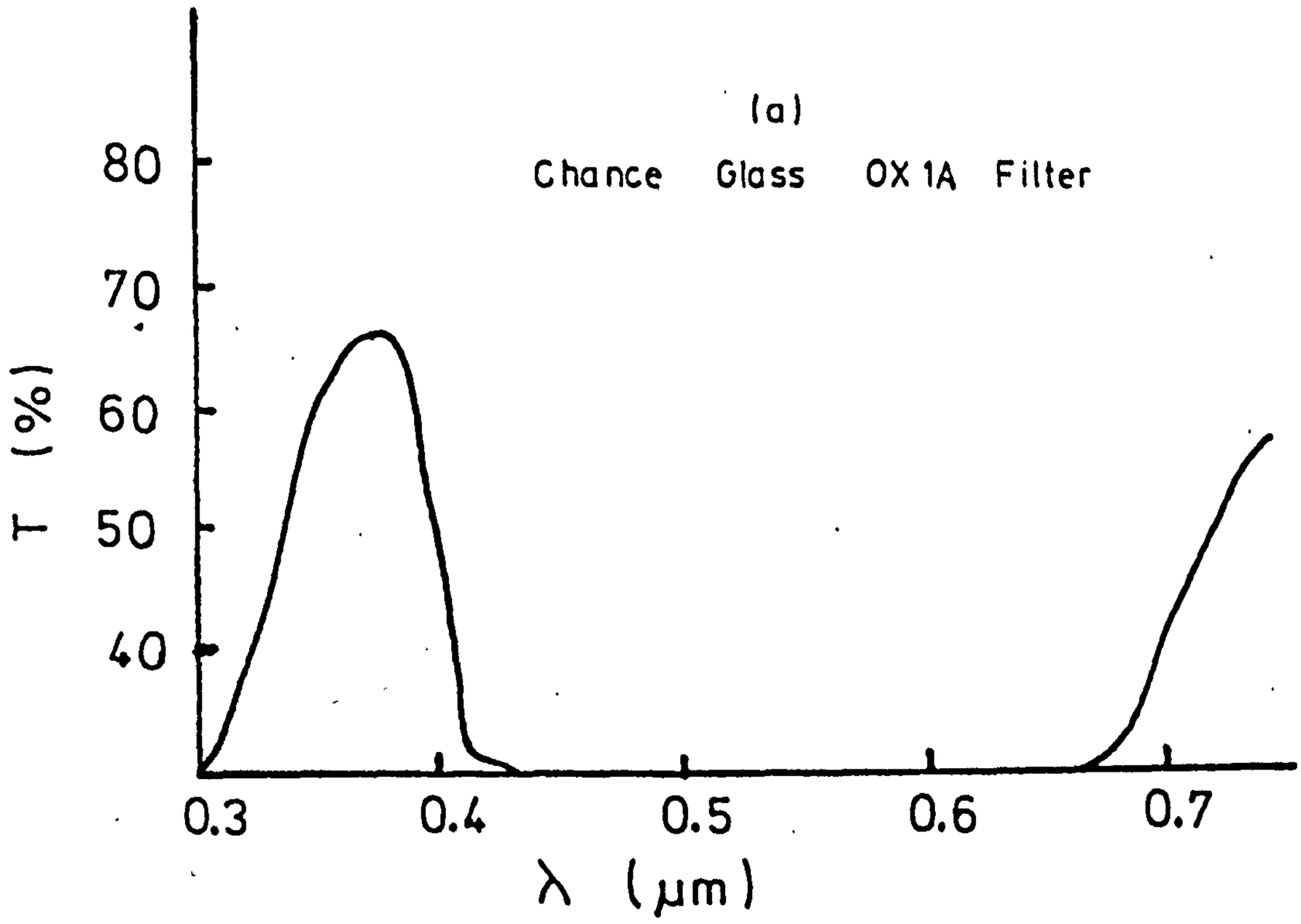

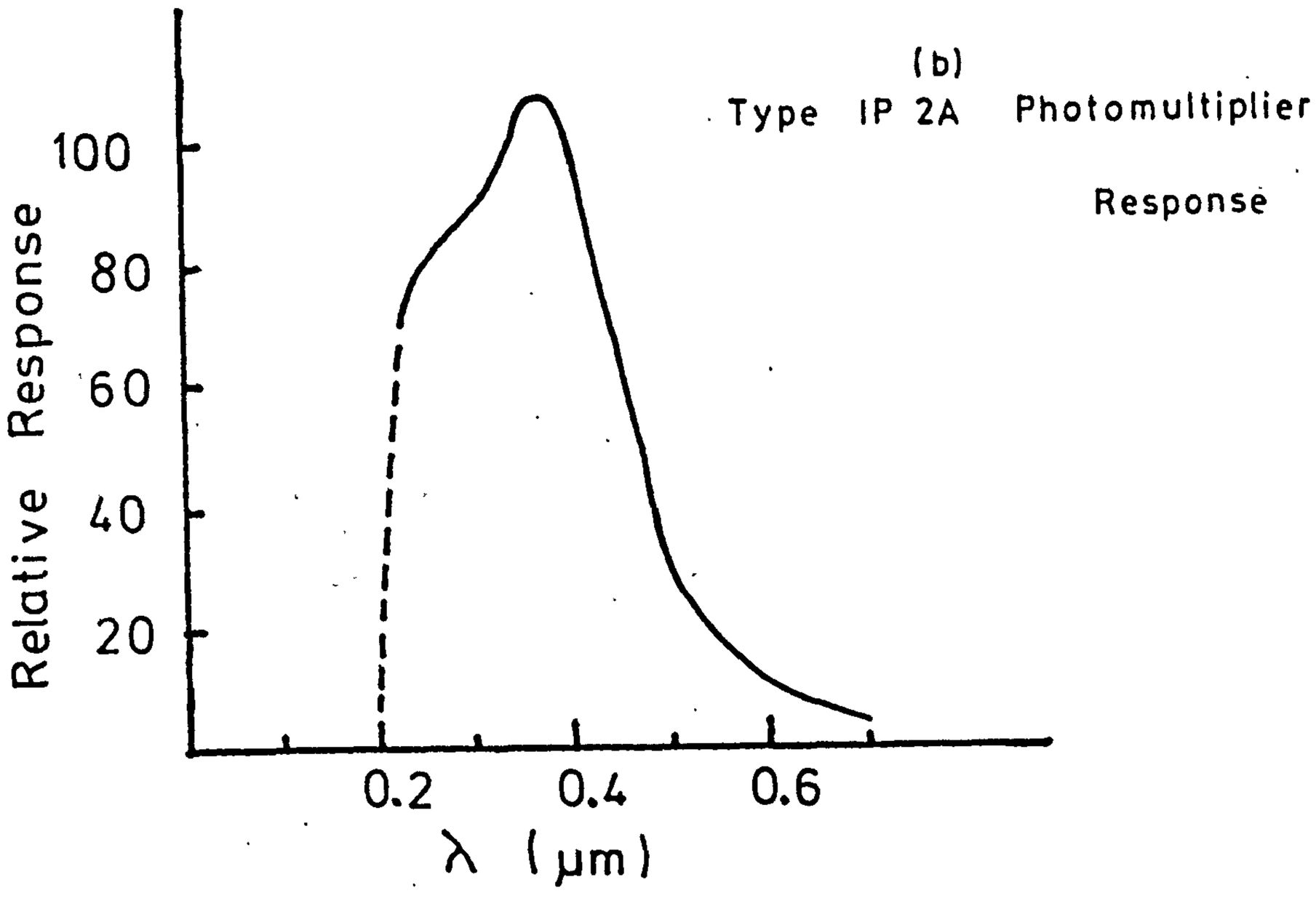

Figure 8.3

Filter and Photomultiplier Characteristics

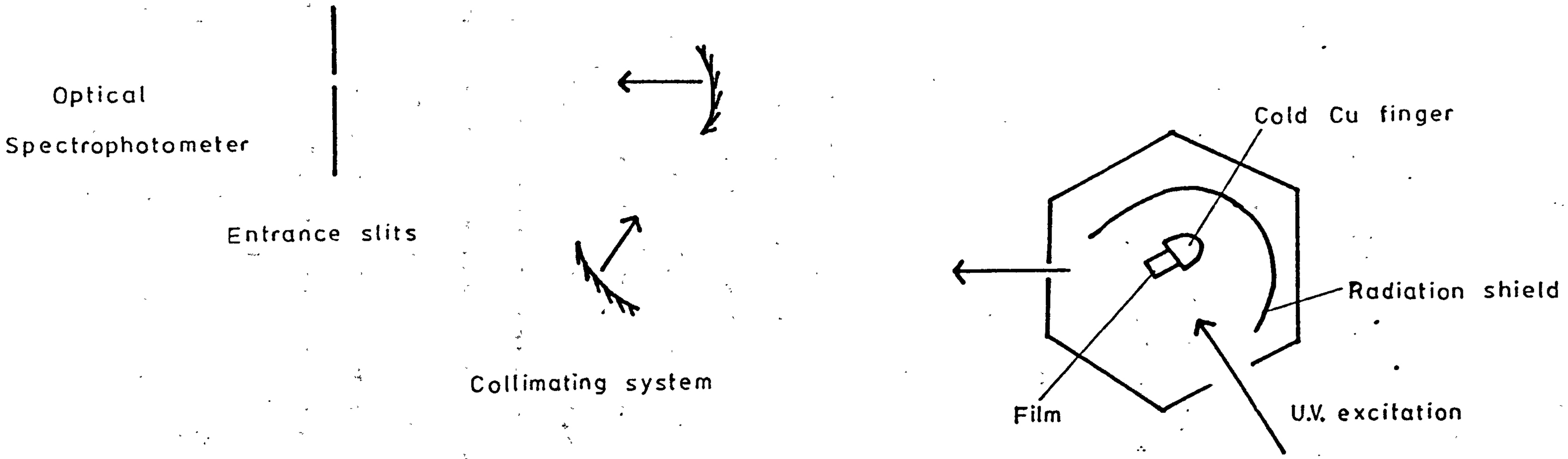

Figure 8.4

Arrangement of Cryostat and Optical Collimation System

0.185 to 3.200 μm. It can be adapted to measure emission when the spectral range is reduced by the limited response of the detectors. In these experiments an R.C.A. type 1P28 photomultiplier was used which limited the range to between 0.2 and 0.62 μm (Figure 8.3b).

The monochromator was of the Littrow type with two interchangeable plane gratings as dispersive elements. In the U.V. and visible regions (0.185 to 1000 μm) the appropriate grating was ruled with 600 lines/mm and had a dispersion of 16Å/min. A block diagram of the whole system is shown in Figure 8.5.

Synchronous motors were used to drive both the paper advance of the recorder and the grating-wavelength scale system.

8.3 Experimental Results

The spectral distribution of the luminescence emitted from the thinner film E41 ($\rho = 1.0 \times 10^5$ Ωcm) is shown in Figures 8.6 and 8.7. The emission can be divided into two distinct spectral regions in the green and in the blue.

Figure 8.6 shows the two peaks in the green at 5173Å and 5236Å which appeared at 4.2 K. These peaks shifted to 5166Å and 5226Å respectively when the temperature was raised to 77 K. The blue emission of this film when shown on the same scale as the green was hardly discernable. However Figure 8.7 shows this region of the spectrum when the sensitivity of the Optica amplifier was increased. At 4.2 K two distinct peaks at 4872 and 4893Å were observed. When the temperature was raised to 77 K these peaks merged to form one band at 4878Å.

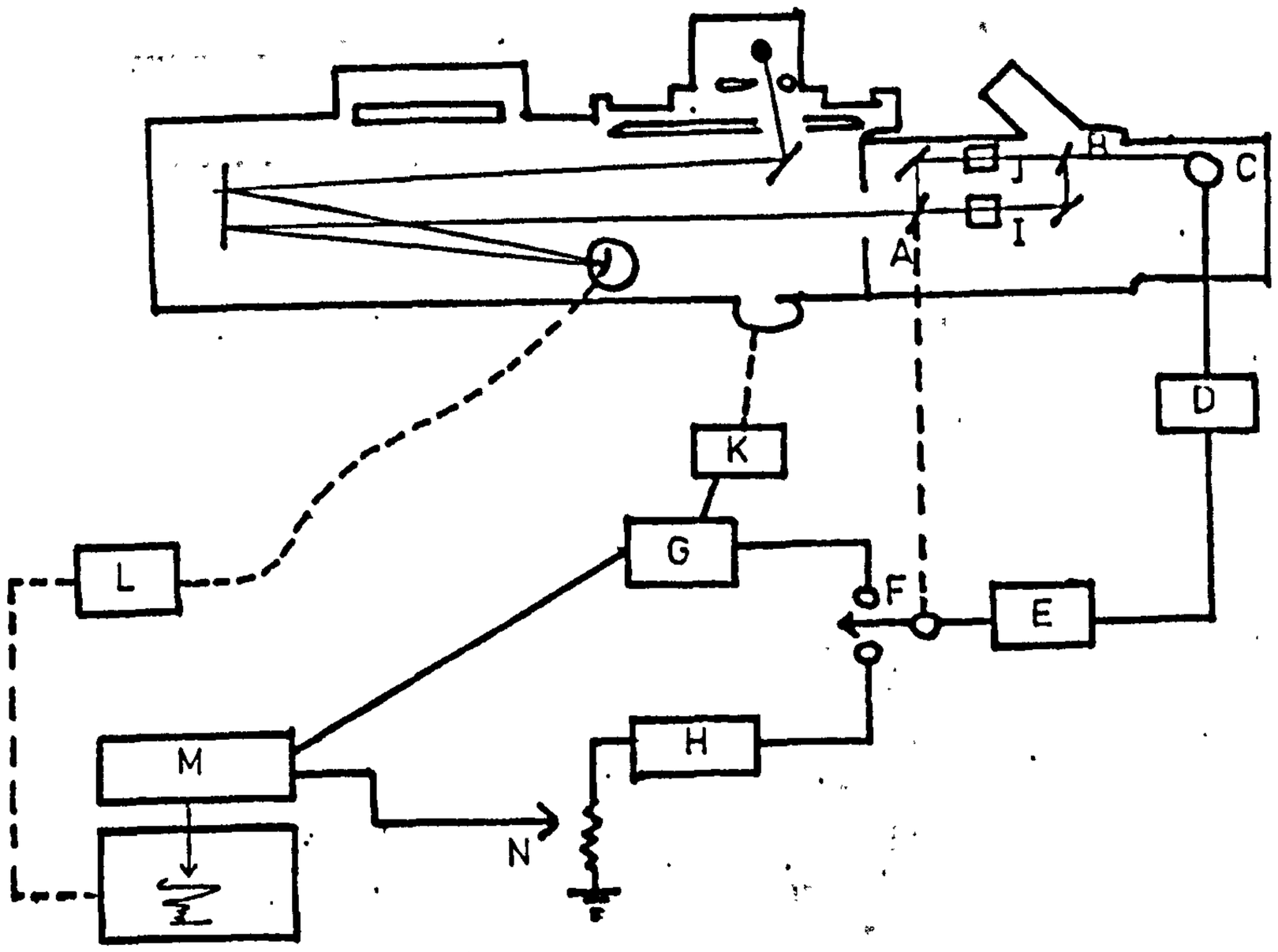

A	Rotating Mirror		G	Reference Demod.	Used For Absorption Measurements
B	Rotating Mirror		H	Sample Demod.	
C	Detector		I	Sample Cell	
D	Pre - Amp.		J	Reference Cell	
E	Amp.		K	Slit Servo	
F	Commutator		L	Wavelength Drive	
			M	Pen Recorder	
			N	100% Adjust	

Figure 8.5

Block Diagram of Optica Spectrophotometer

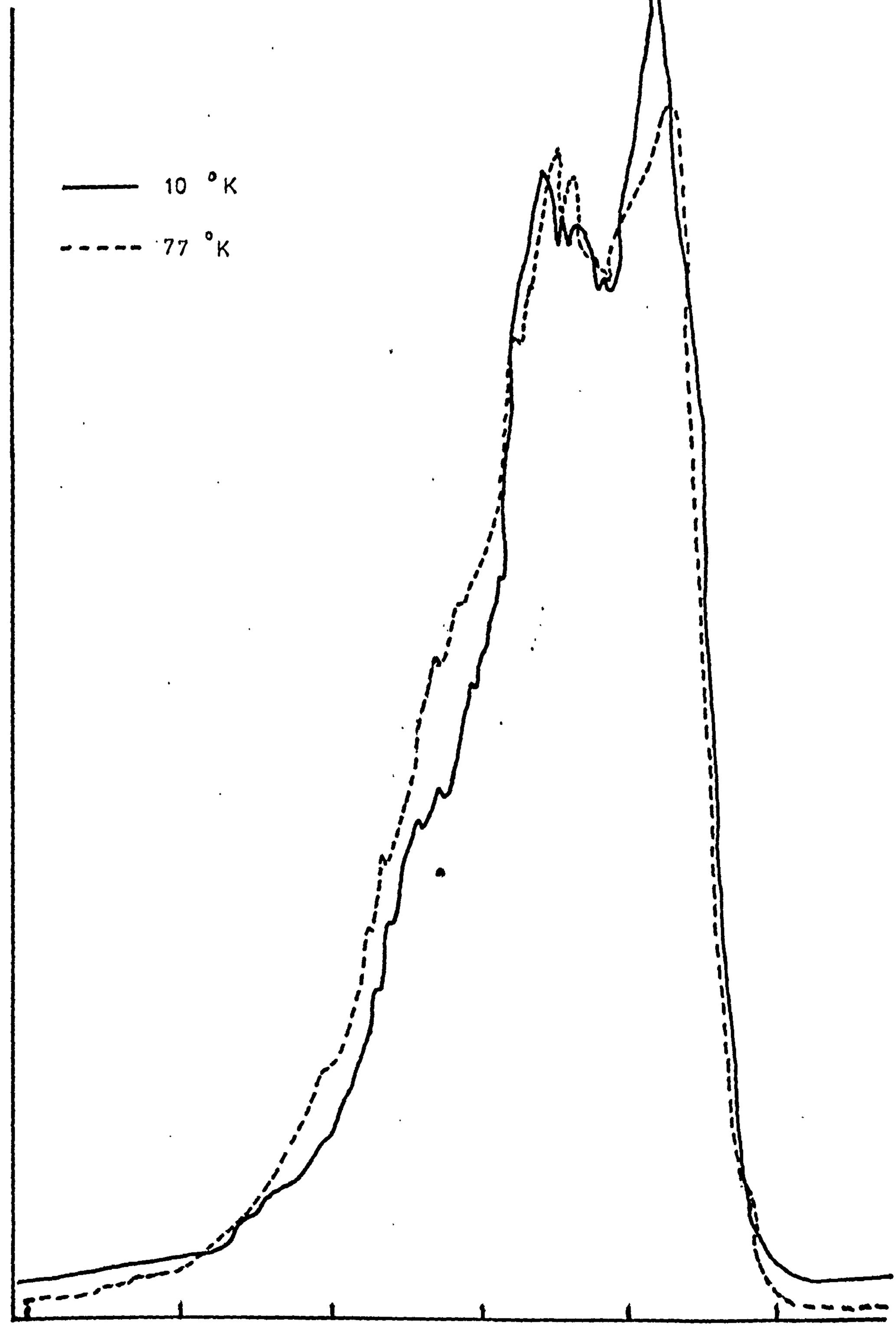

Figure 8.6

Green Emission From Film E41

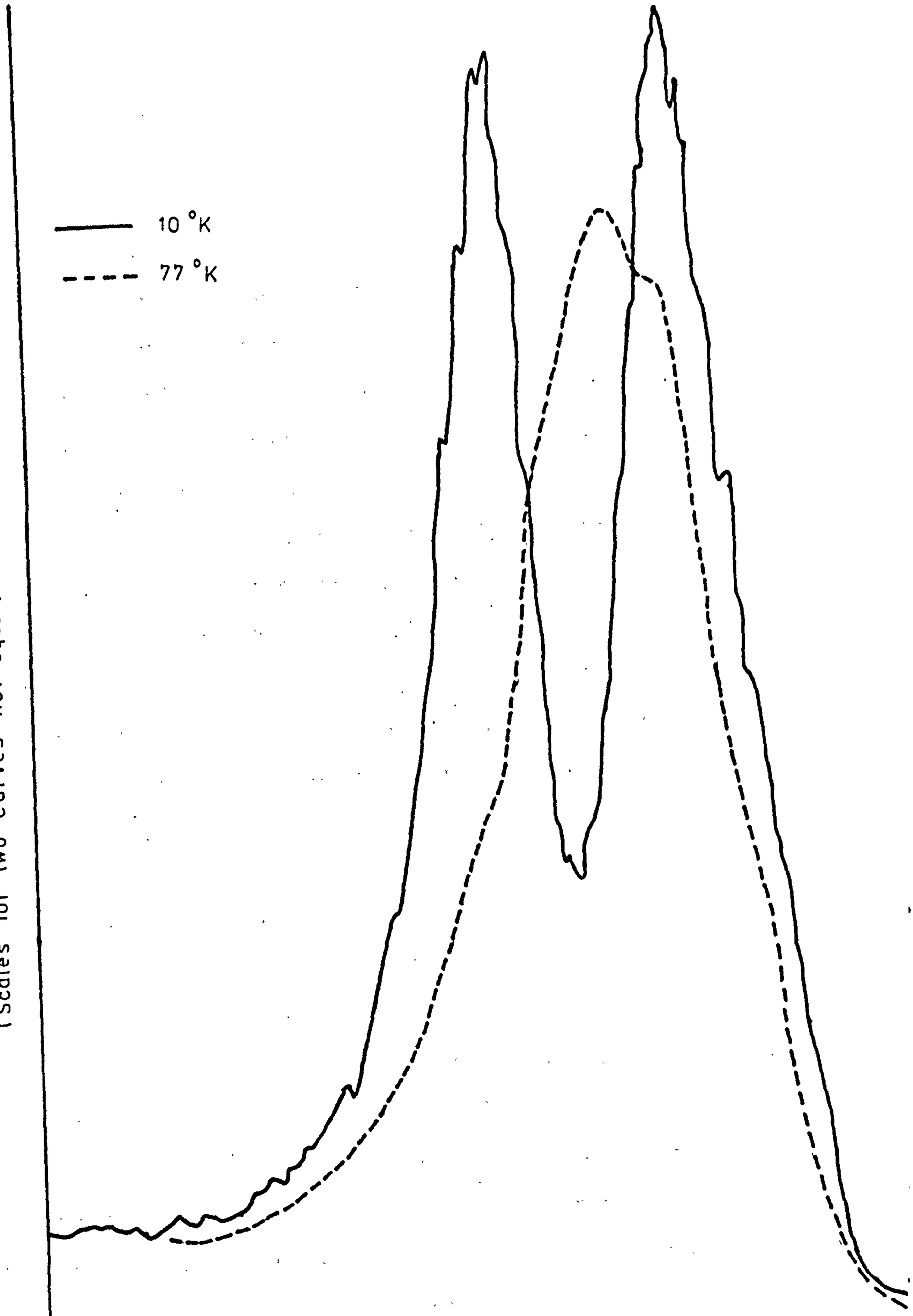

Figure 8.7

Blue Emission from Film E 41

DAMAGED TEXT IN ORIGINAL

The green emission of the thicker film E36 (ρ = 1.0×10^5 Ωcm) showed more structure than that of E41 with peaks at 5170, 5250, 5320 and 5490Å, when excited at 4.2 K (Figure 8.8) At 77 K these peaks shifted to 5147, 5229, 5305 and 5388Å respectively. The blue emission could now be detected using the same sensitivity settings as for the green, but in order to obtain a more accurate determination of the positions of the emission bands, the amplifier sensitivity was increased. Figure 8.9 shows sharp bands in the blue emission of film E36 at 4872 and 4892Å at 4 K merging to form one unresolved band at 4888Å at 77 K. There was no shift in the spectral positions of the blue emission peaks of either film at any temperature when the intensity of U-V excitation was varied down to 1% of its original value. The peaks in the green however shifted towards longer wavelengths by 10Å as the excitation intensity was decreased.

8.4 Interpretation

8.4.1 Green Emission

The first maximum in the spectral distribution of the green emission from film E36 at 77 K appeared at 5170Å. Replicas of the first component were observed on the low energy side of the emission. The mean separation of the components was about 35 meV which is approximately equal to the longitudinal optical (LO) phonon energy of 38 meV. A similar spectral distribution was observed at 4.2 K. This green 'edge' emission has been attributed, in single crystals, to phonon assisted recombination between free electrons and holes bound to acceptor levels some 0.14 to 0.17 eV above

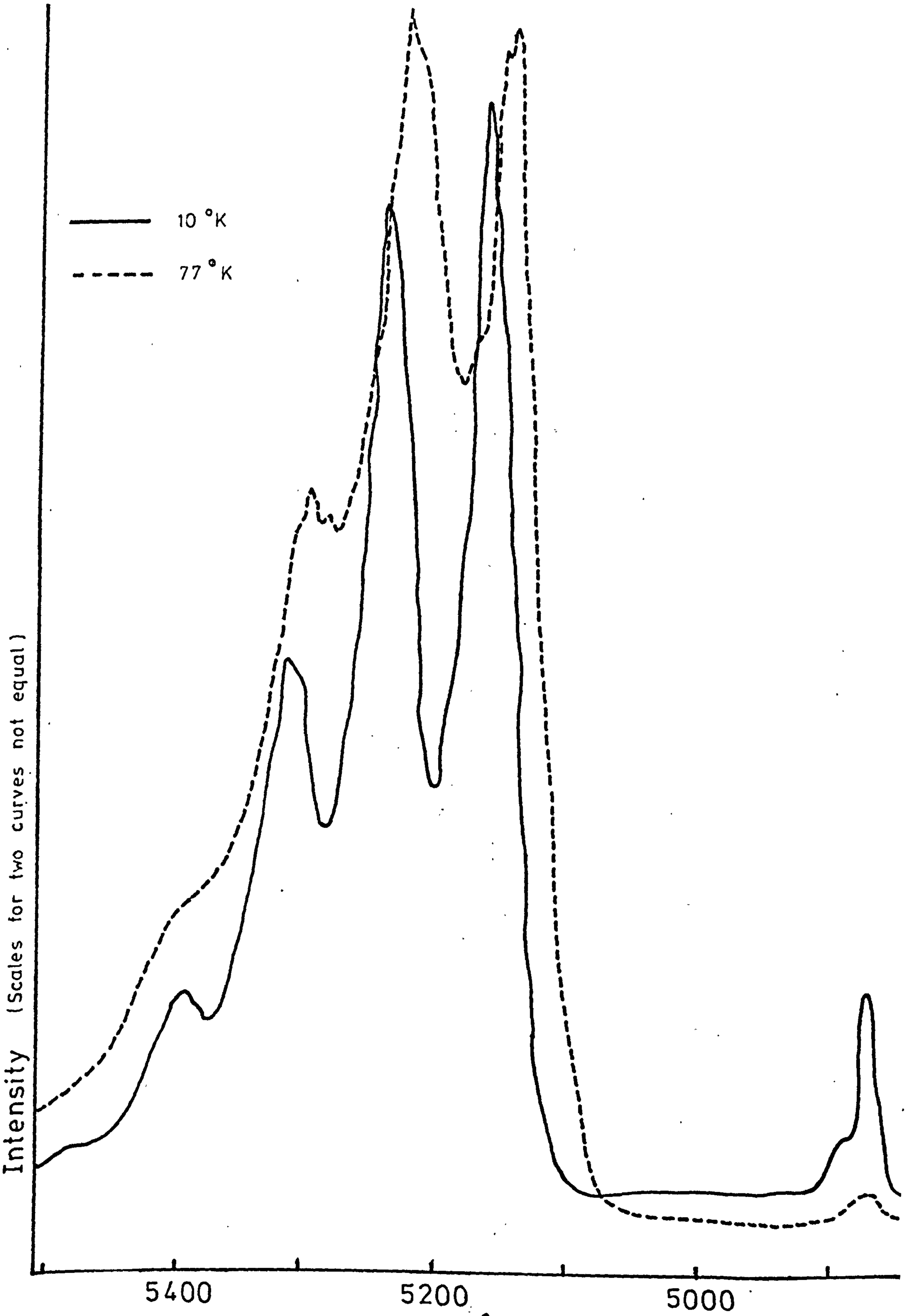

Figure 8.8

Green Emission from Film E 36

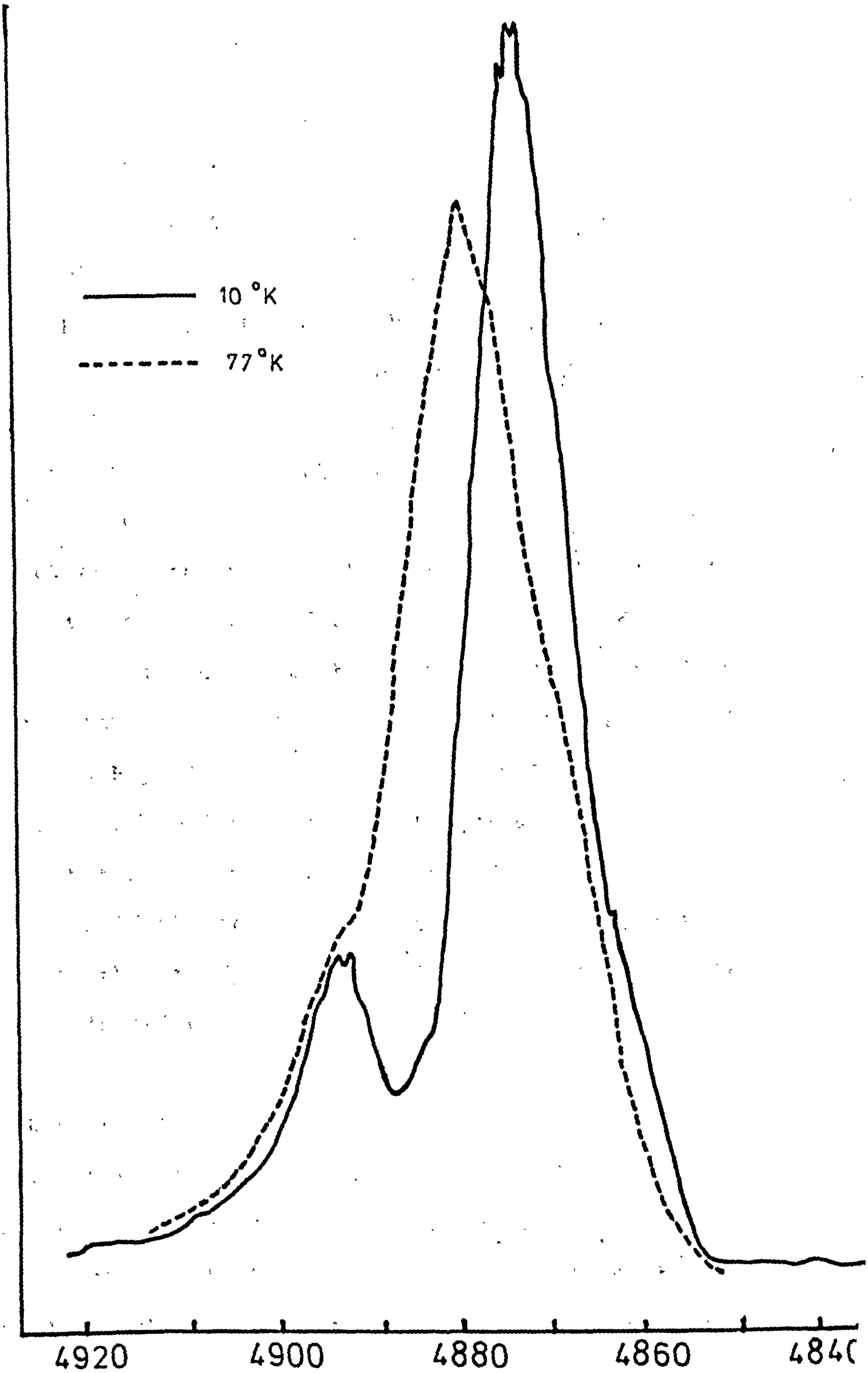

Figure 8.9

Blue Emission from Film E 36

the valence band. (Pedrotti and Reynolds 1960, Colbow 1966). This model put forward by Schon (1942) and Klasens (1940) is supported by the photoconductivity and luminescence measurements of Spear and Bradberry (1965). The shift in the spectral position of the peaks between 4.2 K and 77 K occurs because the bands at 4.2 K are the LES while those at 77 are the corresponding HES. The shift in wavelength therefore gives a measure of the ionisation energy of the donor involved. Our measurements show this acceptor level to be 0.17 eV above the valence band (assuming a value of 2.583 eV for the energy gap of CdS). The shallow donor level was calculated to lie 0.011 eV below the conduction band and this compares favourably with the value of 0.023 eV calculated by Pedrotti and Reynolds (1960) for CdS single crystals.

The green emission from film E41 was of the same general form but showed nothing like the detailed structure and was about half the intensity of the emission from E36. This indicates that the properties of the film E41 were less like those of 'bulk' CdS than E36.

8.4.2 Blue Emission

The blue emission of the films was dominated by two exciton emission lines known as the I_1 and I_2 lines. Zeeman effect studies by Thomas and Hopfield (1964) have shown that I_1 which occurs at 4889Å is associated with the recombination of an exciton bound to a neutral acceptor, whereas I_2 at 4867Å is associated with an exciton bound to a neutral donor. At liquid helium temperatures the I_1 exciton emission was observed at 4892Å and the I_2 line at 4872Å.

It is thought that the acceptor responsible for the I_1 bound exciton emission is also involved in the green edge recombination process (Orr 1970). According to Thomas et al (1967) the acceptor is associated with a cadmium vacancy even though other donor impurities may be juxtaposed with the vacancy. The donors which are responsible for a large part of the I_2 bound exciton emission are probably associated in some way with sulphur vacancies and/or cadmium interstitials. Sulphur vacancies have previously been suggested by Handelman and Thomas (1965) as possible centres for the recombination of excitons to produce emission around 4870Å. Bleha and Peacock (1970) however suggested their emission peak observed at 4875Å from CdS thin films might be due to an excess of cadmium present interstitially in the film. The intensity of both the blue emission and the L.E.S. green emission from the lower resistivity film (E36) was greater than that from E41 by factors of six and two respectively. As the I_2 line was also much stronger relative to both the I_1 line and the green edge emission in the lower resistivity film, we favour the explanation that the emission round the I_2 line is due to an excess of cadmium incorporated in the film, but are unable to conclude whether this cadmium is present in the form of interstials or sulphur vacancies. This is in agreement with the explanation offered in the previous chapter for the decrease in film resistivity with thickness.

8.5 Summary

The luminescent properties of these films deposited

in an enclosed tube from a source at 800°C indicate that their properties resemble more closely those of the bulk material than the films evaporated in a conventional vacuum system. The emission is similar to that previously observed in CdS single crystals and is consistent with the idea that the thicker the films, the lower their resistivity and the larger the amount of excess cadmium they contain.

REFERENCES

Bleha and Peacock (1970) J.A.P. 41 4992

Colbow (1966) Phys. Rev. 141 742

Conradi (1964) Can. J. Phys. 47 2591

Handleman and Thomas (1965) J. Phys. Chem. Sol. 26 1261

Hopfield and Thomas (1961) Phys. Rev. 132 35

Klasens (1940) Nature 158 306

Koller and Coghill (1960) J. Electrochem. Soc. 107 973

Orr (1970) Ph.D. Thesis, Univ. of Durham

Pedrotti and Reynolds (1960) Phys. Rev. 120 1664

Schön (1942) Z. Phys. 119 463

Shalimova et al (1965) Sov. Phys. J. 1 61

Spear and Bradberry (1965) Phys. Stat. Sol. 8 649

Thomas and Hopfield (1959) Phys. Rev. 116 573

Thomas and Hopfield (1964) Phys. Rev. 128 2135

Thomas et al (1964) Proc. 7th Int. Conf. Phys. Semi-Cond. 4. 67

Thomas et al (1967) Proc. Int. Conf. on II-VI Semicond. Comps.

Vlasenko et al (1966) Opt. Spectroscopy 21 261

CHAPTER 9

PHOTOVOLTAIC MEASUREMENTS

9.1 INTRODUCTION

We now move to a discussion of the photovoltaic properties of the CdS-Cu_2S heterojunction. Cells were fabricated both in the thin film form, on films evaporated at I.R.D., and on single crystals.

The majority of the crystals used in this investigation were doped with indium to bring their resistivities down to between 10 and 100 Ωcm. The indium was incorporated in the charge of crushed 'flow' crystals (similar to those used as a source material for vacuum evaporation) and placed in sealed silica growth tubes used in a modified Piper and Polich (1961) technique to grow large crystalline boules approximately 1 cm in diameter.

9.2 Cell Fabrication

9.2.1 Single Crystal Cells

Slices 2 mm thick were cut from the crystalline boules using a wire saw designed by Rushby and Woods (1970). The slices were then polished using '600' grade carborundum and etched for ten minutes in orthophosphoric acid at 90°C to remove surface contamination before being coated on one face with evaporated indium.

The plating solution used to form the p-type Cu_2S layer in the junctions constructed was prepared as follows:

(a) 750 ml. of distilled water was heated and stirred in a closed reaction vessel while oxygen free

nitrogen was continuously bubbled through the liquid to displace oxygen.

(b) 100 ml. of hydrazine hydrate solution was added.

(c) A pH meter (E.I.L. Model 23A) with a calomel reference electrode in a salt bridge container, and a general purpose glass electrode, was used to measure the pH of the solution which was then brought to a value of 2.5 by adding approximately 120 ml. of conc. hydrochloric acid.

(d) Next 10 gm. of CuCl powder was added, and the liquid volume was made up to 1 litre by adding distilled water.

(e) The solution was heated to a temperature of 90°C, and then the pH was accurately adjusted to 2.5 by adding drops of hydrochloric acid or hydrazine hydrate. The plating of Cu_2S was begun by dipping the etched CdS into the bath for a measured period.

During this time oxygen-free nitrogen was continuously bubbled through the liquid, while a magnetic stirrer kept the solution agitated. The combined effect of the hydrazine and the nitrogen was to prevent the formation of Cu^{++} ions. A deep blue copper complex did precipitate from the cold solution, but was readily redissolved in excess acid when the bath was heated again.

The same strength plating solution was used to prepare all the junctions investigated in the present work. Crystals of CdS were etched in cold 40% HCl for five seconds before plating for ten seconds in 2.5 pH at 90°C.

After this they were washed, and then dried in a jet of dry nitrogen. At this stage either initial measurements were made or heat treatment at 200°C in air was carried out.

The indium contact on the crystal was masked with wax to prevent the Cu_2S from forming a short circuit to the ohmic contact. Crystals were fastened to pieces of copper sheet after plating, with a thin layer of silver paste (JMM FSP 43) between the indium and the copper. Electrical contact to the Cu_2S layer was made by a spring-loaded contact.

9.2.2 Thin Film Cells

CdS thin films for solar cell use were evaporated on to silver sprayed kapton substrates plated with zinc. The edges of the films were covered with varnish prior to plating to prevent Cu_2S shorting through to the substrate. The varnish also helped to minimize the possibility of the CdS flaking off the substrate. The p-layer was formed in an identical bath to that used for single crystals, but a 10 second etch in 1 N potassium iodide solution was preferred to the stronger HCl etch. Contact to the Cu_2S layer was provided by a gold covered copper grid with 20 lines per cm and giving a transmission slightly greater than 90%. The grid was fixed in contact with the Cu_2S using adhesive backed Mylar.

9.3 Cell Evaluation

9.3.1 Current-Voltage Characteristics

The electrical circuit and apparatus used to

determine the (I)V characteristics under equivalent A.M.O. sunlight illumination are shown in Figure 9.1. A 1500W quartz halogen strip lamp with a parabolic reflector housing was mounted above a 1 cm deep water filter under which the sample and its heat-sink were placed. The intensity of illumination at the surface of the sample was set to 140 mW cm^{-2} by adjusting the height of the heat-sink table whilst monitoring the short circuit current of a calibrated silicon photovoltaic cell. This intensity of illumination was used throughout the present series of experiments except where otherwise stated.

The open-circuit voltage, OCV, of each cell was measured by a Philips GM6020 valve voltmeter with leads attached to the cell contacts. Separate leads were taken from the cell to a bias supply which was continuously variable from -1.5 to +1.5 volts and consisted of a multi-turn 'helipot' connected as a potential divider. Connections were made from this to a Bryans 21001 X-Y plotter. The current through the cell was measured by recording the potential drop across a one ohm resistor.

9.3.2 Spectral Response

To measure the spectral response a Barr and Stroud VL2 double prism monochromator was used, with a 500W tungsten lamp source run from a stabilised mains supply. No correction was made for the energy distribution of the tungsten lamp.

The intensity of monochromatic light falling on the photovoltaic junction via the VL2 was about one microwatt cm^{-2} at the peak of the response. Both entrance

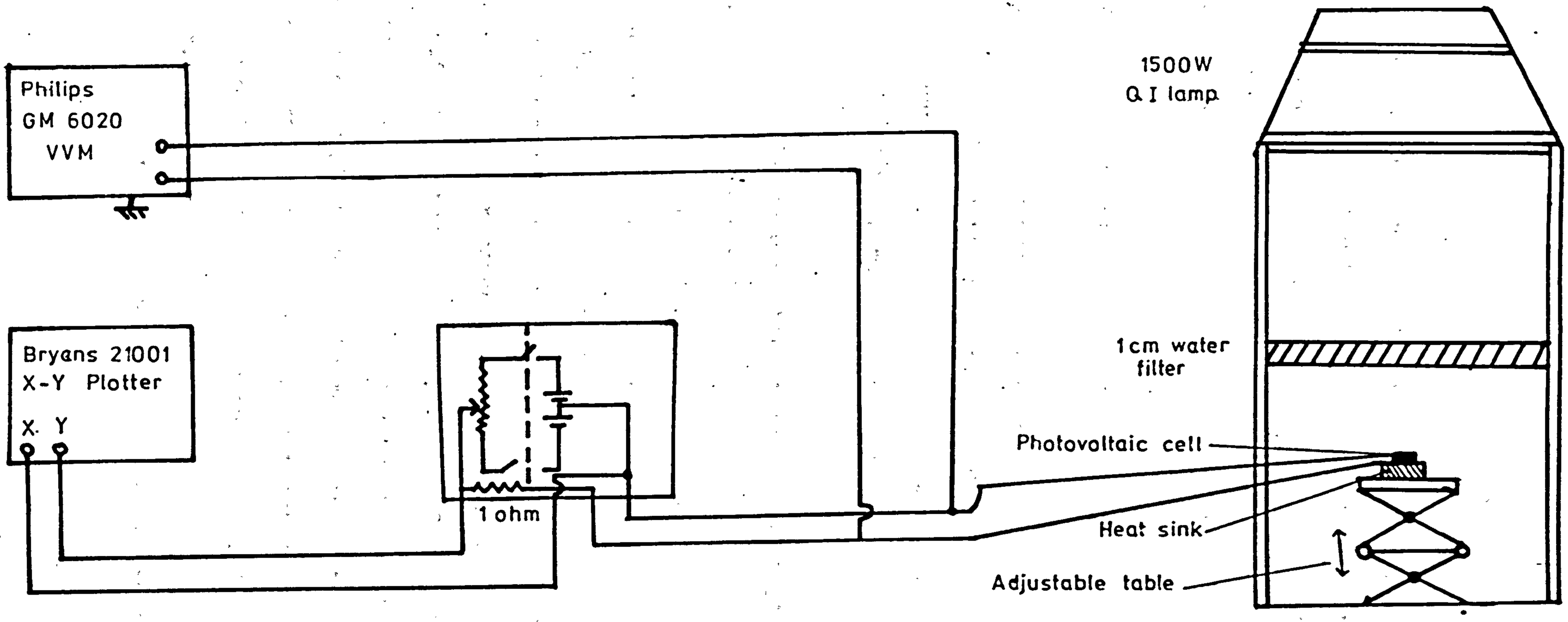

Figure 9.1

Circuit for determining I(V) Characteristics of Photovoltaic Devices

and exit slits of the monochromator were held at the same aperture throughout, giving a bandwidth varying from 380Å at 1.5 microns to 72Å at 0.5 microns.

Only the OCV was monitored (with the GM6020 VVM) since the short-circuit current, SCC, of all the cells was too low to determine accurately over the whole wavelength band.

9.4 Barrier Layer Formation

9.4.1 Experimental Techniques

Using the plating bath described in Section 9.2.1 single crystal slices of CdS doped with varying amounts of indium (1-1000 p.p.m.) were plated for periods up to four hours.

The rate of formation of the Cu_2S layer was monitored in two ways.

(1) The crystal was weighed using an Oertling R20 electronic balance, and lowered into the plating bath in a tantalum basket suspended from the top of the reaction vessel by molybdenum wire. At intervals of 30 minutes the crystal was removed from the bath, dried and reweighed. As Cu_2S has a greater density than CdS the increase in weight of the sample per unit area is a measure of the amount of Cu_2S which has formed. The increase in weight of the sample per unit area as a function of time is shown in Figure 9.2 for crystals doped with 1,10,100 and 1,000 p.p.m. of indium.

(2) Several slices from the same crystalline boule

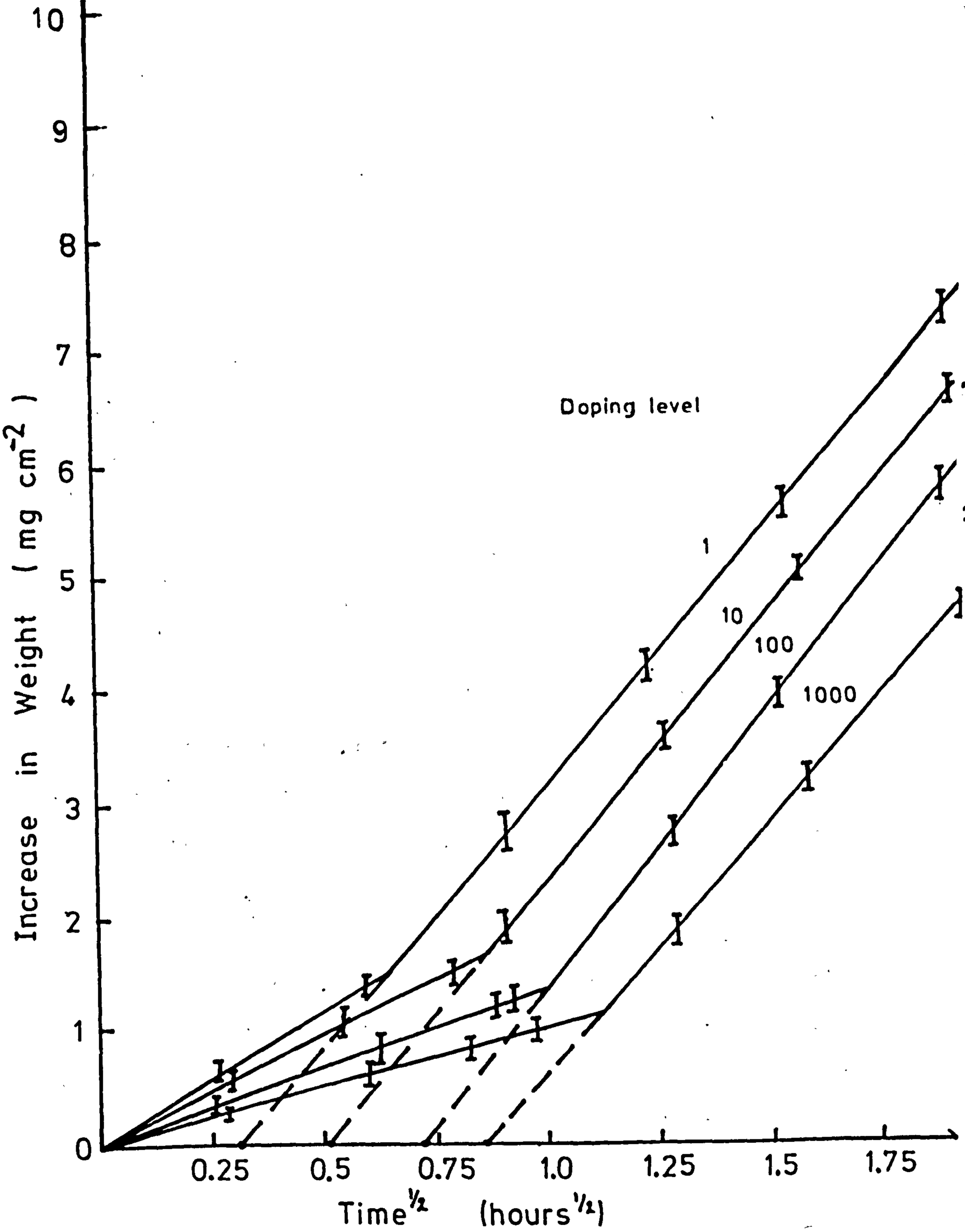

Figure 9.2

$CdS - Cu_2S$ Conversion : Increase in Weight

were stuck on to glass slides using Araldite. The slides were then immersed in the bath for varying periods of time. After plating the crystals were removed by dissolving the adhesive in an organic solvent "De-Solv". The plated crystals were then sectioned using a wire saw and mounted in liquid plastic embedding resin with their sectioned face vertically upwards. The resin block was then polished using '600' grade carborundum and diamond impregnated paste.

The Cu_2S layer was viewed using a Beck 43874 Dimax microscope. Photographs of the crystal were taken and the depth of the Cu_2S layer measured directly from these. The Cu_2S layer appears white on such photographs and can be distinguished plainly from the unconverted CdS and the background as shown in Figure 9.3. The increase in the depth of the Cu_2S layer with time is shown in Figure 9.4.

9.4.2 Experimental Results

The increase in weight of the specimens and the increase in depth of the Cu_2S layer with time followed an identical pattern. The results indicated that the conversion of CdS to Cu_2S is governed by two parabolic laws i.e.

$$R = kt^{\frac{1}{2}}$$

where R is the rate of formation of the Cu_2S, t is the time and k is a constant.

The initial gradients of the lines are dependent on the doping levels in the crystals (Figure 9.5) decreasing by a factor of three as the doping level increases by three orders of magnitude. After this initial induction

Figure 9.3

Cu_2S formed on CdS Single Crystals

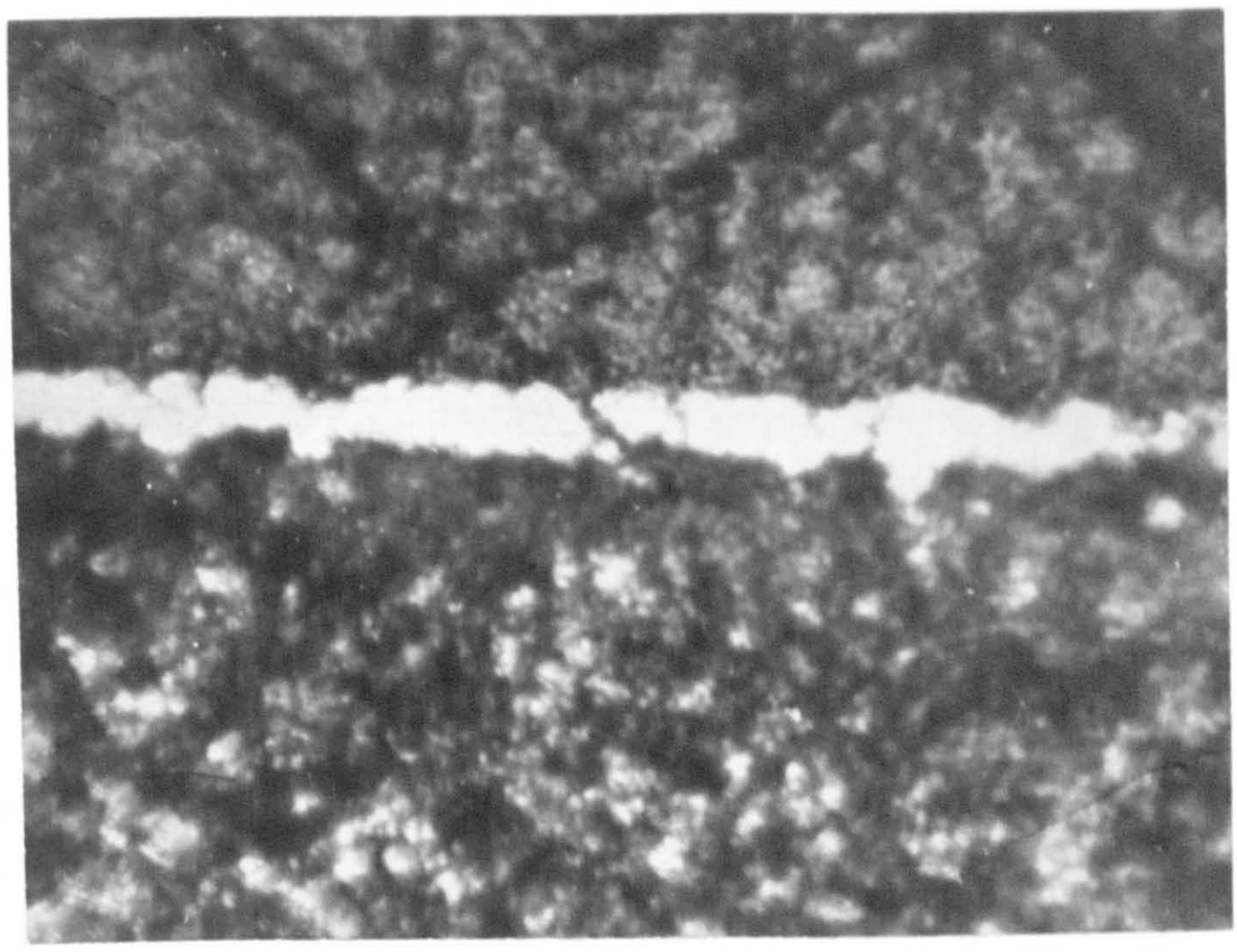

30 minutes plating (Magnification = 30)

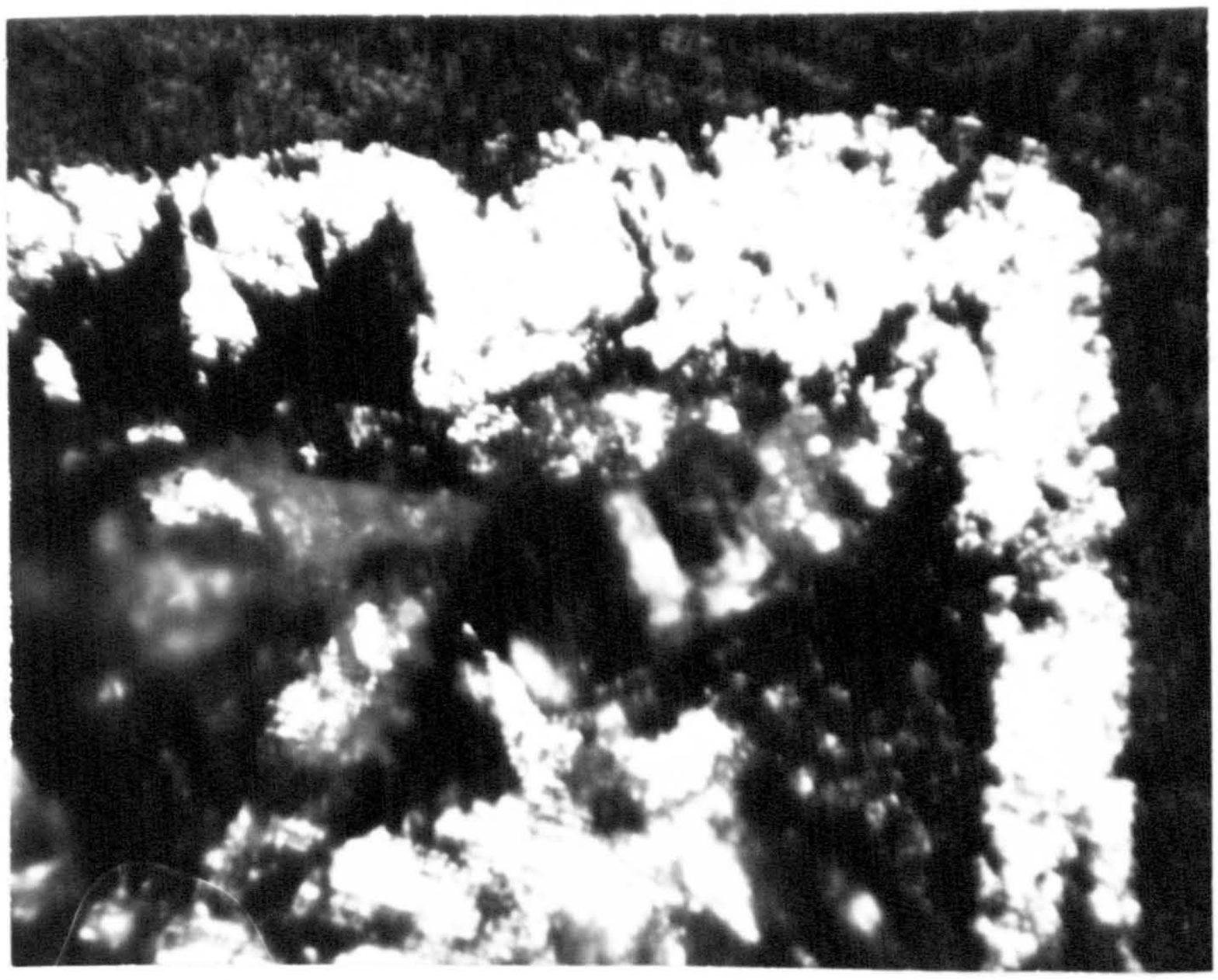

90 minutes plating (Magnification = 50)

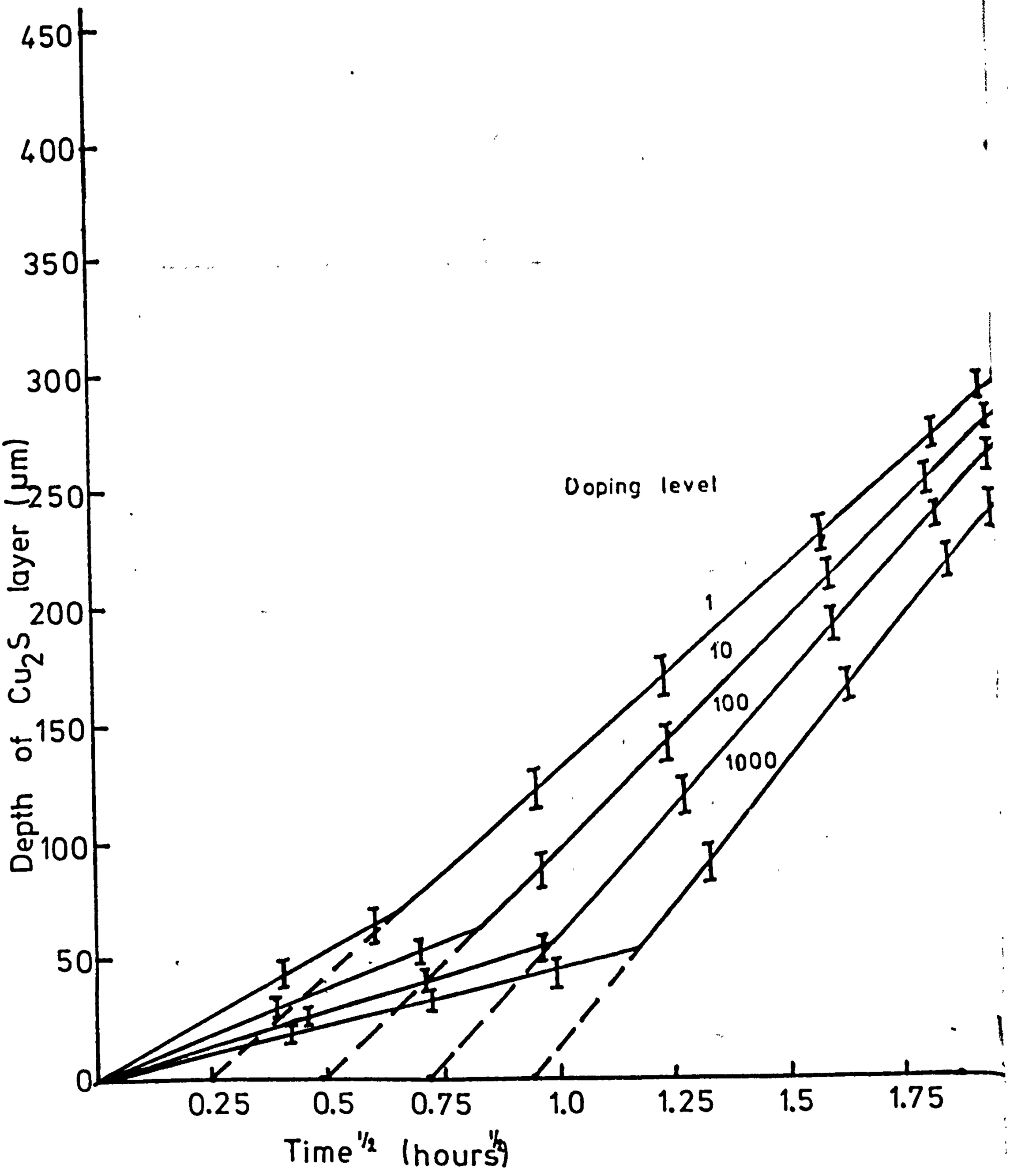

Figure 9.4

CdS-Cu_2S Conversion : Depth of Cu_2S layer

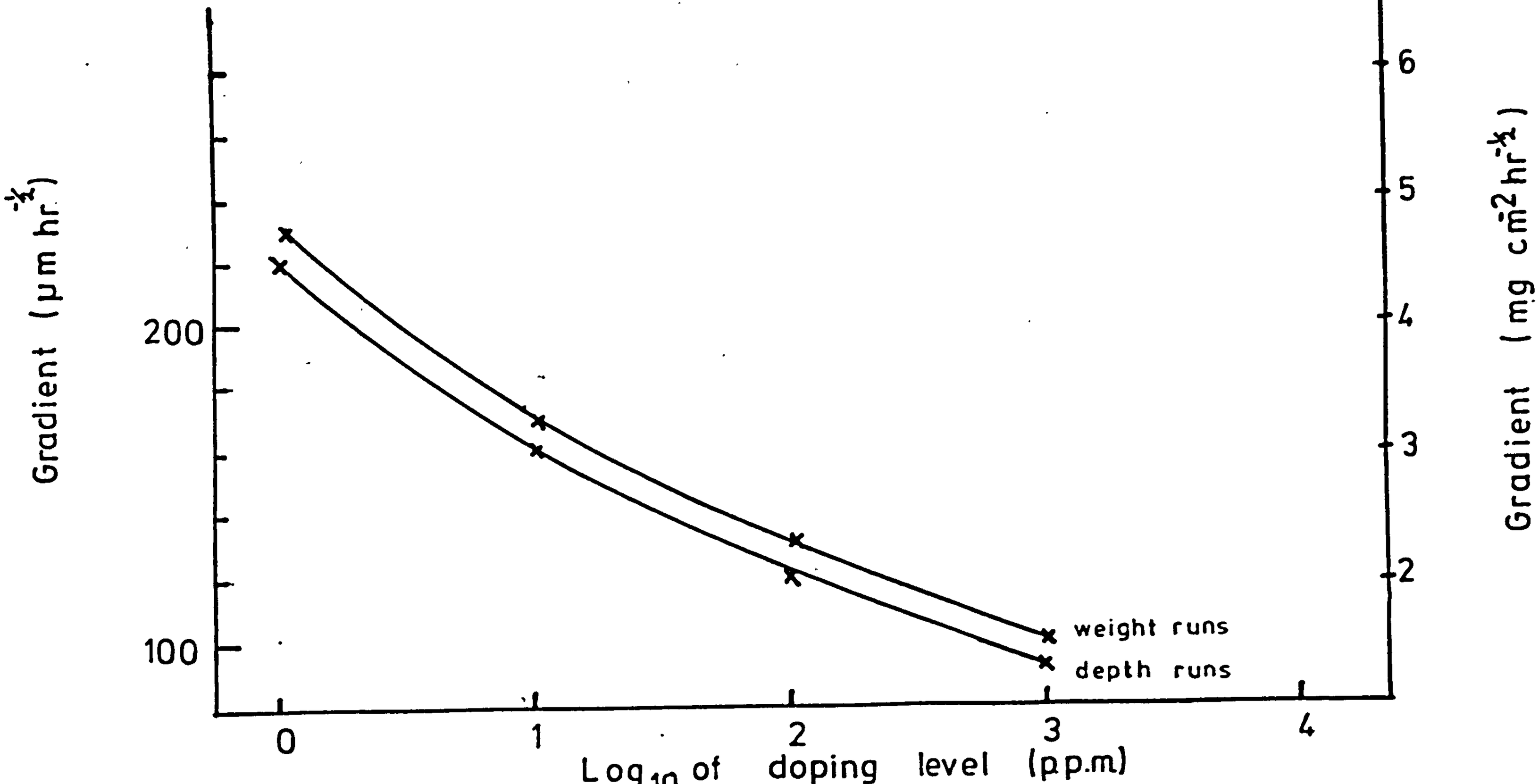

Figure 9.5

$CdS-Cu_2S$ Conversion Initial Gradient versus Doping

period a second parabolic law was observed when the gradients of the lines became approximately equal. The doping therefore only seemed to affect the rate of formation of Cu_2S in its early stages (for about the first 50-75 μm) after that the rate was completely independent of crystal doping and was approximately equal in all samples.

The time, t_{12}, at which the rate of formation of the Cu_2S changed from the first to the second parabolic law varied with doping level as shown in Figure 9.6. It is interesting to note that there is an approximately linear relationship between $t_{12}^{\frac{1}{2}}$ and the doping level.

When the samples were left in the bath for periods greater than four hours, the parabolic laws were no longer obeyed and the rate of formation of Cu_2S was both more rapid and more random. The same experiments were also carried out using crystals doped with 10,100 and 1,000 p.p.m. of gallium and identical results were obtained.

Attempts to measure the depth of the depletion layer formed in these samples between the CdS and the Cu_2S by measuring the variation in the capacitance of a device with voltage were unsuccessful. A capacitance-voltage (C-V) plotter was built to the design of Martin (1970) but in addition to capacitance our devices showed considerable conductance (see Figure 9.9) and with the apparatus available it was impossible to distinguish between these two properties. No meaningful results could therefore be obtained. Lindquist and Bube (1970) have published some photocapacitance results, (i.e. increase in junction capacitance when illuminated with white light) and have used the evidence to support their theory of conduction across the junction by tunnelling.

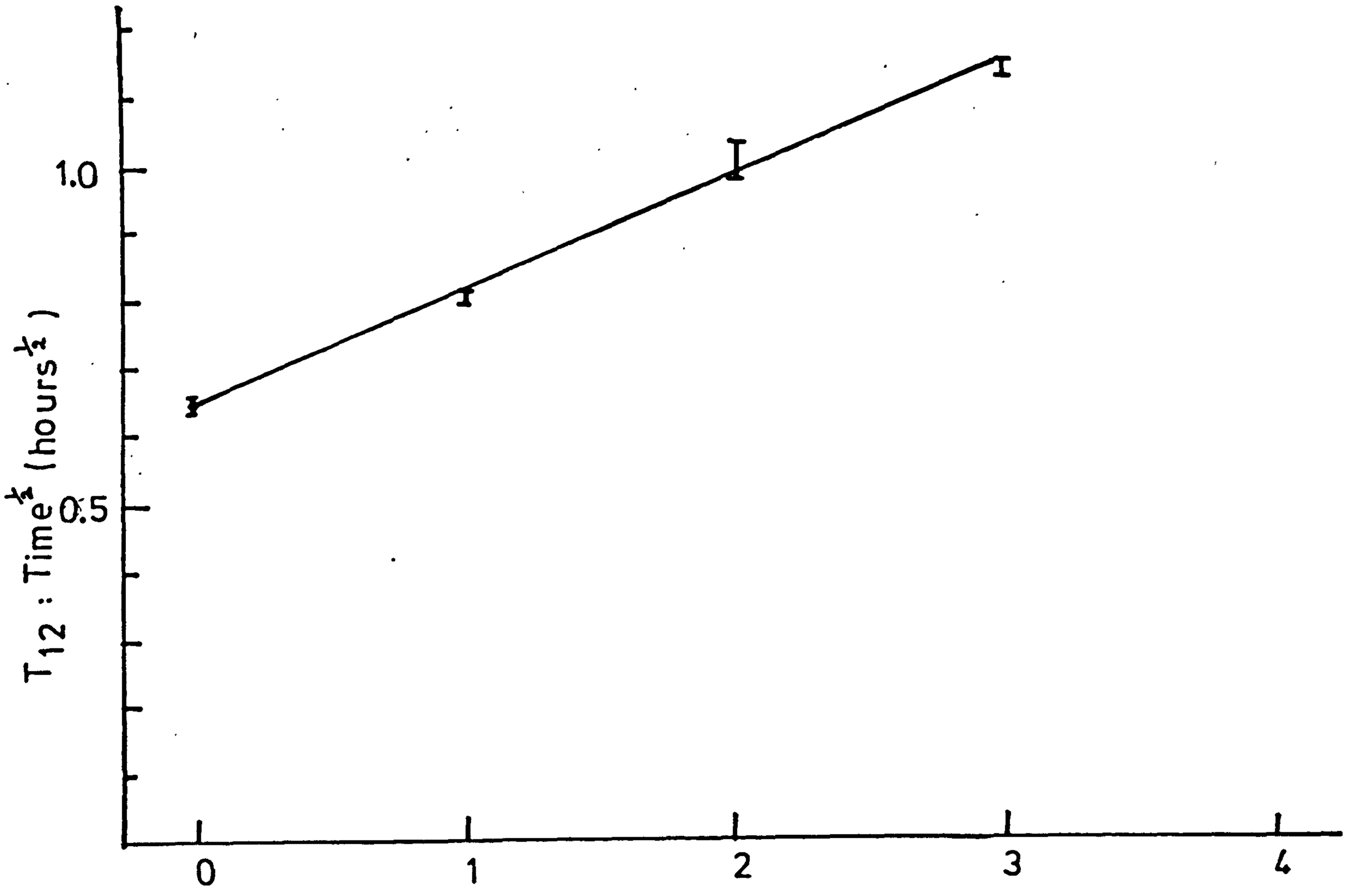

Figure 9.6

CdS-Cu_2S Conversion: Time of Rate Change versus Doping level

However they obtained meaningful results for non-heat treated devices only.

9.5 Cell Properties

9.5.1 Current-voltage Characteristics

In order to obtain the maximum photovoltage it was necessary to heat the cells in air at 200°C to form the intrinsic CdS layer. The usual length of time for this process was 60-120 seconds but the effects of more prolonged heating have been examined in successive stages. The best cells with maximum O.C.V's. of more than 400 mV all possessed an initial O.C.V. of up to 440 mV before any heat treatment. Those cells which had no O.C.V. immediately after plating improved after heating at 200°C but the O.C.V. then obtained never exceeded 400 mV. The O.C.V's. of some of the cells examined are shown at various stages of the heat treatment at 200°C in Figure 9.7.

The S.C.C. was also monitored as a function of the 'bake' time. As only a small area contact to the Cu_2S was used the current collection was inefficient and a gridded contact suitably applied would have allowed larger currents to be drawn. The S.C.C. as a function of baking time for a number of devices is shown in Figure 9.8. The curves are similar in shape to those of Figure 9.7. With most devices the current decreases from a maximum after continued baking.

Typical I(V) plots for a single crystal cell after various bakes are shown in Figure 9.9. It was observed that in general the fill-factor of such boule

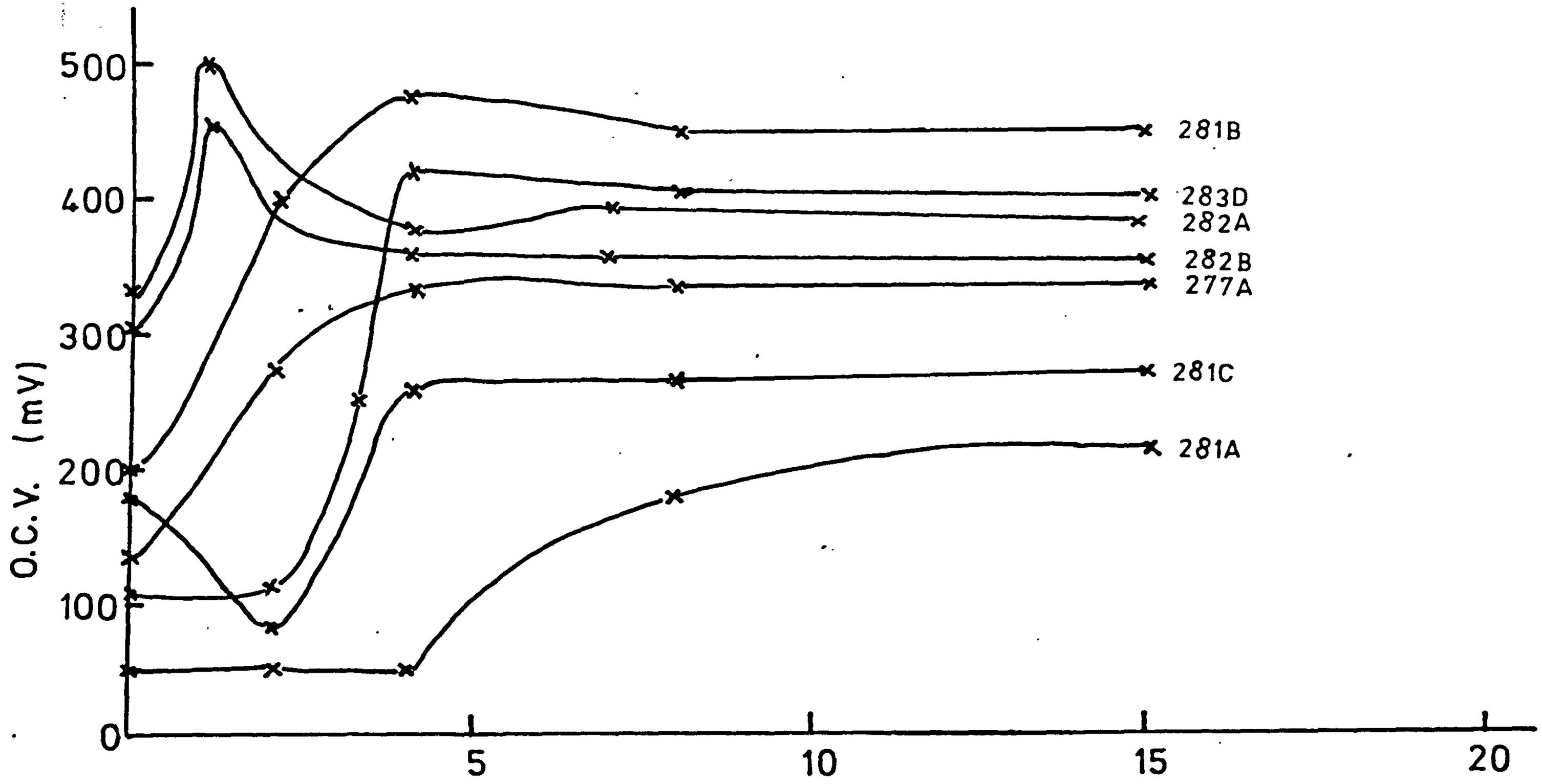

Figure 9.7

OCV Versus Bake Time (Single Crystal Cells)

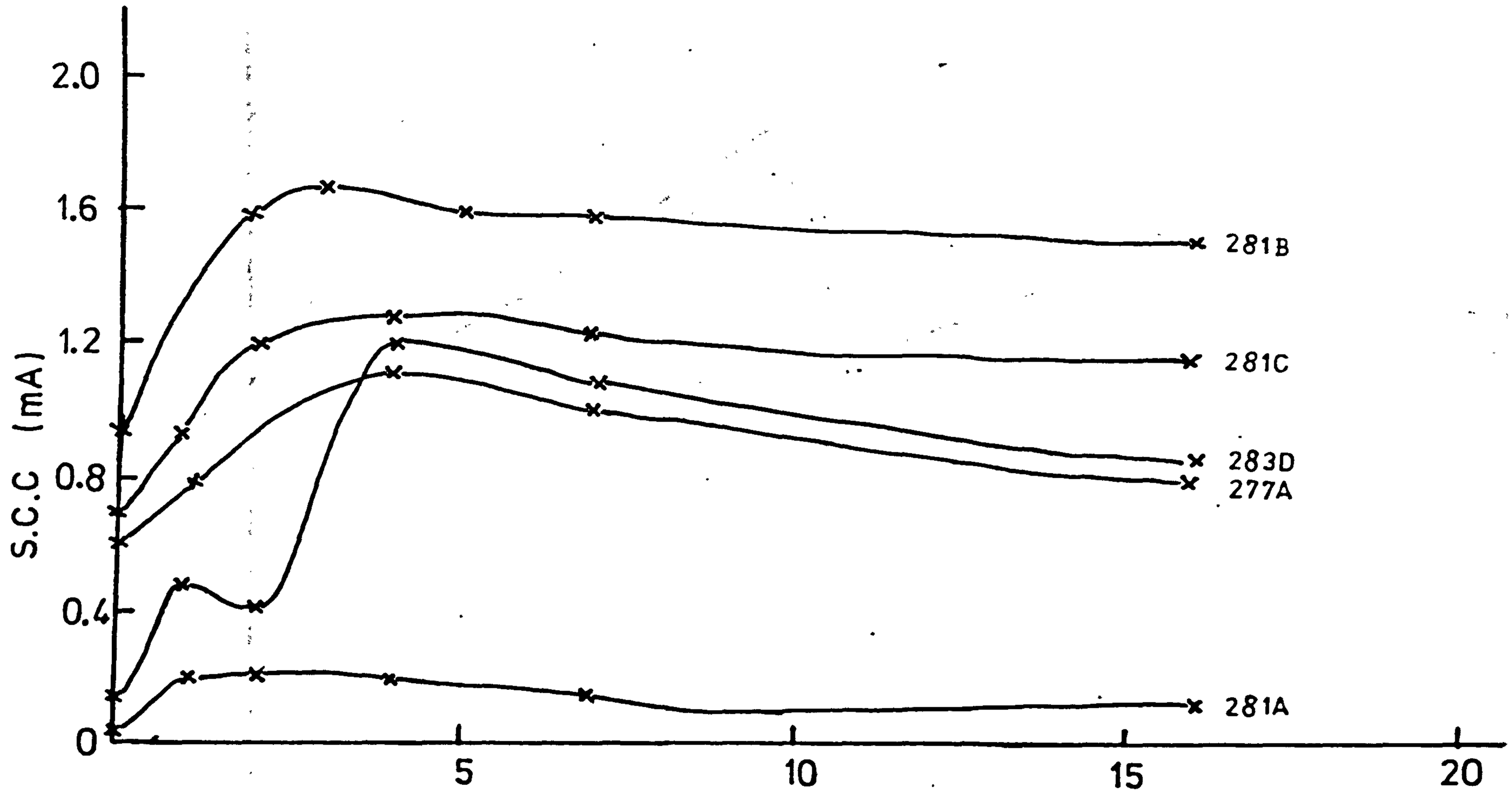

Figure 9.8

S.C.C. Versus Bake Time (Single Crystal Cells)

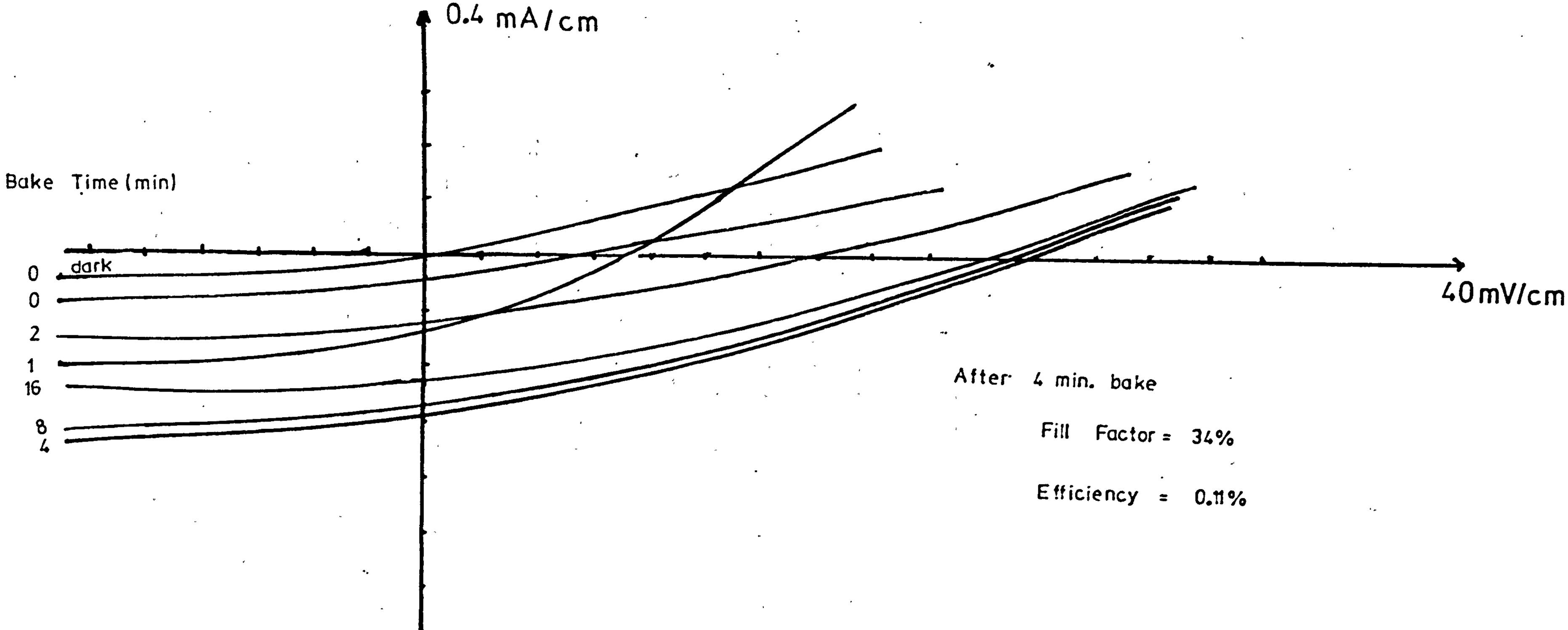

Figure 9.9

I(V) Characteristics of Cell 283D

cells deteriorated after prolonged heat treatment whereas the O.C.V. usually stabilized after about four minutes.

The thin film cells fabricated at I.R.D. behaved in a similar manner. The variation in O.C.V. with bake time for such cells is shown in Figure 9.10. However their S.C.C's. were higher as a grid contact was used and the fill factor also showed an improvement over the single crystal cell. A typical I(V) characteristic for a thin film cell baked at 200°C in air for two minutes is shown in Figure 9.11.

9.5.2 Variation of Photovoltage with Illumination Intensity

So far we have described the results obtained with high intensity illumination of the junction. For satisfactory operation at the Earth's surface or on an outer planet it would be necessary to utilise an intensity of illumination significantly lower than 140 mW cm^{-2}. Therefore the steady state O.C.V. white light response of the boule cells was investigated over four orders of excitation intensity by inserting neutral density filters between the cell and the 140 mW cm^{-2} source.

The CdS:In devices which possessed a high O.C.V. under 140 mW cm^{-2} illumination were most insensitive to low light levels. A lengthy heat treatment in air at 200°C brought about only a slight improvement. Their rate of response to increasing intensity was slow and several tens of seconds were needed under an intensity of micro-watts cm^{-2} before the maximum O.C.V. was reached. This

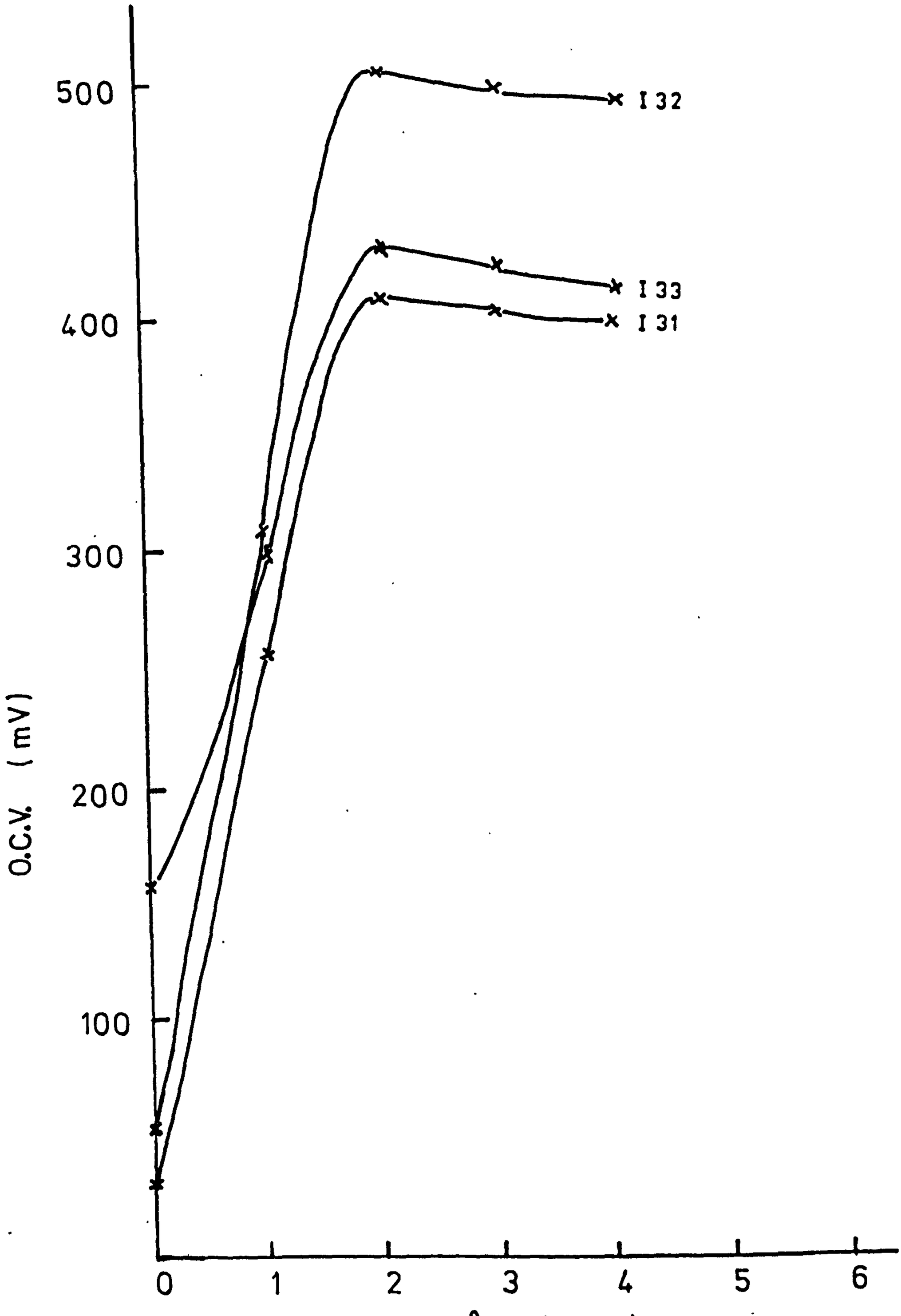

Figure 9.10

O.C.V. Versus Bake Time (I.R.D. Thin Film Cell)

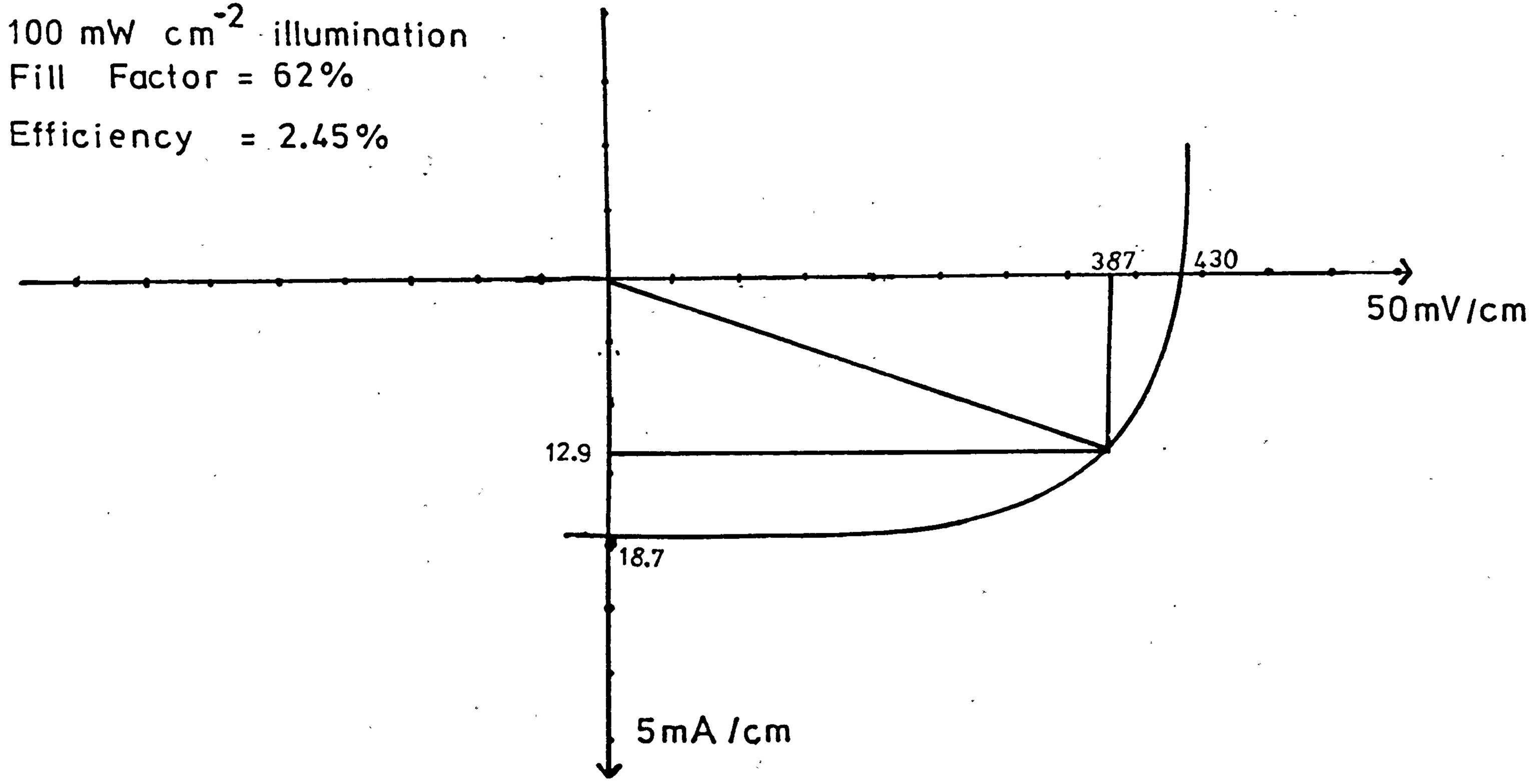

Figure 9.11

I(V) Characteristics of Thin Film Cell I 33

response time increased with prolonged heat treatment. Figure 9.12 shows the variation of O.C.V. with light intensity for two cells after various periods of heat treatment.

High O.C.V's. under weak white illumination have been obtained from cells similar to ours using CdS crystals doped with copper and grown in excess sulphur (Wilson and Woods 1972).

9.5.3 Spectral Response of Photovoltaic Cells

Figure 9.13 shows the spectral response of a typical boule cell after heat treatment for various periods. Unless otherwise stated the points plotted refer to the steady-state values of the O.C.V. reached after several tens of seconds of illumination rather than the initial voltage. Unbaked cells responded quickly (within a few seconds) to changes in the wavelength of illumination but the response of heat treated cells was much slower. Figure 9.13 shows that increasing structure appeared on the curves as the heating proceeded and the relative heights of the two major peaks at 7000Å and 9000Å became roughly comparable. These two peaks are due either to impurities in the CdS or to the Cu_2S. The peak at about 4900Å which is associated with excitation across the band gap of CdS, was not very evident before the cells were heat treated.

After prolonged baking (16-30 minutes) the difference between the initial and steady state values of the O.C.V. became very apparent. Curves illustrating the two responses are shown in Figure 9.14. The slow component

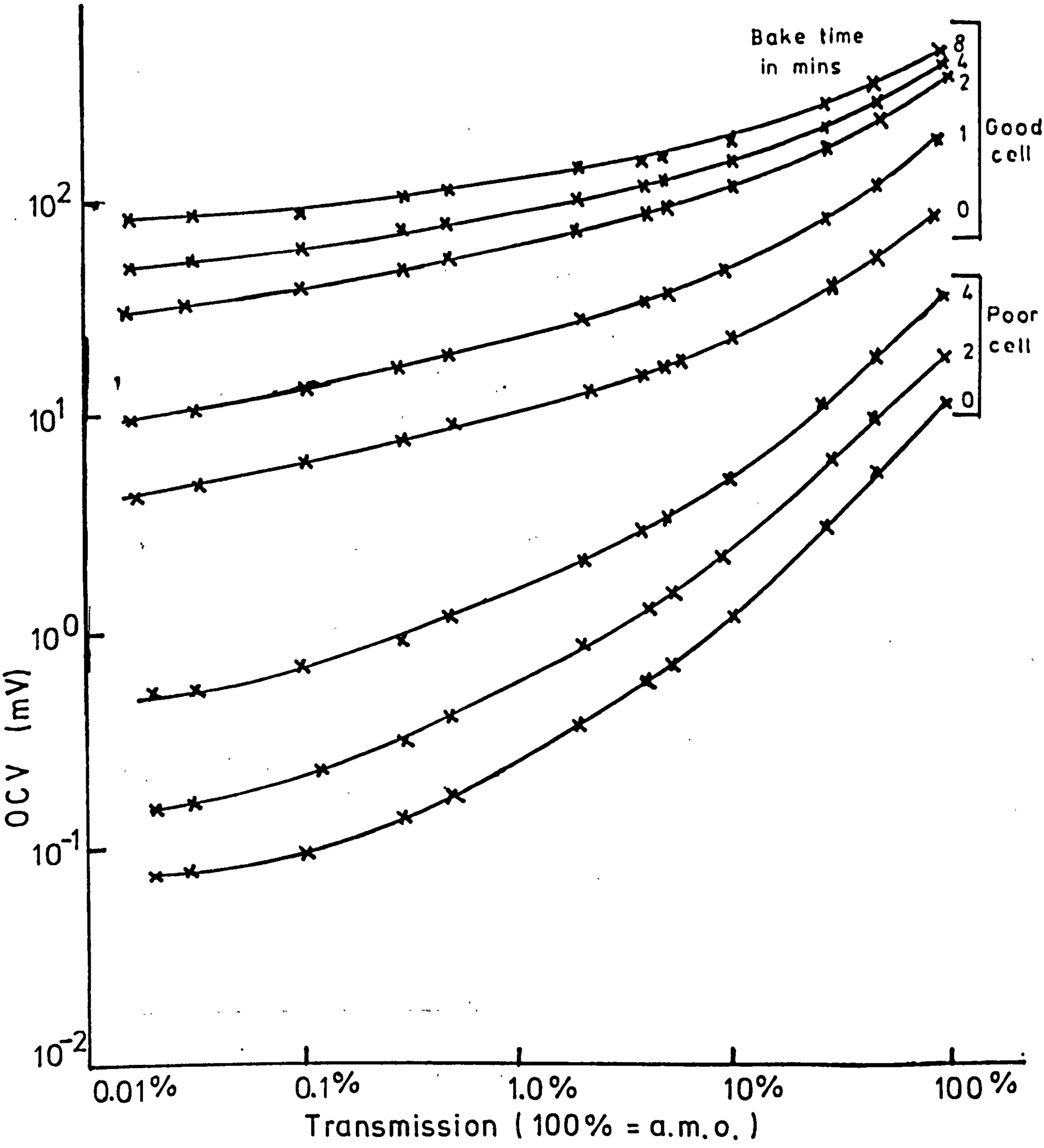

Figure 9.12

Variation of OCV with Illumination Intensity

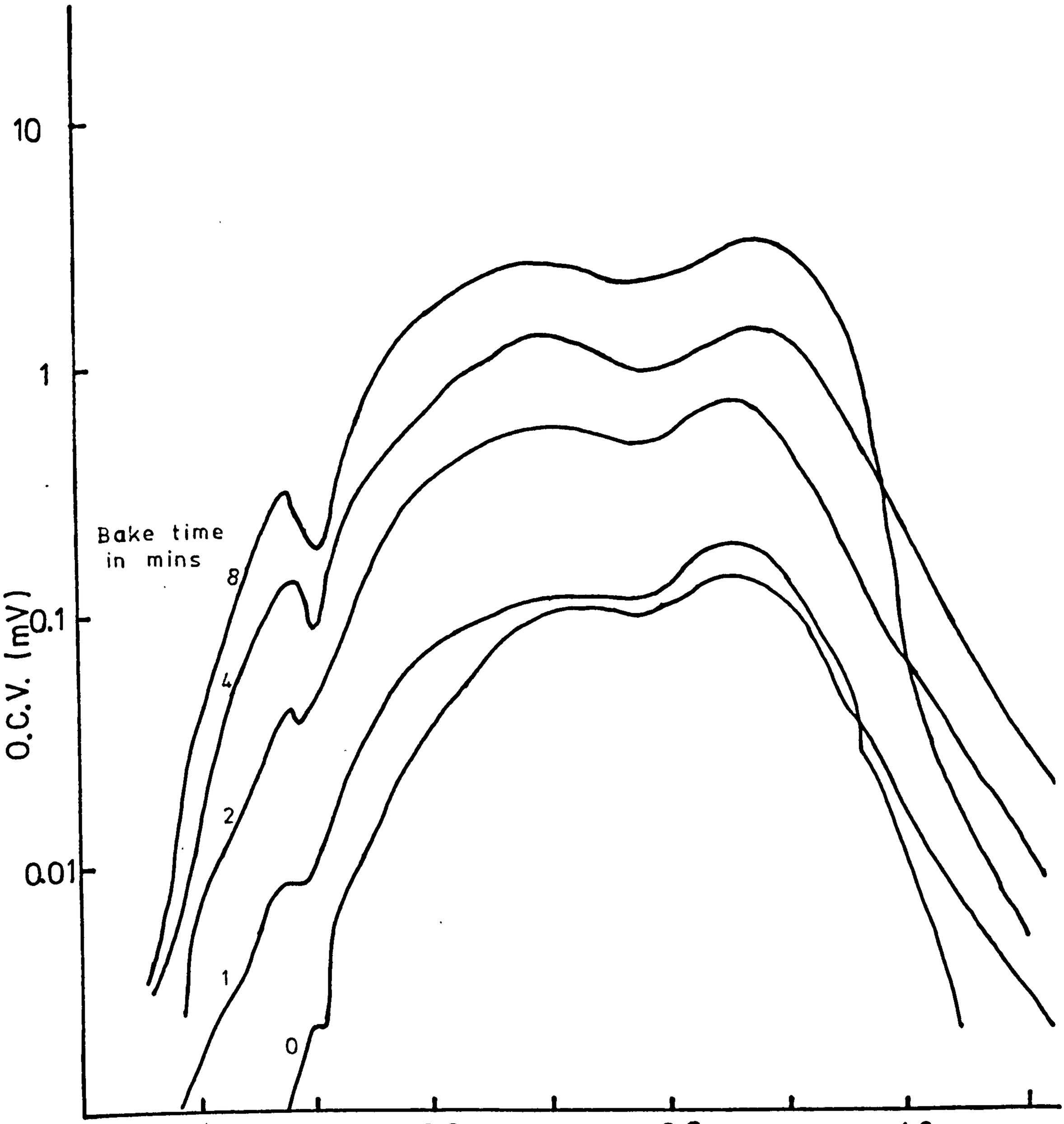

Figure 9.13

Spectral Response of Boule Cell 283 D

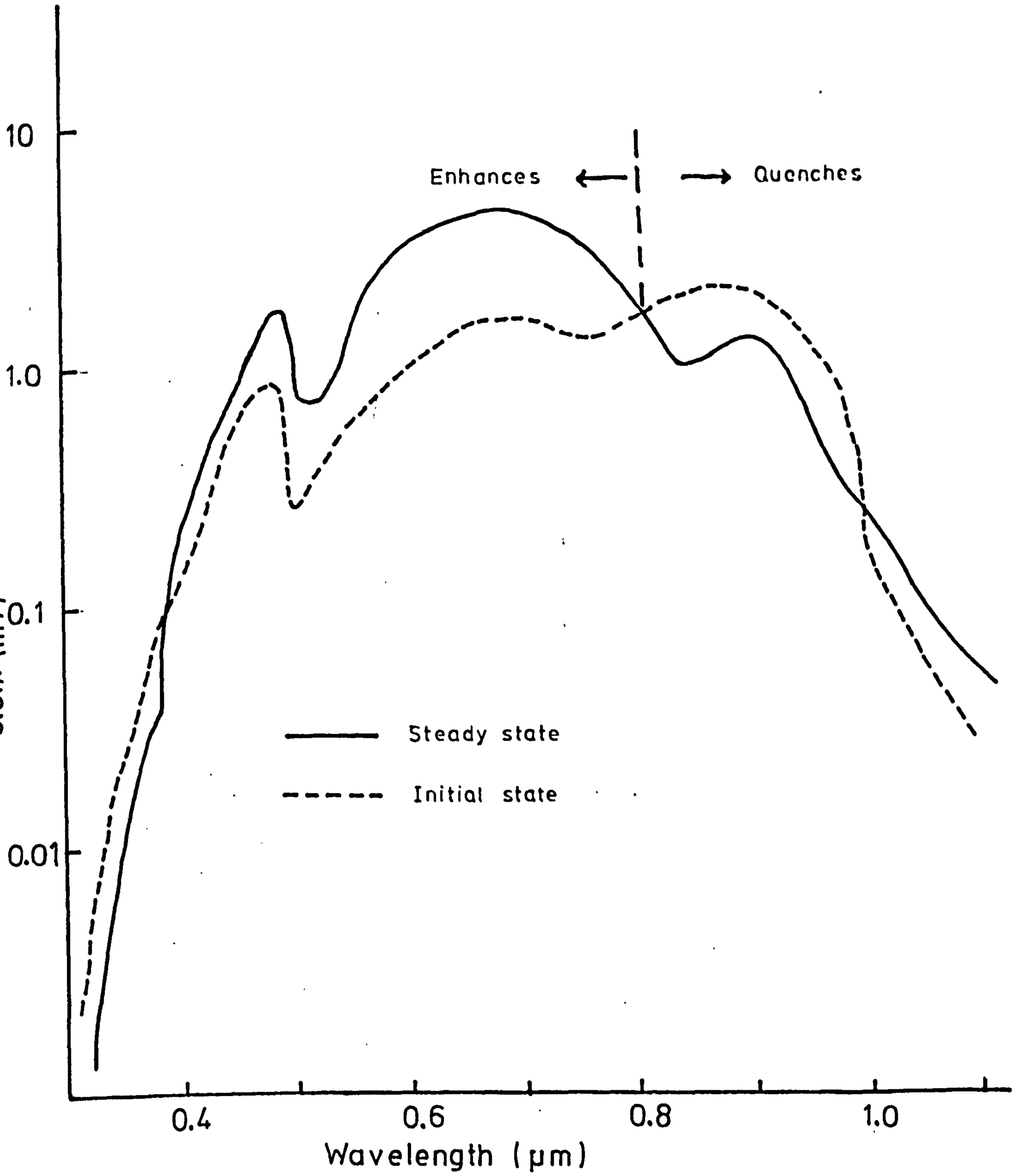

Figure 9.14

Spectral Response of Cell 282 B after 20 mins Baking

of the steady state response enhanced or quenched the initial fast response depending on whether the wavelength of the incident light was shorter or longer than 8000Å. Gill and Bube (1970) have reported a similar phenomenon in the spectral response of the S.C.C. of cells prepared under different conditions. The spectral response of all the cells investigated followed the same shape and behaviour.

9.5.4 Effect of baking the cell prior to plating

During the initial period of the development of the CdS solar cell it was reported by Shiozawa et al (1969) that baking the cell in air prior to the formation of the Cu_2S layer had effects similar to those produced by the normal heat treatment of the completed cell.

To investigate this point cells were therefore prepared from the same boule, some were baked in air at 200°C for varying times prior to forming the junction, while others were prepared in the normal way. The cells were then examined 'as-formed' and after further baking for periods up to 16 minutes.

Baking the cells for periods of 1-8 minutes prior to the formation of the p-type Cu_2S layer decreased their O.C.V. in most cases. Occasionally the O.C.V. remained constant but no specimens showed an increase in O.C.V. as a result of heat treatment prior to plating. Slight improvements in the O.C.V. were obtained when the cells were given a further bake after plating.

However the response of the cells to low level illumination was altered by pre-baking. The O.C.V. of

pre-baked cells tended to saturate at lower illumination intensities than untreated cells (Figure 9.15). This difference was still noticeable when the cells were subjected to further heat treatment after the formation of the Cu_2S layer.

Pre-baking the cell exaggerated the difference between the steady state and instantaneous spectral response. With normal cells this difference was apparent after a post-plating bake of about 16 minutes. Cells pre-baked for 2 minutes however exhibited this difference after a further four minute bake. The spectral response of such a cell is shown in Figure 9.16, where it can be seen that the difference in the two responses is much greater than the corresponding difference for 'normal' cells shown in Figure 9.14.

9.5.5 CdS Surface Quality

Some thin film cells exhibit low fill factors which are attributable to pinhole short-circuits in the CdS layer. Pinhole defects were not of course present in cells formed from CdS boule slices, but care had to be taken to use the same surface treatment for each slice. This was especially important when several cells were manufactured from the same boule. The standard process consisted of removing the cutting marks by polishing with 600 grade carborundum followed by an etch in orthophosphoric acid as described in Section 9.2.1. If instead the surface was roughened by abrasion before chemi-plating a lower O.C.V. resulted. Alternatively the O.C.V. could be improved significantly by polishing the CdS surface with 3 micron

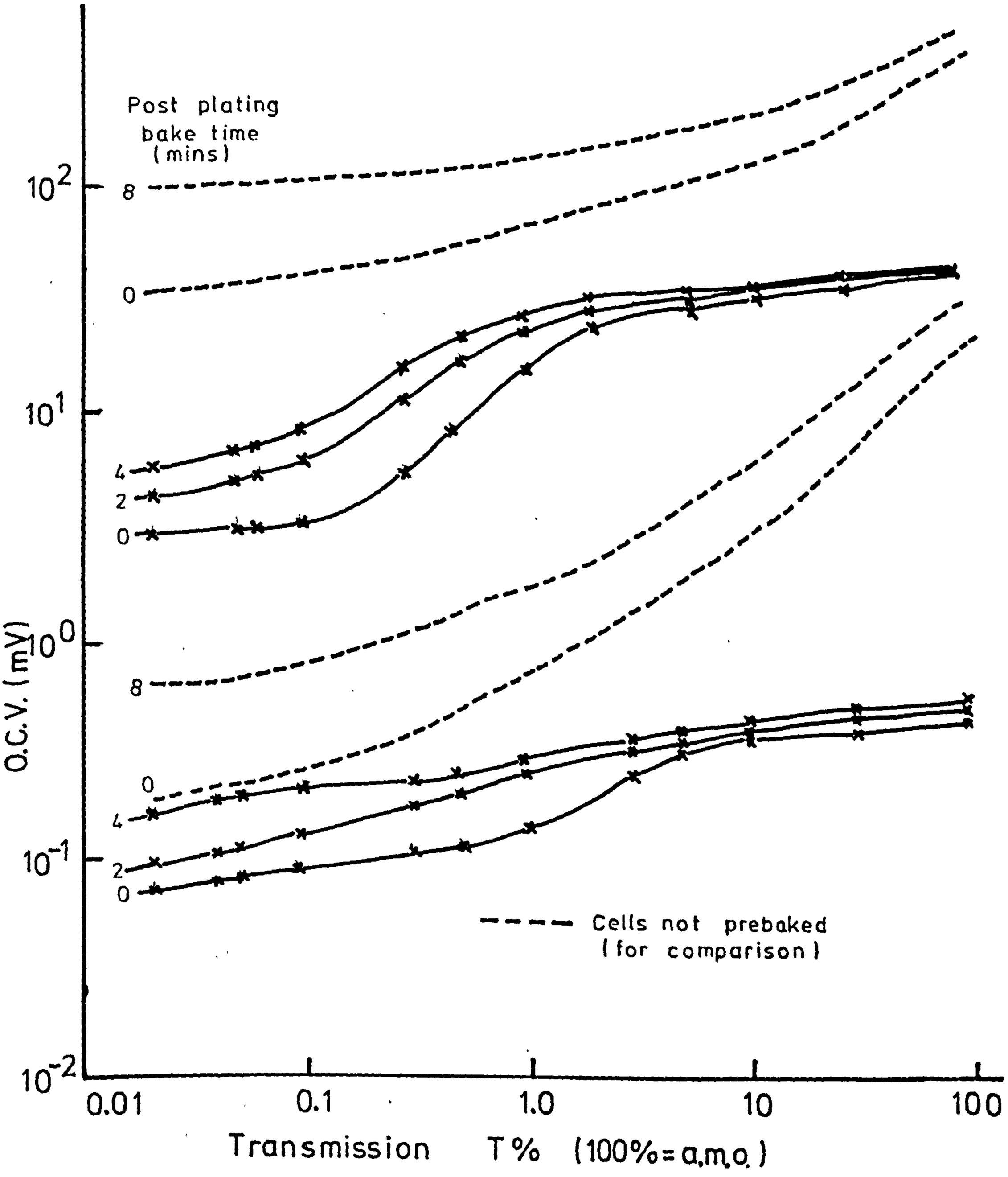

Figure 9.15

OCV Versus Light Intensity for Cells

Pre-baked for 2 minutes

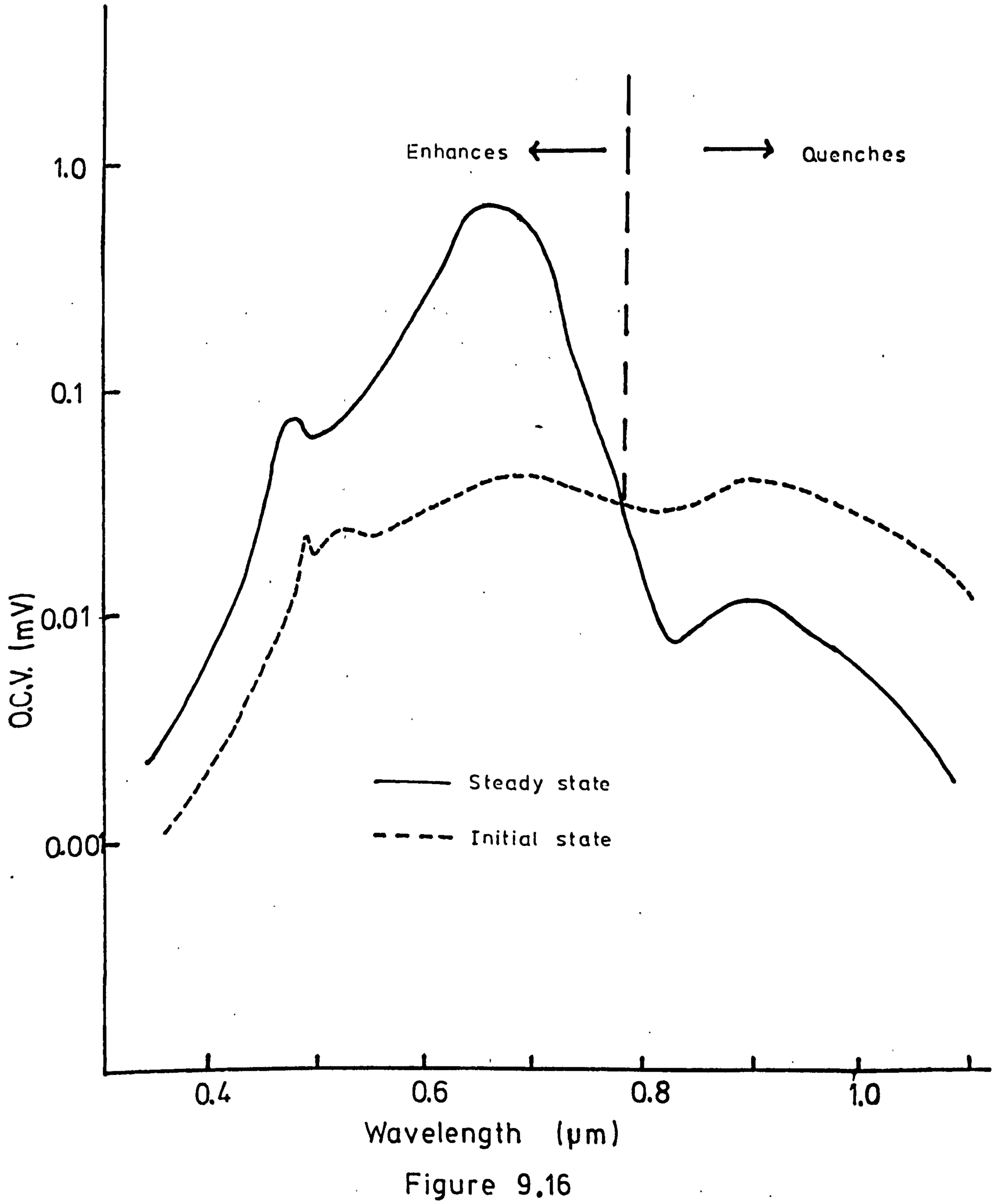

Figure 9.16

Spectral Response of Pre-baked Cell 508∝
after 2 min. pre-plating bake and 4 min.
post-plating bake.

diamond powder before etching in HCl and plating. A comparison between the O.C.V's. of two cells made from the same boule, one highly polished and the other given standard treatments is given in Figure 9.17.

It is obvious that a rough surface forms a larger area junction with more efficient light absorption than a polished surface and this is the reason for administering the brief etch in HCl or KI immediately before the chemi-plating stage. Against this however a rougher surface will have more surface damage together with associated traps and recombination centres. Figure 9.17 shows that the difference between polished and unpolished cells becomes smaller after two minutes heat treatment. This would indicate that the surface damage responsible for the lowering of the cell's O.C.V. was gradually being annealed out.

9.5.6 Thin Film Cells.

Some thin film cells have been fabricated in Durham using CdS thin films evaporated in the closed system described in Chapter 5.

The cells exhibited low O.C.V's of around 60 mV but high S.C.C's of 4 mA for a cell 0.25 cm^2 in area. After baking for two minutes at 200^{o}C the cells had efficiencies of about 1.2% (Figure 9.18). These efficiencies were considerably higher than those exhibited by single crystal cells (typically 0.1-0.7%), but lower than the thin-film cells fabricated at I.R.D. (η = 2.5-3%). However as the I.R.D. cells incorporated a grid electrode as opposed to the

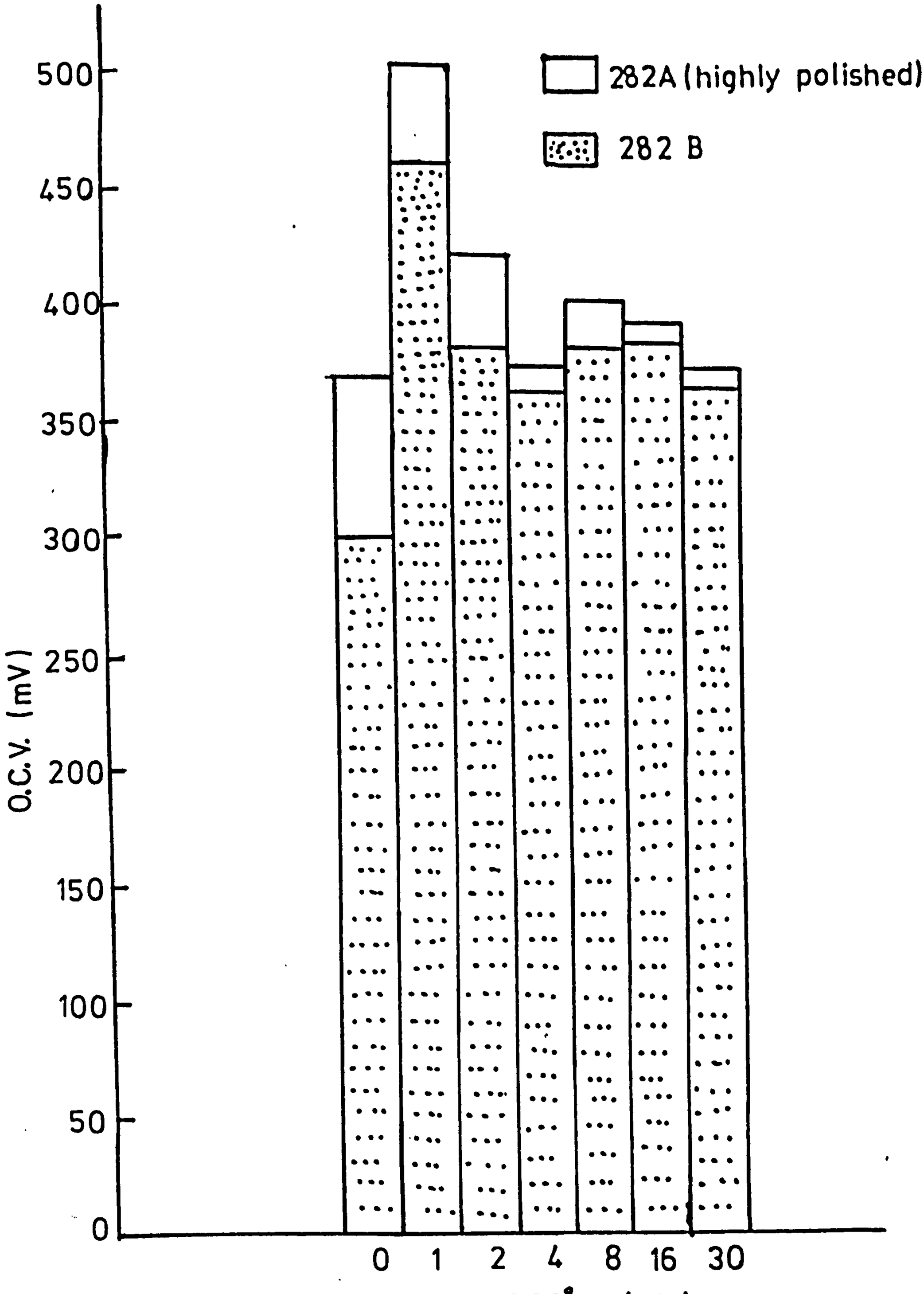

Figure 9.17

Cells 282 O.C.V. and Baking Time

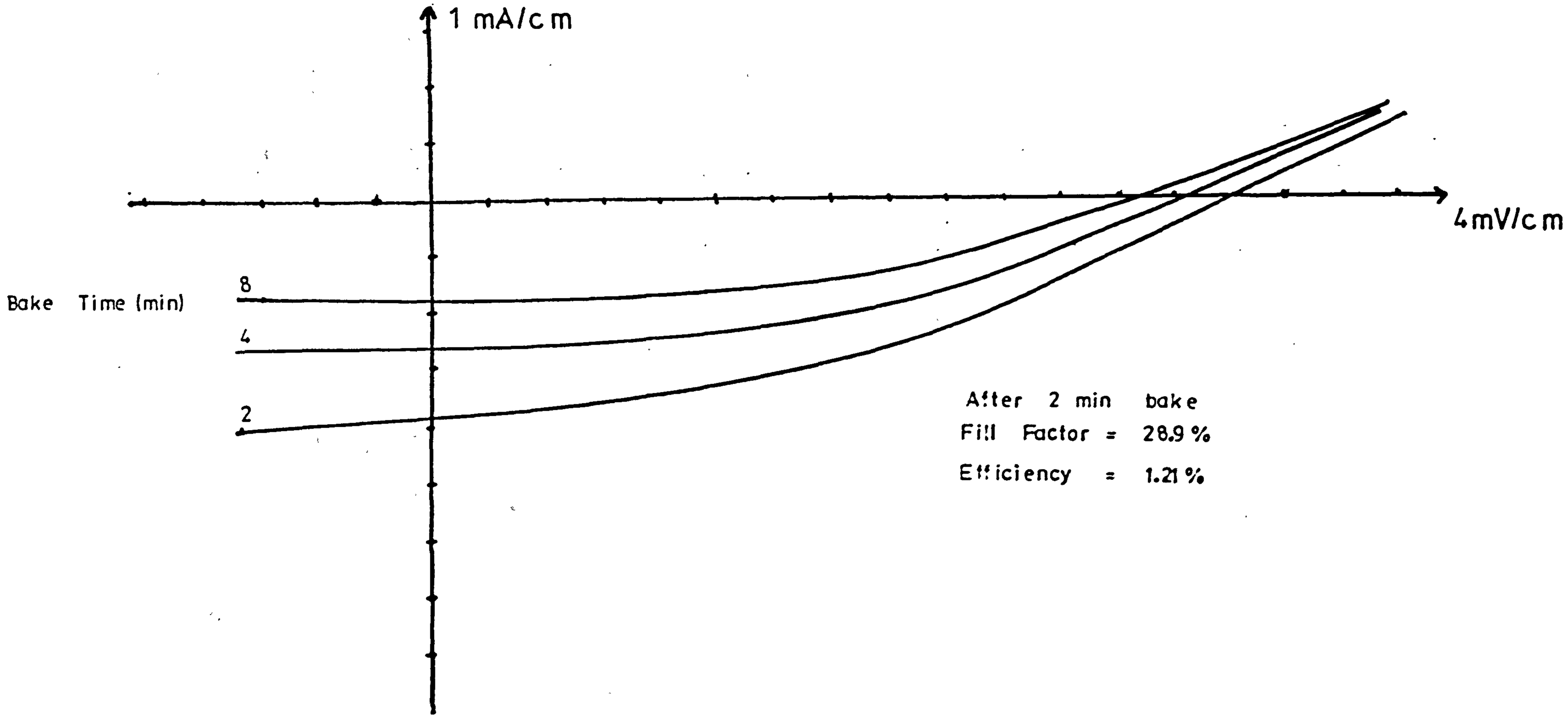

Figure 9.18

Thin Film Cell (film grown in closed system): I(V) Characteristics

point contact method used at Durham, it is reasonable to suppose that the efficiency of these cells, formed on films grown in the enclosed system could be increased to values comparable to or better than the I.R.D. cells after a more rigorous contacting procedure. Baking the thin-film cells for periods greater than two minutes led to a gradual falling off of the O.C.V. and a much more severe drop in S.C.C. as shown in Figure 9.19.

9.6 Cell degradation and Cu_2S Stoichiometry

9.6.1 Introduction

The initial disadvantages of the CdS solar cell, i.e. its degradation when subjected to thermal cycling or ultra-violet radiation have now been overcome by improved encapsulation techniques (Mytton et al 1968). Load effect degradation of the O.C.V., described in Chapter 3 has been attributed to the migration of copper ions through Cu_2S short-circuits which are formed down cracks and grain boundaries in the CdS. This migration results in metallic copper building up along the short until it reaches the top surface. These copper nodules have been clearly observed on the surfaces of degraded, thin film cells by Shiozawa et al (1969). A thermodynamic study of this process however reveals that such a reaction has a threshold of 390 mV and as cells are usually operated below this value in load conditions, this degradation process is not the serious problem it was once thought to be.

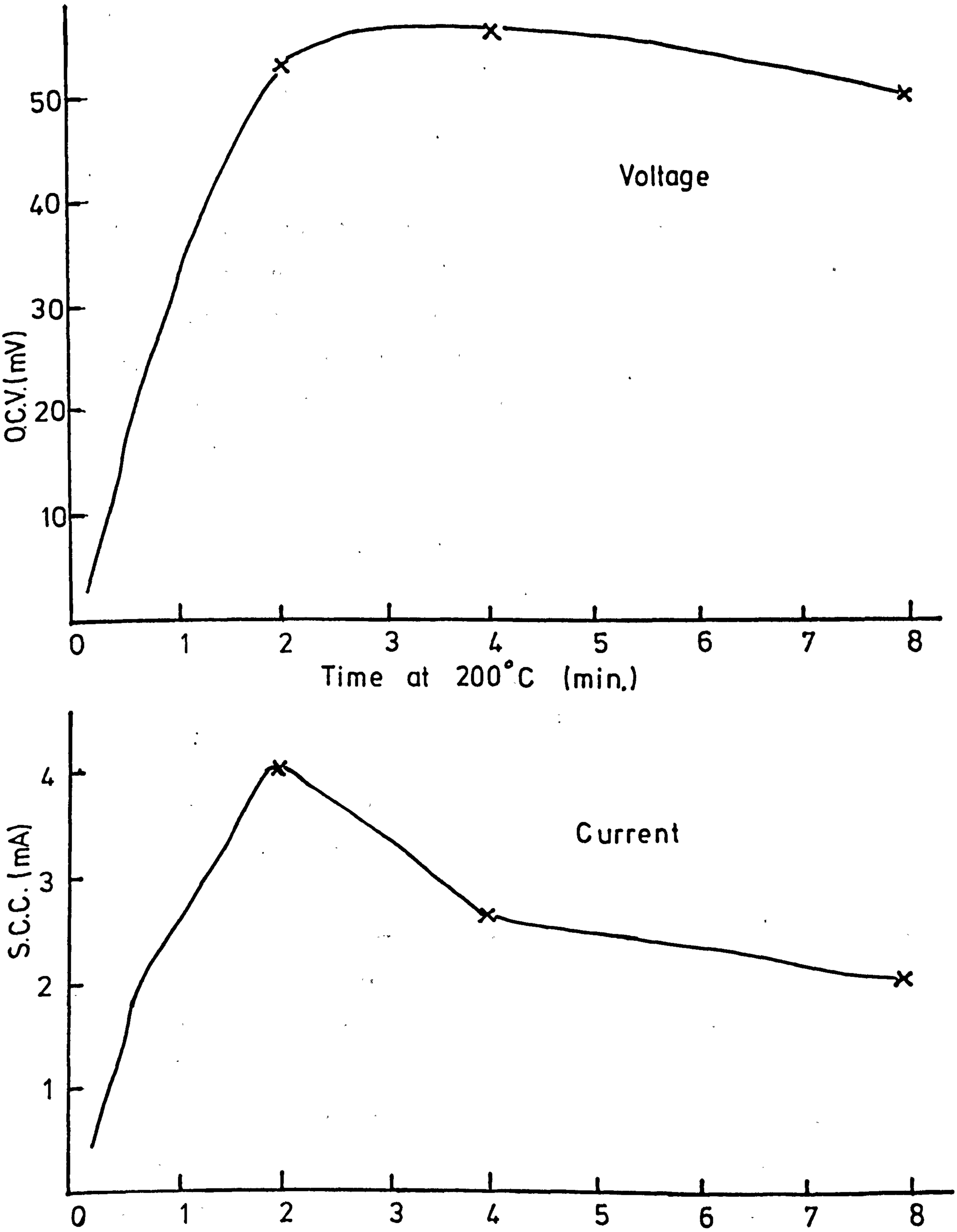

Figure 9.19

Thin Film Cell (film grown in enclosed tube)

Output and Baking Time

Workers both in the United States and Europe have reported degradation in both O.C.V. and S.C.C. when cells are operated at temperatures above 60°C especially in poor vacuum. At first this degradation process was thought to be due either to photochemical changes in the CdS (Kanev et al 1971) or to a sudden increase in the migration of copper through the material. More recently however the effect has been attributed to the gradual photo-assisted oxidation of the Cu_2S (Bogus and Mattes 1972). Palz et al (1972) suggested that the best way to combat the slow deterioration was to ensure good initial stoichiometry in the Cu_2S layer.

9.6.2 Optical transmission of CdS

Single crystal slices of CdS were cut from a boule and both faces polished using 600 grade carborundum followed by 3 micron diamond paste. The transmission of these samples was then measured using the 'Optica' spectrophotometer.

At room temperature the crystals began to transmit light gradually above a threshold of 5250Å and a maximum transmission of 56% was obtained at longer wavelengths. At 77 K the threshold had moved to 4965Å and a maximum transmission of 71% was achieved. The curves in Figure 9.20 show the variation of the transmission as a function of wavelength for a typical sample.

The crystals were then mounted in a water cooled copper block, to ensure isothermal conditions, and illuminated by 140 mW cm^{-2} visible radiation for a period

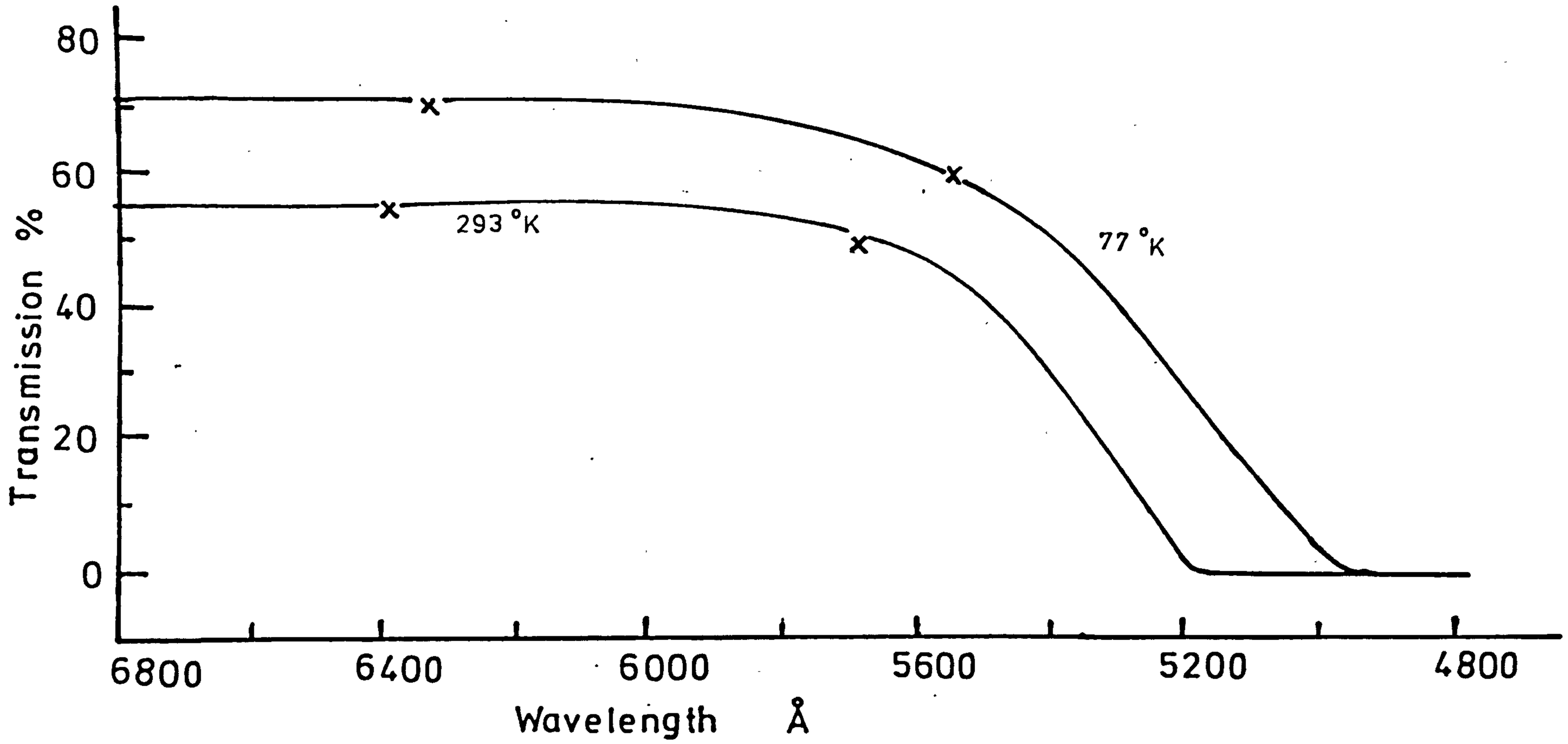

Figure 9.20
Optical Transmission of a CdS Crystal

of 200 hours. After this period further transmission measurements were taken but no change in the threshold or maximum transmission at either temperature was observed. It seemed unlikely therefore that any photochemical changes had taken place in the CdS as a result of a long period of illumination.

9.6.3 Diffusion of Cu in CdS

Copper was evaporated on to both sides of a single crystal slice of low resistivity (≈ 20 Ωcm) CdS, 1 cm in diameter and 2 mm thick. The crystal was then placed in a silica glass tube which was evacuated to a pressure below 10^{-3} torr, flushed with argon and evacuated again. The tube was then sealed off under vacuum. Several samples were prepared in this way and then placed in an oven for seven days at temperatures ranging from 20° to 100°C.

After this heat treatment the crystals were removed from the tube and their dark capacitance measured using a Universal Bridge B221.

The copper penetrating into the CdS forms an insulating layer and so the device can be thought of as two parallel plate capacitors as shown in Figure 9.21. For a parallel plate capacitor

$$C = \frac{\varepsilon_o \varepsilon_r A}{d}$$

where C is the capacitance

ε_o is the permittivity of free space

ε_r is the relative permittivity

A is the device area, and

d is the distance between the plates.

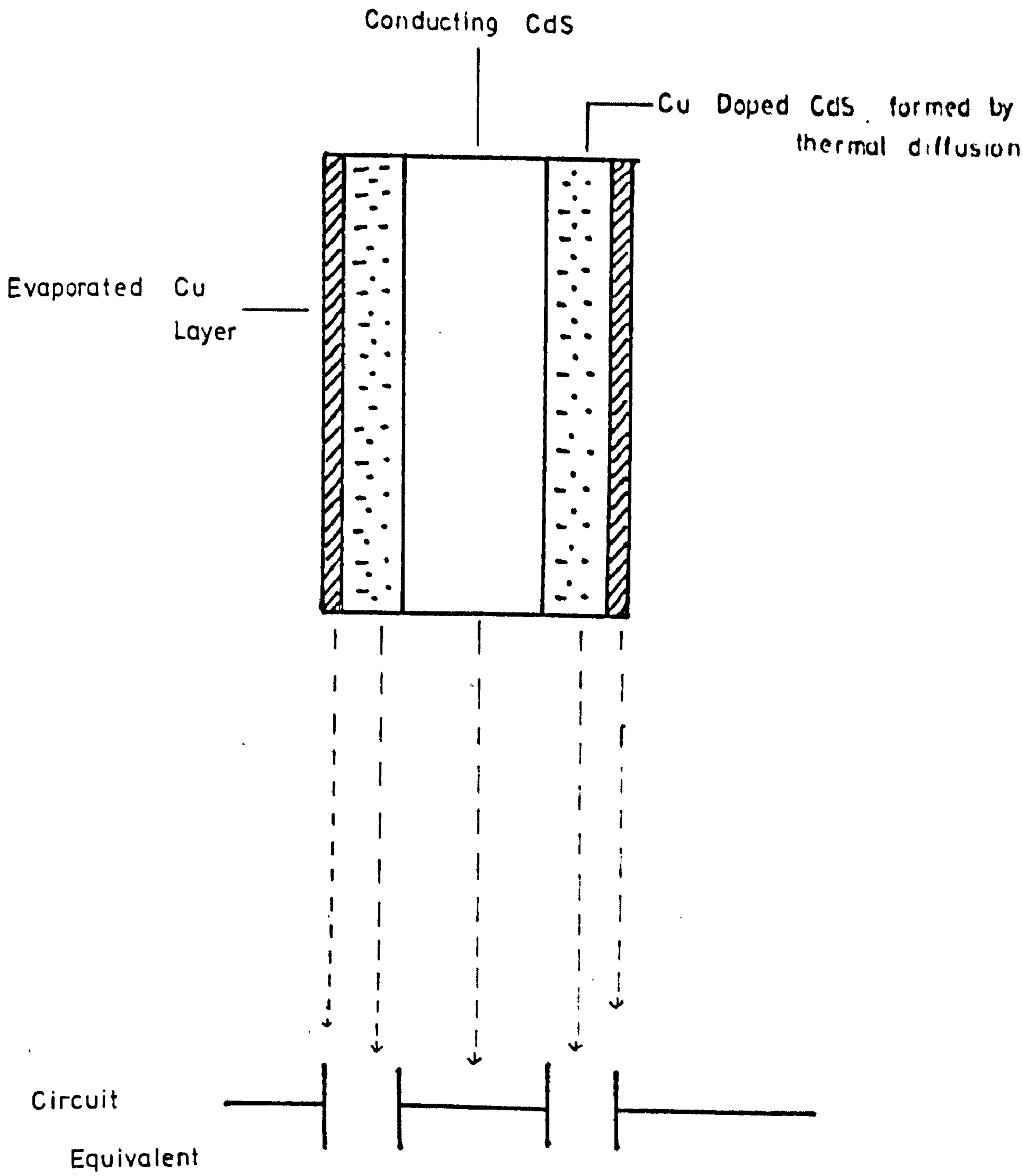

Figure 9.21

CdS Crystal Parallel Plate Capacitor

Using this equation it was possible to calculate the depth of penetration of the copper into the CdS. The results obtained are only approximate as the device was assumed to be two perfect parallel plate capacitors in series and no corrections were made either (1) for any non uniform distribution of Cu in CdS or (2) for the fact that the junction between the CdS and Cu doped CdS is not abrupt or (3) for any edge effects.

The depth of penetration of the Cu into the CdS in seven days as a function of temperature is shown in Figure 9.22. This shows that the penetration increased with temperature over the full range studied. There is no significant increase in the rate of diffusion at 60°C or above. Our results indicate therefore that it is unlikely that either photochemical effects in the CdS, or the migration of Cu through the device contribute significantly to the observed degradation in the output of cells at temperatures above 60°C.

9.6.4 The Stoichiometry of the Cu_2S layer

The advantages to be gained in ensuring strict stoichiometry of the Cu_2S layer are as follows:

(1) The efficiency of the cell is increased

(2) The rate of oxidation at elevated temperatures is reduced.

(3) The oxidation process has to proceed further before the degradation becomes significant (Palz et al 1972).

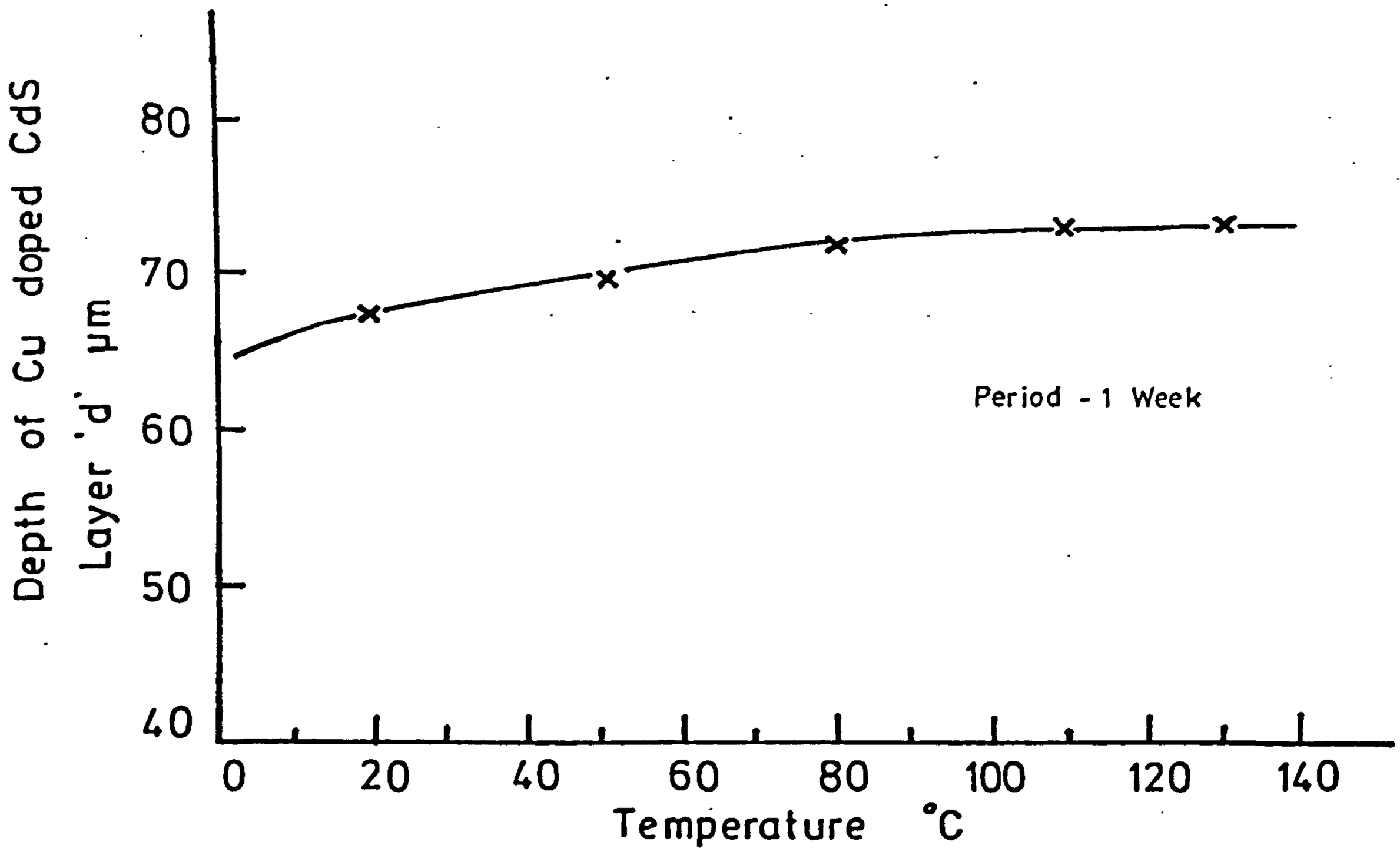

Figure 9.22

Diffusion of Cu into CdS

Rickert and Mathieu (1970) in their physiochemical investigation of the Cu-S system showed theoretically that it was possibly to vary the stoichiometric composition of a compound Cu_xS by changing its electropotential during plating. Accordingly a system was set up to measure the potential of the Cu_2S surface during plating and then to apply a given potential to this reaction interface. Two electrodes were used; (1) Pure copper placed in the bath as a reference electrode, and (2) a platinum electrode to make contact to the CdS/Cu_2S surface. Platinum was selected as it develops only a negligible electropotential when immersed in a bath of copper ions so that the potential of the Cu_2S surface only was measured.

CdS crystals were immersed in the plating bath and the potential of the surface was measured as a function of time. This was done using the Cambridge pH meter as a high resistance voltmeter. The potential remained at a steady value of +21 mV (Cu_2S with respect to the Cu electrode) for immersion periods of up to one minute.

Using a supply consisting of a 'dry cell' battery and a potentiometer, potentials varying from -150 mV to +150 mV were applied to the surfaces of various crystals and thin films during the formation of the Cu_2S layer. The resultant cells were baked for two minutes in air at $200^{o}C$ and then examined under 140 mW cm^{-2} illumination.

The I(V) characteristics of the cells were measured to obtain a curve of resultant O.C.V. as a function of the bias applied in the plating bath. The results are

shown in Figure 9.23. The O.C.V. was enhanced considerably when the Cu_2S was held at a positive potential relative to the Cu reference electrode. Application of a negative potential had a detrimental effect on the O.C.V.

The S.C.C. was also affected by the introduction of a potential bias in the plating bath. By making several cells from the same film and applying potentials of up to +500 mV cells with a wide range of efficiencies were produced.

Figure 9.24 shows that the efficiency of the cells was increased following the application of a positive potential to the Cu_2S surface, that is to say the efficiency increased from the range 2.25 - 2.75% to 2.95 - 3.3%. Maximum efficiencies were obtained for cells plated at a positive potential of 100 mV. Similar results were obtained with single crystal cells.

When trying to form Cu_2S on CdS crystals held at a potential of -100 mV copper nodules began to appear on the surfaces of the crystal. These were observed under a microscope and found to have distinct crystalline facets (Figure 9.25a). Further examination revealed that these nodules formed at intervals along the grain boundaries. In Figure 9.25b the nodule is at the centre and the grain boundary is seen to run from the top to the bottom of the photograph.

Attempts were made to measure the stoichiometry of the Cu_2S formed in those experiments to determine whether the introduction of the potential into the plating process controlled the stoichiometry of the Cu_2S. The samples were investigated using a photo-electron spectroscopy technique

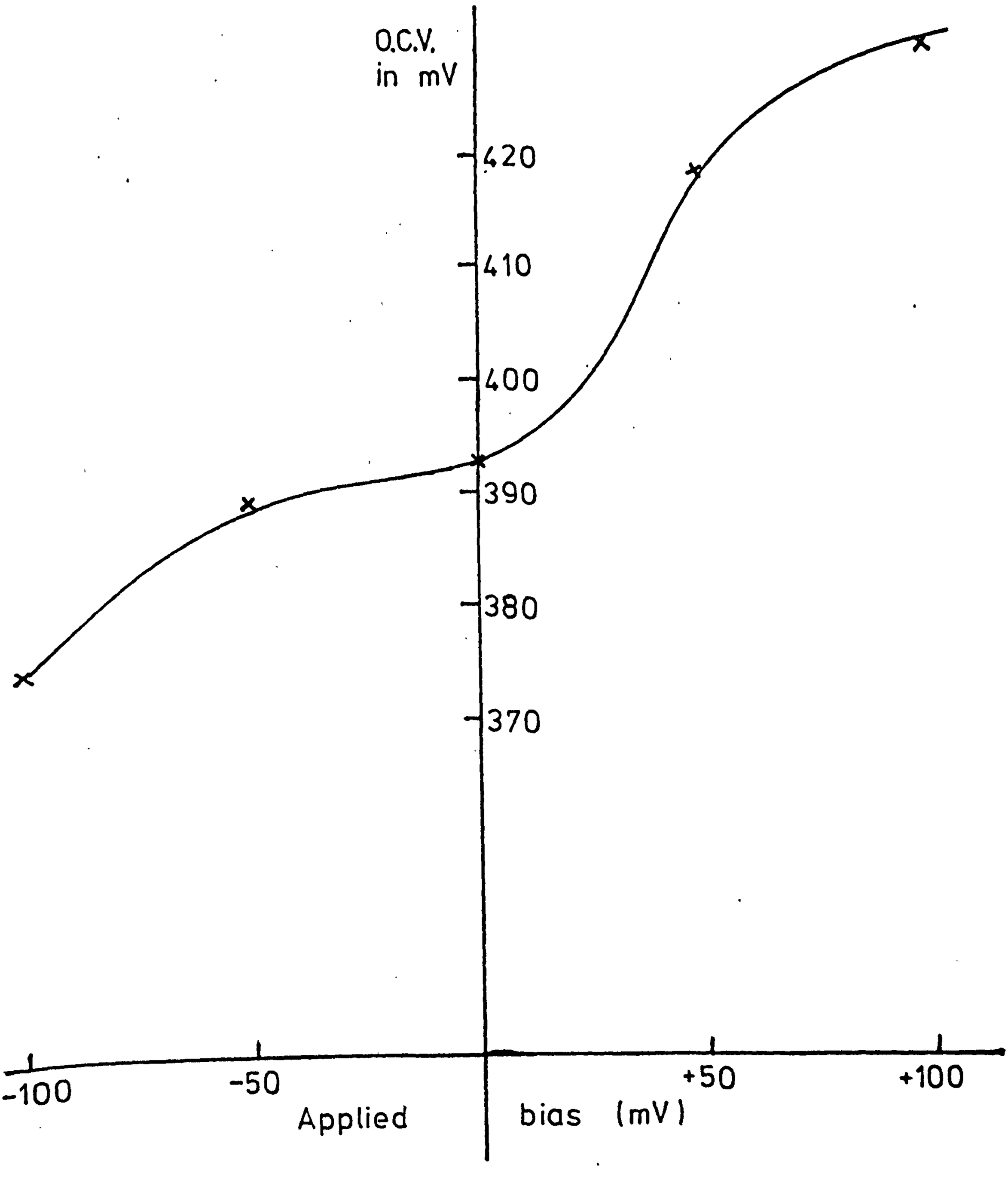

Figure 9.23

Plating Bias Versus Cell O.C.V.

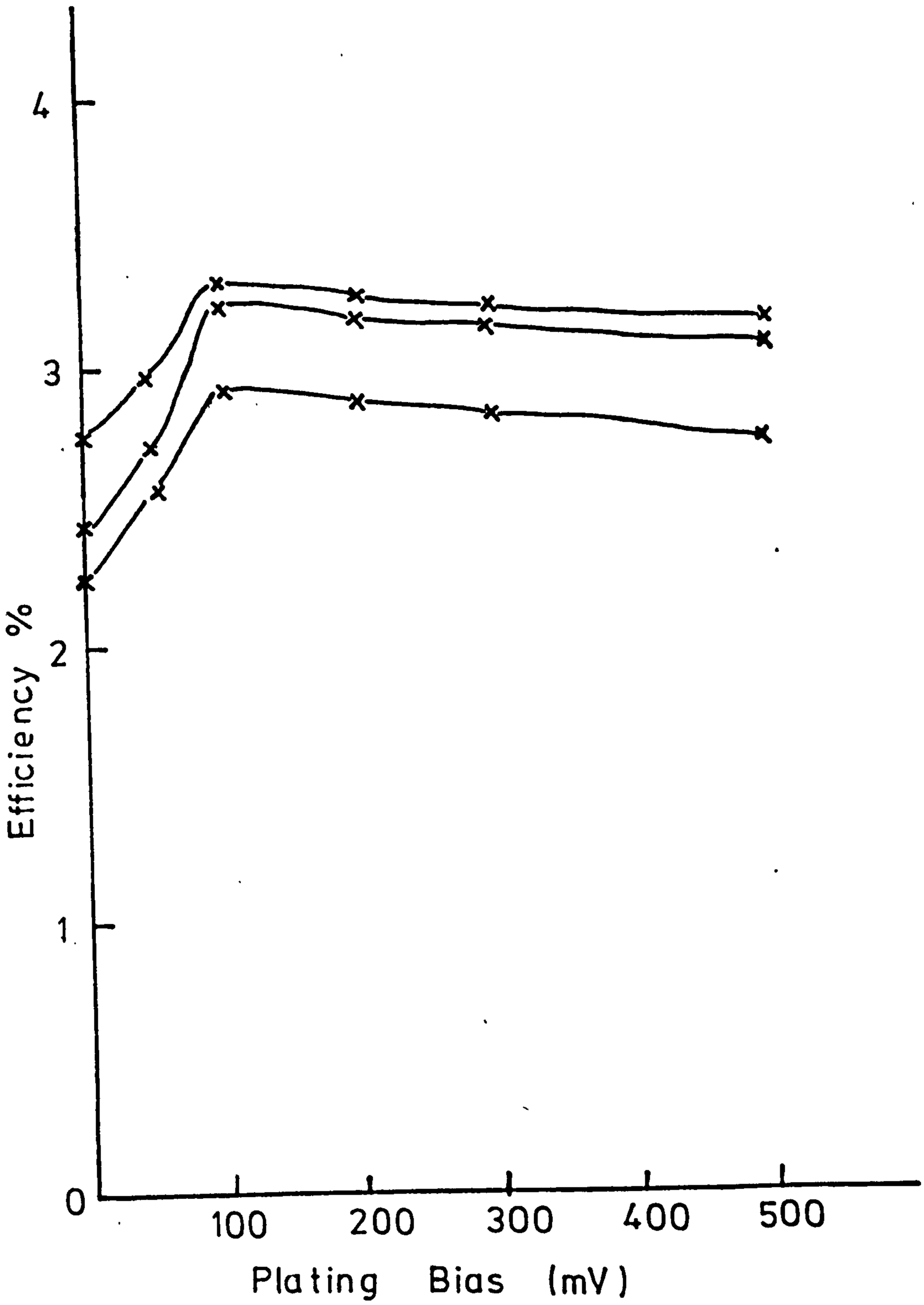

Figure 9.24

Plating Bias Versus Efficiency

Figure 9.25

(a) Copper nodules formed on a CdS crystal

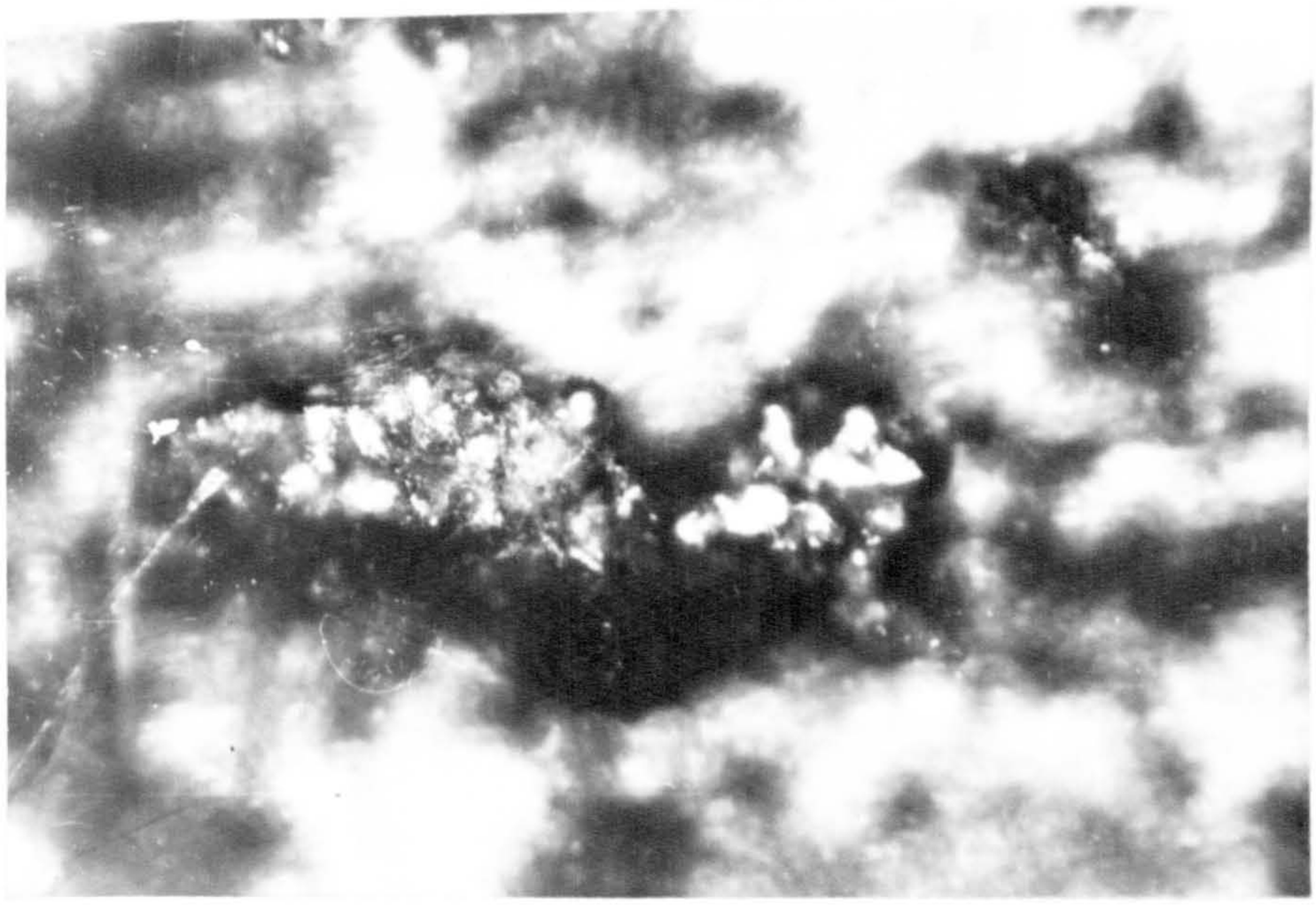

(magnification = 32)

(b) Copper nodule formed at a grain boundary

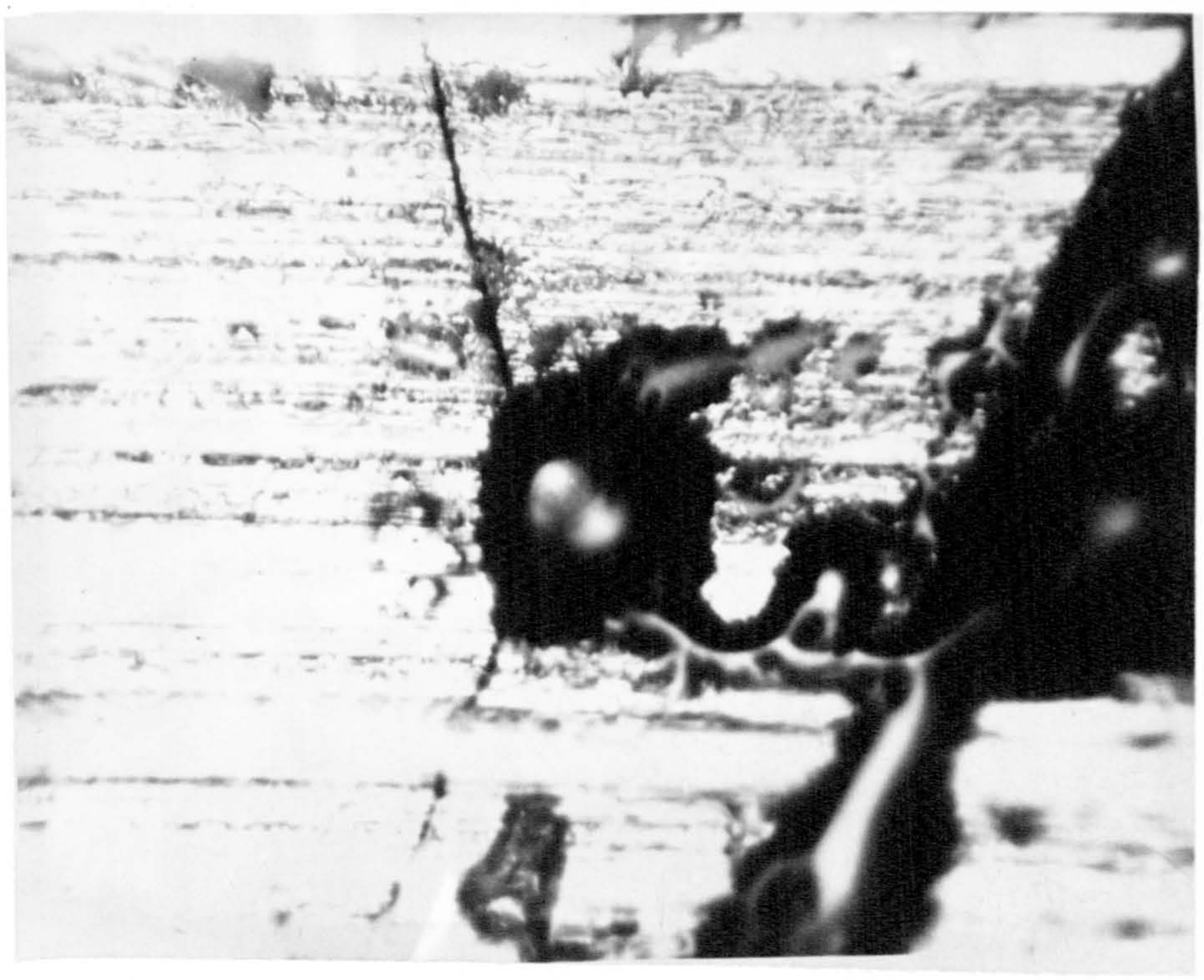

(magnification = 100)

known as E.S.C.A. (Electron Spectroscopy for Chemical Analysis). However this apparatus was very sensitive to the presence of carbon. The corresponding signal associated with carbon which was presumably left as a residue following washing in acetone, masking with wax, encapsulation etc. swamped the small signals expected from changes in the copper and sulphur content. The results showed that with single crystal cells carbon was more abundant in the first 50Å surface layer than either Cd, Cu or S. For thin film cells carbon was less dominant but nevertheless still masked the variation in copper content sought.

The stoichiometry of the cells produced was finally assessed by studying the variation in their S.C.C's. with temperature (Palz et al 1972). Each cell was mounted on a copper block which could be water cooled. The block was then placed on an electrical heating plate. The I(V) characteristics of each cell were measured at various temperatures from 20° to 100°C and from the resultant curves the S.C.C. and O.C.V's. of the cell were determined.

The curves in Figure 9.26 show the variation in S.C.C. as an absolute value as a function of temperature for cells prepared under various bias potentials. There is a noticeable decrease in the S.C.C's. of all cells in the range 75° to 85°C. The interpretation of this sudden decrease will be discussed in the next chapter. Over the same temperature interval the O.C.V. remained constant but dropped to between 95 and 90% of its original value at temperatures above 90°C.

MISSING

PRINT

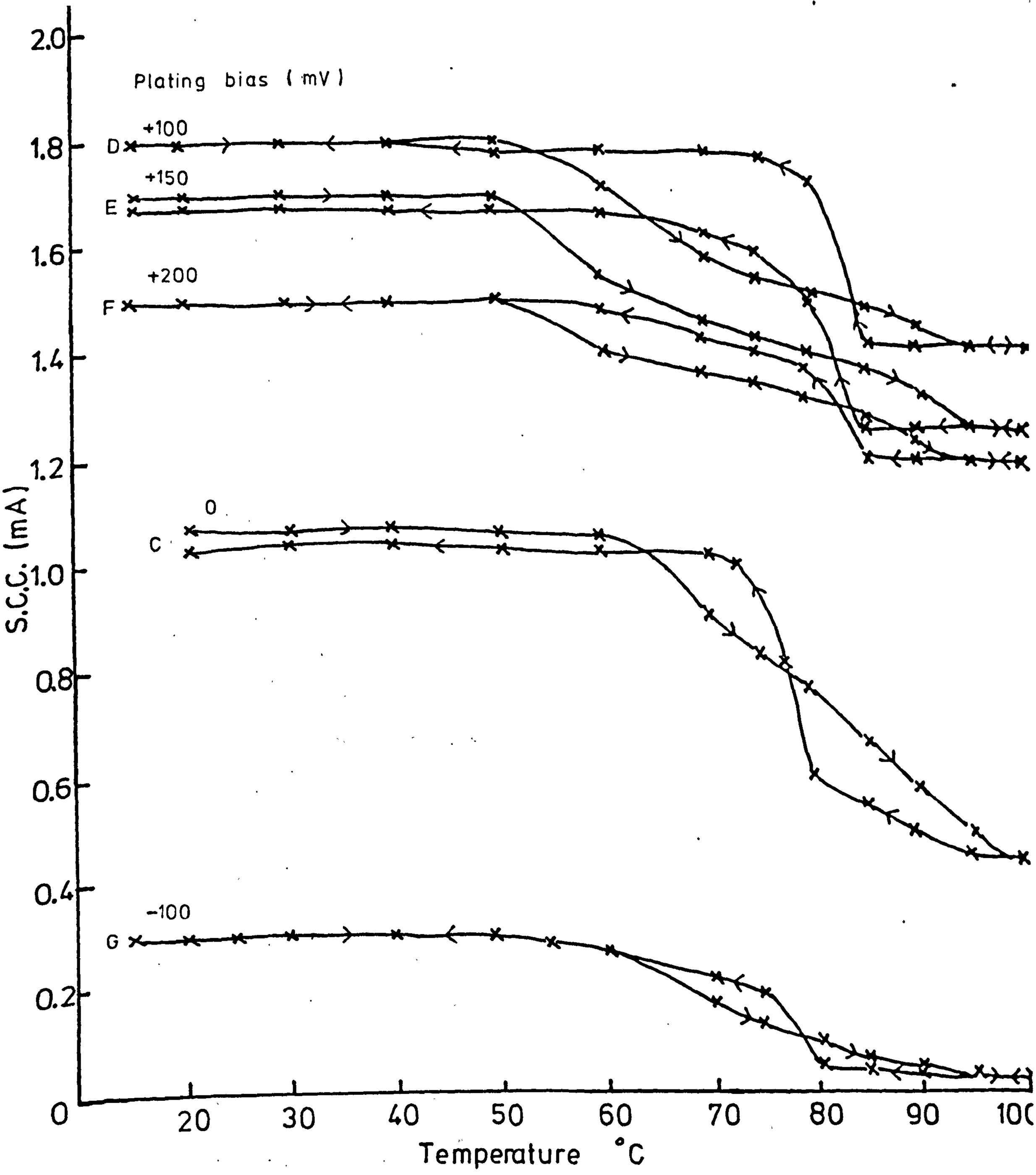

Figure 9.26

S.C.C. Versus Temperature

9.7 Summary

The rate of formation of Cu_2S on CdS by ion transfer is governed by a parabolic law. The presence of In or Ga inhibits this process in its initial stages.

Single crystal CdS cells doped with indium to lower their resistivity had slow response times and poor response at low intensities of illumination. Heat treatment which was essential to achieve high efficiency generally has the effect of slowing the response. After heat treatment, all devices possessed a slow component of the O.C.V. under excitation with wavelengths greater than 0.49 microns. This either enhanced or quenched the initial rapid response according to wavelength. The 0.49 and 0.7 micron peaks in the steady state spectral response became more pronounced with extended heat-treatment at 200°C. Baking a device in air before plating on the Cu_2S layer did not improve either the ultimate O.C.V. or S.C.C. However crystals with highly polished surfaces led to cells with higher O.C.V's.

Cells formed on films grown in a totally enclosed system have higher efficiencies than corresponding single crystal cells. There is no evidence to suggest that photochemical changes in CdS or migration of Cu through the device are responsible for the degradation reported for cells run in poor vacuum at temperatures above 60°C.

Cells fabricated with a positive potential applied to the Cu_2S surface in the plating bath, in an attempt to form stoichiometric Cu_2S, show an increase in efficiency over those plated with a negative or zero applied potential. The interpretation of these results will be continued in the next chapter.

All the cells investigated either in single crystal or thin film form had efficiencies much lower (0.5 - 3.5%) than those normally reported for CdS cells (5-6%). This was due solely to the method of applying the upper contact, where the point contact used or the application of a grid with adhesive backed mylar was distinctly inferior to the commercial technique of applying the grid with gold filled epoxy resin and encapsulating the device in Teflon. This technique was not available for use at either Durham or I.R.D.

REFERENCES

Bogus and Mattes (1972) Proc. 9th IEEE Photovoltaic Specialists Conference

Gill and Bube (1970) J.A.P. 41 3731

Kanev et al (1972) Appl. Phys. Lett. 19 459

Lindquist and Bube (1970) Proc. 8th IEEE Photovoltaic Specialists Conference

Martin (1970) M.Sc. Thesis University of Durham

Mytton et al (1968) Proc. Brighton Power Conference P.643

Palz et al (1972) Proc. 9th IEEE Photovoltaic Specialists Conference

Piper and Polich (1961) J.A.P. 32 1278

Rickert and Mathieu (1970) E.S.R.O. Contract Report No.14

Rushby and Woods (1970) J. Phys. E. 3 726

Shiozawa et al (1969) A.R.L. Report 69-0155

Wilson and Woods (1972) J. Phys. D. 5 1700

CHAPTER 10

DISCUSSION OF PHOTOVOLTAIC MEASUREMENTS

10.1 Introduction

The results described in the previous chapter require more discussion than the brief comments which accompanied their description. It is possible to offer reasonable explanations for much of the behaviour of our cells in terms of the Clevite model for the device (see Section 3.4). Some tentative explanations are also given for the observed results on barrier formation and the effect of introducing fixed potentials into the plating bath.

10.2 Rate of formation of Cu_2S

It was mentioned in Chapter 2 that the mechanism of the formation of a Cu_2S layer on CdS can be represented by the equation

$$2Cu^{+} + CdS \longrightarrow Cu_2S + Cd^{++}$$

If the reaction is taken to the limit therefore, all the CdS becomes Cu_2S (Cook et al 1970). As the molecular weight of CdS is 144.46 and that of Cu_2S is 159.14 this change must be accompanied by an increase in the weight of the sample. For a complete change of the sample from CdS to Cu_2S there would be a corresponding weight increase of 10.1%. The increase in weight of the samples from the present investigation shown in Figure 9.2 corresponds to a conversion of 56% in four hours for the undoped sample, decreasing to 36% in the same period of time for the samples doped with 1,000 p.p.m. of indium.

From the reaction equation it is obvious that once the initial monolayer of Cu_2S has been formed the rate determining step is the diffusion of Cu through the Cu_2S into the CdS.

If H is the thickness of the Cu_2S layer, W is the number of the Cu ions diffusing through it and t is the time, assuming that all the Cu ions diffusing through the Cu_2S react with the CdS then

$$W \alpha H \qquad (1)$$

If we assume that the boundary conditions remain constant, then for a given concentration difference, the rate of diffusion is inversely proportional to the length of the diffusion path which in this case is H, so that

$$dw/dt \alpha \frac{1}{H}$$

Using equation (1) above

$$dw/dt = k'(\frac{1}{w})$$

$$wdw = k' \int dt$$

$$w^2 = kt$$

$$W = k\sqrt{t}$$

or if R is the rate of formation

$$R = K\sqrt{t}$$

where k'k and K are constants.

A parabolic law of this nature has been reported for the oxidation of metals by many workers including Pilling and Bedworth (1923), Vernon (1935), Moore (1950) and Hirashima (1955). Singer and Faeth (1967) and

and Sreedhar et al (1970) reported a parabolic law governing the formation of Cu_2S on CdS but Shiozawa et al (1969) concluded that the rate of formation of Cu_2S was linear with time. The results presented in Figures 9.2 and 9.4 indicate that the formation of the Cu_2S followed two parabolic laws each with a different value of the constant. The initial parabolic laws are affected by the presence of In (or Ga) in the CdS. Shiozawa et al (1968) reported that the presence of indium in their CdS films slowed up the growth of the i-CdS, i.e. inhibited the diffusion of Cu into CdS. Copper will not replace indium in In doped CdS and this is verified by Figure 9.5 where the initial gradient tends to zero as the In doping tends to infinity. This being the case it is surprising that the reaction follows a parabolic law in its initial stages as the assumption that all the Cu ions diffusing through the Cu_2S react with the CdS is invalid.

After an initial period of time a second parabolic law was obeyed and the rate of growth of the Cu_2S layer was approximately equal in all samples regardless of their doping level. This suggests that whatever effect the indium has is overcome after Cu_2S has formed on the first 60 or 70 μm of CdS. This requires that the indium drifts towards the reaction interface and be concentrated in this initial surface layer, rather than being homogeneously distributed throughout the crystal. As the slices were cut from various parts of the boule it is unlikely that such a surface concentration was present in the slice before the cell was fabricated. Darken (1942) reported a similar phenomenon when discussing the oxidation of steel containing copper impurities. The copper was found to accumulate to a marked

degree at or near the oxide-metal interface. The In in CdS might react in a similar way congregating at the initial CdS:Cu_2S interface. We therefore presume that by the time the second parabolic law is in force, there is very little In in the CdS while the first 50-60 μm layer of Cu_2S is heavily doped with In.

An alternative explanation for the lowering of the rate of Cu_2S formation in the presence of In can be given in terms of ion pairing between the In and Cu. It is quite possible that the inward diffusing Cu is attracted to the Cd vacancies associated with In^{+++}. The lower diffusion rate would be consistent with the idea that the diffusing Cu is captured by centres consisting of a complex of a foreign donor and a cation vacancy. This explanation has been offered by Aven and Halsted (1965) to explain similar results on the diffusion of Cu into ZnS and ZnSe doped with varying amounts of aluminium. If Aven and Halsted are correct the first stage in the conversion of indium doped CdS to Cu_2S is a compensation process. In makes the samples highly conductive and this has to be compensated first of all before the second mechanism takes place. The quantity of copper required for compensation will be directly proportional to the indium concentration. However the quantity of copper is directly proportional to $\sqrt{t}$, where t is the time and therefore

$$\sqrt{t} \alpha \text{ In Concentration}$$

Figure 9.6 shows this to be the case and therefore suggests that this second explanation is more likely to be the correct one.

Unfortunately no direct correlation can be made between these results and those previously published for the diffusion of Cu into CdS for example by Szeto and Somorjai (1966) and Clark (1959) as these workers quote results only in the temperature range 450-700°C.

10.3 Cell Performance

10.3.1 Heat treatment after plating

Heat treatment modified the responses of the cells to a variety of stimuli. As well as the magnitudes of the O.C.V. and S.C.C., the spectral response and response times were also affected.

These phenomena can be understood as associated with the thermally enhanced diffusion of Cu from the Cu_2S into the n-CdS to form a compensated layer of high resistivity CdS. As the period of heating at 200°C was increased this layer grew and its influence became more obvious. The initial heat treatment also affected the surface reflectivity of the Cu_2S and it became darker and more matte.

As the O.C.V. and S.C.C. both increased during the initial stages of heating, there must have been either more efficient light absorption or increased carrier collection, in addition to an increase in barrier height. When the height of the barrier reached its constant value and the O.C.V. was at a maximum , the low light level response improved, but the S.C.C. and O.C.V. began to decrease slightly.

The best cells possessed an O.C.V. of appreciable magnitude before any heat treatment indicating that a potential barrier of some height must already have existed between the Cu_2S and CdS. The intermediate i-CdS layer helps to increase the S.C.C. by photoconductive effects which (1) aid electron transport across the junction, (2) allow large O.C.V's. to develop by reducing recombination currents and (3) prevents tunnelling between p^+ and n^+ regions which brings about unstable diode behaviour as observed in the I(V) characteristics of unheated cells. It is also thought that the poorer cells had defects in the junction region which tended to short out the photovoltage. The subsequent formation of the i-CdS layer however widened the junction region and removed these short-circuits.

The long time constant effects observed in baked cells are similar in nature to those which exist in high resistivity, photoconductive CdS. Such material contains electron traps which are responsible for the slow response of photoconductivity. Several tens of seconds are required before the traps reach thermal equilibrium following a change in the illumination. The quenching and enhancement behaviour of the slow component of the O.C.V. spectral response to monochromatic radiation is typical of the photoconductive effects in CdS connected with the capture and release of holes at recombination centres.

The increase in the O.C.V. of baked cells on exposure to 4900Å radiation is due to increased light absorption in the CdS layer. As the Cu_2S does not appear to become more transparent to illumination with continued heating, the light absorption must be more efficient in the

CdS. The only possible change in the CdS is an increase in width of the insulating layer so that it must be this which is actively involved in light absorption at 4900Å.

10.3.2 Heat treatment prior to plating

Baking cells prior to the formation of the Cu_2S also brought about the introduction of long time constants, and the quenching and enhancement behaviour of the slow component of the O.C.V. response under monochromatic illumination. This is consistent with the idea that these phenomena are associated with trapping effects and the capture and release of holes at recombination centres in the CdS. Since the Cu_2S was not formed when the baking took place it is unlikely that the observed effects were due to any changes in this p-type layer.

It is not obvious why the O.C.V's. of some pre-baked cells were lower than cells fabricated from the same boule given normal treatment. One possibility is that in the poorer polycrystalline slices the heating brings about a small amount of surface migration and recrystallization which decreases the number of grain boundaries down which the Cu_2S can penetrate, thus reducing the effectiveness of the junction.

10.3.3 Spectral Response

The maxima of the three peaks of the O.C.V. spectral response were located at wavelengths 4900Å, 7000Å and 9000Å which correspond to photon energies of 2.53 eV, 1.77 eV and 1.38 eV. The first of these is attributed to direct band to band transitions in CdS. The other two peaks

have, in the past, been thought to be caused by absorption in the Cu_2S layer which has two band gaps of 1.8 eV (direct) and 1.2 eV (indirect). If this were so it would be difficult to explain why their relative heights change after heat treatment, and particularly why the absorption at 7000Å increased in baked cells. This could be connected with the change in composition of the copper sulphide layer with heating when it becomes deficient in copper (Section 2.5). This might produce changes in the absorption coefficient and energy gaps, but the effect however is unlikely to be large.

It is more probable that the peak at 7000Å is due mainly to the absorption of photons by centres in copper doped CdS. Gill et al (1968) came to a similar conclusion following their experiments on the S.C.C. spectral response of Cu_2S-CdS heterojunctions.

Copper doped CdS has a photoconductive maximum at 6,500Å so that it is possible that the increase in the O.C.V. at 7000Å is brought about by an increase in the number of copper impurities in the CdS. Only the band at 9000Å is due to excitation processes in the Cu_2S across the indirect gap. The measurements of Bube et al (1962) are in agreement with these ideas. They reported the existence of Cu levels 1.7 eV below the conduction band in heavily copper doped CdS. Further support for this suggestion is provided by Nakayama (1962) who reported cells with thick Cu_2S layers which had spectral responses centred at 9000Å as opposed to cells with thin layers giving large responses at 6400Å and less at 9000Å.

10.3.4 Surface Quality

Crystals which were highly polished with 3 micron diamond paste led to cells with higher O.C.V's. than those given the standard polish with 600 grade carborundum (see Figure 9.17). As mentioned previously one would expect that a rough surface would form a larger area junction, with more efficient light absorption. However, it would seem that the diamond paste polish produces much less surface damage, together with the associated traps and recombination centres than a polish with silicon carbide and this results in higher O.C.V's. being obtained.

10.4 Thin Film Cells

Cells fabricated on the thin films evaporated in enclosed tubes looked very promising with efficiencies greater than corresponding cells on single crystals. The S.C.C. of the cells was very high 16 mA cm^{-2} and this was thought to be due to the low resistivity (4-8 Ωcm) of the CdS layer. However the low O.C.V. of the cells indicates that the junction formed between the CdS and Cu_2S has only a low barrier height. This could be a function of the structure of these films about which little is known. Another possibility is that the resistivity of the base layer is too low for a large O.C.V. to be produced. Further work is required to established this point. If the O.C.V. of such devices could be increased to the normal level of 400-500 mV without any detrimental effect on the S.C.C. efficiencies around 7% could be achieved. This represents a very high value for cells where the current is drawn from only a point contact.

10.5 Cu_2S Stoichiometry

Most workers now attribute the degradation observed in CdS solar cells, operated for long periods of time, as due to the oxidation of Cu_2S to $Cu_{2-\delta}S$ where δ is the copper deficiency. For example

$$Cu_2S + {}^{\delta}/_{2}\, O_2 \longrightarrow Cu_{2-\delta}S + \delta CuO$$

Rickert and Mathieu (1970) have shown that it is possible to control the stoichiometry of the Cu_2S formed in the plating bath by controlling its electropotential. The basis of this reasoning is outlined below:-

We shall consider a galvanic cell which consists of an electrode under consideration and the standard hydrogen electrode as a reference electrode. The cell voltage E which can be measured is by definition identical to the electrode potential. It can be correlated with the Gibbs free energy of the corresponding reversible cell reaction according to

$$\Delta G = -nFE \qquad (2)$$

where nF is the number of Faradays transported. At constant temperature T and constant pressure p the Gibbs free energy ΔG only depends on the chemical potential μ of the reaction partners.

$$\Delta G = \sum_i V_i \mu_i \qquad (3)$$

where V is the stoichiometric coefficient of component i and μ_i is the chemical potential of component i. Using (2) and (3) we have

$$E = -\frac{1}{nF} \sum_i V_i \mu_i \qquad (4)$$

The chemical potential μ of mixed phases depends upon the activity, a, of the components according to the equation

$$\mu_i = \mu_o + RT \ln a_i \qquad (5)$$

where μ_o is the chemical potential in the standard state

a = fc and is the activity

f is the activity coefficient, and

c is the concentration.

The activity coefficient is equal to 1 in ideal solutions. Equations (4) and (5) show that changes in electrode potentials can also be written as functions of the activities of the components participating in the reaction. Rickert and Mathieu have shown that individually the activities of both copper (a_{Cu}) and sulphur (a_s) decrease with increasing potential E. However the chemical potentials in mixed phases, especially in solid compounds, are not independent being correlated by the Gibbs-Dunhem equation

$$\sum_i V_i \, d\mu_i = 0 \qquad (6)$$

Applying this equation to Cu_xS leads to

$$x d\mu_{Cu} + d\mu_s = 0$$

This implies that an increase in the chemical potential μ_{Cu} of copper as a result of a change in the copper activity, a_{Cu}, has to bring about a decrease in the chemical potential μ_s, of sulphur and a corresponding decrease in the sulphur activity, a_s. Consequently one can change the stoichiometric composition of Cu_xS by fixing the electropotential E.

To assess the stoichiometry of the Cu_2S layers prepared in this investigation we will compare our results

with those of Palz et al (1972). Figure 10.1 shows the relationship they obtained for the O.C.V. of Cu_xS-CdS cells as a function of x. (The parameter x was measured by means of coulometric titration experiments). Studying Figure 9.23 we can see that the changes in O.C.V. produced as a result of applying a potential to the CdS in the plating bath are consistent with a change in Cu_xS composition from x = 1.97 to x = 1.98.

This argument is given further support by the measurements of S.C.C. as a function of temperature. Palz et al have shown that with pure chalcocite (x=2) or pure djurleite (x=1.95) there is only a slight variation in S.C.C. with temperature. In the presence of a chalcocite-djurleite mixture (2>x>1.95) however there is a noticeable decrease in the S.C.C. of the cells at temperatures in the range 80-85^{o}C. Bougnot et al (1971) have attributed this decrease to a phase change within the mixed material. Palz's results are shown in Figure 10.2. The S.C.C. of the cells used in the present investigation decreased significantly at around 80^{o}C (Figure 9.26) and this is consistent with the suggestion that even by applying fixed potentials to the reaction surface it was not possible to grow perfectly stoichiometric Cu_2S. It would also appear that the cells plated without applied bias also consist of a djurleite/chalcocite mixture, whereas the change in S.C.C. with temperature of the sample plated with a negative applied bias shows less of a variation of S.C.C. with temperature implying that the composition of the barrier layer might be approaching pure djurleite.

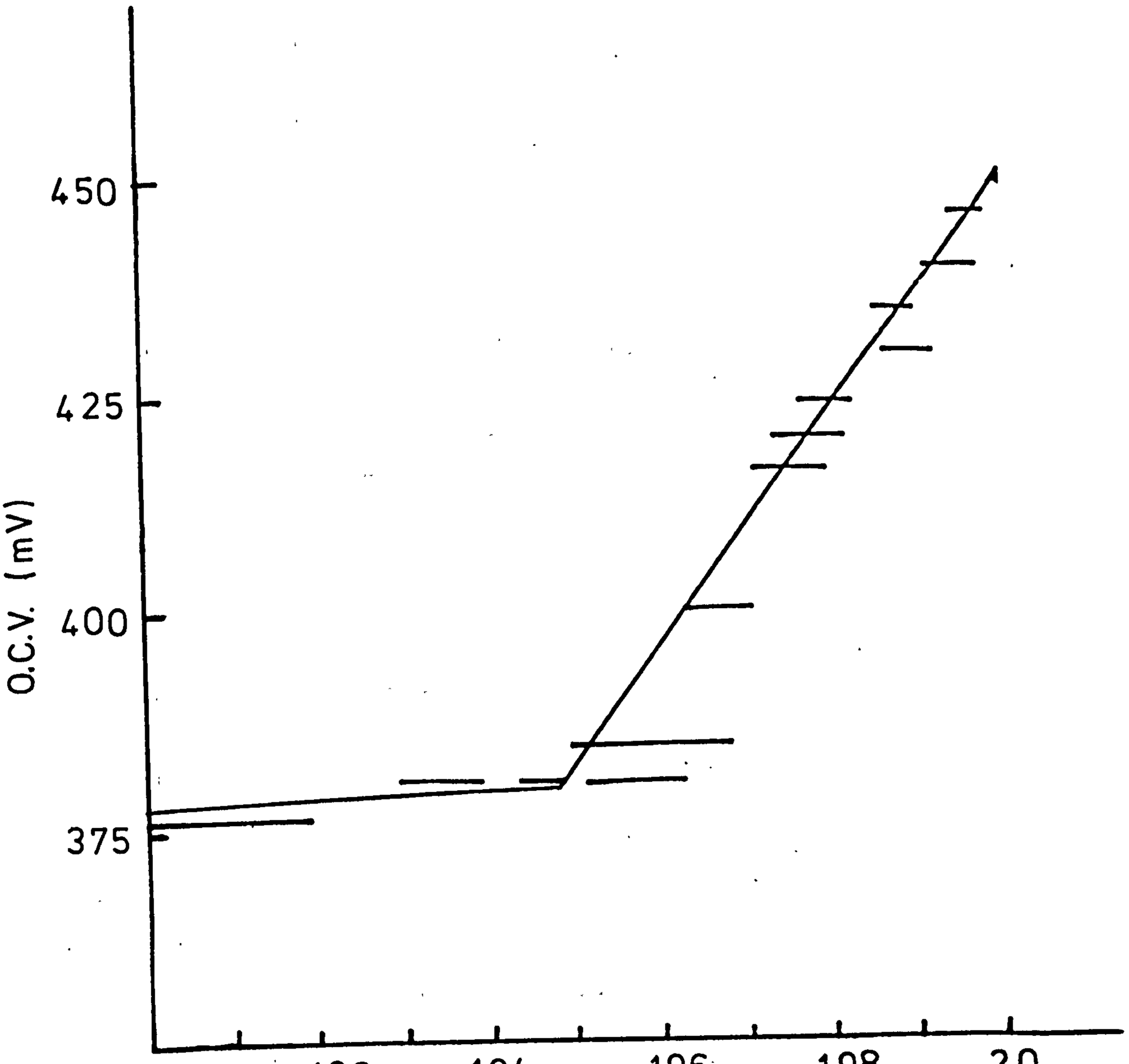

Figure 10.1

Open Circuit Voltage as a Function of x in Cu_xS (Palz 1972)

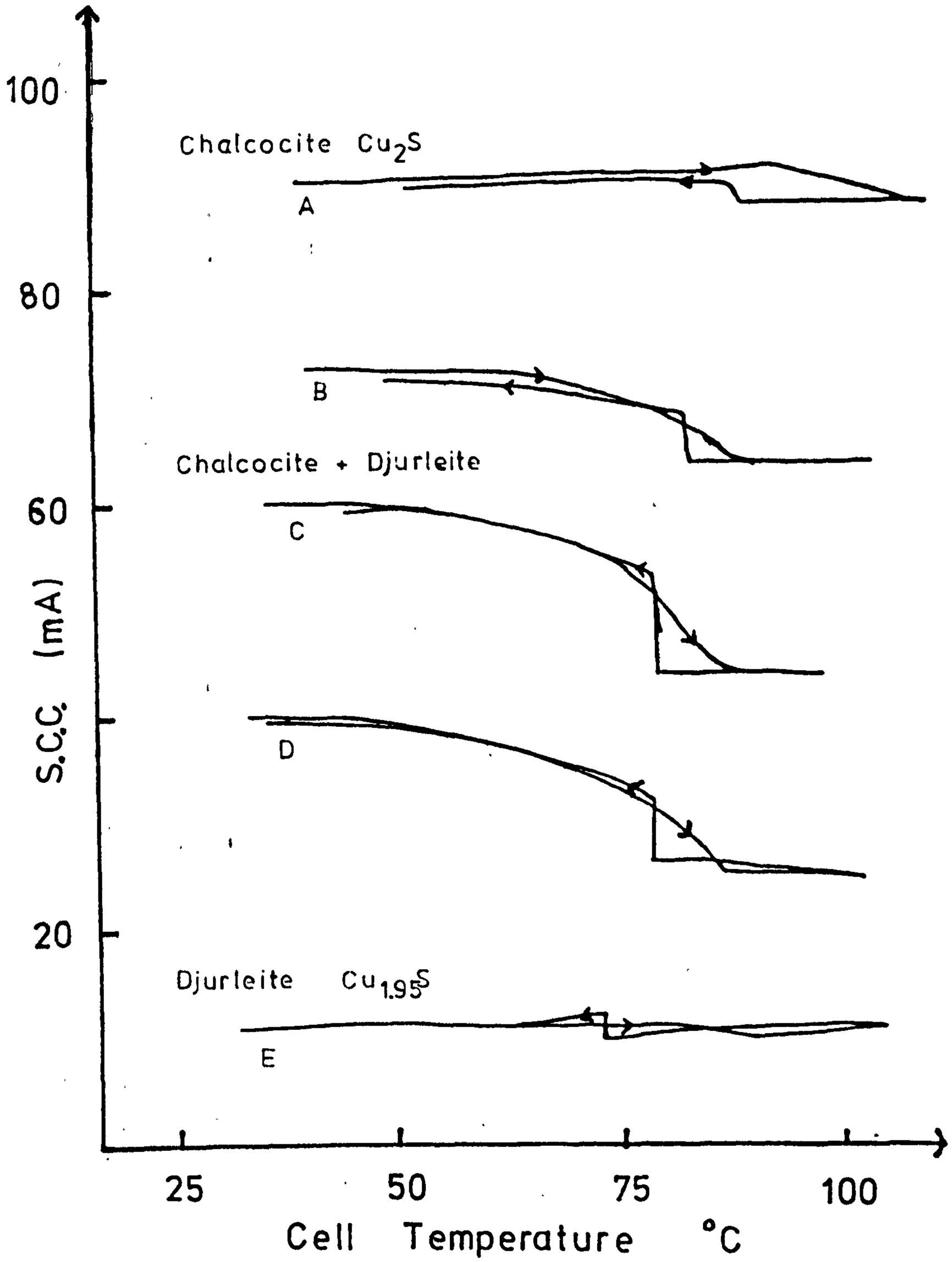

Figure 10.2

S.C.C. as a Function of Cell Temperature
(Palz 1972)

10.6 Conclusions

Most of the experimental observations on cell performance can be explained in terms of the Clevite model. In particular the effect of heat treatment on the cells can be attributed to the growth of an insulating layer of CdS between the Cu_2S and the bulk CdS formed by the thermal diffusion of Cu ions into the CdS.

The application of fixed positive potentials to the reaction surface in the plating bath with respect to a copper electrode immersed in the solution improved the stoichiometry of the copper sulphide layer, but failed to produce perfect Cu_2S.

REFERENCES

Aven and Halsted (1965) Phys.Rev. 137 228A

Bougnot et al (1971) University of Montpellier CNES Contract 274

Bube et al (1962) Phys. Rev. 128 532

Clark (1959) J A.P. 30 957

Cook et al (1970) J.A.P. 41 3058

Darken (1942) Metals Technology August p.157

Gill et al (1968) 7th IEEE Photovoltaic Specialists Conf.

Hirashima (1955) J. Phys. Soc. Jap. 10 1055

Moore (1950) J. Chem. Phys. 18 231

Nakayama (1962) Japan J.A.P. 8 430

Palz et al (1972) 9th IEEE Photovoltaic Specialists Conf.

Pilling and Bedworth (1923) J. Inst. Met. 29 529

Rickert and Mathieu (1970) E.S.R.O. Contract Report CR14

Shiozawa et al (1968) 7th IEEE Photovoltaic Specialists Conf.

Shiozawa et al (1969) ARL Report 69-0155

Singer and Faeth (1967) App. Phys. Lett. 11 130

Sreedhar et al (1970) Radiant Eff. G.B. July P.103

Szeto and Somorjai (1966) J. Chem. Phys. 44 3490

Vernon (1935) Trans. Farad Soc. P.1668.

CHAPTER 11

SUMMARY

11.1 CdS Thin Films

In the course of this work polycrystalline CdS thin films with reproducible properties have been prepared by the evaporation of the compound. Three different systems were used; an electron beam heated source, a resistively heated source, and a totally enclosed tube heated externally by a furnace. By considering the processes of evaporation and condensation some understanding of the importance of the substrate temperature, source temperature (deposition rate) and film thickness in determining the properties of the film was achieved. Two approaches were used for this (1) an equilibrium approach using the CdS phase diagram and (2) the non equilibrium approach where the dissociation of CdS into two species with different sticking coefficients was considered. From this it was concluded that a film will contain only CdS if the substrate temperature is higher than the critical temperatures for the nucleation of cadmium and sulphur. At lower temperatures both free sulphur and free cadmium may exist.

The equilibrium theory predicts that the CdS source will become rich in cadmium with time, and since CdS evaporates congruently the deposited film will become richer in cadmium as the evaporation proceeds. This has been found to occur in practice with films evaporated either in an enclosed tube or in the resistively heated system and manifests itself by lowering the resistivity

of the films with thickness by increasing the carrier density. With the majority of films less than 1 micron thick the Hall mobility was dominated by surface scattering phenomena. In the thicker films it is controlled by the inter-crystallite barrier height.

Films evaporated from an electron beam heated source did not display the continually decreasing resistivity with thickness because no single source was heated for long enough for the appropriate effects to appear. The method did however yield films with higher resistivities than those produced from a resistively heated source and this is attributed to a lower impurity content. Metal impurities from the heating element would be screened from the substrate by the focussed electron-beam evaporation.

Electron microscope studies have shown that epitaxial films of CdS could be grown on the (100) face of NaCl using either the electron gun or resistively heated sources.

By growing films in a totally enclosed system it was possible to prepare films with very low resistivity (≈ 5 Ωcm). These produced very promising photovoltaic cells, but such a method is not suitable for the mass production of large area devices.

11.2 CdS:Cu_2S Photovoltaic Cells

The formation of Cu_2S on CdS can be explained in terms of a simple diffusion model and is governed by a parabolic law. The rate of formation of Cu_2S is initially

inhibited by the presence of In or Ga in the CdS. Although light is absorbed in the Cu_2S layer, the properties of the n-type CdS have been seen to determine the behaviour of the devices particularly after heat treatment. Many of the results on the baked cells can be explained by the thermally enhanced diffusion of Cu into CdS to form a compensated i-CdS region. This region has both photoconductive properties and the ability to absorb light to create free electrons. The voltage output of single crystal cells was increased by polishing their surfaces with diamond paste.

The spectral response of the cells can be divided into three bands:

(1) at 4900Å due to direct band to band transitions in the CdS.

(2) at 7000Å due to the absorption of photons by centres in the copper doped i-CdS layer, and

(3) at 9000Å due to excitation across the direct gap of Cu_2S.

The stoichiometry of the Cu_2S layer was also found to be important. By applying fixed potentials to the CdS:Cu_2S reaction surface in the plating bath it was possible to improve the stoichiometry, but comparison of the resulting O.C.V's. and the variation of the S.C.C's. with temperature, with the results of other workers, indicates that the average composition of the copper sulphide layer was Cu_xS where $1.98 \leq x < 2.0$.

11.3 Suggestions for future work

The results described in this thesis indicate several interesting areas for future work. The main ones are listed below.

(1) An investigation into the structure of CdS thin films formed in the enclosed system to determine whether the low O.C.V's. produced by these films when made into cells is a function of their structure or their resistivity.

(2) To devise a system where it is known that the evaporation proceeds under equilibrium conditions. (This was originally thought to be the situation with the enclosed system but the results proved it to be otherwise). If the equilibrium theory is correct, as CdS evaporates congruently, films grown in such a system would not become increasingly cadmium rich and consequently more conducting.

(3) To continue the analysis of the photoluminescence of CdS films produced in the enclosed system, particularly between 4.2 K and 77 K.

(4) To measure the stoichiometry of the Cu_2S layer either directly with an electron microprobe analyser or by coulometric titration when a value of δ, the copper deficiency can be calculated. This latter method has the disadvantage of being destructive.

11.4 Epilogue

Commenting on the present energy crisis Professor D. Bryce-Smith of Reading University said, "We use power like a drunk with a legacy and now we are wondering where the next round of drinks will come from. We are intoxicated with power use."

The energy available in natural sunlight, if properly utilized could provide all the energy requirements of our industrial society into the foreseeable future, without relying on the potentially hazardous applications of nuclear energy. In this thesis the CdS Photovoltaic Cell has been described and reference made to similar devices using Si, GaAs etc. The "green-house effect" has also been studied as a means of heating by incorporating what are known as solar walls into buildings. Such an experiment has been tried at St. George's School,Wallasey but has only met with limited success. Recently however photochemical reactions e.g. photosynthesis, have been examined as a means of energy conversion. Other possibilities include the use of the wind, the tides, and ocean heat. In conclusion it should be stated that although solar power (in any form) is pollution free, it is doubtful whether its cost could ever be reduced to less than twice that of nuclear energy.